UNIVERSITY OF Hull

Investigating the Role of MicroRNAs as Modulators of Sensitivity to Neoadjuvant Chemoradiation Therapy in Oesophageal Adenocarcinoma Patients

Being a thesis submitted for the Degree of Doctor of Philosophy in the University of Hull

by

Becky Ann Selina Bibby, BSc

December 2015

Declaration

I, the undersigned, declare that this work has not been previously submitted as an exercise for a degree at this or any other University.

Unless otherwise stated, this thesis is the sole work of the author, who gives permission for the library to lend or copy this work upon request.

_____

Becky Bibby

December 2015

Summary

Oesophageal cancer is the eight most common cancer and the sixth leading cause of deaths worldwide. There are two major histological subtypes of oesophageal cancer, with the most predominant subtype in Europe and the USA being oesophageal adenocarcinoma (OAC). The standard of care for OAC patients with locally advanced disease is neoadjuvant therapy and surgical resection. Unfortunately, ~70% of patients do not respond to neoadjuvant therapy and non-responders gain no benefit from the aggressive treatment regimen whilst compromising their quality of life.

There is an unmet clinical need for biomarkers predicative of patient's response to neoadjuvant chemoradiation therapy (neo-CRT). In a pre-treatment setting, predictive biomarkers indicative of patient response could enable the stratification of patients and would ensure individual patients receive the most effective treatment. However, the greater clinical benefit for patients may come from the development of new or combination therapeutics for OAC. Novel chemosensitising and radiosensitising therapeutics could be administered with neo-CRT to enhance tumour sensitivity, improve CRT efficacy and increase survival rates for OAC patients.

MicroRNAs (miRNA/miRs) are short non-coding RNA that function to regulate gene expression at the post-transcriptional level. A single miRNA can potentially target hundreds or thousands of mRNA and subsequently alter the expression of multiple genes and proteins. As essential regulators of gene expression, miRNA are involved in all cellular processes and are dysregulated in cancer and other diseases. Furthermore, miRNA have been identified as predictors and modifiers of tumour sensitivity to chemotherapy and radiotherapy in numerous cancer types. Playing a causal role in disease development and progression, miRNA are promising biomarkers and therapeutic targets.

In this study miRNA were investigated as biomarkers of OAC patient response to neo-CRT and as potential therapeutic targets through which to enhance tumour sensitivity to neo-CRT. In pre-treatment OAC biopsies, 67 miRNA that were differentially expressed between responders and non-responders to neo-CRT were identified. MiR-330-5p and miR-187 were downregulated in the pre-treatment biopsy samples of the neo-CRT non-responders. The functional roles of miR-330-5p and miR-187 were investigated as modulators of tumour sensitivity to CRT. *In vitro* the silencing of miR-330-5p enhanced, albeit subtly, cellular resistance to radiation. Furthermore, silencing miR-330-5p altered the expression of extracellular proteases and protease inhibitors, including MMP1. *In vivo* a pilot study indicated miR-330-5p silencing enhanced tumour growth and may alter tumour sensitivity to cisplatin. *In vitro* miR-187 overexpression enhanced cellular sensitivity to radiotherapy and cisplatin, implying that the downregulated miR-187 expression in the non-responders may confer resistance to CRT. Furthermore, miR-187 induced apoptosis *in vitro* and induction of apoptosis is a potential mechanism by which miR-187 enhances radiosensitivity. MiR-187 altered the expression of genes encoding extracellular proteins, including *C3* and other immune related genes. Both miR-330-5p and miR-187 are potential regulators of the secretome, thus emphasising the role of miRNA as modulators of the tumour microenvironment. This study has identified miR-330-5p and miR-187 as potential therapeutic targets that could augment OAC tumour sensitivity to neo-CRT.

Acknowledgements

Thank you to my supervisor Dr Stephen Maher. I have thoroughly enjoyed my PhD experience and my research project and for this I am very grateful to Stephen. I am proud of what I have achieved during my PhD and could not have done this without Stephen's encouragement and support.

Thank you to my Mam and Dad who always support me in all my endeavours. Thanks to my family and friends who have listened to me talk endlessly about my work every time we catch up, and despite this always enquire as to how I am getting on. Without doubt my Mam has had to listen to me go on more than anyone else, but still regularly enquired as to how my cells were doing and took a genuine interest in microRNA. Thank you to my Dad for proof-reading the introduction of the thesis and telling me that he actually enjoyed reading it.

Thank you to the University of Hull for my PhD scholarship and the Cancer and Polio Research Fund (CPRF) and Irish Cancer Society for financially supporting this research. Thanks to the University of Hull cancer group staff and students for help, guidance, support and feedback throughout. A special thank you to Hannah, Anna and Flore-Anne who have taken the same journey as me, we have supported one another throughout and the experience has been all the better for it. Hannah in particular has put up with me ranting over coffee on a daily basis. We have also had many in depth chats about our research, the weather and life and have become the best of friends. Thanks to Dr Elena Rosca for help with statistics and the supportive and honest advice. Thank you to Dr Chris Cawthorne and Dr Niamh Lynam-Lennon who have contributed to the work presented in this thesis and have been a great help to me.

Thank you to the patients treated at St James hospital that consented to their tissue samples being used in this study, in the hope that this research will benefit patients suffering with oesophageal cancer in the not so distant future.

Dedication

This thesis is dedicated to my parents and my sisters.

Abbreviations

3’	3 prime
5’	5 prime
3’ UTR	3 prime untranslated region
5-FU	Fluorouracil
5’ UTR	5 prime untranslated region
^{18}F-FDG	Fludeoxyglucose
Abs	Absorbance
aCGH	Array comparative genomic hybridization
Ago	Argonaut protein
AGT	Alkylguanine DNA alkytransferase
AJCC	American joint committee on cancer
Akt	Protein kinase B
Amp^R	Ampicillin resistance
ANOVA	Analysis of variance
ASR	Age standardised incidence rate
APS	Ammonium persulfate
ATM	Ataxia telangiectasia mutated kinase
ATP	Adenosine triphosphate
ATR	ATM Rad3 related kinase
BCA	Bicinchoninic acid
BCL2	B-cell lymphoma 2
BER	Base excision repair
BMI	Body mass index
BSA	Bovine serum albumin
cDNA	Complementary deoxyribonucleic acid
CGH	Chromosomal genomic hybridization
CHARM	Compact Hough and radial map
CLL	B cell chronic lymphocytic leukaemia
CMA	Chromosomal microarray analysis
CMV	Cytomegalovirus
CN-LOH	Copy neutral loss of heterozygosity
copGFP	Copepod green fluorescent protein
CRT	Chemoradiation therapy
CSC	Cancer stem cell
CT	Computed tomography
CTLs	Cytotoxic T lymphocytes
CTR1	Copper transporter 1
DAMPs	Damage associated molecular patterns
DAPI	4’, 6-diamidino-2-phenylindole
DEPC	Diethylpyrocarbonate
DGCR	DiGeorge syndrome chromosomal region
DMSO	Dimethyl sulfoxide
DNA	Deoxyribonucleic acid
dNTPs	Deoxyribose nucleotide triphosphates
DR	Direct response
dsDNA	Double stranded DNA
BO	Barrett’s oesophagus
E.coli	*Escherichia coli*
EDTA	Ethylenediainetetraacetic acid
ELISA	Enzyme-linked immunosorbent assay

EMT	Epithelia to mesenchymal transition
EtOH	Ethanol
EU	European Union
EUS	Endoscopic ultrasound
FBS	Foetal bovine serum
FITC	Fluorescein isothiocyanate channel
FPKM	Fragments per kilobase of transcript per million mapped reads
G	Grade
G418	Geneticine
gDNA	Genomic DNA
GFP	Green fluorescent protein
GLUT1	Glucose transporter 1
GO	Gene ontology
GORD	Gastro-oesophageal reflux disease
GP	General Practitioner
GSH	Glutathione
G:U	Wobble pair G-U
HCV	Hepatitis C virus
HGD	High grade dysplasia
HR	Homologous recombination
HRP	Horseradish peroxidise
IC_{50}	Half maximal inhibitory concentration
IFN	Interferon
IgG	Immunoglobulin G
IHC	Immunohistochemistry
IMC	Intramucosal carcinoma
IRES	Internal ribosome entry site
Kan^R	Kanamycin resistance
KEGG	Kyoto encyclopaedia of genes and genomes
LB	Lysogeny broth
LGD	Low grade dysplasia
M	Metastasis
M1	Marker 1
M2	Marker 2
MEP	microRNA expression profile
miR/miRNA	microRNA
miRISC	microRNA induced silencing complex
miRNA*	microRNA passenger strand
miRZIP	microRNA ‘zip down’ or silencing
MMP	Matrix metalloproteinase
MMR	Mismatch repair
mRNA	Messenger RNA
N	Node/nodal
n	Sample size
NCBI	National centre for biotechnology information
neo-CRT	Neoadjuvant chemoradiation therapy
Neo^R	Neomycin resistance
NER	Nucleotide excision repair
NHEJ	Non-homologous end joining
NK	Natural killer
Non-pCR	Non-pathological complete response
ns	Not significant

OAC	Oesophageal adenocarcinoma
OD	Optical density
OE33 P	OE33 parent
OE33 R	OE33 radioresistant
OSC	Oesophageal squamous carcinoma
P	Probability
p21	Protein 21
p53	Protein 53
p-Akt	Phosphorylated protein kinase B
PBS	Phosphate buffered saline
p-bodies	Processing bodies
pCR	Pathological complete response
PCR	Polymerase chain reaction
PET	Positron emission tomography
PI	Propidium iodide
pre-miRNA	Precursor microRNA
pri-miRNA	Primary microRNA
PRRs	Pattern recognition receptors
Puro	Puromycin
PVDF	Polyvinylidene fluoride
qPCR	Quantitative polymerase chain reaction
R0	Tumour negative resection margin
R1	Tumour positive resection margin
Ran-GTP	Ras related nuclear protein- guanosine triphosphate
RB	Retinoblastoma
RIPA	Radioimmunoprecipitation assay
RISC	RNA induced silencing complex
RNA	Ribonucleic acid
RNase	Ribonuclease
RNA-seq	Ribonucleic acid sequencing
ROS	Reactive oxygen species
RPMI-1640	Roswell park memorial institute-1640
RT	Reverse transcription
SEM	Standard error of the mean
SDS	Sodium dodecyl sulfate
SDS-PAGE	Sodium dodecyl sulphate-polyacrylamide gel electrophoresis
SH3GL2	SH3 domain protein 2A
S phase	Synthesis phase
ssDNA	Single stranded DNA
SUV	Standard uptake value
T	Tumour
TBE	Tris/borate/EDTA
TBS	Tris-buffered saline
TBST	Tris-buffered saline containing 0.1% Tween-20
TEMED	N, N, N’, N’-tetramethylethylenediamine
TGFβ	Tumour growth factor beta
T_H1	T helper 1
T*is*	Tumour *in situ*
TLR	Toll-like receptor
TMA	Tissue microarrays
TNM	Tumour node metastasis
TP53	Tumour protein 53

TRBP	Transactivating response RNA-protein
Tregs	T regulatory
TRG	Tumour regression grade
UK	United Kingdom
USA	United States of America
VEGFA	Vascular endothelial growth factor A

Units

∞	infinity
bp	base pairs
°C	degrees Celsius
cm	centimetre
g	grams
× *g*	acceleration due to gravity
Gy	gray
h	hour
kb	kilobase
kDa	kiloDalton
kg	kilogram
L	litre
M	molar
m	meter
MBq	megabecquerel
mg	milligram
min	minute
mL	millilitre
mM	millimolar
mm	millimetre
ms	milliseconds
µg	microgram
µL	microlitre
µM	micromolar
µm	micrometer
ng	nanogram
nM	nanomolar
nm	nanometre
nt	nucleotide
pg	pictogram
rmp	revolutions per minute
s	seconds
U	units
V	volts
v/v	volume per volume
w/v	weight per volume

Publications, presentations and awards

Bibby BAS, Reynolds JV, Maher SG. MicroRNA-330-5p as a putative modulator of neoadjuvant chemoradiotherapy sensitivity in oesophageal adenocarcinoma. *PLoS ONE* 2015 doi: 10.1371/journal.pone.0134180

Reid G, **Bibby BAS**, Moody HL, Maher SG. MicroRNA and Cancer *in* Epigenetic Cancer Therapy. Stephen Gray (Ed), *Elsevier*, July 2015

National Cancer Research Institute Conference, Liverpool UK, November 2015
Poster presentation, shortlisted for the BACR Gordon Hamilton-Fairley Young Investigator Award and awarded a BACR/CRUK student travel award

CRUK International Symposium on Oesophageal Cancer, Oxford UK, June 2015
Oral and poster presentation

International Postgraduate Medical Conference, Charles University Czech Republic, November 2014
Oral presentation, awarded 1st prize and ORPHEUS diploma

National Cancer Research Institute Conference, Liverpool UK, November 2013
Poster presentation and awarded the NCRI prize award bursary

Genetics Society Workshop, Milton Keynes UK, March 2013
Science communication workshop, funded 3 day workshop

Chapter 1 General Introduction

1.1 Oesophageal adenocarcinoma

1.1.1 Incidence rates

Oesophageal cancer is the eighth most common cancer worldwide (Ferlay et al., 2015). In 2012 there were approximately 400,000 oesophageal cancer deaths worldwide (Ferlay et al., 2015). The oesophageal cancer 5-year survival rate in Europe was 12.6% between 2005 and 2007 (Anderson et al., 2015). In 2015 the predicted mortality for oesophageal cancer in the EU is ~22,300 deaths, with the highest predicted mortality rate in the UK at 8.51 deaths per 100,000 men (Castro et al., 2014). In England and Wales between 1971 and 1998 the incidence of oesophageal cancer increased by 67% in men and 34% in women (Newnham et al., 2003). Furthermore, only 25% of patients diagnosed with oesophageal cancer between 1992 and 1994 were alive after 1 year and only ~5% of patients were alive after 5 years (Newnham et al., 2003). During the last decade the largest regional improvements in the 5 year survival rate where in the UK, Ireland and central Europe (Anderson et al., 2015). However, the prognosis for oesophageal cancer patients is poor across Europe where the 1 and 5 year relative survival rates are 36% and 11%, respectively (Anderson et al., 2015).

There are two distinct histological subtypes of oesophageal cancer; oesophageal adenocarcinoma (OAC) and oesophageal squamous cell carcinoma (OSC). OSC arises from the squamous cell epithelium in the upper and middle regions of the oesophagus. OAC arises from the columnar epithelium in glandular tissue of the lower oesophagus, proximal to the gastro-oesophageal junction. Globally OSC is the predominant subtype with ~398,000 cases in 2012 compared to ~52,000 cases of OAC (Arnold et al., 2015). However, the geographical distribution of OSC and OAC incidence does vary significantly across countries and continents and this reflects the distinct aetiological factors associated with the two subtypes. The highest OSC incidence rates are in South-

Eastern and Central Asia (Arnold et al., 2015). The highest OAC incidence rates are in Europe, North America and Oceania and the countries with the highest incidence rates in 2012 were the UK, Netherlands and Ireland (Fig 1.1) (Arnold et al., 2015).

OAC is considered to be an epidemic in the West and developed world (Edgren et al., 2013). The OAC incidence rate has rapidly increased since the 1980s, particularly in the UK and USA where the incidence of OAC has increased at a faster rate than any other malignancy (Botterweck et al., 2000; Edgren et al., 2013). Up until the 1970s OAC was considered a relatively rare form of oesophageal cancer compared to OSC. In the late-1970s the incidence of OSC was 6-fold greater than OAC in the USA (Pohl & Welch, 2005). Since then the incidence of OAC has risen at a phenomenal rate and by the mid-1990's the incidence rates for OSC and OAC were approximately equal (Pohl & Welch, 2005). In the USA, between 1975 and 2000, OSC incidence decreased 40% and during the same period OAC increased 500% (Pohl & Welch, 2005). By the late 1990's the incidence rates of OAC began to exceed those of OSC in some Northern European countries (Castro et al., 2014). Between 1980 and 2002 there was a steep increase in OAC incidence rates in Denmark, Netherlands, England and Scotland (Castro et al., 2014). In 2012 the incidence of OAC in Northern and Western Europe accounted for 22.8% of cases worldwide, compared to the incidence of OSC which accounted for 3.5% of cases worldwide (Arnold et al., 2015). Estimates suggest inflection points, at which OAC progressed to epidemic status, occurred around the 1960s and 1970s in the UK and USA, and as recently as early-1990s in Sweden (Edgren et al., 2013). Interestingly inflection points vary significantly even between bordering countries, such as Sweden and Finland and Sweden and Norway (Edgren et al., 2013).

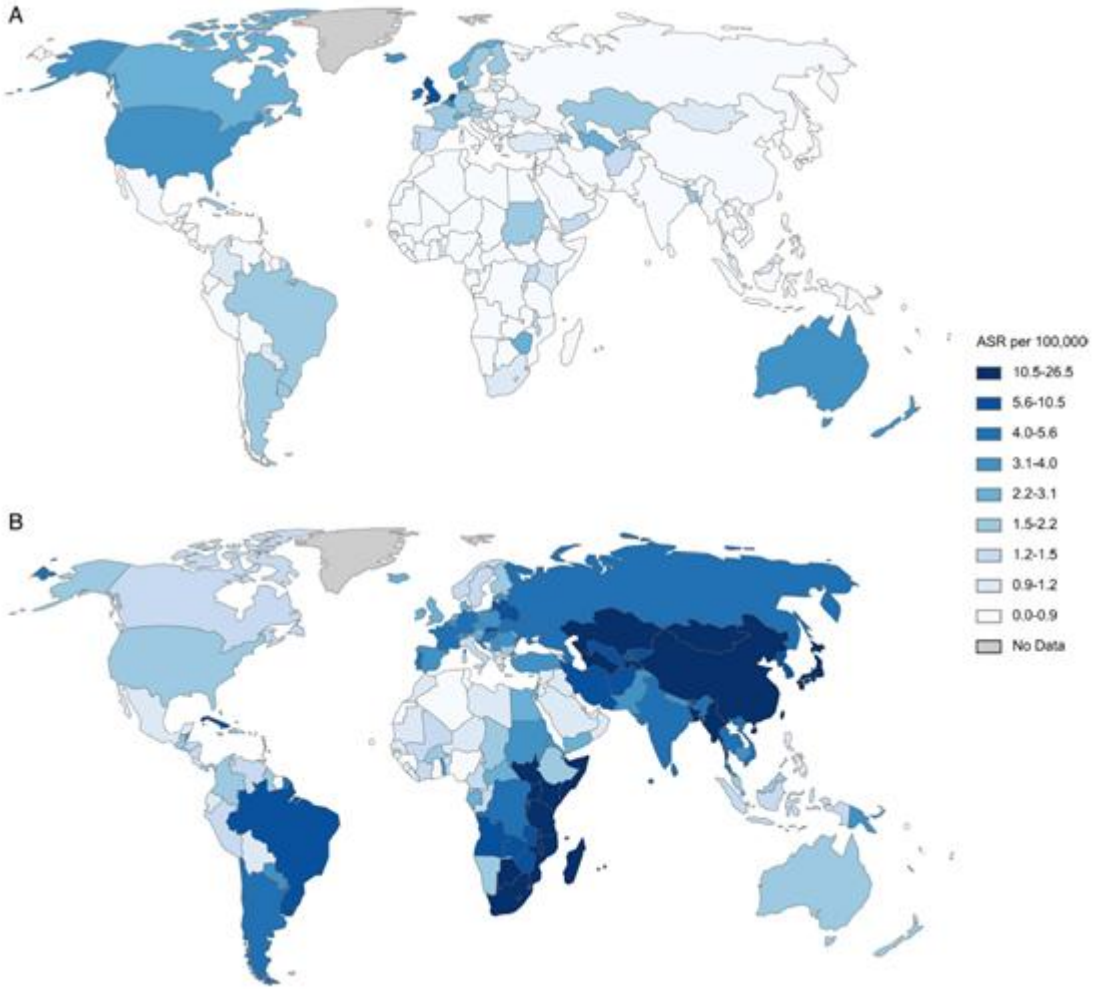

Fig 1.1 Global distribution and incidence rates of OAC and OSC. The age standardised incidence rate (ASR) of OAC (A) and OSC (B) per 100,000 men. The figure illustrates the distinct distribution of the oesophageal cancer subtypes worldwide. The highest incidence rates for OAC are in the UK, Netherlands and Ireland. The highest incidence rates for OSC are across Asia, a region commonly referred to as the oesophageal cancer belt. Incidence rates of OSC are also highest across East Africa. The epidemiology of OSC and OAC reflects their distinct aetiological factors and illustrates the significantly greater global burden of OSC relative to OAC. Figure adapted from (Arnold et al., 2015).

The rapid increase in OAC raised concerns regarding the diagnosis and classification of oesophageal cancers. In the USA a study investigating the changing trends in oesophageal cancer concluded that the rapid increase in OAC was representative of an increase in the disease.(Pohl & Welch, 2005). The rapid increase in OAC is accepted as a genuine representation of incidence, because factors such as improved diagnosis, over-diagnosis and reclassification cannot explain the rapid increase in the disease (Pohl & Welch, 2005; Pohl et al., 2010; Edgren et al., 2013). There is no definitive explanation as to why the incidence of OAC has risen to epidemic status in the West (Pohl et al., 2010; Edgren et al., 2013).

1.1.2 Aetiology and epidemiology

The greatest risk factor in the development of OAC is the chronic acid reflux disease Barrett's Oesophagus (BO) (Hvid-Jensen et al., 2011). BO is characterised by chronic tissue inflammation which causes a transition in the oesophagus from normal stratified squamous epithelium to single layered mucin-secreting columnar epithelium (Jankowski et al., 2000a). Tissue inflammation and a dysregulated immune response provide the ideal microenvironment for OAC development (Picardo et al., 2012). BO increases the risk of OAC by 30-125 fold and approximately 1.6-3% of the population have BO (Jankowski et al., 2000a; Gilbert et al., 2011). The development of OAC occurs in step-wise progression from no reflux disease to gastro oesophageal reflux disease (GORD) to BO to OAC (Theisen et al., 2003). Few patients (~10%) will progress from GORD to BO, of these only ~0.5% will progress from BO to OAC (Schneider & Corley, 2015). In the UK and the Netherlands the incidence of BO increased up until 2003, since then BO incidence rates have reached a plateau (Solaymani-Dodaran et al., 2004; Masclee et al., 2014). The onset of OAC in patient

with BO can occur 4-10 years after the initial BO diagnosis (Masclee et al., 2014; Arnold et al., 2015). The reported plateau in BO in the UK and the Netherlands may contribute towards a predicted decrease in the rate of OAC incidence in the next decade (Castro et al., 2014; Masclee et al., 2014).

Patients at high risk of developing OAC are difficult to identify because the majority of risk factors associated with the disease are common amongst the general population. Those at highest risk are Caucasian males over 60 years of age with existing gastro oesophageal reflux disease. Lifestyle factors associated with OAC risk are low intake of fruit and vegetables, high BMI and abdominal obesity (Pohl et al., 2013). There is a continued debate as to the contributions of smoking and alcohol consumption to OAC but generally these show a weak correlation with disease incidence (Pohl et al., 2013; Thrift et al., 2014). An explanation for the rapid increase in OAC incidence in Western population remains elusive, although it is broadly attributed to unhealthy lifestyle and poor diet which subsequently induce GORD. Obesity is an independent risk factor for OAC and is a significant health issue in the West, however obesity trends in the USA and UK do not match the trends in OAC incidence (Lagergren, 2011; Edgren et al., 2013). High intake of fruit, vegetables and fibre lower the risk of developing OAC and can provide a protective effect in patients considered to be at high risk of developing the disease (Kubo et al., 2010). The increase in OAC incidence correlates with a decrease in *Helicobacter pylori* infection in Western population (Khalifa et al., 2010). *Helicobacter pylori* lowers gastric acid secretion and reflux and is proposed to offer a protective effect against developing OAC (Fischbach et al., 2012). Different combinations of risk factors are associated with the step-wise progression of the disease (Pohl et al., 2013) (Table 1.1). Risk factors associated with the BO to OAC transition

Table 1.1 Aetiological factors associated with step-wise disease progression from GORD to OAC.

Disease Stage	Aetiological factors
Development of GORD	• Abdominal obesity • Hiatal hernia • Absent *H.pylori* infection
GORD to BO	• Male gender • Age • Duration of GORD • Hiatal hernia • Body mass index (BMI)
BO to OAC	• Male gender • White ethnicity • Smoking • Low fruit and vegetable dietary intake • Length of BO segment

include male gender, white ethnicity, smoking, unhealthy diet and a BO segment greater than 3 cm in length from the top of the gastric folds (Pohl et al., 2013). The treatment of GORD or BO with protein pump inhibitors and anti-inflammatory drugs may provide a protective effect against development of OAC (Liao et al., 2012; Masclee et al., 2015). BO is regarded as a clinically detectable precursor to OAC, although BO is regarded first and foremost as a defence mechanism in which an adaptive epithelium is developed to withstand the corrosive acid reflux in the lower oesophagus (Orlando, 2006). Understanding OAC development and progression from BO will ultimately provide patients with better outcomes. However there is concern that too much significance has been attached to BO in the progression of OAC, whilst other risk factors may have been under investigated or are yet to be identified (Rajendra, 2015).

The incidence of OAC is 3-9 times higher in men than in women, depending on geographical location (Arnold et al., 2015). To date there is insufficient evidence to explain the vast difference in gender risk. For females, breastfeeding may reduce OAC risk and female sex hormones may provide a protective effect against disease development (Cronin-Fenton et al., 2010). Male and female obesity rates are similar in the West, however visceral adipose tissue around the abdomen is more often observed in males (Chen et al., 2012). The altered levels of the cytokines leptin and adiponectin secreted by visceral adipose tissue have been shown to induce proliferation and inhibit apoptosis in OAC cells (Ogunwobi & Beales, 2008). In females, oestrogen modulates leptin sensitivity and favours subcutaneous body fat accrual as oppose to visceral abdominal fat deposition (Morita et al., 2006; Chen et al., 2012). Abdominal obesity also increases the mechanical intra-abdominal pressure on the oesophagus which may contribute to reflux disease and development of OAC.

The step-wise progression from GORD to BO to OAC over ~10 years should provide the opportunity for early diagnosis and prevention of OAC. However, disease progression is relatively asymptomatic and less than 5% of patients diagnosed with OAC have a precancerous diagnosis of BO (Corley et al., 2002).

1.1.3 Diagnosis and staging

Early diagnosis of OAC is essential to successful treatment and patient survival. For patients diagnosed at the earliest possible stage the 5 year survival rate is 90% (Visbal et al., 2001). Unfortunately patients are generally diagnosed at an advanced stage as the disease is relatively asymptomatic. Overall the prognosis for OAC patients is poor, with a 5-year survival rate of ~17% (Jankowski et al., 2000b). The step-wise progression of OAC occurs over several years which should enable early diagnosis or ideally, disease prevention. BO is regarded as a clinically detectable precursor to OAC. BO is monitored to detect the transition from metaplastic to dysplastic status, which is indicative of early stage neoplastic progression. Worldwide BO screening or surveillance is a common clinical practise which aims to monitor alterations in BO and detect early disease progression from BO to OAC. The surveillance programmes identify patients who are at risk of developing OAC or patients who are in the early stages of OAC (Bhat et al., 2015). These patients receive curative treatments and have far great survival rates than symptomatic patients presenting at the clinic. However the majority of BO patients will never progress to OAC, only ~1% of BO cases progress to OAC (Hvid-Jensen et al., 2011; Schneider & Corley, 2015). This is reflected in BO surveillance studies which generally report the risk of non-dysplastic BO progressing to OAC at a rate of 0.12-0.4% per year (Domper Arnal et al., 2015). This increases to ~1% risk of progression to OAC in patients with low grade BO dysplasia and ~5% for high

grade BO dysplasia (Domper Arnal et al., 2015). Despite the wide spread use of surveillance programmes worldwide the majority (80-93%) of patients diagnosed with OAC have not had a previous diagnosis of BO (Bhat et al., 2015). Furthermore, 40% of OAC patients have no prior history of heartburn or acid reflux (Spechler & Souza, 2014). Considering the majority of patients diagnosed with OAC have not previously been diagnosed with BO and annually <1% of patients under BO surveillance progress to OAC, the clinical and cost effectiveness of BO surveillance programmes is under scrutiny (Rajendra, 2015; Rubenstein & Thrift, 2015).

Selecting patients who should be enrolled in a BO surveillance programme is a major challenge because the risk factors associated with BO and OAC are common. In the USA, 20% of adults report GORD-like symptoms on a weekly basis (El-Serag, 2007). On average, 10% of GORD progresses to BO emphasising the need for stringent but sensitive surveillance programmes (Schneider & Corley, 2015). Numerous models for patient selection have been proposed, but it is not clear what the criteria should be for enrolling patients in surveillance programmes, or where the threshold of risk should be set (Spechler & Souza, 2014). The current screening and surveillance programmes are not reducing OAC mortality rates and in the UK OAC is predicted to increase 40% by 2020 (Steevens et al., 2010). The Barrett's Oesophagus Surveillance Study (BOSS) in the UK will assess the benefits of surveillance and aims to identify patients who would benefit from screening as well as the time intervals that should be implemented for clinical and cost effective outcomes (Old et al., 2015). The BOSS trial will be the first randomised controlled study in the assessment of BO surveillance.

Dysplastic BO is categorised as low or high grade (LGD/HGD). The next stages of disease progression from BO into OAC are intraepithelial carcinoma, intramucosal carcinoma (IMC) and invasive carcinoma (Coron et al., 2013). Patients with HGD or

IMC are eligible for endoscopic treatments which involve tissue resection or tissue ablation therapy (Blevins & Iyer, 2015). These treatments aim to prevent submucosal invasion and further disease progression by removal of the entire BO segment or ablation of the BO segment, whilst preserving the oesophagus. Endoscopic treatments are minimally invasive and potentially curative. In the UK there have been significant improvements in the clinical outcomes for patients treated with endoscopic therapies (Haidry et al., 2015).

Staging the patient's disease at diagnosis is critical in determining their treatment regimen. Multiple diagnostic modalities are used to stage OAC which is determined by tumour, node, metastasis (TNM staging) and histological grade (Table 1.2) (Rice et al., 2010). Endoscopy and histological analysis of tumour tissue biopsies are used for initial diagnosis. Endoscopic ultrasound (EUS), computed tomography (CT) and positron emission tomography (PET) are used to stage the disease following diagnosis. The multi-modal technologies are used to determine the depth of tumour invasion at the primary site and detect metastatic disease (Khanna & Gress, 2015). EUS is able to detect disruption of the layers in wall of the oesophagus tissue which correlates to local tumour invasion. EUS is used to determine T stage (tumour size) and has been shown to be the most accurate method for N staging (lymph nodes affected) (Foley et al., 2014b; Khanna & Gress, 2015). CT is used to assess the primary tumour and can detect lymph node metastasis, if the appearance of the node is enlarged (Khanna & Gress, 2015). CT is particularly useful for determine the location and size of tumours but is unable to accurately assess depth of invasion. PET with fludeoxyglucose (^{18}F-FDG) is used to detect tissues with high metabolic activity.

Table 1.2 TNM classification and staging for OAC.

T classification				
T*is*	High grade dysplasia			
T1	Tumour invades lamina propria, muscularis mucosa (T1a) or submucosa (T1b)			
T2	Tumour invades muscularis propria			
T3	Tumour invades adventitia			
T4	Tumour invades adjacent strictures; T4a resectable, T4b unresectable			
N classification				
N0	No regional lymph node metastasis			
N1	1 to 2 positive lymph node metastasis			
N2	3 to 6 positive lymph node metastasis			
N3	≥7 positive lymph node metastasis			
M classification				
M0	No distant metastasis			
M1	Distant metastasis			
Histological grade				
G1	Well differentiated			
G2	Moderately differentiated			
G3	Poorly differentiated			
G4	Undifferentiated			
Staging	**T**	**N**	**M**	**G**
0	*is*	0	0	1
IA	1	0	0	1-2
IB	1	0	0	3
	2	0	0	1-2
IIA	2	0	0	3
IIB	3	0	0	Any
	1-2	1	0	Any
IIIA	1-2	2	0	Any
	3	1	0	Any
	4a	0	0	Any
IIIB	3	2	0	Any
IIIC	4a	1-2	0	Any
	4b	Any	0	Any
	Any	N3	0	Any
IV	Any	Any	1	Any

Tumours have high metabolic activity and can be detected using PET. PET imaging is the most sensitivity method for detecting metastasis to lymph nodes or secondary sites and is used for M staging (Bunting et al., 2015). PET/CT examination are performed together to detect anatomical spatial distribution (CT) and metabolic activity (PET). These multiple diagnostic modalities are used in conjunction with one another to stage OAC at diagnosis.

Early tumours, graded T1a, are limited to the mucosa and these patients can receive curative endoscopic therapies (Khanna & Gress, 2015). Unfortunately patients are generally asymptomatic during the early stages of the disease and the majority of patients diagnosed with OAC have advanced disease. It is often the case that patients do not consult their GP until more serious symptoms arise, consequently ~75% of patients diagnosed with OAC have symptomatic dysphagia (Khanna & Gress, 2015). Tumours invading the submucosa (T1b-T4) have a 15-50% risk of lymph node metastasis and require more intensive treatments (Liu et al., 2005; Khanna & Gress, 2015). The standard of care for patient diagnosed with locally advanced or metastatic disease, is neo-adjuvant therapy followed by surgical resection (Coron, 2013).

1.1.4 Neoadjuvant therapies and surgery

At diagnosis 50% of OAC patients have locally advanced or metastatic disease (Khanna & Gress, 2015). The majority of oesophageal cancer patients do not receive curative treatment due to advanced disease, physical fitness and comorbidities. The standard treatment for patients with operable OAC is neoadjuvant therapy and surgical resection. The neoadjuvant therapies are utilised to treat metastatic disease and improve operability by down staging the primary tumour (Enzinger & Ilson, 2000).

In the UK the current standard of care for OAC patients is neoadjuvant chemotherapy, in response to the OE02 and MAGIC trials which reported a 6-13% increase in 2 year survival rate with neoadjuvant chemotherapy and surgery compared to surgery alone (Gwynne et al., 2013). Patients are mostly likely to receive a combination of two or three chemotherapeutics; cisplatin, carboplatin, oxaliplatin, fluorouracil (5-FU), capecitabine, paclitaxel or epirubicin (Gwynne et al., 2013). Conversely in Ireland, Netherlands and USA the standard of care is neoadjuvant chemoradiation therapy (neo-CRT) (Messager et al., 2015). The benefits of neoadjuvant chemotherapy compared to neo-CRT were assessed in a phase III study with 119 OAC patients, unfortunately, this study closed early and the data did not reach statistical significance (Stahl et al., 2009). However, more patients achieved a complete pathological response (pCR) with neo-CRT compared to patients treated with neoadjuvant chemotherapy, 15.6% and 2% respectively (Stahl et al., 2009). The neo-CRT patients also had improved 3 year survival rates (47.4%) compared to with neoadjuvant chemotherapy (27.7%). The CROSS trial reported neo-CRT and surgery significantly improved patient survival compared to surgery alone, median overall survival 49.4 months versus 24 months (van Heijl et al., 2008). Complete resection (R0) improves patient prognosis, 73% of patients with surgery alone had R0 compared to 92% with neo-CRT (Courrech Staal et al., 2010). In the UK the current NEOSCOPE trial is underway to select one of two neo-CRT regimens which will then be taken forward into a future trial to directly compare neo-CRT and neoadjuvant chemotherapy (Mukherjee et al., 2015). The two neo-CRT regimens under investigation are oxaliplatin-capecitabine chemoradiation or carboplatin-paclitaxel chemoradiation (Mukherjee et al., 2015).

Approximately 25% of patients have a pCR following neo-CRT and their 5 year survival rate significantly increases from ~17% to ~60% (Walsh et al., 1996; Geh et al.,

2006). However, 60-70% of OAC patients display little or no response to neoadjuvant therapies (Allum et al., 2009). Furthermore, for some patients the disease progresses during treatment and the delay to surgery worsens their prognosis (Kelsen, 2000; Cunningham et al., 2006). Significant clinical benefit would be gained if biomarkers indicative of patient response to treatment could be identified and applied in a pre-treatment setting. The likelihood of a patient responding to treatment could be predicted at the point of diagnosis and patients could be stratified to facilitate the administration of the most effective treatment regimens. Furthermore, monitoring patient response during neoadjuvant therapy could identify non-responders who would benefit from immediate salvage surgery. This approach could also identify those patients with a pCR, for whom definitive CRT without surgery could be an option. Predictive biomarkers of chemo and radioresistance could prevent unnecessary treatment and trauma for patients, improve patient survival rates and result in the delivery of cost effective treatments. Furthermore, understanding the tumour biology underlying resistance to CRT could aid the development of novel therapeutics which could enhance the efficacy of CRT. To achieve these aims, understanding the basis and fundamental biology of the tumour is the prerequisite to identifying the mechanisms of tumour resistance to CRT.

1.2 Tumour biology

1.2.1 Hallmarks of cancer

Cancer cells arise from normal cells which have acquired selective advantages and functional capabilities described as the hallmarks of cancer (Hanahan & Weinberg, 2011). The most significant factor in the transition of a normal cell to a cancer cells is genomic alterations. Germ line and somatic gene mutations, in combination with

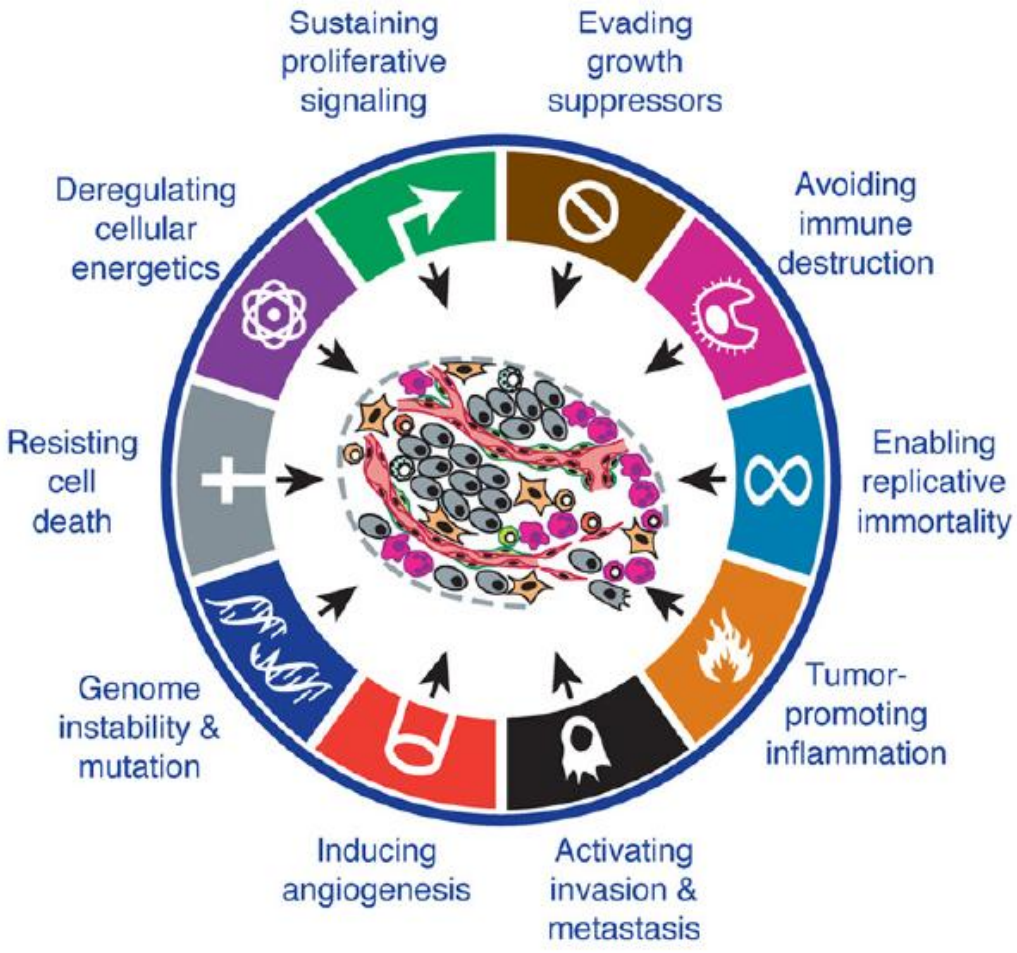

Fig 1.2 The hallmarks of cancer. There are eight hallmarks of cancer and two enabling characteristics (genome instability and tumour promoting inflammation). The hallmarks represent a simplified set of principles which underpin the complexity of cancer. During disease progression and tumorigenesis cancer cells acquire some or all of these features. The tumour microenvironment and the tumour stromal cells are as influential as the cancer cells in driving tumour growth and progression. Figure adapted from (Hanahan & Weinberg, 2011).

epigenetic regulation of gene expression, drive the normal to cancer cell transition. There are two enabling characteristics and eight functional capabilities that ultimately enable cancer cells to survive, proliferate and disseminate (Fig 1.2) (Hanahan & Weinberg, 2011). The dynamic and complex tumour microenvironment is comprised of the parenchyma and the stroma (Fig 1.3). The neoplastic cancer cells are the parenchyma, they initiate and drive tumour progression by recruiting normal cell types from the surrounding tissue (Hanahan & Weinberg, 2011). In addition to the cancer cells there are the cancer stem cells (CSCs). The CSCs have the capacity to self-renew and produce differentiated cell types (Cho & Clarke, 2008). The CSCs are more resistant to chemotherapy and radiotherapy, and are able to initiate tumour growth and disease recurrence after treatment (Ishii et al., 2008). The stromal compartment contains the tumour stromal cells and extracellular matrix. The endothelial cells, immune cells and fibroblasts are non-neoplastic cells recruited to the tumour microenvironment by the cancer cells, they are collectively known as the tumour associated stromal cells. The immune cells include mast cells, neutrophils, lymphocytes and macrophages which have pro- and anti-tumorigenic functions. The cancer associated fibroblasts produce and secrete components of the extracellular matrix including collagen and glycoproteins (Rasanen & Vaheri, 2010). The crosstalk between cancer cells and the tumour associated stromal cells, and the continuous remodelling of the extracellular matrix collectively promotes tumour growth and disease progression (Pietras & Ostman, 2010).

Sustained proliferative signalling

The proliferation of normal cells is tightly regulated to control cell growth and division. The ability of the cancer cell to overcome the tight regulations modulating cellular proliferation is the hallmark most often used to describe the fundamental

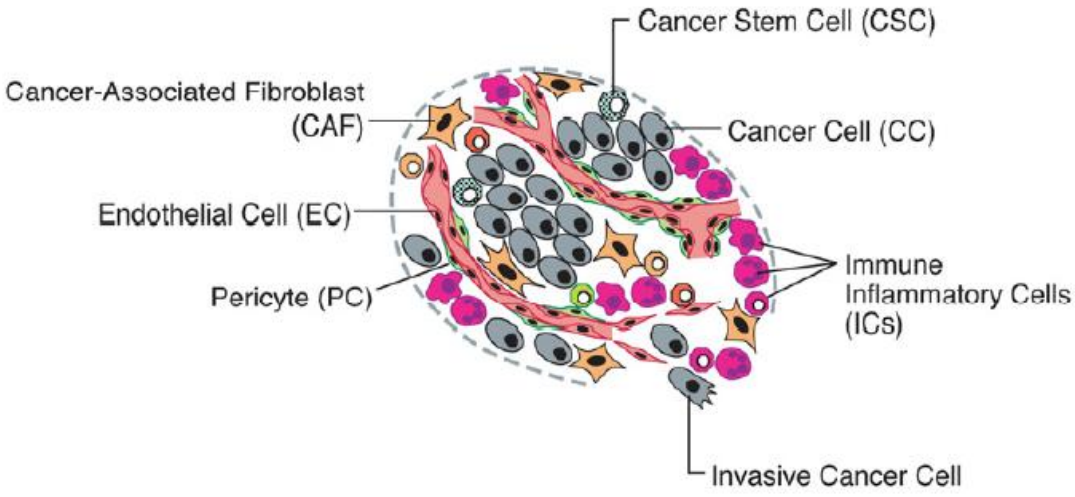

Fig 1.3 The tumour microenvironment. The solid tumour is composed of two compartments; the parenchyma and the stroma. The parenchyma is the neoplastic cancers cells and CSCs. The stroma is comprised of the non-neoplastic tumour stromal cells and the structural extracellular matrix. The cancer cells and CSCs are the initiators and drivers of tumorigenesis. The cancer cells recruit non-neoplastic cell types from the surrounding tissues to support tumour growth and progression, these non-neoplastic cells are known as the tumour stromal cells. The endothelial cells are the building blocks of the tumour associated vasculature and are accompanied by the structural supporting pericytes. The cancer associated fibroblast produce the structural components that form the extracellular matrix which is the structural scaffold of the tumour tissue. The immune cells have both tumour promoting and tumour suppressive functions. Inflammation produces a milieu of extracellular signalling factors which have pro-tumorigenic and anti-tumorigenic effects. Each element of the tumour microenvironment contributes to cancer cell invasion and metastasis. Dissemination of cancer cells from the primary tumour follows the epithelial-to-mesenchymal transition in the cancer cells, and their subsequent infiltration of the systemic vasculature or lymphatic system. Figure adapted from (Hanahan & Weinberg, 2011).

difference between the normal cell and the cancer cell. In the cancer cell the normal pathways governing growth and division are dysregulated. Cancer cells can become hyper-responsive to proliferation signals, by increasing the expression of growth factor receptors on the cell surface and upregulating the production of growth factors to stimulate autocrine proliferation (Witsch et al., 2010). Cancer cells can also stimulate the tumour associated stromal cells which reciprocate by supplying more growth factors (Cheng et al., 2008). Alternatively, the cancer cell can uncouple growth receptor stimulation from the proliferation signalling pathways induced by extracellular growth factors, thus enabling growth factor independent proliferation (Witsch et al., 2010). Sustained proliferation expands into other hallmarks including evasion of growth suppressors, resisting cell death and enabling replicative immortality.

Evasion of growth suppressors

To enable sustained proliferation cancer cells do not only enhance growth factor mediated signalling pathways but also repress anti-proliferative growth suppressing signalling, via the negative regulation of tumour suppressors such as the retinoblastoma protein (RB) and tumour protein 53 (TP53). The RB and TP53 proteins are signalling hubs and instrumental mediators of proliferation, apoptosis and senescence (Hanahan & Weinberg, 2011). The anti-proliferative functions of TGFβ are redirected to promote epithelial to mesenchymal transition (EMT) which induces another hallmark; invasion and metastasis (Ikushima & Miyazono, 2010). Furthermore, the proliferating cancer cells abolish contact inhibition which ordinarily suppresses cellular proliferation (Curto et al., 2007).

Resisting cell death

Apoptosis is a mechanism of programmed cell death which removes abnormal and potentially neoplastic cells to conserve the normal homeostasis of the tissue. Normal cells which are damaged or have acquired a mutational change that may provide a survival advantage at the expense tissue homeostasis are removed in an act of self sacrifice. Apoptosis can be induced by intrinsic or extrinsic signalling pathways and involves multiple proteins which are pro-apoptotic or anti-apoptotic (Adams & Cory, 2007). Cancer cells upregulate anti-apoptotic proteins and survival signalling pathways to evade apoptosis. The *TP53* gene encodes the tumour suppressor and 'guardian of the genome' protein p53 (Lane, 1992). The p53 protein has multiple functions and can induce apoptosis (Junttila & Evan, 2009). Hence the loss of p53, which is a frequent and early event in cancer progression, promotes evasion of apoptosis. To resist the induction of apoptosis by extrinsic ligands, the cancer cell can uncouple the downstream signalling pathways from the cell surface death receptor (Hanahan & Weinberg, 2011).

Enabling replicative immortality

Normal cells undertake a limited number of growth and division cycles before undergoing apoptosis. To proliferate the cell must completely duplicate its DNA and with each cycle of growth and division the risk of incurring a mutation increases. The number of divisions a cell can undertake is in part controlled by the telomeres (Blasco, 2005). The telomeres are multiple tandem hexanucletoide repeats which protect the ends of the chromosomes from end to end fusion (Blasco, 2005). With each division the telomeres gradually shorten until the protective telomere is eroded and the cell becomes senescent. The transition into the senescent state is irreversible, senescent cells are viable non-proliferating cells which subsequently undergo crisis apoptosis. To overcome this mechanism of limited growth and division the cancer cells overexpress

telomerase (Blasco, 2005). Telomerase is a specialised DNA polymerase which effectively maintains the telomeres between cycles of division. Telomerase adds more repeat segments to the ends of the DNA to prevent the telomeres eroding, thus the cancer cell avoids senescence and it is able to replicate indefinitely.

Inducing angiogenesis

The proliferating cancer cells require a blood supply for the delivery of oxygen and nutrients and removal of waste and carbon dioxide. The endothelial cells which form the vessels of the systemic vasculature are generally quiescent cells. The cancer cells orchestrate the 'angiogenic switch' which induces sprouting of vessels from the existing vasculature (Hanahan & Folkman, 1996). The tumour vasculature supply is essential for sustaining tumour growth, and provides the opportunity for cancer cells to metastasis away from the site of the primary tumour. Angiogenesis is modulated by pro-angiogenic and anti-angiogenic factors (Hanahan & Weinberg, 2011). The milieu of pro-angiogenic and anti-angiogenic factors induces the sprouting of imperfect vessels which are enlarged, distorted and leaky (Nagy et al., 2010). The VEGFA gene encodes pro-angiogenic ligands and the expression of VEGFA is frequently upregulated by hypoxia and oncogenic signalling (Ferrara, 2009).

Activating invasion and metastasis

As tumour growth increases and a vasculature supply is acquired, the cancer cells undergo an epithelial-to-mesenchymal transition (EMT) (Klymkowsky & Savagner, 2009). Interactions between the cancer cells, stromal tumour cells and the dysregulated intracellular signalling pathways induces the EMT phenotype (Jones & Thompson, 2009). Loss of the cell-cell adhesion molecule E-cadherin and the loss of cell matrix attachment proteins are associated with migration and the EMT (Hanahan & Weinberg, 2011). Crosstalk between cancer cells and the stromal tumour cells promotes

infiltration of immune cells, including macrophages which produce matrix metalloproteinases (MMPs) and cathepsin proteases which degrade components of the extracellular matrix and enhance local tumour invasion (Qian & Pollard, 2010). The dissemination of cancer cells from the primary tumour to secondary sites occurs in a stepwise progression (Nagy et al., 2010). The cancer cells enter the blood vessels by intravasation and are transported in the vasculature and lymphatic networks to distant tissues. The cancer cells escape from the vessels by extravasation and proliferate to form micrometastasis which can further progress to macroscopic tumours. For cancer cells to colonise the new tissue microenvironment they must adapt to the new site and the cancer cells do not always achieve this hence, not all micrometastasis progress to macroscopic tumours (McGowan et al., 2009).

Reprogrammed energy metabolism

To meet the high energy demand imposed by uncontrolled proliferation, the cancer cells reprogramme their energy metabolism pathways (Hanahan & Weinberg, 2011). In a normal oxygenated cell, energy in the form of ATP is produced by aerobic oxidative phosphorylation in the mitochondria. The cell imports glucose and glycolysis converts a single glucose molecule into two pyruvate molecules, simultaneously producing two ATP molecules. This first step of glucose metabolism does not require oxygen. The pyruvate molecules are oxidised to carbons dioxide by oxidative phosphorylation, which produces 26 ATP molecules. The cancer cells within a solid tumour are starved of oxygen under hypoxic conditions. To produce energy under anaerobic conditions the cell relies on glycolysis to produce ATP. However, cancer cells undergo a ‘metabolic switch’ and prefer to produce ATP energy by glycolysis under aerobic conditions, despite glycolysis producing ~18 fold less energy than oxidative phosphorylation. This is known as the Warburg effect and to date there is no definitive

explanation as to why the cancer cell prefers glycolytic metabolism (Warburg et al., 1927). To facilitate increased uptake of glucose for energy metabolism, the cancer cell upregulates the glucose transporter GLUT1 (DeBerardinis et al., 2008). Under hypoxic conditions the cancer cell also upregulates the expression of GLUT1 and glycolytic enzymes (Semenza, 2010). The pyruvate produced by glycolysis can subsequently be metabolised to lactate, this is achieved under anaerobic conditions. Lactate can be secreted as a waste product and imported into oxygenated cells which can metabolise the lactate to produce ATP (Semenza, 2008). The symbiosis between lactate secreting and lactate utilising cells enable the cells to maintain energy metabolism with fluctuating oxygen availability.

Evasion of immune destruction

Immune surveillance can identify and eliminate incipient cancer cells providing a barrier against tumour initiation and development. In particular, $CD8^+$ cytotoxic T lymphocytes (CTLs), $CD4^+$ T_h1 helper T cells and natural killer (NK) cells contribute to immune surveillance and eradication of cancer cells (Hanahan & Weinberg, 2011). Therefore cancer cells must avoid detection by the immune response to initiate tumour growth and progression. To evade immune destruction cancer cells secrete immunosuppressive factors such as TGFβ which paralyse CTLs and NK cells, the cancer cell also recruits immunosuppressor cell such as Tregs which dampen the immune response (Kim et al., 2007).

In addition to the eight hallmarks there are two enabling characteristics which facilitate the acquisition of the cancer hallmarks. These are genome instability and tumour-promoting inflammation. Genetic alterations provide cancer cells with mutant phenotypes which can offer a selective advantage. Genomic instability enables cancer cells to acquire the hallmarks and dominate the local tissue microenvironment. The

stepwise progression of tumour initiation and growth can be considered as a succession of clonal expansions (Greaves & Maley, 2012). The idea of tumour development progressing through a series of clonal expansions has recently been challenged by the big bang model (Sottoriva et al., 2015). The clonal expansion model is based on a sequence of advantageous mutations which occur over time. The clones which arise during tumour progression compete against one another and later clones can out compete earlier clones (Greaves & Maley, 2012). Conversely, the big bang model suggests that after the initial transformation of normal cells to cancer cells the tumour develops from a number of clones which are present from the start (Sottoriva et al., 2015). This model suggests that all of the important gene mutations are acquired at the start, during the transformation of the normal cell to the cancer cell and this is subsequently followed by a 'big bang' of sudden tumour growth. In essence these cells were 'born to be bad' from the point of transformation. In the big bang model there are no selection pressures and the clones do not compete during tumour progression.

The second enabling characteristic is tumour promoting inflammation. The immune response can destroy cancer cells and eradicate tumours however, the inflammatory response also has a paradoxical effect in promoting tumour development and the acquisition of cancer hallmarks (DeNardo et al., 2010). Inflammation contributes growth factors, survival factors, proangiogenic factors and extracellular matrix modifying proteases which facilitate EMT, angiogenesis, invasion and metastasis (Hanahan & Weinberg, 2000).

Cancer cells within the tumour microenvironment drive tumour growth and progression. Furthermore, the cancer cells and tumour microenvironment dictate tumour sensitivity to chemo and radiotherapy. Cancer cells employ a variety of mechanisms to

resist and survive the cytotoxic effects of chemo and radiotherapy and these resistance mechanisms are supported by the hallmarks of cancer.

1.2.2 Tumour resistance to CRT

The vast majority of cancer patients will receive chemotherapy or radiotherapy as curative treatments or during palliative care. Chemotherapeutic drugs and radiation therapy primarily induce DNA damage which ultimately induces cell death. In normal cells, proliferation and cell cycle progression are strictly regulated. The hallmark most commonly associated with cancer cells is their ability to overcome the strict regulatory mechanisms associated with proliferation. The uncontrolled and rapid proliferation of cancer cells is exploited by chemo and radiotherapy. To enhance the efficacy of chemo and radiotherapy these treatments are fractionated and administered over a period of time to ensure sufficient levels of DNA damage, and subsequently cell death, are induced in the cancer cell population.

Chemotherapy and radiotherapy: mechanisms of action

Chemotherapeutics are chemical substances which are cytotoxic to proliferating cells. There are various chemotherapeutic drugs currently used in the clinic, these drugs are categorised by their cytotoxic mechanism and include alkylating agents, anti-metabolites, anti-microtubule agents, topoisomerase inhibitors and cytotoxic antibiotics.

The alkylating agents cisplatin, carboplatin and oxaliplatin are platinum based chemotherapeutics which intercalate with DNA through covalent bonding. The alkylating agents form intrastrand and interstrand crosslinks with the DNA (Eastman, 1987). These DNA adducts disrupt DNA replication and transcription which subsequently induces cell death. The alkylating agents are cell cycle independent, they

can access and bind to the DNA during all stages of the cell cycle (Malhotra & Perry, 2003).

Capecitabine and 5-FU are anti-pyrimidine metabolites which are incorporated into DNA and RNA. 5-FU is administered to patients intravenously. Capecitabine is administered orally as a prodrug which is metabolised in the liver to produce 5-FU. Within the cell 5-FU is converted into one of three metabolites (Wohlhueter et al., 1980). Fluorouridine triphosphate is incorporated into RNA as a uracil substitute. Flurodeoxyuridine is misincorporated into the DNA and binds to the thymidine synthase enzyme (Longley et al., 2003). The thymidine synthase enzyme is the only source of *de novo* thymine base production in the cell, inhibition of thymine synthase inhibits DNA synthesis (Parker, 2009). The cytotoxic effects of 5-FU are S phase cell cycle dependent. The metabolites of 5-FU interfere with RNA function, induce DNA damage and interfere with DNA replication and transcription to induce cell death.

Paclitaxel is an anti-microtubule taxane agent which stabilises microtubules and inhibit microtubule disassembly. Microtubules are essential structural components in the cytoskeleton and are associated with multiple cellular processes. During cell division microtubules form the mitotic spindle, paclitaxel inhibits normal microtubule function and induces mitotic catastrophe and cell death during G_2/M phase of the cell cycle (Malhotra & Perry, 2003).

Epirubicin is an anthracycline and topoisomerase inhibitor. The topoisomerase II enzyme relieves supercoiled DNA during replication by inducing temporary dsDNA breaks which are immediately repaired. Epirubicin inhibits topoisomerase II and interferes with DNA replication during S phase of the cell cycle (Nitiss, 2009).

Radiotherapy therapy is the targeted administration of X-rays to destroy cancer cells and tumour tissue. The X-rays penetrate the tumour tissues inducing cytotoxic

damage in proliferating cells. Radiotherapy X-rays are targeted to the site of the tumour to minimise off target effects on the normal healthy tissue. Radiation mediated cell death is induced by direct and indirect damage effects. Radiation directly induces single and double strand breaks in the DNA. In addition, radiation induces reactive oxygen species (ROS) and free radicals which induce DNA damage, cell stress and indirectly alter cellular signalling pathways. The accumulation of radiation mediated DNA breakages and ROS damage ultimately induce cell death.

Chemotherapy and radiotherapy are the foundations of cancer therapy in the clinic today. Patients generally receive a combination of two or three chemotherapeutics, with or without radiotherapy, administered in fractionated doses. Resistance to chemo and radiotherapy is a significant challenge in the treatment of cancer. Combination therapies aim to overcome resistance by challenging the tumour with a variety of cytotoxic mechanisms to overwhelm the repair and survival pathways, exceed the sublethal threshold of cellular damage and induce cell death (Wahl & Lawrence, 2015). Cancer cell resistance to the cytotoxicity of chemo and radiotherapy can be inherent or acquired. Evasion of apoptosis and resisting cell death in favour of survival are inherent mechanisms of resistance (Stegeman et al., 2014). Alternatively, cancer cells can respond and adapt to evolve acquired mechanisms of resistance such as enhanced DNA repair or drug efflux. In addition to cancer cells, the tumour microenvironment plays a critical role in mediating sensitivity and resistance to chemo and radiotherapy (Castells et al., 2012).

DNA repair

The DNA repair pathways enable cells to reverse or undo DNA damage. In the cancer cell these pathways are essential to repairing the dsDNA breaks, ssDNA breaks, DNA crosslinking and DNA base modifications induced by chemo and radiotherapy

(Longley & Johnston, 2005). The major DNA repair pathways in the cell are direct repair (DR), base excision repair (BER), nucleotide excision repair (NER), mismatch repair (MMR), homologous recombination (HR) and non-homologous end-joining (NHEJ).

The DR pathway is mediated by the alkylguanine DNA alkytransferase protein (AGT) (Gerson, 2004). Alkyl and methyl DNA adducts, such as those formed by the platinum chemotherapeutics, are quickly and efficiently repaired by AGT. The AGT protein transfers DNA adducts from the DNA bases onto the cysteine residue within its active site (D'Incalci et al., 1988). The BER pathway recognises and removes DNA bases damaged by alkylation, oxidation or radiation (Chan et al., 2006). The damaged base is excised and the site is subsequently repaired by polymerases and ligase III. The NER pathway recognises and repairs bulky DNA lesion formed by the alkylating chemotherapeutic agents which intercalate with the DNA (Hanawalt, 2002). These bulky DNA lesions distort the DNA and disrupt DNA replication and transcription if they are not removed by NER machinery. The MMR pathway recognises and repairs incorrect base pairings. Deficient MMR enhances resistance to some chemotherapeutics including cisplatin and topoisomerase II inhibitors, because MMR normally recognises DNA adducts and induces apoptosis (Longley & Johnston, 2005). The HR and NHEJ are responsible for the repair of dsDNA breaks which are considered to be the most cytotoxic form of DNA damage (Scott & Pandita, 2006). The dsDNA breaks are induced by radiation, free radicals and chemotherapeutics. In addition, the ssDNA breaks which are encountered during replication can cause the collapse of the replication fork and dsDNA breaks (Strumberg et al., 2000). The immediate responders to dsDNA breaks are the ataxia telangiectasia mutated kinase (ATM) and the ATM Rad3 related kinase (ATR). The ATM and ATR kinases subsequently phosphorylate multiple proteins which coordinate the cell cycle, DNA repair and apoptosis (Bassing &

Alt, 2004). The HR pathway repairs dsDNA breaks with high fidelity during the S/G_2 phase, by using the homologous sequence on the sister chromatid as a template to repair the break and restore the original DNA sequence (Johnson & Jasin, 2001). Conversely, NHEJ repairs dsDNA break during G_0/G_1 by aligning and ligating the broken ends of the DNA without restoring the original sequence (Cahill et al., 2006). This can induce further genomic instability, mutations and deletions. Chemotherapeutics and radiation therapy need to induce sufficient DNA damaging to exceed the sublethal threshold, beyond which the cancer cell cannot sufficiently repair the damage or continue to survive.

Cell cycle distribution and evasion of apoptosis

The uncontrolled proliferation of cancer cells is exploited by chemotherapeutics and radiation, which induce DNA damage and cell death in rapidly proliferating cells whilst most normal cells are spared. However, the ability of cancer cells to resist cell death is a critical factor in chemo and radioresistance. To avoid apoptosis and mitotic catastrophe, in response to DNA damage, cancer cells can induce cell cycle arrest and transition to G_0/G_1 phase (Ye et al., 2013). The transition from G_1 to S phase commits the cell to completion of the cell cycle and cell division. However, there is evidence to suggest that in response to radiation induced DNA damage, cancer cells can arrest in G_2 phase and G_2 slippage can subsequently bypass mitosis (Ye et al., 2013). The tetraploid cancer cells then enter a quiescent or senescent state (Ye et al., 2013). In a normal cell senescence is irreversible and the cell will not re-enter the cell cycle, in comparison quiescence is a dormant non-proliferative state which is reversible. In cancer cells senescence can be reversed and the cell can potentially re-enter the cell cycle and continue proliferating (Wu et al., 2012).

The concept of cell cycle mediated drug resistance is defined as cellular insensitivity to chemotherapeutics or radiation, due to the position of the cells in the cell cycle at the time of treatment (Shah & Schwartz, 2001). Radiation and paclitaxel primarily induce mitotic catastrophe by DNA damage and microtubule stabilising, respectively. Hence the cytotoxicity of radiation and paclitaxel peak during the G_2/M phase of the cell cycle (Donaldson et al., 1994; Pawlik & Keyomarsi, 2004). In comparison, 5-FU is only cytotoxic to cells during S phase of the cell cycle. Whereas cisplatin DNA adduct formation is cell cycle independent but is most cytotoxic in the late stages of G_1 immediately prior to S phase (Stewart, 2007). Combination therapies aim to enhance cytotoxicity and induction of apoptosis through additive or synergistic effects. The sequencing and scheduling of multiple therapies should take into consideration the phase of the cell cycle in which each therapeutic is most effective. The administration of cisplatin followed by paclitaxel has antagonistic effects, because cisplatin induces G_2 arrest which subsequently reduces sensitivity to paclitaxel, which is most effective during mitosis (Zaffaroni et al., 1998). Conversely, paclitaxel administration prior to cisplatin has synergetic effects. The paclitaxel increases cisplatin uptake, inhibits the repair of cisplatin DNA damage and may synchronise cycling cells, thereby promoting accumulation of cells in the G_1 phase where cisplatin exerts peak cytotoxicity (Donaldson et al., 1994).

Drug influx and efflux

Decreased influx and increased efflux of chemotherapeutic drugs restricts cellular accumulation and subsequently limits the cytotoxic effects of the drugs in the cancer cell. The influx and efflux of drugs is modulated in part by plasma membrane transporters, such as the influx copper transporter CTR1 and the multidrug resistant efflux transporters (Borst et al., 2000; Ishida et al., 2002). In addition to the

accumulation of the drugs within the cell, the localisation of the drugs at the site of action is also critical to exceed the sublethal threshold of cytotoxicity. The alkylating chemotherapeutic drugs exert their cytotoxic effects in the nucleus. The localisation of platinum chemotherapeutics in the cytoplasm sequesters the drug from the nucleus and promotes resistance (Siddik, 2003). Intracellular pH can also alter cellular sensitivity to chemotherapeutics, such as cisplatin, which is inactivated by high intracellular pH (Chau & Stewart, 1999).

Glutathione detoxification, metabolism and mitochondria

The DNA damage induced by chemotherapeutics or ROS can be limited by restricting their accessibility to the nucleus. Glutathione (GSH) is an antioxidant frequently upregulated in the cancer cell. GSH detoxification neutralises the DNA damaging molecules produced by chemotherapeutics and radiation (Stewart, 2007). Furthermore, the glycolytic metabolism of the cancer cell alters the redox state of the cell in favour of scavenging and neutralising ROS (Good & Harrington, 2013). The mitochondria are the energy hub of the cell and are critical mediators of apoptosis. Dysregulated mitochondrial metabolism and function are associated with evasion of apoptosis and resistance to chemo and radiotherapy (Aichler et al., 2013; Guaragnella et al., 2014; Lynam-Lennon et al., 2014).

Cancer stem cells

The relapse, recurrence and dissemination of tumour growth after initial tumour regression following chemo or radiotherapy is attributed to the cancer stem cells (CSCs) (Ishii et al., 2008). The CSC is an undifferentiated, self renewing cell which can produce differentiated daughter cells. CSCs constitute a small proportion of cells in the tumour, which are more resistant to CRT. The CSCs maintain a non-proliferative state in G_0 of the cell cycle, hence CSCs are less susceptible to the DNA damaging effects of

chemo and radiotherapy (Ishii et al., 2008). Furthermore, CSCs have a more efficient drug efflux mechanism which enhances resistance to CRT (Zhou et al., 2001). Following treatment the dormant CSCs can re-enter the cell cycle, proliferate and thus repopulate the tumour. Chemo and radiotherapy can also induce CSC transformation into an invasive cell type, which can disseminate and establish tumour growth at distant sites (Ishii et al., 2008).

Tumour microenvironment

In the tumour microenvironment the tumour vasculature is an essential delivery vehicle for chemotherapeutic drugs and the supply of oxygen in the tumour vasculature which is essential for the formation of ROS during radiation therapy. The leaky and disorganised structure of the tumour vasculature causes fluctuations in oxygen availability, ranging from normoxia to anoxia (Hardee et al., 2009). The absence of oxygen in the tumour tissue impedes the generation of ROS and the expression of hypoxia inducible factor (HIF1α) enhances radioresistance (Fu et al., 2015). The endothelial cells of the tumour vasculature are in turn damaged and destroyed by radiation which can subsequently induce hypoxia as well as pro-vasculogenic stimuli (Lerman et al., 2010; Barker et al., 2015). Furthermore, radiation induced endothelial cell death promotes a pro-survival immune response in the tumour (Kozin et al., 2010). Cellular stress induced by ROS can stimulate an immune response through the generation of damage associated molecular patterns (DAMPs) which are exposed on the cell surface or secreted into the extracellular environment (Schaue & McBride, 2010). The DAMPs are recognised by the pattern recognition receptors (PRRs) which include Toll-like receptors (TLRs) and RIG-1-like receptors (Takeuchi & Akira, 2010). The DAMP-PRR mediated damage response can induce immunogenic cell death in response to tissue damaged caused by chemo and radiotherapy (Apetoh et al., 2007).

In addition to the cancer cells, the contributions of the CSC population, the tumour vasculature, hypoxia and immune response are also critical factors and mediators of chemo and radio resistance. Understanding the resistance mechanisms exploited by the tumour to evade cell death in response to chemo and radiotherapy will enable the development of novel therapeutics, which could enhance tumour sensitivity to therapy. For the vast majority of cancer patients, improving the efficacy of chemo and radiotherapy with the addition of targeted therapies would improve response and overall survival. For the 70% of OAC patients who do not respond to neo-CRT, enhancing tumour sensitivity and the efficacy of CRT would have a significant clinical benefit.

1.2.3 Strategies to enhance tumour sensitivity to CRT

The vast majority of cancer patients treated with curative intent will receive chemotherapy and/or radiotherapy therefore, improving patient response and the efficacy of CRT would be beneficial to the majority of cancer patients (Delaney et al., 2005). Targeted therapies which act as chemosensitisers and/or radiosensitisers have the potential to enhance tumour sensitivity, treatment efficacy and improve patient outcomes.

Chemotherapy and radiotherapy primarily induce DNA damage which subsequently initiates apoptosis and cell death. Defective DNA damage repair mechanisms and evasion of apoptosis enables cancer cells to survive the cytotoxic insult of chemo and radiotherapy (Shabbits et al., 2003; Helleday et al., 2008). In comparison to normal cells, the cancer cells have defective DNA damage repair pathways which may be upregulated or downregulated (Helleday et al., 2008). Targeting the abnormal DNA repair pathways utilised by cancer cells should selectively enhance the sensitivity of the cancer cells to CRT (Bolderson et al., 2009). Therefore, manipulating the DNA

damage response and signal transduction pathways with targeted therapies in addition to chemo and/or radiotherapy could enhance tumour sensitivity and patient response to CRT. Inhibiting DNA repair in cancer cells could effectively increase DNA damage and promote apoptosis. In response to DNA DSBs the protein kinase ATM induces cell cycle arrest and phosphorylates downstream DNA repair proteins thus facilitating DNA repair (Begg et al., 2011). The DNA-dependent protein kinase (DNA-PK) is a component of the NHEJ repair pathway which facilities the repair of DSBs (Begg et al., 2011). Inhibiting ATM and DNA-PK using small molecule inhibitors has been shown to enhance radiosensitivity *in vitro* and *in vivo* (Veuger et al., 2003; Hickson et al., 2004). The inhibition of DNA repair in combination with continued progression through the cell cycle and DNA replication further aggravates the levels of DNA damage (Shah & Schwartz, 2001). Poly ADP-ribose polymerase (PARP) facilitates BER and the repair of DNA SSBs (Begg et al., 2011). The unrepaired SSBs and abasic sites can stall the DNA replication fork and subsequently induce lethal DSBs. Small molecule inhibitors of PARP-1 have been shown to enhance radiosensitivity and have entered clinical trials as potential radiosensisting agents (Albert et al., 2007).

Tumour sensitivity to CRT could also be enhanced by targeting the signal transduction pathways which promote cell survival in response to cytotoxic insult. The PI3K-Akt, NF-κB and MAPK signalling pathways inhibit apoptosis in response to DNA damage (Begg et al., 2011). These signalling cascades involve multiple proteins which are potential therapeutic targets. One such example is the epidermal growth factor receptor (EGFR) which activates the PI3K-Akt signalling pathway thus promoting cell survival in response to CRT (Toulany et al., 2006). The anti-EGFR antibody cetuxiamb specifically blocks EGFR and inhibits downstream activation of the PI3K-AKT pathway (Begg et al., 2011). Cetuximab and radiotherapy significant increased locoregional control and overall patient survival in a head and neck cancer phase III

clinical trial (Bonner et al., 2010). In addition to cetuximab, receptor tyrosine kinase EGFR inhibitors also enhanced radiosensitivity (Feng et al., 2007). However the mechanisms by which the PI3K-Akt, NF-κB and MAPK signalling pathways mediate tumour response to CRT are not fully understood. In addition, the breadth and complexity of these signalling cascades suggests targeting individual components of these pathways may not necessarily have a substantial impact on tumour sensitivity to CRT.

The tumour microenvironment is also instrumental in dictating tumour response and sensitivity to CRT and hypoxia is an attractive target for enhancing tumour sensitivity to CRT (Karar & Maity, 2009). Hypoxic cells are often non-diving cells hence they are less susceptible to the cytotoxic damage of CRT furthermore, radiation induced DNA damage and generation of free radicals is oxygen dependent (Wouters & Brown, 1997; Tredan et al., 2007). Restoring or enhancing tumour oxygenation during or prior to radiotherapy could enhance tumour sensitivity to CRT. Inhaling carbogen (95% oxygen and 5% carbon dioxide) prior to and during radiotherapy has been shown to enhance blood oxygen tension, reduce tumour hypoxia and enhance tumour sensitivity to radiotherapy in multiple cancer types (Kaanders et al., 2002). In addition to carbogen the oxygen mimicking drugs nimorazole and nicotinamide have been demonstrated to enhance the efficacy of radiotherapy in head and neck cancer patients (Kjellen et al., 1991). An alternative approach to targeting tumour hypoxia is the development of therapeutics which selectively kill hypoxic cells. For example the drug tirapazamine is converted into DNA damaging radicals in the absence of oxygen, drugs such as these are not radiosensitisers but administered in conjunction with radiotherapy have the potential to enhance treatment efficacy (Rischin et al., 2010).

Tumour resistance to chemotherapy and radiotherapy is mediate by a combination of mechanisms, including cellular response to cytotoxic insult and the pre-existing tumour microenvironment. To enhance tumour sensitivity to CRT it is necessary to understand the mechanisms of resistance in individual patient tumours to aid selection of the most effective drugs (Begg et al., 2011). Simultaneously targeting multiple mechanisms of tumour resistance to CRT would presumably be far more effective than targeting a single mechanism or a single protein. Therefore, a relatively new class of regulatory RNA molecule known as miRNA are of particular interest in the development of novel chemo and radio sensitising agents. MiRNA function to regulate gene expression at the post transcriptional level and are predicted to regulate the expression of 30-60% of all protein coding genes (Friedman et al., 2009). A single miRNA can potentially repress the translation of thousands of mRNA thus simultaneously altering the expression of thousands of proteins (Peter, 2010). Furthermore, miRNA have been identified as modulators of cellular sensitivity to chemo and radiotherapy as well as regulators of the tumour microenvironment (Hummel et al., 2010; Soon & Kiaris, 2013).

1.3 MicroRNA

1.3.1 Discovery

During the 1970's and 1980's researchers investigating neural development in *C.elegans* identified the mutated *lin-4* gene in nematodes with a developmental timing defect (Horvitz & Sulston, 1980). In 1993, the genomic locus encoding the *lin-4* gene was reported to encode two small RNA transcripts, 22 and 61 nucleotides in length (Lee et al., 1993). A second independent study reported the 3'UTR of the *lin-14* mRNA contained sequences complementary to the two small non-protein-coding RNA products

of the *lin-4* gene (Ambros & Horvitz, 1984). The two small RNAs produced by the *lin-4* gene bound to the 3'UTR of the *lin-14* mRNA by complementary base pairing and subsequently repressed translation of the mRNA (Lee et al., 1993). Several years later a second RNA was identified in *C.elegans*. The *lethal-7* (*let-7*) gene encoded a 21 nucleotide RNA transcript complementary to the 3' UTR of five heterochronic genes involved in development; *lin-14, lin-28, lin-41, lin-42* and *daf-12* (Wightman et al., 1991; Reinhart et al., 2000). Unexpectedly, these nematode studies had identified a novel mechanism of gene regulation which is conserved in plants and animals (Bartel, 2004). The small non-protein coding RNA molecules identified as modulators of post-transcriptional gene expression were termed microRNA. The *let-7* gene was the first miRNA gene to be identified in humans (Pasquinelli et al., 2000). In 2001, numerous small non-protein-coding RNAs were identified, including 21 novel human miRNA (Lagos-Quintana et al., 2001; Lau et al., 2001; Lee & Ambros, 2001). Intensified research efforts identified additional miRNA in mammals, insects and plants and highlighted the evolutionary conservation of miRNA in eukaryotes (Bartel, 2004). To date there are ~1900 human miRNA precursor sequences and ~2600 mature human miRNA sequences in the miRBase (Kozomara & Griffiths-Jones, 2014).

1.3.2 MiRNA biogenesis

MiRNA genes are located throughout the genome as individual genes, polycistrons or within introns of pre-mRNA (Bartel, 2004). The miRNA genes are transcribed in the nucleus by RNA polymerase II or III which produces a single-stranded RNA transcript 1-7 kb in length (Fig 1.4) (Lee et al., 2004; Borchert et al., 2006). This primary miRNA (pri-miRNA) transcript folds into an imperfect hairpin structure as a result of Watson-Crick base pairing and is processed in the nucleus by

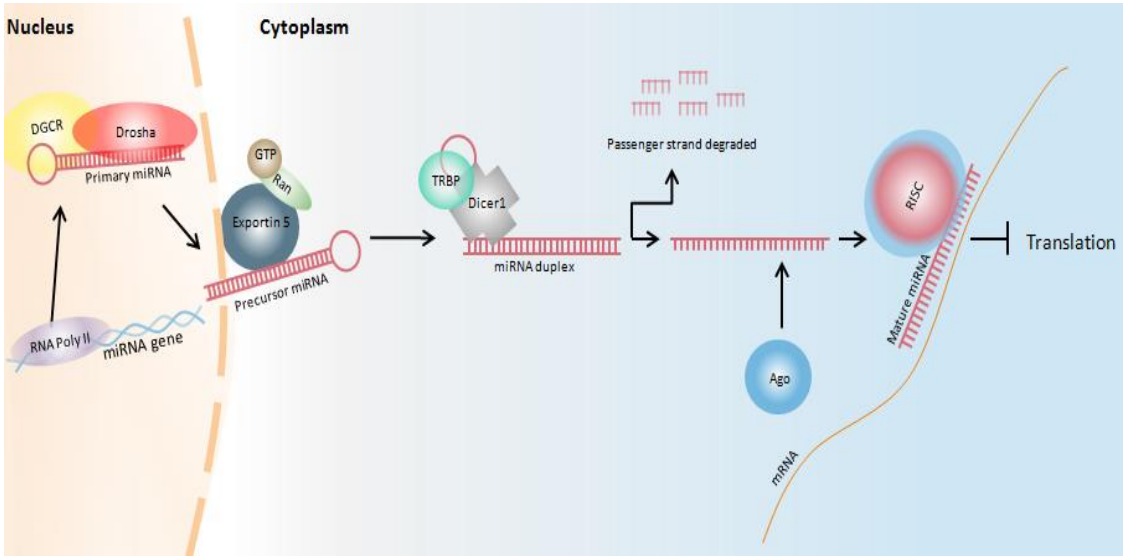

Fig 1.4 MicroRNA biogenesis. MiRNA genes are transcribed in the nucleus by RNA polymerase II to produce a long, single stranded RNA. The primary-miRNA (pri-miRNA) folds into a hairpin structure and is processed by Drosha and DGCR. The 5' and 3' ends of the hairpin structure are asymmetrically cleaved to produce the precursor-miRNA (pre-miRNA). The pre-miRNA is exported from the nucleus to the cytoplasm, via exportin-5 and Ran-GTP on the nuclear membrane, and is further processed in the cytoplasm by Dicer and TRBP. The loop of the hairpin structure is cleaved to produce the miRNA duplex. Within the miRNA duplex one arm is the passenger strand and the other is the mature miRNA. The passenger strand is degraded whilst the mature strand complexes with Argonaute proteins. The Ago proteins constitute the major functional element of the RNA induced silencing complex (RISC). The exposed bases of the mature miRNA, in the miRISC, bind to complementary mRNA via imperfect complementary base pairing. Subsequently, translation of the mRNA is repressed thereby downregulating gene expression at the protein level. Figure adapted from (Gray, 2015).

Drosha and DGCR (Lee et al., 2002; Han et al., 2004). The 5' and 3' ends of the hairpin structure are asymmetrically cleaved producing a precursor-miRNA (pre-miRNA) which is exported to the cytoplasm via exportin-5 on the nuclear membrane (Bohnsack et al., 2004). In the cytoplasm Dicer and TRBP cleave the loop structure off the hairpin leaving a miRNA duplex (miRNA-miRNA*) (Ketting et al., 2001; Schwarz et al., 2003). Thermodynamic stability of the strands determines which arm of the duplex will be incorporated into the RNA-induced silencing complex (RISC) as the mature miRNA, whilst the passenger strand (miRNA*) is degraded (Schwarz et al., 2003; Peters & Meister, 2007). Some miRNA genes produce two functional miRNA if both the -3p and -5p strands of the duplex are mature, active miRNA then there is no passenger strand. Furthermore, alternative strands can function as the mature miRNA in different tissue types and during pathological stages. For example, miR-140-3p is the mature miRNA stand in mouse ovaries and testis however miR-140-5p is the mature miRNA strand in cartilage (Tuddenham et al., 2006; Rakoczy et al., 2013). Recent nomenclature guidelines acknowledge the potential for both the -3p and -5p miRNA to be functional active. The current guidelines suggest the strands of the miRNA duplex should be annotated as the -3p or -5p in miRNA studies and should replace the miRNA/miRNA* annotation (Desvignes et al., 2015).

1.3.3 MiRNA function

MiRNA are short, non-protein-coding RNA that act as regulators of gene expression at the post-transcriptional level (Bartel, 2004). The exposed bases of the mature miRNA within the RISC bind target mRNA sequences via complementary base pairing (Schwarz et al., 2003). The mRNA seed site is a sequence of approximately seven nucleotides, and is essential for miRNA binding to targets. These sequences are

often highly conserved between species (Pasquinelli et al., 2000; Lewis et al., 2003; Friedman et al., 2009). The mRNA seed site is frequently, but not exclusively, located in the 3' UTR. The seed site in the mRNA binds to the seed region at the 5' end of the miRNA (Lewis et al., 2003; Saito & Saetrom, 2010). The 5' UTR and coding sequence of the mRNA can also contain seed sites and the miRNA with the RISC (miRISC) can potentially bind to any region of the mRNA (Lytle et al., 2007; Tay et al., 2008). The miRISC has less competition at the 3' UTR because this region is furthest away from the ribosome and translational machinery (Bartel, 2004; Grimson et al., 2007; Saito & Saetrom, 2010). Furthermore, target mRNA generally have longer 3' UTR compared to ubiquitously expressed genes, which tend to have shorter 3' UTRs depleted of miRNA binding sites (Stark et al., 2005). The general consensus is that the 3' UTR is the most accessible region of the mRNA, however a recent study identified ~42% of miRNA interactions occurring in the coding region compared to ~23% in the 3' UTR (Helwak et al., 2013).

Stringent seed sites have perfect Watson-Crick base pairing between the mRNA and miRNA (Saito & Saetrom, 2010). However, the miRISC can also tolerate G:U wobble and mismatch binding between the miRNA seed and mRNA seed site, current estimates suggest ~60% of miRNA and mRNA interactions contain bulged or mismatched nucleotides (Helwak et al., 2013). In mammals miRNA binding is generally the result of imperfect complementary base pairing, where as near-perfect complementary base pairing is most commonly observed in plants (Bartel, 2004). The imperfect nature of miRNA target binding enables a single miRNA to target multiple mRNAs in addition, a single mRNA can be targeted by multiple miRNA hence there is a significant degree of redundancy between miRNA (Lim et al., 2005).

The miRISC targets complementary mRNA and downregulates gene expression at the post-transcriptional level, thereby decreasing protein expression. The exact mechanism of miRISC mediated translational repression remains unclear (Wilczynska & Bushell, 2015). The levels of target mRNA, frequently remain unchanged by miRNA targeting, but a decrease in protein expression is observed (Lee et al., 1993; Bartel, 2004). This observation is explained by the miRISC repressing translation without mRNA degradation. The miRISC can repress the translation of mRNA targets at the initiation or post-initiation stage, or both (Petersen et al., 2006; Chendrimada et al., 2007). At the post-initiation stage the miRISC can displace or stall the ribosomal subunits during translation. At the initiation stage the miRISC preventing ribosomal subunits binding to the mRNA and initiating translation. Alternatively mRNA targets can be guided by the miRISC into processing bodies (P-bodies), sequestering them from the ribosome and translational machinery (Peters & Meister, 2007; Filipowicz et al., 2008). Endonucleases can subsequently enter P-bodies and degrade the sequestered mRNA, or the mRNA can later be released back into the cytoplasm for translation if protein levels decrease below the requirements of the cell. This would suggest miRNA-mediated repression is dynamic and reversible (Brengues et al., 2005; Bhattacharyya et al., 2006). More recent studies suggest mRNA destabilisation and degradation occurs more frequently than previous thought. Destabilisation of the mRNA, as a result of the miRISC interaction, may account for ~84% of decreased protein expression (Guo et al., 2010). The destabilisation of mRNA can be induced by the gradual shortening of the poly A tail, resulting in mRNA degradation by progressive decay (Parker & Song, 2004). The miRISC can directly cleave the mRNA targets, although this is dependent on stringent complementary binding between the mRNA and miRNA (Bartel, 2004). Translational repression and mRNA degradation may be sequential or independent mechanisms (Wilczynska & Bushell, 2015). It has been suggested that repression may

be the primary event which is followed by mRNA destabilisation and degradation (Djuranovic et al., 2012). Furthermore, the mechanism of miRISC mediated translation repression is potentially context dependent and influenced by other cellular factors (Wilczynska & Bushell, 2015).

The functional roles of miRNA are expanding beyond the translation repression of mRNA in the cytoplasm. The miRISC can also upregulate gene expression via the recruitment of translational proteins to the mRNA (Vasudevan et al., 2007). MiRNA also localise to subcellular compartments including the endoplasmic reticulum, mitochondria, P-bodies, multivesicular bodies, stress granules and the nucleus (Leung, 2015). The miRNA which re-localise to the nucleus are known to function as components of the epigenetic machinery (Roberts, 2014). The miRISC in the nucleus can silence or activate gene expression at the transcriptional level via promoter binding. Alternatively, the miRNA can recruit components of the epigenetic machinery which subsequently alter the epigenetic status of the gene via DNA methylation or chromatin remodelling (Roberts, 2014). In the endoplasmic reticulum miRNA and miRISCs are loaded into microvesicular bodies which are subsequently released into the extracellular environment in exosomes (Leung, 2015). The uptake of miRNA in the recipient cell can modulate gene expression, thus the extracellular miRNA are considered to function like hormones (Cortez et al., 2011). Extracellular miRNA are detectable in bodily fluids and are key molecules in cell-to-cell and cell-to-extracellular environment communication (Neviani & Fabbri, 2015).

1.3.4 MiRNA and cancer

The first link between miRNA and cancer was reported in B cell chronic lymphocytic leukaemia (CLL). The deleted 13q14 chromosomal region was reported to

encode two miRNA genes; *miR-15a* and *miR-16-1* (Calin et al., 2002). Intensified research efforts established differential miRNA expression profiles between normal and cancer tissue. Compared to normal tissue, the miRNA expression in cancer tissue is globally downregulated (Lu et al., 2005). The expression levels of ~200 miRNA could accurately distinguish between normal and malignant tissue (Lu et al., 2005). Furthermore, the miRNA expression profiles also reflected the developmental lineages and differentiation state of the tumours. The downregulated expression of miRNA in cancer tissue was further supported by the identification of miRNA genes in regions of chromosomal instability (Calin et al., 2004). Approximately 50% of miRNA genes are located within cancer-associated genomic regions or chromosomal fragile sites, and are susceptible to amplification, translocation or deletion (Calin et al., 2002; Farazi et al., 2013). Aberrant miRNA expression has also been attributed to epigenetic DNA methylation and chromatin remodelling, which can upregulate or downregulate miRNA expression (Gray, 2015). Furthermore, abnormalities in the expression of the proteins involved in miRNA biogenesis and processing can significantly alter miRNA expression profiles (van Kouwenhove et al., 2011).

In normal tissues miRNA function as master regulators of gene expression and it is estimated that ~60% of genes are regulated by miRNA (Friedman et al., 2009). Therefore it is feasible, and highly likely, that miRNA directly or indirectly regulate all cellular processes. Dysregulation of a single miRNA has the potential to alter the expression of hundreds of genes. Consequently, aberrant miRNA expression plays a causal role in cancer development and progression. Oncomirs are cancer associated miRNA which have either tumour suppressor or tumour promoting functions (He et al., 2005; Johnson et al., 2005; Esquela-Kerscher & Slack, 2006). Tumour suppressive miRNA are frequently downregulated in cancer resulting in the upregulation of oncogenes and tumorigenesis, conversely oncogenic miRNA promote cancer

development and progression (Li et al., 2010). In CLL, miR-15a and miR-16-1 act as tumour suppressor via the negative regulation of the antiapoptoic B cell lymphoma 2 gene (*Bcl2)* (Cimmino et al., 2005). The ectopic expression of miR-15a and miR-16-1 repressed *Blc2* expression and induced apoptosis in a leukaemia cell model (Cimmino et al., 2005). The oncogenic miRNA miR-21 is overexpressed in most cancer types (Mendell & Olson, 2012). In glioblastoma miR-21 expression is increased 5-100 fold and inhibits apoptosis (Chan et al., 2005). Furthermore, miR-21 was one of the first miRNA to be studied *in vivo*. The overexpression of miR-21 was sufficient to initiate tumorigenesis in a mouse model with no predisposing mutations, subsequent inactivation of miR-21 induced apoptosis and tumour regression (Medina et al., 2010). The expression and functions of miRNA are tissue-type specific, therefore, a single miRNA can act as a tumour suppressor and an oncogene in different settings. For example, miR-330-3p was found to act as a tumour suppressor in prostate cancer by down regulating Akt phosphorylation, thus inactivating survival pathways and promoting apoptosis (Lee et al., 2009). Conversely, miR-330-3p acts as an oncogene in glioblastoma cell lines, promoting cellular proliferation and migration by down regulating the tumour suppressor gene *SH3GL2* (Qu et al., 2012).

The eight cancer hallmarks are associated with the tumour suppressor and oncogenic functions of individual miRNA (Ruan et al., 2009; Berindan-Neagoe et al., 2014). Aberrant miRNA expression could potentially be considered an independent hallmark of cancer, due to the universal dysregulation of miRNA expression across all cancer types and the extensive contributions of miRNA in cancer development and progression. Furthermore, miRNA are known to directly and indirectly regulate the tumour microenvironment. The releases of miRNA into the extracellular environment can facilitate cell-to-cell and cell-to-stroma communication in the tumour microenvironment. Numerous miRNA have been reported to modulate angiogenesis,

hypoxia, immune response and extracellular matrix remodelling in the tumour microenvironment (Soon & Kiaris, 2013). The release of miRNA into the systemic vasculature and extracellular bodily fluids can also facilitate communication between distant sites and these miRNA are considered to have hormone-like functions (Neviani & Fabbri, 2015).

Despite the vast number of miRNA cancer expression profiles reported in the literature, a limited number of miRNA have been characterised and the functions of most miRNA are as yet unknown. Alterations in the intracellular and extracellular miRNA expression profiles identified in cancer highlight the potential use of miRNA as clinical cancer biomarkers. Furthermore, understanding the functional role of dysregulated miRNA in cancer development will identify miRNA for therapeutic targeting.

1.3.5 MiRNA cancer biomarkers and therapeutics

MiRNA play a causal role in cancer and differential miRNA expression between normal and cancer tissues makes miRNA attractive biomarkers. Ideal biomarkers are sensitive, consistent and specific. In the clinic the method for biomarker detection should be fast, accurate and inexpensive. Biomarkers which can be detected non-invasively are particularly useful in the clinic. MiRNA are ideal biomarkers because they are stable biological molecules that are readily extractable from tissue, blood, urine and saliva and they can be accurately measured using high throughput qPCR (Gilad et al., 2008; Grimm, 2009). MiRNA cancer biomarkers have potential applications in diagnostics, prognostics, tumour staging, identifying clinical subtypes and predicting and monitoring patient response to treatment (Hummel et al., 2010). Potential miRNA biomarkers have been identified in most cancers and devising miRNA profiles or

signatures constituting several miRNA are far more robust than individual miRNA, this is impart due to the intra and inter heterogeneity of tumour tissue (Kent et al., 2014).

MiRNA biomarkers have the potential to predict patient response before and during treatment. In a pre-treatment setting miRNA biomarkers could aid therapeutic stratification for patients in the transition towards personalised and precision medicine (Hummel et al., 2010). In addition, miRNA modulate the sensitivity of the cancer cells and the tumour microenvironment by direct and indirect mechanisms. Determining the functional roles of the miRNA which modulate tumour sensitivity to chemo and radiotherapy may also identify opportunities for therapeutic intervention.

There are two therapeutic strategies to targeting miRNA; replacement therapy and knockdown therapy. Downregulated tumour suppressor miRNA expression can be restored with functional miRNA mimics. Alternatively, overexpressed oncogenic miRNA expression can be inhibited or silenced by miRNA antisense mimics known as antagomirs (Krutzfeldt et al., 2005). The identification of miRNA which modulate or contribute to tumour resistance are potential therapeutic targets which could be manipulated to enhance tumour sensitivity and the efficacy of CRT. This approach is exemplified by miR-200c of the miR-200 miRNA family. The miR-200 family have been reported *in vitro* to modulate sensitivity to chemotherapy and radiotherapy in multiple cancer types (Feng et al., 2014). The overexpression of miR-200c in lung cancer cell models enhanced radiosensitivity *in vitro* by inhibiting DNA repair, increasing ROS and upregulating p21 (Cortez et al., 2014). *In vivo* the delivery of miR-200c mimics in xenograft lung cancer models enhanced tumour sensitivity to radiotherapy. Replacement miR-200c therapy in combination with radiation has the potential to enhance radiosensitivity in non-small cell lung cancer patients.

The most advanced clinical application of a miRNA therapeutic is for the treatment of hepatitis C virus (HCV). The expression of miR-122 promotes the replication of the HCV in the liver. Miravirsen is a miR-122 single-stranded antagomir that inhibits the biogenesis and function of the miRNA, which subsequently inhibits replication of the virus (Gebert et al., 2014). Miravirsen was the first miRNA targeted therapy to enter clinical trials in 2010 and has generated promising results in phase 2a trials. Another pharmaceutical company, MiRNA Therapeutics, focus on the development of miRNA oncology replacement therapies. Their lead target is miR-34a, a tumour suppressor which modulates proliferation, cell cycle progression and apoptosis and is frequently down regulated in multiple cancers (Bader, 2012). The miR-34a therapeutic, MIRX34, is a liposome-formulated mimic of the tumour suppressor miR-34a. The miRNA mimics are encapsulated in an ionisable liposome which enhances retention time, avoids immune response and displays a promising safety profile in pre-clinical studies (Bader, 2012). The miR-34a replacement mimic induces cell cycle arrest, senescence and apoptosis *in vitro* and *in vivo*. MIRX34 has generated promising results in current phase 1 clinical trials and is schedule to progress to phase 2 trials in 2017.

MiRNA play a causal role in cancer development and progression and are promising biomarkers and therapeutics. Aside from identifying dysregulated miRNA there is a need to understand the functional role of these miRNA in cancer progression. The therapeutic targeting of miRNA is dependent on our understanding of the mechanistic contributions of specific miRNA in tumorigenesis.

1.3.6 MiRNA and OAC

Of the ~20,000 publications on miRNA and cancer only ~0.5% (<100 publications) are miRNA OAC related studies. The majority of these studies identify miRNA which are dysregulated miRNA in OAC. Few of these studies report the targets and functions of individual miRNA in OAC.

The expression profiling of miRNA in normal oesophagus, BO and OAC tissues has identified the sequential upregulation and downregulation of several miRNA (Fassan et al., 2011). Distinct miRNA expression patterns have been identified in the transition of BO to OAC (Yang et al., 2009). These miRNA signatures are potential biomarkers of disease progression. In combination with the BO surveillance programmes these miRNA signatures could indicate disease progression in tissue biopsies, prior to obvious changes observed with endoscopy. During disease progression from normal oesophagus tissue to BO and then OAC, the miR-106b-25 polycistron is progressively upregulated due to genomic amplification (Kan et al., 2009). The upregulation of miR-93 and miR-106b modulates cell cycle progression by inhibiting p21 protein expression, whilst miR-25 inhibits apoptosis via negative regulation of the proapoptotic protein Bim (Kan et al., 2009). These miRNA expressed from the miR-106b-25 polycistron are considered to be drivers of OAC development and progression.

Several miRNA have been identified as prognostic markers in clinical patient biopsies. The expressions of miR-99b, miR-199a-3p and miR-199a-5p were significantly upregulated in patients with lymph node metastasis (Feber et al., 2011). Furthermore, increase expression of miR-30e correlated with a 2.5 fold increase in the risk of disease recurrence following surgery (Hu et al., 2011). In tissue biopsy samples from BO and OAC patients, the downregulated expression of miR-375 was associated

with poor patient survival. In combination with a panel of inflammatory cytokines the downregulated expression of miR-372 was identified as a predictive marker of poor prognosis (Nguyen et al., 2010). The expression of miR-148a was inversely correlated with tumour differentiation status (Hummel et al., 2011a). Furthermore, *in vitro* the ectopic overexpression miR-148a enhanced cellular sensitivity to cisplatin and 5-FU (Hummel et al., 2011b). Further studies are needed to assess miR-148a as a replacement therapy which could enhance patient sensitivity and response to chemotherapy in OAC.

There are numerous studies which have identified potential miRNA biomarkers in OAC, but few studies have further investigated the functional roles of these miRNA in OAC. Following CRT the expression of miR-145 was reportedly upregulated in OAC patients and correlated with shorter disease free survival (Derouet et al., 2014). *In vitro* overexpression of miR-145 enhanced metastasis related phenotypes including invasion and protection against anoikis, supporting the role of miR-145 in disease recurrence post-treatment (Ko et al., 2012; Derouet et al., 2014). In another study, upregulation of miR-196a during disease progression was demonstrated to target and downregulated annexin A1 thus promoting evasion of apoptosis (Luthra et al., 2008).

The majority of OAC patient present with advanced disease and the only treatment options available at this stage are neoadjuvant therapy and surgery. Predicting the patient's response to neoadjuvant therapy prior to treatment would have a significant clinical benefit, particularly for the ~70% of patients who show little or no response to treatment. The delay to surgery in patients who do not respond to the neoadjuvant chemotherapy or CRT can worsen the patient's prognosis, for these non-responders immediate surgery may be an option. In a recent study, a validated miRNA signature predictive of OAC patient response to neoadjuvant CRT has been reported (Skinner et al., 2014). Skinner *et al* identified a four miRNA signature which predicts, in a pre-

treatment setting, patients with a high probability of a pCR and patients with a low probability of a pCR (Skinner et al., 2014). In a discovery patient cohort (*n*=10) miRNA expression profiling was undertaken in pre-treatment patient biopsies. Of the 754 miRNA analysed, 44 were selected and further validated in a model cohort (*n*=43). Four miRNA were significantly differentially expressed in the patients with pCR compared to non-pCR patients. The expression levels of the four miRNA (miR-505*, miR-99b, miR-451 and miR-145*) were used to devise a miRNA expression profiling score. The downregulated expression of these four miRNA, in pre-treatment patient tumours, was significantly associated with pCR.

In another OAC study, miR-31 was downregulated in pre-treatment biopsies taken from patients who did not respond to neo-CRT. Furthermore, in an OAC isogenic cell model of radioresistance, miR-31 was also downregulated (Lynam-Lennon et al., 2012). Ectopic re-expression of miR-31 *in vitro* re-sensitised radioresistant cells to the cytotoxic effects of radiation. Further investigation identified 13 DNA repair genes as downstream targets of miR-31, indicating downregulation of miR-31 results in enhanced DNA repair mechanisms and radioresistance (Lynam-Lennon et al., 2012). The downregulated expression of miR-31 in the treatment naive tumours of OAC patients is a potential biomarker of resistance to CRT. The identification of miR-31 mediated regulation of DNA repair mechanisms may contribute to radioresistance, thus replacing miR-31 in patient tumours in combination with CRT may improve tumour sensitivity and treatment efficacy.

In addition to these two studies which have identified potential miRNA biomarkers indicative of patient response to neo-CRT, there is need to develop new therapeutics for OAC. The biomarkers could enable stratification of OAC patients prior to neoadjuvant chemotherapy or CRT however, for those patients predicted to be non-

responders there are no alternative treatments. Identifying miRNA which modulate tumour response and sensitivity to chemotherapy and radiotherapy could enable the development of targeted miRNA therapy. Replacement or silencing of miRNA prior to, or during, neoadjuvant therapy could enhance patient sensitivity and response to chemotherapy and radiotherapy. This approach has been undertaken in other cancer types but there have been no studies of this kind in OAC.

1.4 Project rationale

Unfortunately the majority of OAC patients do not respond to neo-CRT. The non-responders gain no benefit from the aggressive neo-CRT treatment regimen whilst quality of life is compromised. There is an unmet clinical need for biomarkers predicative of patient response to neo-CRT. However, the greater clinical benefit for patients would come from the development of new or augmented therapeutics for OAC.

Dysregulated miRNA expression plays a causal role in cancer development and progression. Furthermore, miRNA are known to predict and modulate tumour response to CRT. In a pre-treatment setting, miRNA biomarkers indicative of patient response would enable the stratification of patients and ensure individual patients receive the most effective treatment. In addition to identifying miRNA biomarkers, understanding the functional relevance of the miRNA that modulate tumour resistance to CRT could provide an opportunity for therapeutic intervention. The development of novel miRNA therapeutics targeting tumour resistance could be administered in combination with CRT to enhance tumour sensitivity. Synergistic CRT and targeted miRNA therapies could significantly improve the efficacy of neo-CRT and survival rates for OAC patients.

1.4.1 Project hypothesis

MiRNA are predictors and modifiers of OAC tumour sensitivity to CRT. Therefore, miRNA are potential biomarkers predictive of patient response to neo-CRT and therapeutic manipulation of miRNA expression could improve the efficacy of CRT.

1.4.2 Project aims and objectives

1. Identify differentially expressed miRNA between diagnostic pre-treatment biopsies from OAC patients who responded to neo-CRT and patients who did not.
2. Determine the functional significance of select miRNA as modulators of tumour sensitivity to CRT using *in vitro* cell models and *in vivo* tumour xenografts.
3. Elucidate the targets, pathways and potential molecular mechanisms by which these miRNA modulate tumour sensitivity to CRT using *in vitro* cell models.

Chapter 2 Materials and Methods

2.1 Reagents and materials

Chemicals, reagents and consumables were purchased from Fisher UK, unless otherwise stated. Reagents in powder form were prepared in deionised distilled water, unless otherwise stated. An OHAUS Explorer analytical balance (OHAUS Europe, Switzerland) was used for weighing solids with up to 4 decimal places of accuracy. An OHAUS Scout Pro balance (OHAUS Europe, Switzerland) was used for weighing larger quantities of solid to 2 decimal places of accuracy. Volumes less than 2 mL were measured using a range of adjustable volume pipettes (PIPETMAN Gilson, USA). Volumes between 2-25 mL were measured with polystyrene serological pipettes and electronic pipette fillers (PIPETBOY Integra, Switzerland). Volumes greater than 25 mL were measured with graduated cylinders.

2.1.1 Preparation of chemotherapeutic drugs

Stock solutions of *cis*-diamminedichloroplatinum (cisplatin) and 5-Flurouracil (5-FU) were prepared in phosphate buffered saline (PBS) and dimethyl sulfoxide (DMSO), respectively. Solutions were sterile filtered and then aliquoted and stored at -20°C. Upon thawing a yellow crystal precipitate was visible in the cisplatin solution. Prior to use the solution was incubated at 37°C and mixed thoroughly until the precipitate had fully solubilised.

2.1.2 Irradiation

X-ray irradiation was performed using an RS-2000 Pro biological research irradiator (Rad Source Technologies, Georgia, USA) at a dose rate of 1.87 Gy/min.

2.2 Patient samples

2.2.1 Patient recruitment and sample acquisition

Pre-treatment diagnostic endoscopic biopsies were obtained from patients diagnosed with operable oesophageal cancer. Tumour tissue biopsies (10-20 μg) were acquired by a qualified endoscopist prior to the patient receiving neo-CRT. Adjacent normal tissue was also taken for histological confirmation. Routine tissue staining was performed by the St. James's Hospital (Dublin) Central Pathology Laboratory using haematoxylin and eosin. Patient biopsy samples were placed in RNA later (Ambion, UK) with and refrigerated for 24 h before storage in the biobank (-80°C). Ethical approval and written informed consistent were obtained prior to recruitment of patients at St James's Hospital Dublin, Ireland (Lynam-Lennon et al., 2012).

2.2.2 Patient treatment and pathological assessment

Patients received neo-CRT, consisting of two courses of 5-FU (15 mg/kg infused over 16 h on days 1-5 and day 35-39) and two courses of cisplatin (75 mg/m^2 infused over a period of 6 h on days 6 and 40). In addition to chemotherapy patients received radiotherapy starting on the first day of the first course of chemotherapy. Radiotherapy was administered over 5 days in fractionated doses of 2 or 2.67 Gy/fraction. The patients received 22 or 15 daily fractions of radiation over 4.5 or 3 weeks, respectively. Patients received a cumulative dose of 44 or 40.5 Gy of radiotherapy (Maher et al., 2009). Surgical resection was performed within approximately 1 month of completion of the neo-CRT regimen. Resected oesophagectomy specimens were assessed by an experienced pathologist who graded and staged the specimens. A tumour regression grade (TRG 1-5) was allocated based on the method of Mandard (Mandard et al., 1994). Patients assigned TRG 1 and 2 were

considered responders to neo-CRT. TRG 1; complete regression, absence of residual cancer cells and fibrosis extending through the different layers of the oesophagus wall. TRG 2; presence of rare residual cancer cells scattered through the fibrosis. Patients assigned TRG 3-5 were considered non-responders to neo-CRT. TRG 3; increase in the number of cancer cells but fibrosis still predominated. TRG 4; residual cancer outgrowing fibrosis. TRG 5; absence of regressive changes.

2.2.3 RNA isolation from patient biopsy samples

Total RNA was extracted from patient biopsy samples (10-20 μg) using the All-In-One purification kit as per the manufacturer's instructions (Norgen Biotek, Ontario, Canada). RNA extractions were quantified and sample quality assessed using the NanoDrop ND-1000 (Thermo Scientific, UK) (section 2.5.2).

2.2.4 MiRNA expression arrays in patient biopsy samples

The pre-treatment biopsy tissue samples of 9 responders and 10 non-responders to neo-CRT were selected for global miRNA expression analysis. The pre-treatment patient samples were extracted from the biobank and total RNA was extracted for qPCR based miRNA expression arrays as described in section 2.2.3. RNA (40 ng) was converted to cDNA using Universal RT primers and miRNA reverse transcription kit (Exiqon, Denmark), as per the manufacturer's instructions. The expression of 742 miRNA were analysed in each of the 19 patient samples using Human miRCURY LNA Universal RT miRNA arrays, panel I and II (Exiqon, Denmark), and a 7900HT RT-PCR system (Applied Biosystems, UK). Analysis was performed using GenEx 5.0 software

(MultiD Analyses AB, Sweden), with global normalization to the mean used for data normalization. One sample was set as the calibrator for analysis.

2.3 Cell lines

The OE33, OE19 and SK-GT-4 oesophageal adenocarcinoma cell lines were purchased from European Collection of Cell Culture (ECACC, UK). The OE33 cell line was established from a 73-year old female patient, with a stage 2a tumour taken from the lower oesophagus with confirmed Barrett's metaplasia. The OE19 cell line was established from a 72-year old male patient, with a stage 3 tumour tissue taken from the oesophageal gastric junction. The SK-GT-4 cell line was established from an 89-year old male patient with a well differentiated adenocarcinoma, which arose from a Barrett epithelium and had invaded into but not through the muscle layer. The radioresistant isogenic model, OE33 P and OE33 R, was previously established within the group (Lynam-Lennon et al., 2010). The OE33 R cell line was irradiated with 2 Gy fractioned doses of radiation, cumulative to 50 Gy, to induce a radioresistant phenotype, while the OE33 P cell line was mock-irradiated to maintain a control passage matched isogenic model.

2.3.1 Tissue culture

RPMI-1640 media with phenol red and without L-Glutamine (BioWhittaker Lonza, Switzerland) was supplemented with 10% heat-inactivated foetal bovine serum (BioWhittaker Lonza, Switzerland), 1% penicillin-streptomycin antibiotic 5000 U/mL (BioWhittaker, Lonza, Switzerland) and 1% L-Glutamine substitute (GlutaMAX, Invitrogen, UK). All cell lines were cultured in RPMI-1640 media with supplements,

hereafter termed complete media, in T75 cm^2 filter cap tissue culture flasks (Greiner Bio-One, UK). Cells were maintained in a 37°C incubator, 95% humidified air and 5% CO_2 (Nuaire IR Direct Heat CO_2 Incubator, Red Laboratory Technology, USA). Aseptic technique and Faster BH-EN 2004 laminar flow hoods (Faster S.r.l, Italy) were used for tissue culture work. The equipment and reagents were sterilised with 70% EtOH before entering the workspace of the laminar flow hood. Tissue culture reagents were stored at 4°C and warmed to 37°C in a water bath prior to use. Cells were observed daily under the microscope (Olympus CKX41, × 10 magnification).

2.3.2 Subculture

Cells were maintained in an exponential growth phase by subculturing cells at 80 - 90% confluency. Exhausted medium was discarded to waste and cells were washed with approximately 5 mL sterile PBS (BioWhittaker Lonza, Switzerland). Adherent cells were detached from the flask with 1.5 mL trypsin-EDTA (BioWhittaker, Lonza, Switzerland). The trypsin was inactivated after 3-5 min, with the addition of 5 mL complete media when >95% of the cells were detached. The cell suspension was split into daughter T75 cm^2 flasks at ratio 1:2 - 1:10 and medium was added to a total volume of 20 mL. Passage numbers were noted to indicate the number of times the cells had been subcultured.

2.3.3 Preparation of frozen cell stocks

Cells were frequently frozen down and stored in liquid nitrogen to maintain early passage cell stocks. Each confluent flask (80 - 90%) was washed with PBS, trypsinsed and then trypsin was inactivated with complete media as in subculturing

(section 2.3.2). The cell suspension was centrifuged for 5 min at 300 × *g* to pellet the cells. Medium was decanted to waste and the cell pellet was resuspended in 5 mL PBS then centrifuged again for 5 min at 300 × *g*. The PBS was decanted to waste and cells were resuspended with the gradual addition of 1.5 mL freeze mix (90% FBS, 10% DMSO). The suspension was aliquoted into cryovials (500 µL per vial) and labelled with the cell line, date and passage number. Cell freeze downs were stored at -80°C overnight using Nalgene Mr Frosty containers for the optimal freezing rate of -1°C/minute. For long term storage frozen cell stocks were stored in the vapour phase of liquid nitrogen.

2.3.4 Reconstitution of frozen cell stocks

Frozen cells were quickly thawed by hand and transfer to T25 cm^2 or T75 cm^2 flasks containing pre-warmed complete media (7 mL or 20 mL, respectively). Alternatively thawed cells were transferred to a 50 mL falcon tube with 5 mL complete medium and centrifuged for 5 min at 300 × *g*. Medium was decanted to waste and the cells were resuspended in 2 mL complete medium before transferring to the tissue culture flask.

2.3.5 Haemocytometry and viability determination

Confluent flasks were washed with PBS, trypsinsed and inactivated with media as in subculturing (section 2.3.2). The cell suspension was centrifuged for 5 min at 300 × *g* to pellet the cells. The supernatant was discarded and the cells were thoroughly resuspended by pipetting in 1-3 mL complete media. To achieve a single cell suspension the cell suspension was passed through a 70 µm cell strainer. For the viable

cell count the cell suspension was diluted 1:2 or 1:10 with trypan blue dye (0.4%, Gibco). For a 1:2 dilution, 100 µL cell suspension was combined with 100 µL of trypan blue. For a 1:10 dilution, 20 µL cell suspension was combined with 180 µL of trypan blue. The solution was mixed thoroughly and 9 µL was applied to a haemocytometer (Superior Marienfeld, Germany). Using the microscope (Olympus CKX41, × 10 magnification) cells in the four large corner squares of the grid were counted. Viable cells with intact cell membrane exclude the trypan blue dye and non-viable cells take up the dye and appear blue. Positively staining cells were not included in the count. Cells touching the right and bottom sides of the counting field were included in the count, cells touching the top and left sides of the field were not included in the count. The total count was divided by four and multiplied by the dilution factor, 2 or 10, then multiplied by 10^4 to calculate the number of cells/mL.

2.3.6 Mycoplasma screening

Cell cultures were tested on average every 3 months for mycoplasma contamination using the MycoAlert Mycoplasma Detection Kit (Lonza, Switzerland). The assay required 1 mL of exhausted medium taken from a flask of cultured cells. The medium was centrifuged 300 × *g* for 5 min to pellet any cells and 100 µL of the cell free supernatant was pipetted into the well of an opaque white 96-well plate (each sample was run in triplicate). A 100 µL volume of MycoAlert™ Reagent was added to each well. The plate was incubated for 5 min and read with a luminometer (1000 ms integration time) (Fluoroscan Ascent FL, Thermoscientific, UK). A 100 µL volume of MycoAlert Substrate was subsequently added to each well and the plate was incubated for a further 10 min, followed by a second reading with a luminometer (1000 ms integration time). In mycoplasma negative samples the second reading does not increase

compared to the first. To calculate the ratio of the two readings the second reading was divided by the first reading. Calculated ratio values <0.9 were indicative of a mycoplasma negative sample, and values >1.2 were indicative of a mycoplasma positive sample. Mycoplasma positive cells lines were re-tested, and if positivity confirmed they were discarded.

2.4 MicroRNA plasmids

MicroRNA overexpression and silencing plasmid constructs were purchased from System Biosciences (USA) and Origene (USA). The miRNA precursor constructs and anti-miRNA silencing constructs were cytomegalovirus (CMV) promoter driven vectors that also encode the GFP reporter gene (Appendix 1). The miRNA-330 (PMIRH330PA-1 System Biosciences) and miR-187 (PMIRH187PA-1 System Biosciences or PCMVMIR187 Origene) plasmid constructs produced a precursor miRNA hairpin that is processed by the endogenous cell machinery to produce the mature form of the miRNA. The anti-miR-330-5p vector (MZIP-330-5p-PA-1 System Biosciences) encoded the antisense miR-330-5p sequence. The anti-miR-330-5p produced by the vector binds irreversibly to the endogenous miR-330-5p in the cell thereby silencing and permanently inhibiting the function of the miRNA. The corresponding control vectors, hereafter referred to as miR-VC, are empty vectors or vectors encoding a scrambled non-functional sequence in place of the miRNA insert (CD511B-1, MZIP000-PA-1, PCMVMIR). Plasmids were supplied as live bacterial streaks, from which bacterial stocks were grown for plasmid extraction (section 2.4.2).

2.4.1 Preparation of chemically-competent *E. coli*

Glycerol stocks of DH5α *E.coli* were thawed and plated on Lysogeny Broth agar plates (LB agar; 10 g tryptone, 10 g NaCl, 5 g yeast in 1 L with 2% agar) using a spreader and aseptic technique. Plates were incubated overnight at 37°C. A single colony was used to inoculate 5 mL LB in a sterilin, which was grown overnight in a rotary shaker at 37°C. In a 500 mL conical flask, 100 mL LB was inoculated with 0.5 mL of the overnight culture and grown for 2-3 h at 37°C. After 2 h the optical density at 600 nm (OD_{600}) was measured at 30 min intervals using a spectrophotometer (Libra S32 UV/Visible spectrophotometer, Biochrom, UK). Cells in early exponential growth phase are needed to produce competent cells, equating to an OD_{600} of approximately 0.2. The culture was cooled on ice for 10-20 min and then divided between two pre-cooled falcon tubes. The tubes were centrifuged at 3000 × *g* for 10 min to pellet the bacterial cells. The supernatant was decanted to waste and the cell pellets were resuspended in 5 mL ice-cold 0.1M $MgCl_2$. Tubes were centrifuged 3000 × *g* for 5 min to pellet the cells. The supernatant was decanted to waste and the cells were again resuspended in 5 mL of ice cold 0.1M $CaCl_2$ and incubated for 5 min on ice. The tubes were subsequently centrifuged at 3000 × *g* for 5 min and the supernatant again decanted to waste. The cells were resuspended in 1 mL ice cold 0.1M $CaCl_2$ and incubated for 1.5 h on ice. Chemically-competent cells were supplemented with 15% glycerol and 100 µL aliquots were stored at -80°C until required.

2.4.2 Bacterial transformation

Chemically-competent DH5α *E.coli* (section 2.4.1) or XL10-Gold *E.coli* (Agilent Technologies, California, USA) were used for propagation of the miRNA plasmids (section 2.4). The bacterial cells and the plasmid were thawed on ice, and then

1-2 µL of the plasmid was added per 100 µL chemically-competent cells. The tube was mixed thoroughly and incubated on ice for 15 min. The mixture was then heat-shocked for 45 sec at 42°C and incubated on ice for a further 2 min. Bacteria were plated, using a spreader and aseptic technique, on thermo-stable ampicillin- or kanamycin-containing agar (Fast-Media *E.coli* LB Agar, InvivoGen, USA). The plates were incubated overnight at 37°C, and the next day a single colony was picked and used to establish a starter culture by inoculating 5 mL LB ampicillin or kanamycin medium (Fast-Media *E.coli* LB Liquid, InvivoGen, USA). The culture was grown for ~8 h at 220 rpm and 30°C in a rotary incubator. A second larger culture was prepared from the resulting starter culture by inoculating 400 mL LB ampicillin or kanamycin medium with 0.5 mL starter culture in a 2 L conical flask, which was subsequently grown overnight at 30°C in a rotary shaker. Prior to plasmid DNA purification the OD_{600} was measured to determine the recommended culture volume stated for use with the plasmid purification kit. The culture was aliquoted into falcon tubes and centrifuged at 6000 × *g* for 15 min at 4°C to pellet the transformed bacterial cells prior to plasmid purification (section 2.4.3). Exhausted medium was decanted to waste and sterilised before being discarded. Cell pellets were stored at -20°C for up to 6 months before plasmid purification.

2.4.3 Plasmid purification

Transformed *E.coli* cell pellets were thawed on ice immediately prior to plasmid purification using the NucleoBond Xtra Midi Plus Kit (Macherey-Nagel, Fisher, UK) according to the manufacturer's instructions. Briefly, the cell pellet was thoroughly resuspended in 8 mL resuspension buffer containing RNase A, then 8 mL lysis buffer was added and mixed by gently inverting the tube 5 times. The resulting suspension was incubated at room temperature for 5 min. Meanwhile a NucleoBond Xtra Column Filter

was equilibrated with 12 mL equilibration buffer applied around the inner rim of the column filter. After 5 min of lysis, 8 mL neutralisation buffer was added to the lysed cell suspension and gently mixed by inverting the tube 10-15 times before applying the homogenous suspension to the NucleoBond Xtra Column Filter. The column filter cleared the suspension of cell debris and precipitate, whilst the plasmid DNA was bound to the NucleoBond Xtra Silica Resin at the bottom of the column. The resin consists of hydrophilic, macroporous, positively-charged silica beads to which the negatively charged backbone of the plasmid DNA binds with high specificity. The column was subsequently washed with 5 mL equilibration buffer and the column filter then discarded. The column was again washed with 8 mL wash buffer to improve plasmid purity. The plasmid was eluted from the silica resin with 5 mL elution buffer, and the flow-through containing the plasmid was collected in a clean tube. To precipitate the plasmid DNA, 3.5 mL room temperature isopropanol was added to the tube and the solution was vortexed thoroughly (Stuart SA7 Vortex, Fisher UK). The plasmid DNA was further purified with the additional NucleoBond Finalizers. The plasmid solution was loaded onto a second silica membrane with a 1 mL syringe. The membrane was washed with ethanol and the plasmid eluted with 250 µL 5mM Tris-HCl pH 8.5. Plasmid DNA concentration and purity was measured using the NanoDrop ND-1000 (section 2.4.4). Plasmid DNA preparations were stored at -20°C.

2.4.4 Plasmid DNA quantification

Plasmid DNA samples were quantified using the NanoDrop ND-1000 (Thermo Scientific, UK). The pedestal was cleaned with H_2O and blanked with the appropriate reference solution. For DNA measurements 5mM Tris-HCL solution was used as the blank. The pedestal was loaded with 1 or 2 µL of sample. The plasmid DNA

concentration was measured in ng/mL. DNA samples were analysed for protein contamination (Abs 260:280, a ratio ≥ 1.8 was indicative of a pure yield).

2.4.5 Liposomal-based transfection of cell lines

Lipofectamine 2000 Transfection Reagent is a cationic lipid which forms liposomes around the plasmid DNA. The positively charged DNA-lipid complexes fuse with the negatively charged cell membrane and enter the cell via endocytosis. Thawed plasmid DNA and Lipofectamine 2000 Transfection Reagent (Invitrogen, UK) were separately diluted in Opti-MEM reduced serum media (Invitrogen, UK). The DNA-lipid complexes were prepared by combining the DNA and transfection reagent in a 1:2 ratio. The solution was gently mixed and incubated for 5-10 min to allow DNA-lipid complexes to form. The DNA-lipid complexes were applied immediately to seeded cells in suspension (reverse transfection) or to adherent cells that had been seeded 24 h prior to transfection (forward transfection). Transfection efficiency was assessed 24 h post-transfection using fluorescent microscopy to observe GFP expression. Successful transfection corresponded to >75% of cells expressing GFP.

2.4.6 Fluorescent microscopy

The Olympus IX71 inverted microscope and CellD software were used to take images of transfected cells and to confirm successful transfection by visualising GFP. Bright field images of cells were taken at 2-5 ms exposure times with × 10 magnification. The FITC channel was used to image GFP at 100-200 ms exposure. Both images were taken in the same field of view. The Axio Vert.A1 inverted microscope and ZEN 2012 software (Carl Zeiss, Germany) were used to take images of DAPI

stained cells in the invasion assay (section 2.7.4). The DAPI channel was used to image DAPI stained nuclei with × 10 or × 5 magnifications.

2.5 Gene expression analysis

2.5.1 RNA extraction from cell lines

For total RNA extraction and purification, including miRNA, the RNeasy Mini Kit was used as per the manufacturer's instructions (Qiagen, UK). Sterile RNAase and DNase free filter tips were used throughout all RNA experiments (TipOne Starlab, UK). Briefly, cell pellets ($<5 \times 10^4$ cells) were resuspended in 350 µL RLT lysis buffer and pellets $>5 \times 10^4$ cells were resuspended in 600 µL RLT lysis buffer. One volume of 70% ethanol was added to the lysate and mixed well by pipetting. RNeasy Mini columns were inserted into the top of 2 mL collection tubes. Up to 700 µL of the lysate was added to the columns, which were then centrifuged at 8000 × *g* for 15 s at room temperature. The RNA binds to the silica column membrane whilst impurities are washed through the column, and the flow through discarded to waste. A 700 µL volume of RW1 buffer was added to the column, and centrifuged 8000 × *g* for 15 s at room temperature. The flow through was discarded and 500 µL RPE buffer was added to the column and centrifuged at 8000 × *g* for 15 s at room temperature. The flow through was discarded and 500 µL Buffer RPE was added to the column and centrifuged at 8000 × *g* for 2 min at room temperature. The flow through was subsequently discarded and the column was transferred to a new 1.5 mL collection tube. A 30-50 µL volume of RNase-free water was pipetted directly onto the column membrane and centrifuged for 1 min at 8000 × *g* to elute the RNA from the silica membrane of the column. The concentration and purity of the eluted RNA was measured on the NanoDrop ND-1000 (section 2.5.2).

RNA extracts were stored at -20°C in the short term (< 1 month) or -80°C in the long term (>1 month).

2.5.2 RNA quantification

Total RNA extracts were quantified using the NanoDrop ND-1000 (Thermo Scientific). The pedestal was cleaned with H_2O and blanked with the appropriate reference solution. For all RNA samples RNase free-water was used as the blank. The pedestal was loaded with 1 or 2 µL of sample. The RNA concentration was measured in ng/mL. RNA samples were analysed for protein contamination (Abs 260/280, a ratio of ~2 was indicative of a pure yield) and phenol contamination (Abs 260/230, a ratio ≥ 1.7 was indicative of a pure yield).

2.5.3 Reverse transcription/cDNA synthesis for miRNA

The miScript II RT Kit (Qiagen, UK) or the TaqMan MicroRNA Reverse Transcription Kit (Applied Biosystems, UK) were used for miRNA cDNA synthesis, using total RNA extracts (section 2.5.1).

The miScript II RT Kit was used to prepare cDNA for SYBR-based quantitative polymerase chain reaction (qPCR). Working on ice throughout, the RNA samples were first diluted to 2 µg in 12 µL RNase-free water. The reverse transcription mix was prepared in 1.5 mL tubes with an additional 10% to allow for pipetting error (volumes per reaction; 4 µL HiSpec buffer, 2 µL nucleic acid mix, 2 µL reverse transcriptase mix) and 8 µL of the resulting reaction mix was added to each 0.2 mL PCR tube containing diluted RNA, to give a total volume of 20 µL per tube. Samples were mixed and pulse centrifuged (Miniplate Spinner MPS1000 Labnet, UK) to pool the contents in the tubes.

The thermal cycler (C1000 Thermal Cycler, BioRad, UK) was programmed to heat samples for 60 min at 37°C followed by 5 min at 95°C. Samples were kept on ice if immediately proceeding to qPCR, otherwise the samples were store at -20°C until required.

The TaqMan MicroRNA Reverse Transcription Kit was used to prepare cDNA for TaqMan-based qPCR. Working on ice throughout, the RNA samples were firstly diluted to 10 ng in 5 µL RNase-free water. Reverse transcription mix was prepared by combining 0.15 µL dNTPs, 1 µL MultiScribe reverse transcriptase, 1.5 µL reverse transcription buffer, 0.19 µL RNase inhibitor and 4.16 µL RNase-free water per reaction plus an additional 10% to allow for pipetting error. To each PCR tube containing 5 µL diluted RNA, 7 µL of the reverse transcription reaction mix and 3 µL of the 5× RT primer were added to give a total volume of 15 µL. Samples were mixed briefly and pulse centrifuged (Miniplate Spinner MPS1000, Labnet, USA) to pool tube contents. The thermal cycler (C1000 Thermal Cycler, BioRad, UK) was programmed to heat samples for 30 min at 16°C, 30 min at 42°C and 5 min at 85°C. Samples were kept on ice if immediately proceeding to qPCR, otherwise the samples were store at -20°C until required.

2.5.4 qPCR for miRNA analysis

Both SYBR-based and TaqMan-based qPCR detection methods were used to analyse relative miRNA expression.

The miScript SYBR Green PCR Kit and miScript primer assays (Qiagen, UK) were used for qPCR analysis of miRNA using the cDNA template produced with the miScript II RT Kit (section 2.5.3). Each sample was run in triplicate wells to allow for the exclusion of outliers in the final analysis. A 1 µL volume of cDNA, equal to 100 ng,

was pipetted into the individual wells of a 96-well PCR plate (Applied Biosystems, UK). Reaction mix was prepared (volumes per reaction; 10 µL SYBR green master mix, 2 µL universal primer, 2 µL miRNA primer assay, 5 µL RNase-free water) and following thorough mixing 19 µL of the mix was pipetted into each of the wells containing cDNA (Table 2.1). Non-template controls were also loaded into the PCR plate (1 µL of RNase free water and 19 µL of the reaction mix).The total volume per well was 20 µL. The PCR plate was covered with optically clear adhesive film (Applied Biosystems, UK) and pulse centrifuged (Miniplate Spinner MPS1000 Labnet, USA) to pool well contents. The PCR system (Step One Plus Real Time PCR System, Applied Biosystems, UK) was programmed using the advanced set up option to run the cycling conditions; initial activation for 15 min 95°C, denaturing for 15 s at 94°C, primer annealing for 30 s at 55°C, and primer extension for 30 s at 70°C. Fluorescent data collection was performed at the extension step, and the protocol ran for 40 cycles of denaturation, annealing and extension.

As an alternative the TaqMan Universal PCR Master Mix and TaqMan miRNA Assays (Applied Biosystems, UK) were used for qPCR analysis of miRNA using the cDNA template produced with the TaqMan MicroRNA Reverse Transcription Kit (section 2.5.3). Each sample was run in triplicate wells to allow for the exclusion of outliers in the final analysis. A 1.33 µL volume of cDNA, equal to ~1 ng, was pipetted into the individual wells of a 96-well PCR plate (Applied Biosystems, UK). Reaction mix was prepared (volumes per reaction; 10 µL master mix, 1 µL miRNA assay, 7.67 µL RNase-free water) and 18.67 µL of the mix was pipetted into each of the wells containing cDNA. Non-template controls were also loaded into the PCR plate (1.33 µL of RNase free water and 18.67 µL of the reaction mix).The total volume per well was 20 µL. The PCR plate was covered with optical adhesive film (Applied Biosystems, UK) and centrifuged (Miniplate Spinner MPS1000, Labnet, USA). The PCR system

(Step One Plus Real Time PCR System, Applied Bioscience, USA) was programmed using the advanced set up option to run the cycling conditions; initial activation 10 min 95°C, denaturing 15 s at 95°C, annealing/extension 60 s at 60°C. Data collection was performed at the annealing/extension step, and the protocol ran for 40 cycles of denaturation, annealing and extension.

The PCR data files were opened in the Step One Plus software (Applied Bioscience, USA) and the baselines on the amplification plots were adjusted to intersect the early exponential phase, for accurate determination of the cycle threshold (C_t). The relative expression of the miRNA targets was calculated using the $2^{-\Delta\Delta Ct}$ Livak method (Livak & Schmittgen, 2001).

Table 2.1 qPCR primers

Target	miRNA/ mRNA	Manufacturer	Catalogue no.	TaqMan/ SYBR
miR-330-3p	miRNA	Qiagen	MS00031738	SYBR
miR-330-5p	miRNA	Qiagen	MS000094520	SYBR
RNU6	miRNA	Qiagen	MS00033740	SYBR
miR-187-3p	miRNA	Applied Biosystems	001193	TaqMan
RNU48	miRNA	Applied Biosystems	001006	TaqMan
E2F1	mRNA	Qiagen	QT00016163	SYBR
MMP1	mRNA	Qiagen	QT00014581	SYBR
MMP7	mRNA	Qiagen	QT00001456	SYBR
B2M	mRNA	Qiagen	QT00088935	SYBR
PYROXD2	mRNA	Qiagen	QT00047271	SYBR
APC	mRNA	Qiagen	QT02407671	SYBR
PTEN	mRNA	Qiagen	QT00086933	SYBR
JUN	mRNA	Qiagen	QT00242956	SYBR
TNF	mRNA	Qiagen	QT00029162	SYBR
CXCL10	mRNA	Qiagen	QT01003065	SYBR
CDK6	mRNA	Qiagen	QT00019985	SYBR
MMP1	mRNA	Applied Biosystems	Hs00899658_m1	TaqMan
C3	mRNA	Applied Biosystems	Hs00163811_m1	TaqMan
CFB	mRNA	Applied Biosystems	Hs00156060_m1	TaqMan
TRANK1	mRNA	Applied Biosystems	Hs00389727_m1	TaqMan
APOL2	mRNA	Applied Biosystems	Hs01935263_s1	TaqMan
OAS1	mRNA	Applied Biosystems	Hs00973637_m1	TaqMan
IL28	mRNA	Applied Biosystems	Hs00820125_g1	TaqMan

IFNB1	mRNA	Applied Biosystems	Hs01077958_s1	TaqMan
IL22RA1	mRNA	Applied Biosystems	Hs00222035_m1	TaqMan
B2M	mRNA	Applied Biosystems	Hs00187842_m1	TaqMan

2.5.5 Reverse transcription cDNA synthesis for mRNA

The QuantiTect RT Kit (Qiagen, UK) or random hexamers (Invitrogen, UK) were used for mRNA cDNA synthesis using total RNA extracts (section 2.5.1).

The QuantiTect RT Kit was used to prepare cDNA for SYBR-based qPCR. Prior to cDNA synthesis potential genomic DNA contamination was eliminated from the RNA sample. Briefly, the RNA samples were adjusted to 1 µg in 12 µL RNase-free water in 0.2 mL PCR tubes. A 2 µL volume of gDNA wipeout buffer was added, tubes were mixed thoroughly, and the samples incubated for 2 min at 42°C in a thermal cycler (C1000 Thermal Cycler, BioRad, UK). Following incubation the tubes were kept on ice. The reverse transcription mix was prepared (volumes per reaction; 1 µL reverse transcriptase, 4 µL RT buffer, 1 µL RT primer mix) and 6 µL of the reaction mix was added to the 14 µL reaction volume used in the genomic elimination step. Samples were mixed and pulse centrifuged (Miniplate Spinner MPS1000, Labnet, USA) to pool tube contents. The thermal cycler was programmed to heat samples for 15 min at 42°C for reverse transcription and 3 min at 95°C to inactivate the reverse transcriptase mix. Samples were stored on ice if immediately preceding to qPCR, otherwise the samples were store at -20°C.

Random hexamers and were used to prepare cDNA for TaqMan based qPCR. High quality total RNA was reverse transcribed to cDNA using random hexamer oligodeoxyribonucleotides that prime mRNA for cDNA synthesis. Briefly, a volume of 1 µL of random hexamers (Promega, Wisconsin, USA) was added to 1.0 µg total RNA, and the volume adjusted to 11 µL with RNase-free water. The reaction mixture was then

incubated at 70^{o}C for 10 min and then placed on ice. The reverse transcription mix was prepared. Volumes per reaction; 0.5 µL RNasin (40 U/µL) (Promega, Wisconsin, USA), 0.5 µL 10 mM dNTP's (stock prepared as a 1:1:1:1 ratio of dATP, dCTP, dGTP, dTTP) (Promega, Wisconsin, USA), 4 µL reverse-transcription reaction buffer (250 mM Tris HCl, 375 mM KCl, 15 mM $MgCl_2$) (Invitrogen, UK), 2 µL 0.1 M dithiothreitol (DTT) (Invitrogen UK), 0.5 µL superscript II (200 U/µL) (Invitrogen, UK) and 0.5 µL RNase-free water. The reverse transcription mix was added to the RNA and random hexamer reaction and mixed well by pipetting. Samples were pooled by centrifugation and incubated at 37^{o}C for 1 h.

2.5.6 qPCR for mRNA analysis

Both SYBR-based and TaqMan-based qPCR detection methods were used to analyse relative mRNA expression.

The QuantiTect SYBR Green PCR Master Mix and QuantiTect primer assays (Qiagen, UK) were used for qPCR analysis of mRNA, using the cDNA template produced with the QuantiTect RT Kit (section 2.5.5). Each sample was run in triplicate wells to allow for the exclusion of outliers in the final analysis. A 1 µL volume of diluted cDNA equating to 20 ng was pipetted into the individual wells of a 96-well PCR plate (Applied Biosystems, UK). The reaction mix was prepared with an additional 10% to allow for pipetting error (volumes per reaction; 10 µL SYBR green PCR master mix, 2 µL primer assay, 7 µL RNase-free water) and 19 µL of the mix was pipetted into each well containing cDNA (Table 2.1). Non-template controls were also loaded into the PCR plate (1 µL of RNase free water and 19 µL of the reaction mix). The PCR plate was covered with an optically-clear adhesive film (Applied Biosystems, UK) and pulse centrifuged (Miniplate Spinner MPS1000, Labnet, USA) to pool well contents. The

PCR system (Step One Plus Real Time PCR System, Applied Biosystems, UK) was programmed using the advanced set up option to run the cycling conditions; initial activation for 15 min at 95°C, denaturing for 15 s at 94°C, annealing for 30 s at 55°C, and extension for 30 s at 72°C. Fluorescent data collection was performed at the extension step, and the protocol ran for 40 cycles of denaturation, annealing and extension.

Alternatively, the TaqMan Universal PCR Master Mix and TaqMan mRNA Assays (Applied Biosystems, UK) were used for qPCR analysis of mRNA using the cDNA template produced with the random hexamers (section 2.5.5). Each sample was run in triplicate wells to allow for the exclusion of outliers in the final analysis. A 1 µL volume of cDNA, equal to 20 ng, was pipetted into the individual wells of a 96-well PCR plate (Applied Biosystems, UK). Reaction mix was prepared with an additional 10% to allow for pipetting error (volumes per reaction; 10 µL master mix, 1 µL mRNA assay, 8 µL RNase-free water) and 19 µL of the mix was pipetted into each of the wells containing cDNA. Non-template controls were also loaded into the PCR plate (1 µL of RNase free water and 19 µL of the reaction mix).The total volume per well was 20 µL. The PCR plate was covered with optical adhesive film (Applied Biosystems, UK) and centrifuged (Miniplate Spinner MPS1000, Labnet, USA). The PCR system (Step One Plus Real Time PCR System, Applied Bioscience, USA) was programmed using the advanced set up option to run the cycling conditions; initial activation 10 min 95°C, denaturing 15 s at 95°C, annealing/extension 60 s at 60°C. Data collection was performed at the extension step, and the protocol ran for 40 cycles of denaturation, annealing and extension.

The PCR data files were opened in the StepOne Plus software (Applied Bioscience, USA) and the baselines on the amplification plots were adjusted to intersect

the early exponential phase, for accurate determination of the cycle threshold (C_t). The relative expression of the miRNA targets was calculated using the $2^{-\Delta\Delta Ct}$ Livak method (Livak & Schmittgen, 2001).

2.5.7 Digital gene expression sequencing

Total RNA extracts were prepared as previously described (section 2.5.1). The gene expression sequencing was outsourced to LC Sciences (Texas, USA). The samples were prepared for shipping as advised by LC Sciences. Briefly, 6 µg total RNA was prepared in 50 µL DEPC (diethylpyrocarbonate) water, 5 µL 3M NaOAc, pH 5.2 and 150 µL absolute ethanol to give a final volume of 205 µL. Samples were stored at -80°C prior to shipping on dry ice. High-throughput sequencing was performed using Illumina sequencing by synthesis technology. LC Sciences provided analysed gene expression data, GO (Gene Ontology) and KEGG (Kyoto Encyclopaedia of Genes and Genomes) analysis.

2.6 Protein expression

2.6.1 Protein extraction

Working on ice throughout, medium was firstly discarded and cells were washed with ice-cold PBS. Adherent cells were scraped in 1 mL PBS using a cell scraper or cells were typsinised as described in section 2.3.2. The cell suspension was transferred to a clean tube and centrifuged for 5 min at 400 × *g* at 4°C to pellet the cells. The PBS or medium was discarded and the cell pellet was resuspended in 30 - 100 µL ice-cold RIPA lysis buffer (50 mM Tris, 150 mM NaCl, 0.1% SDS, 1% Triton X-100) containing protease inhibitors (complete protease inhibitor cocktail, Roche, UK) and

phosphatase inhibitors (PhosStop, Roche, UK). Cells were incubated on ice for 30 min, and then centrifuged for 5 min at 6300 × *g* at 4°C to pellet the insoluble protein fraction. The supernatant was aliquoted into a clean tube and stored at -20°C until required.

2.6.2 Protein quantification

The concentrations of the protein extracts were determined with the Pierce Bicinchoninic Acid (BCA) Protein Assay Kit (Thermo Scientific, UK). BCA undergoes a colour change in the presence of protein. This assay is based on the biuret reaction in which Cu^{+2} is reduced to Cu^{+} in the presence of protein under alkaline conditions. The chelation between the BCA molecules and the reduced copper ions causes the formation of a purple coloured product, the absorbance of which is linear with increasing protein concentration. The concentration of protein in an unknown sample is calculated by producing a standard curve of known protein concentrations. Bovine serum albumin (BSA) at 2 mg/mL was provided with the kit. From this stock of BSA serial dilutions were performed with RIPA buffer to produce a range of known protein concentrations (8 protein standards in the range 2000 - 25 μg/mL and a RIPA buffer only blank). In a 96-well plate, 10 μL of the standards were loaded into duplicate wells. In addition to the standards, 10 μL of the unknown protein samples were loaded into duplicate wells. In some cases it was necessary to dilute the unknown sample such that the absorbance measurement fell within the measurable range of the assay (125 - 2000 μg/mL). Generally, a 4-10 fold dilution of the unknown protein sample with RIPA buffer was sufficient. The BCA reagent was prepared by combining 50 parts of reagent A (BCA-based reagent) and 1 part reagent B (4% cupric sulphate). A 200 μL volume of the working reagent was added to each well and the plate was covered with foil and

incubated at 37°C for 30 min. Absorbance was measured at 595 nm (Absorbance Microplate Reader ELx800, Biotech, USA). The absorbance of the RIPA buffer blank was subtracted from the absorbance of the standards and unknown protein samples, and duplicate samples were averaged. A standard curve was produced for the BSA protein standards by plotting absorbance (y-axis) vs. BSA concentration (x-axis). Protein concentration of the unknown sample was calculated from the standard curve using the equation of the line y=mx+c, where y=absorbance, m=gradient, x=protein concentration (μg/mL) and c= y-intercept of the line.

2.6.3 SDS-PAGE

Quantified protein samples were loaded and electrophoresed by SDS-PAGE. The polyacrylamide gel separates proteins based on charge and size. Large molecular weight proteins migrate slowly through the polyacrylamide and separate out towards the top of the gel. Small molecular weight proteins migrate faster and separate out at the bottom of the gel.

SDS-PAGE gels were hand cast (10% or 12%) or precast 4-20% gradient gels (Mini-PROTEAN TGX Stain-Free Precast Gels, BioRad). Hand cast gels were prepared according to established recipes (Appendix 2). The BioRad mini-PROTEAN Tetra System gel casting apparatus was assembled according to the manufacturer's instructions. The large glass spacer plate and the short plate were sandwiched together and clamped into the casting frames, with the spacer plate at the back. The bottom edges of the plates were level to ensure the polyacrylamide solution did not leak when loaded between the plates. The casting frames with glass plates were clamped into the casting stand. The resolving gel was prepared and loaded between the glass plates using a Pasteur pipette leaving room (~1.5 cm) at the top of the short plate for the stacking gel

and well comb. Isopropanol was gently pipetted on top of the resolving gel solution to ensure the gel set with a straight and level edge, and to facilitate the polymerisation reaction. Once the resolving gel had set (~1 h), the casting stand was lifted and tilted to remove the layer of isopropanol using absorbent tissue. The stacking gel was prepared and applied on top of the resolving gel with a Pasteur pipette. The stacking solution was used to fill remaining space and a 10 or 15 well comb was inserted, ensuring no bubbles had formed in the staking gel around the comb.

Once the stacking gel had set (~15 min) the electrophoresis system (Mini-PROTEAN Tetra Cell, BioRad, UK) was assembled. Up to four gels were run simultaneously per tank, with two gels clamped into each gasket and the short plate facing in towards the centre of the gasket. If only a single gel was used the buffer dam was secured in the other side of the gasket. Gasket(s) were secured in the tank, such that positive and negative electrodes were in the correct orientation. The gasket and tank were filled with 1× running buffer (10× running buffer: 30.2 g Tris base, 144 g glycine, 100 mL 10% SDS made up to 1 L with H_2O). The wells of the gel were flushed with a 1 mL syringe and a 25-gauge needle filled with running buffer to clear the wells of residual polyacrylamide gel before loading the samples.

Based on BCA assay quantification (section 2.6.2), samples were prepared such that 30 - 50 μg of protein was loaded per well. Concentrated protein samples were diluted with RIPA buffer (containing protease and phosphtase inhibitors). Loading buffer constitutes a proportion of the 20 μL total volume, 5 μL of the total volume was loading buffer. Samples were mixed and heated to 95°C for 8 min (Techne Dri-Block DB-3D, Sigma Aldrich, UK). Samples were centrifuged briefly to pool the entire sample in the bottom of the tube, and 20 μL of sample was loaded per well. Molecular weight markers were loaded into the first and/or last lanes (5 μL 1kB PageRuler Plus

Prestained Protein Ladder, ThermoScientific, UK and 2 μL of the Precision Plus Protein WesternC Standards, BioRad, UK). The gel electrophoresed for 1-2 h at 100-150 V (PowerPac Universal, BioRad, UK) until the dye front reached the bottom of the gel. The glass plates were carefully separated and the gel was transferred to a dish containing 1× transfer buffer for 3-5 min (10× transfer buffer: 30.2 g Tris base, 144 g glycine made up to 1 L with H_2O) to equilibrate the gel prior to Western blotting.

2.6.4 Western blotting

Proteins in the polyacrylamide gel were transferred onto a PVDF (polyvinylidene fluoride) 0.2 μm transfer membrane (Thermo Scientific, UK) for Western blotting. The PVDF is probed for a specific protein using primary antibodies that bind specifically to an epitope within the protein of interest. The PVDF is then probed with a secondary antibody that specifically binds to the primary antibody. The secondary antibody is linked to the enzyme horseradish peroxidise (HRP). When a chemiluminescent substrate is applied to the PVDF, the HRP catalyses a hydrogen peroxide substrate producing light (chemiluminescence), which is detected on X-ray film (autoradiography) or with a chemiluminescent imaging system (Molecular Imager ChemiDoc XRS with Image Lab 3.0 software, BioRad, UK).

To assemble the transfer cassettes, sponges and filter papers were first soaked in 1× transfer buffer (section 2.6.3). The PVDF was activated in methanol for 5 s followed by equilibration in 1× transfer buffer. The transfer cassette was assembled (on the clear side of the cassette) in the following order; sponge, 2 filter papers, PVDF, gel, 2 filter papers and sponge. Between each component a roller was used to gently remove air bubbles between the layers and the stack was kept moist with 1× transfer buffer. The cassette was closed, secured and slotted into the transfer gasket in the tank, such that

positive and negative electrodes were in the correct orientation. The current flows from negative to positive and the negatively charged proteins were transferred onto the PVDF. A magnetic stir bar in the bottom of the tank and an ice pack were used to dissipate the heat generated during transfer. The tank was filled to the blotting mark with 1× transfer buffer and the transfer ran at 100 V for 1.5-2 h.

When disassembling the cassette the orientation of the PVDF was noted by cutting the top right corner. The PVDF was then blocked with 5% milk (skimmed dried milk powder) 1× TBS supplemented with 0.1% Tween (TBST) (10× TBS: 88 g NaCl, 24 g Tris base made up 1 L in ultrapure H_2O) solution for 1 h with agitation. The blocking step prevents non-specific binding of the antibodies to the PVDF. The PVDF was first probed with the primary antibody diluted in 5 mL 5% milk TBST, or 5% BSA TBST, in a 50 mL tube (Table 2.2). The PVDF was transferred to the tube and incubated on a roller for 2 h at room temperature or overnight at 4°C, depending on the recommendations of the antibody manufacturer's. The PVDF was washed 3 times, at 10 min intervals, with 1× TBST and then probed with the secondary antibody (Table 2.2). The secondary antibody was diluted in 5 mL 5% milk TBST in a 50 mL tube, and the PVDF was incubated on a roller for 1 h at room temperature. When using the Protein WesternC Standards 0.25 µL StrepTactin HRP conjugate (BioRad, UK) was added to the diluted secondary antibody. The PVDF was washed 3 times, at 10 min intervals, with 1× TBST.

The chemiluminescent substrate was prepared according to the manufacturer's instructions (Clarity Western ECL Substrate, BioRad). Two reagents were combined in a 1:1 ratio, for a single PVDF membrane 1-2 mL of substrate solution was required. Substrate solution was applied to the PVDF and incubated for 5 min. The PVDF was sandwiched between two sheets of acetate and any bubbles and excess solution were

removed by blotting with paper towel. The PVDF was imaged using a chemiluminescent imaging system (Molecular Imager ChemiDoc XRS with Image Lab 3.0 software, BioRad, UK) or autoradiography (section 2.6.7). Western blots were analysed using densitometry (section 2.6.8).

Table 2.2 Antibodies

Target	Manufacturer	Catalogue no.	Species	Dilution
E2F1	Santa Cruz	sc-251	Mouse mAb	1:1000
turboGFP	Origene	TA150041	Mouse mAb	1:10000
β-actin	Santa Cruz	sc-69879	Mouse mAb	1:10000
MMP1	R and D Systems	MAB901	Mouse mAb	1:1000
MMP7	R and S Systems	MAB9071	Mouse mAb	1:1000
cleaved PARP	Cell Signaling	#5625	Rabbit mAb	1:1000
cleaved caspase-3	Cell Signaling	#9664	Rabbit mAb	1:1000
GAPDH	Ambion	AM4300	Mouse mAb	1:1000
Anti-rabbit	Cell Signaling	#7074	Goat pAb	1:2000
Anti-mouse	Dako	P0260	Rabbit pAb	1:2000

mAb, monoclonal antibody; *pAb*, polyclonal antibody

2.6.5 Antibody-based arrays

Antibody-based arrays were used to assess the relative expression levels of 32 proteases and 35 protease inhibitors (Proteome Profiler antibody arrays, R and D Systems, UK) as per the manufacturer's instructions. Briefly, the nitrocellulose membranes were pre-spotted with capture antibodies, in duplicate. Conditioned serum free media was prepared and concentrated as outlined in section 2.6.6, with the exception of the concentrating column centrifugation time which was reduced to 30 min. Approximately 200 µL of concentrated media was recovered and quantified using the BCA assay (section 2.6.2). Each membrane was blocked for 1 h using the array buffer provided. Samples were prepared and incubated for 1 h (75 µg protein plus 1.4 mL of array buffer and 15 µL of the relevant antibody cocktail). The samples were applied to the blocked membrane and incubated overnight at 4°C on a rocking platform

shaker. Membranes were washed with the provided buffer, for 30 min with two buffer changes during that time. The membranes were subsequently incubated with Streptavidin-HRP for 30 min on a rocking platform shaker, then washed again for 30 min with two buffer changes during that time. Chemiluminescent substrate was provided, and prepared according to the manufacturer's instructions. To each membrane 1 mL of chemiluminescent solution was applied and incubated for 1 min. The membranes were sandwiched between two sheets of acetate and any bubbles and excess solution were removed. Autoradiography was used to develop blots on X-ray film (section 2.6.7) and these were analysed using densitometry (section 2.6.8).

2.6.6 Gelatin zymography

Zymography is a technique used to detect hydrolytically active enzymes, such as matrix metalloproteinases (MMPs). Samples are prepared in non-reducing sample buffer and are separated using conventional SDS-PAGE. The substrate, which is degraded by the enzyme of interest, is incorporated into the polyacrylamide gel. Following electrophoretic separation of the proteins under non-denaturing conditions, the proteins in the zymogram are re-natured and subsequently degrade the substrate embedded within the gel (Frankowski et al., 2012).

The MMP1 protein is produced as an inactive enzyme precursor, or zymogen, which is transported out of the cell into the extracellular environment (Tallant et al., 2010). The enzyme is activated in the extracellular environment and degrades interstitial collagens (types I, II and III). Gelatin zymography was used to detect the presence and activity of MMP1 in conditioned serum free media. In 6 cm dishes, 8×10^5 cells were seeded in complete medium and incubated for 48 h to reach ~70% confluency. The medium was discarded, cells were washed with PBS and 2.5 mL of serum free RPMI

1640 was applied. Cells were incubated for 24 h, and then the conditioned medium was subsequently decanted into a 15 mL tube and centrifuged at 4°C for 5 min at 300 × *g* to pellet non-adherent cells and debris. The conditioned medium was then transferred into a centrifugal filter column (5 kDa molecular weight cut-off) to concentrate the protein (Vivaspin® 4 Sartorius, Fisher UK). Columns were centrifuged at 4°C for 60 – 70 min at 4000 × *g* in a centrifuge with a swing bucket rotor (5804R, Eppendorf, Cole-Parmer, UK). Approximately 100 µL of concentrated protein sample was recovered after this time.

Samples were prepared for zymography by combining 20 µL concentrated medium with 5 µL 5× sample buffer (5× non-reducing sample buffer; 313 mM Tris, pH 6.8, 10% SDS, 50% glycerol, 0.05% bromophenol blue). In addition, a serial dilution 1:8–1:20 of the concentrated protein samples were also prepared for zymography. Gelatin gels were prepared using the same procedure and equipment as SDS-PAGE (section 2.6.3). The gels contained 1 mg/mL gelatin and 10% acrylamide (recipe for two gels; 8.3 mL 2.65 mg/mL gelatin, 5.25 mL 1.5M Tris, pH 8.8, 7 mL 30% acrylamide, 165 µL 50% glycerol, 165 µL 10% SDS, 10 µL TEMED, 100 µL 10% APS). Prepared samples, 25 µL, were loaded into individual wells and tanks were filled with cold running buffer (section 2.6.3). Gels were ran at 120 V for 2 h. Gels were transferred into renaturing wash buffer (2.5% Triton-X, 50 mM Tris pH 7.4, 5 mM $CaCl_2$) for 1 h, during which time the buffer was changed three times. The zymogram was rinsed in deionised water and incubated in developing buffer (50 mM Tris, pH 7.4, 5 mM $CaCl_2$) at 37°C overnight. Zymograms were stained with coomassie stain (0.125% w/v coomassie brilliant blue R-250, 1% v/v acetic acid, 45% v/v ethanol, 54% v/v water) for 1 h and destained with solution I (62.5% v/v ethanol, 25% v/v acetic acid, 12.5% v/v water) for 30 min and solution II (0.05% v/v ethanol, 7% v/v acetic acid, 92.95% v/v water) for 1 h. Zymograms were washed with water for 30 min and stored in gel

preservative solution (3% v/v glycerol, 30% v/v methanol, 67% v/v water). Zymograms were imaged using the coomassie setting on the imager (Molecular Imager ChemiDoc XRS with Image Lab 3.0 software, BioRad, UK). The images appear as a 'reverse' coomassie, with the zymogram staining gelatin blue and the hydrolase activity of the enzyme visible as a white band/cleared area.

2.6.7 Autoradiography

The PVDF membrane, sandwiched between two sheets of acetate, was secured in the autoradiography developing cassette (Hypercassette, Amersham Biosciences, USA). Working in the dark room, a sheet of X-ray film was placed over the acetate and the cassette was firmly closed. The exposure time varied between different antibodies, but exposure times were typically in the range of 5-180 s. The film was removed from the cassette and agitated in a tray containing developer solution (Universal Champion Photochemistry, Malaysia) for ~20 s, then washed briefly in water and agitated in fixer solution (Universal, Champion Photochemistry Malaysia) until the film had turned from opaque to transparent. Once the film was transparent it was again briefly washed with water and left to air dry at room temperature.

2.6.8 Densitometry

Blots developed on X-ray film were imaged on the chemiluminescent imaging system using the white light option (Molecular Imager ChemiDoc XRS with Image Lab 3.0 software, BioRad, UK). Alternatively blots imaged on the chemiluminescent imaging system directly were opened from saved files. Using the Image Lab 3.0 software the volume tool was selected and boxes, of the same dimensions, were drawn

around the bands of interest. The analysis table option was selected and the volume intensity of each band was recorded in a spreadsheet. For each sample/ lane the volume intensity of the band(s) of interest were normalised against the β-actin loading control, by dividing the volume intensity of the band of interest by the volume intensity of the β-actin band. The relative densities of the samples were then normalised to the control sample.

2.6.9 Phospho-Akt ELISA

Levels of phosphorylated Akt (p-Akt) were measured in protein extracts using an enzyme-linked immunosorbent assay (ELISA) (DuoSet p-Akt 1/2/3 ELISA, R&D Systems) according to the manufacturer's instructions. Briefly, a 96-well plate was coated with the capture antibody. Under aseptic conditions a 100 µL volume of capture antibody solution (1080 µg/mL) was applied to each well and incubated overnight at room temperature. The wells of the plate were washed thoroughly 3 times with the wash buffer supplied with the kit. A 300 µL volume of blocking buffer was added to each well and the plate was incubated at room temperature for 2 h. The wells of the plate were washed thoroughly 3 times with wash buffer. The standards were prepared according to manufacturer's instructions (seven standards 20,000-312.5 pg/mL range). Protein extracts were prepared from cultured cells (section 2.6.1) and the protein concentration was determined (section 2.6.2). The samples were loaded in duplicate. A 100 µL volume of sample containing 100 µg protein was added to each well and the plate was incubated for 2 h at room temperature. The washing steps were repeated as previously described and 100 µL streptavidin-HRP conjugate was added to each well, and the plate was incubated for 20 min in the dark. The reaction was stopped by adding 50 µL stop solution to each well and the optical density was measured at 450 nm using a

microplate reader (Absorbance Microplate Reader ELx800, Biotech, USA). The absorbance readings of the duplicate samples were averaged and the blank reading was subtracted. Sample readings were normalised to the relevant control.

2.6.10 Immunohistochemistry

Tissue microarrays (TMA) were constructed from formalin-fixed paraffin-embedded pre-treatment tumour biopsies using 0.6 mm cores. Immunohistochemistry was performed using a Vectastain Elite ABC Kit (catalogue number PK-6100, Vector Laboratories, UK), as per the manufacturer's instructions. Slides were deparaffinised, rehydrated and heated-antigen retrieval was performed using Trilogy solution (Cell Marque Corporation, California, USA). Endogenous peroxidase activity was blocked using hydrogen peroxide (3%) for 30 min and sections were blocked using horse serum and incubated with rabbit-anti-human C3 antibody (5 µg/mL, catalogue number Ab97462, Abcam, UK) for 1 h at room temperature. Sections were then incubated with secondary antibody/horseradish peroxidise for 30 min at room temperature. Diaminobenzidine (Sigma, UK) was used to visualise staining and sections were counter-stained with haematoxylin, dehydrated and mounted. Stained sections were scanned using a scanscope XT digital scanner and ImageScope software (Aperio Technologies, UK).

The TMAs of the pre-treatment tumour biopsies (7 responders, 16 non-responders) were assessed by three independent scores. The percentage positivity and staining intensity scores were assigned separately for the epithelium and stromal compartments of the TMA cores. The percentage positivity was the percentage of cells stained positive for C3 using the following categories; 0%, 10%, 25%, 50%, 75%, 90%

and 100%. The staining intensity was categorised as negative (0), weak (1), medium (2) and strong (3). The three sets of scores were complied and analysed.

2.7 Cell-based assays

2.7.1 Clonogenic assay

Cells were harvested and counted as previously described (section 2.3.2). The cells were seeded at a density of 500-3000 cells per well in a 6-well plate with 2 mL medium and allowed to adhere overnight in the incubator. For chemotherapy-based clonogenic assays, the medium was carefully removed so as not to disturb the adhered single cells from the base of the well. Treatment and control media were prepared from frozen stock solutions (section 2.1.1) and 2 mL treatment or control medium was added to each well. The plates were returned to the incubator and after 24 h of treatment the medium was removed and replaced with 3 mL complete medium. For radiation-based clonogenic assays, the plates were transported to irradiator and were exposed to 2 or 4 Gy radiation as described in section 2.1.2). The plates were incubated for 7 - 14 days. Approximately 50 cells constituted a visible colony, and from 7 days onwards plates were checked daily to determine whether or not sufficient colony numbers and colony sizes were developing in the wells. Medium was aspirated from the plates (Intergra Vacsafe, Switzerland) and 2 mL PBS was gently applied to wash the wells and then aspirated from the plates. Approximately 2 mL crystal violet fix and stain solution (0.1% w/v crystal violet, 70% v/v methanol, 30% v/v deionised H_2O) was applied to each well. Plates were incubated for 1 h at room temperature. Crystal violet solution was removed from the wells with a Pasteur pipette and crystal violet waste was inactivated with NaOH. Plates were submerged in a water bath to wash the remaining crystal violet solution from the wells and were air dried at room temperature. Colonies

were counted using a GelCount instrument (Oxford Optronics, UK). CHARM (compact Hough and radial map) algorithm settings were optimised for counting colonies for each cell line, and the average number of colonies per plate was used to calculate the surviving fraction (Appendix 3). The plating efficiency was equal to the average number of colonies per plate divided by the number of cells seeded per well. The surviving fraction was equal to the average number of colonies per plate divided by the plating efficiency of the control, multiplied by the seeding density. To calculate the surviving fraction of treated cells (cisplatin, 5-FU or radiation), the plating efficiency for the untreated control (PBS, DMSO or mock-irradiated) was used in the calculation.

2.7.2 MTS cell proliferation/viability assay

The CellTiter 96 AQ_{ueous} One Solution Proliferation Assay (Promega, UK) is a colourmetric assay for the determination of viable cells in proliferation or cytotoxicity assays. The one solution reagent contains the tetrazolium compound MTS which is added to cell culture media and is reduced by the metabolically active viable cells to produce a soluble, coloured formazan product. Absorbance of the coloured product can be measured at Abs 490 nm. The quantity of the formazan product is proportional to the number of viable cells.

Cells were seeded into 96-well plates at a density of 1000 cells/well in 100 μL medium, with each sample loaded in triplicate, including a medium only control. The plates were incubated at 37°C overnight to allow cells to adhere. Medium was removed from the wells and 100 μL treatment or vehicle control medium was added. Plates were returned to the incubator. A 20 μL volume of MTS reagent (Promega, UK) was applied to the wells 24, 48 or 72 h post-treatment. The plates were incubated for 3-4 h at 37°C. Absorbance measurements were taken at 490 nm (Absorbance Microplate Reader

ELx800, Biotech, USA). The absorbance readings for each triplicate were averaged and the media only absorbance value was subtracted from the sample readings.

2.7.3 MT cell viability assay

The Real-Time Glo MT Cell Viability Assay (Promega, UK) is a nonlytic, bioluminescence assay for the determination of viable cells in real-time proliferation or cytotoxicity assays. The MT cell viability substrate contains a cell-permeant prosubstrate which is added to cell culture media with the NanoLuc luciferase. The prosubstrate is reduced by metabolically active viable cells to produce a substrate which diffuses from the cell. The substrate is used by the NanoLuc luciferase to produce a luminescent signal which is proportional to the number of viable cells in culture. The MT cell viability reagent is stable in cell culture at 37°C for at least 72 h, enabling real-time cell viability measurements.

Cells were seeded in white opaque 96-well plates at a density of 3000 cells per/well in 50 µL medium, with each sample loaded in triplicate, including a medium only control. The plates were incubated at 37°C overnight to allow cells to adhere. The 2× MT reagent was prepared by diluting 2 µL MT cell viability substrate and 2 µL NanoLuc enzyme in 1 mL medium (RealTime-Glo™ MT Cell Viability Assay, Promega, UK). To each well, 50 µL MT reagent mix was added, and the plate was returned to the incubator. The first luminescence reading (0 h) was taken 30 min after the addition of the MT reagent using a luminometer (1000 ms integration time) (Fluoroscan Ascent FL, Thermoscientific, UK). Immediately after the first reading plates were treated with 2 Gy radiation or were mock-irradiated. Plates were returned to the incubator and luminescence readings were taken at 4, 24 and 48 h post-treatment. The 0 h pre-treatment reading was normalised to 1 and the change in viability over the

time course was calculated from the time point reading (4, 24 or 48 h) divided by the 0 h reading.

2.7.4 Invasion assay

The Corning BioCoat Growth Factor Reduced matrigel Invasion Chamber (8 micron membrane) assay was used to measure cellular invasion (VWR, UK). Matrigel inserts were rehydrated with 500 µL serum free medium for 2 h at 37°C. Cells were harvested and counted as previously described (section 2.3.2). A cell suspension of 5×10^4 cell/mL was prepared in serum free medium supplemented with 0.1% BSA. The wells of a 24-well plate were filled with 750 µL medium, supplemented with 10% FBS, as a chemo-attractant. The rehydration medium was carefully removed from the matrigel inserts, and the inserts were placed in the top of the wells of the 24-well plate, ensuring no bubbles were trapped between the insert and the medium in the well. Inserts without matrigel were used as a control. Cells were immediately seeded into the inserts at a density of 2.5×10^4 cells per insert. Plates were incubated for 24 h in the tissue culture incubator. Invasive cells were stimulated by the chemo attractant and invaded through the matrigel layer and across the membrane. The invasive cells adhered to the surface of the lower membrane on the outside of the insert.

After incubation the matrigel and non-invasive cells were removed by 'scrubbing'. Using a cotton tipped swab the matrigel was removed from inside the insert, by apply gently but firm pressure over the upper surface of the membrane. Control inserts were also 'scrubbed' to remove non-invasive cells adhered to the upper membrane surface. This procedure was repeated a second time with a swab moistened with medium. Inserts were washed in PBS and fixed in methanol for 15 min. The inserts were inverted and the membrane was cut away from the plastic using a scalpel.

Membranes were mounted onto glass sides with mounting media containing DAPI stain (ProLong Gold Antifade Mountant with DAPI, Invitrogen, UK). Membranes were mounted onto slides with the lower membrane, where the invasive cells were adhered, in contact with the DAPI mounting medium. Glass cover slips were secured over the membrane and mounting medium and the cover slip was sealed and secured with clear nail varnish. Slides were dried and stored in the dark at 4°C. Slides were visualised under the microscope using the DAPI filter and × 10 magnification (section 2.4.6). All of the DAPI stained nuclei on the membrane were counted using Image J software or by manually counting the DAPI stained nuclei. Data was expressed as invasion index. The first calculation was the percentage invasion; (number of cells invading through the matrigel insert membrane / number of cells migration through the control insert membrane) ×100. The second calculation (invasion index) was the percentage invasion of the test cell (i.e. miRZIP-330-5p) divided by the percentage invasion of the control cell (i.e. miRZIP-VC); (% invasion test cell / % invasion control cell).

2.7.5 Propidium iodide-based flow cytometry cell death assay

Propidium iodide (PI) is a fluorescent molecule that intercalates with DNA. Viable cells with an intact cell membrane exclude PI. Cells in the latter stages of apoptosis and necrosis loose membrane integrity and are permeable to PI. The uptake of PI can be measured using flow cytometry in the FL-2 channel. Cells were seeded and reverse transfected (section 2.4.5) in 6-well plates, 5×10^5 cells/well for 24 h or 3.5×10^5 cells/well for 48 h. Cells were harvested 24 or 48 h post-transfection. Cells harvested after 48 h were supplemented with 1 mL/well complete medium 24 h post-transfection. Both adherent and non-adherent cells were recovered. Medium containing the non-adherent cells was collected in flow cytomtery (Falcon) tubes. The adherent cells were

washed with PBS, and the PBS wash was added to the tubes. Trypsin was applied to detach the adherent cells, then medium was subsequently added to inactive the trypsin and the resulting cell suspension was added to the tubes. Tubes were centrifuged at 300 × *g* for 5 min to pellets the cells. The supernatant was discarded to waste and cells were resuspended in 500 µL PBS. Tubes were then centrifuged for 5 min at 300 × *g* to pellets the cells. The supernatant was discarded and the cells were thoroughly resuspended in 500 µL PBS or 500 µL PI solution (1/4000 dilution of 1 mg/mL PI stock in PBS). Sample were analysed on the FACSCalibur (BD Biosciences, USA).

2.8 *In vivo* tumour xenografts

2.8.1 Preparation of tumour cells for *in vivo* implants

Cells were prepared for subcutaneous injection into CD1 nude mice. Mice were injected with 4×10^6 cells prepared with matrigel (matrigel basement membrane matrix, BD Biosciences, USA). The addition of matrigel has previously been reported to enhance uptake and growth of subcutaneously injected tumour cells (Fridman et al., 2012). Sub-confluent cells were harvested and counted as previously described (section 2.3.2). Cell pellets were stored on ice to preventing gelling when mixed with the matrigel. The cell pellet was dispersed by gentle tapping. The volume of the dispersed pellet was determined using a pipette with the plastic tip cut to create a larger bore, to enable uptake of the cell pellet. Cells were resuspended in a 1:1 mixture of serum free medium and matrigel, taking into account the volume of the pellet, to give a final concentration of 4×10^7 cells/mL. The serum free medium was added to the pellet first and allowed to cool on ice before the addition of the matrigel. For each cell line, six mice were injected, subcutaneously on the right flank, with 0.1 mL of cell suspension mixture. Tumour measurements were recorded 2-4 times per week once palpable.

2.8.2 *In vivo* cisplatin treatment

Mice were treated with 2.5 mg/kg cisplatin twice per week. Treatment began when the tumour volume reached ~200 mm^3. Cisplatin was prepared fresh each week in sterile saline solution and delivered by intraperitoneal injection.

2.8.3 *In vivo* ^{18}F-FDG PET-CT imaging

Mice were weighed and then anaesthetised using and induction chamber and 2% isoflurane (oxygen 2 L/min). Mice were transferred onto an anaesthetic face mask on a heat bed and were injected subcutaneously with 50 mL/kg of sterile saline. The mouse tail was immersed in warm water to dilate the tail vein prior to the implantation of a catheter. Mice were transferred to the temperature controlled imaging bed and attached to an anaesthetic face mask. Mice were injected intravenously with ~10 MBq of ^{18}F-FDG in a total volume < 200 µL at the start of the 90 min PET imaging session. A CT scan was acquired, and temperature and respiration were monitored throughout scanning.

2.9 Statistical analysis

The standard deviation (SD) is the variability or scatter between the individual data points that are used to calculate the average. The standard error of the mean (SEM) is calculated from the SD and the sample size (*n*). The SEM is equal to the SD divided by the square root of *n*. The SEM quantifies the precision of the mean and is a measure of the deviation between the sample mean and the true population mean.

Data are presented throughout as the mean ± SEM. The SEM error bars estimate how far the sample mean deviates from the true mean. Statistical tests were used to

determine if there was a significant difference between two or more set of data. Statistical tests generate a *P* value, which indicates the probability of observing the difference between the data sets even if the population means are identical. Statistical significance was set at $p<0.05$ i.e. there was a 5% chance of observing differences as large as those observed between the groups of data even if the population means were identical. Statistical tests were performed using GraphPad InStat v3 (GraphPad software Inc, California, USA). When comparing two sets of data a *t*-test was used, for more than two sets of data an analysis of variance (ANOVA) was employed. The reported P values are from two-tailed statistical tests, the two-tailed tests are more conservative as they do not require the user to select the group that is assumed to have the larger mean. The data sets were analysed using a paired *t*-test or repeated measures ANOVA if the experimental design involved a control and treated group(s) that were prepared and handled in parallel. The unpaired *t*-test or one-way ANOVA was used to analysis data sets that were not paired or matched. The one-sample *t*-test was used to determine if the mean of a single data set deviated from the hypothetical mean. The Wilcoxon matched pairs test was used to analyse non-parametric paired data sets. The Mann Whitney U-test was used to analyse unmatched patient samples. The Spearman rank test was used to analyse correlation and regression between two nonparametric data sets. The statistical tests that were used for each experiment are disclosed in the figure legends. Graphs were produced using GraphPad PRISM 6 (GraphPad software Inc, California, USA).

Chapter 3 MicroRNA Expression Profiling in OAC Patients

3.1 Introduction

The standard of care for patients diagnosed with OAC is neoadjuvant chemoradiation therapy (neo-CRT) or neoadjuvant chemotherapy followed by surgical resection. The aim of neoadjuvant therapies is to abolish or at least shrink the volume of the tumour and prevent disease progression. Tumour regression can ease the difficulty of surgery and improve patient outcome. Furthermore, systemic chemotherapy can prevent metastasis of locally advance disease and can also treat micrometastasis that may not have advanced to a clinically detectable threshold. The overall consensus is that a combination of neoadjuvant therapy and surgery is more effective than surgery, chemotherapy or radiotherapy alone (Dai & Shah, 2015). Neo-CRT has been reported to increase the rate of pCR, R0 resection and local tumour control all of which improve patient outcome and disease free survival (Campbell & Villaflor, 2010). In 2012 the CROSS trial reported a significant increase in overall and disease free-survival in patients who received neo-CRT and surgery compared to surgery alone (van Hagen et al., 2012). In the UK trials are ongoing to establish the optimal neoadjuvant treatment regimen for patients. The NEOSCOPE trial is currently evaluating the addition of radiotherapy to current neoadjuvant chemotherapy, which is the UK standard of care at this time (Mukherjee et al., 2015).

Of the patients who receive neo-CRT, 18-35% have a pCR which is a proxy for improved prognosis and a reported 50-60% increase in 5 year survival rate (Geh et al., 2006; Stahl et al., 2009). Unfortunately, the majority of patients (~60-70%) do not respond to neo-CRT and the 5 year survival rate for OAC patients after treatment is 23% (Allum et al., 2009). Consequently, the patients who fail to respond to neo-CRT are subjected to an aggressive treatment regimen from which they gain little or no benefit. In some cases the patient's disease progresses during the neoadjuvant therapy regimen, thereby increasing the difficulty and reducing the success of surgery which

adversely affects patient prognosis (Kelsen, 2000; Skinner et al., 2014). The identification of biomarkers in a pre-treatment setting, which predict patient response to neo-CRT, could aid treatment stratification for patients at the point of diagnosis. Furthermore, novel therapeutic agents targeting biological molecules that modulate response to treatment could enhance patient response to conventional CRT as part of multimodal, synergistic treatment regimens. Considering the 50-60% increase in the 5 year survival rate for patients with a pCR, additional therapies to enhance the efficacy of conventional CRT could significant improve prognosis for the majority of OAC patients.

MiRNA are a family of short non-coding RNAs that repress the translation of mRNA targets (Bartel, 2004). Perfect Watson-Crick binding between the miRNA and its mRNA target is not essential, therefore a single miRNA can potentially target thousands of mRNA (Peter, 2010). MiRNA are predicted to regulate 30-60% of protein coding genes and are essential regulators of normal cellular processes. Approximately 50% of miRNA genes are located within cancer-associated genomic regions or chromosomal fragile sites and are susceptible to amplification, translocation or deletion (Calin et al., 2004). There is global downregulation of miRNA expression in cancer tissue compared to normal tissue and dysregulated miRNA expression plays a causal role in the development and progression of cancer. Cancer associated miRNA are referred to as ‘oncomirs’ and they may act as tumour suppressors or oncogenes (Esquela-Kerscher & Slack, 2006). The link between dysregulated miRNA expression and cancer has potential clinical applications as miRNA are promising cancer biomarkers and novel therapeutic targets. Furthermore, miRNA have been identified as predictors and modulators of chemo and radiotherapy sensitivity in cancer (Hummel et al., 2010). Advances in miRNA profiling techniques have identified miRNA signatures predictive of treatment response by screening patient tissue samples. Predictive miRNA

signatures are promising clinical biomarkers however, these miRNA are also potential modulators of treatment response and hold greater promise as therapeutic targets. In this study the aim was to identify and investigate the role of miRNA that potentially modulate tumour response and sensitivity to CRT in OAC.

3.2 Rationale, aims and objectives

In this chapter, the aim was to identify miRNA which were differentially expressed between OAC patients who responded and OAC patients who did not respond to neo-CRT. Global miRNA expression profiling of diagnostic pre-treatment patient biopsies from responders and non-responders was employed to identify differentially expressed miRNA. Beyond this chapter the functions of selected miRNA were investigated as modulators of CRT sensitivity.

- Identify differentially expressed miRNA in OAC neo-CRT responders and non-responders using diagnostic pre-treatment biopsy specimens and miRNA arrays.

3.3 Materials and methods

3.3.1 Patient sample acquisition, treatment and pathological assessment

Diagnostic pre-treatment endoscopic biopsies were taken from patients diagnosed with operable OAC (section 2.2.1). Patient biopsy samples were stored in RNA later (Ambion, UK) and refrigerated for 24 h before storage in the biobank (-80°C). Patients under took a neo-CRT regimen consisting of; 5-FU, cisplatin and fractioned doses of radiotherapy totalling 40.5 or 44 Gy (section 2.2.2). Surgical resection was performed within 1 month of neo-CRT regimen completion. A tumour regression grade (TRG 1-5) was allocated based on the Mandard method (Mandard et al., 1994). For the purpose of this study TRG 3 patients were not included.

3.3.2 MiRNA expression arrays in patient samples

Total RNA was extracted from the patient biopsy samples and quantified using the nanodrop (sections 2.2.3 and 2.5.2). The pre-treatment biopsy tissue samples of 9 responders and 10 non-responders were selected for miRNA expression analysis (Table 3.1). The expression of 742 miRNA were analysed in each of the 19 patient biopsy specimens using Human miRCURY LNA Universal RT miRNA arrays, panel I and II (Exiqon, Denmark) and a 7900HT RT-PCR system (Applied Biosystems, UK) (section 2.2.4). Analysis was performed using GenEx 5.0 software (MultiD Analyses AB, Sweden) with global normalization of the mean used for data normalization.

3.4 Results

3.4.1 MiR-330-5p and miR-187 were downregulated in the pre-treatment biopsies from neo-CRT non-responders

Diagnostic pre-treatment endoscopic biopsy samples were taken from OAC patients and stored in the biobank. Following diagnosis those patients who were considered suitable received neo-CRT followed by surgical resection. At the point of surgical resection a tumour regression grade (TRG) was allocated by an experienced pathologist. Patients allocated TRG 1 and 2 were considered responders to neo-CRT and patients allocated TRG 4 and 5 were considered non-responders. Patients allocated TRG 3 on the border between responders and non-responders, these tumours displayed histological evidence of tumour and fibrotic tissue in equal measure and were excluded from this study. The miRNA expression profiles of pre-treatment biopsies, taken from 9 responders and 10 non-responders, were determined via qPCR based arrays (Table 3.1). Of the 742 miRNA analysed, 67 miRNA were differentially expressed between responders and non-responders (Appendix 4).

Of the 67 differentially expressed miRNA, miR-330-5p was the most downregulated miRNA in the non-responders (responders 0.54 ± 8.09 *vs.* non-responders -12.72 ± 1.23) (Fig 3.1 A). The expression of miR-330-5p was significantly higher in patients with TRG 1 and 2 compared to TRG 4 patients (Fig 3.1 B). The two outlier values in the responders group corresponded to the two biopsy samples that were not derived from tumours graded clinical stage T3 (T*is* 18.37 and T2 -12.84).

The expression of miR-187 was also downregulated in the non-responders (responders 0.55 ± 0.73 *vs.* non-responders -0.97 ± 0.98) (Fig 3.2 A). There was significantly higher miR-187 expression in patients with TRG 1 and 2 compared to TRG 4 patients (Fig 3.2 B).

Table 3.1 OAC patient cohort characteristics.

Patient demographics		miRNA profiling arrays patient cohort (*n*=19)
Gender	Male	17
	Female	2
Age (years)[1]		65 (37-75)
Tumour Differentiation	Well	0
	Moderate	8
	Poor	11
Histology	OSC	1
	OAC	18
Clinical TNM staging	T*is*	1
	T1	0
	T2	1
	T3	17
	T4	0
	N0	8
	N1	11
	Mx	5
	M0	14
Overall clinical TNM stage	0	0
	I	0
	IIa	7
	IIb	2
	III	10
	IV	0
TRG	1	4
	2	5
	3	0

	4	8
	5	2

OSC, oesophageal squamous cell carcinoma; *OAC*, oesophageal adenocarcinoma; *TNM*, tumour-node-metastasis clinical staging classification; *Tis*, tumour *in situ*; *N0*, lymph node negative; *N1*, lymph node positive; *Mx*, distant metastasis could not be evaluated; *M0*, no distant metastasis; *TRG*, tumour regression grade.
[1]Values are median (range)

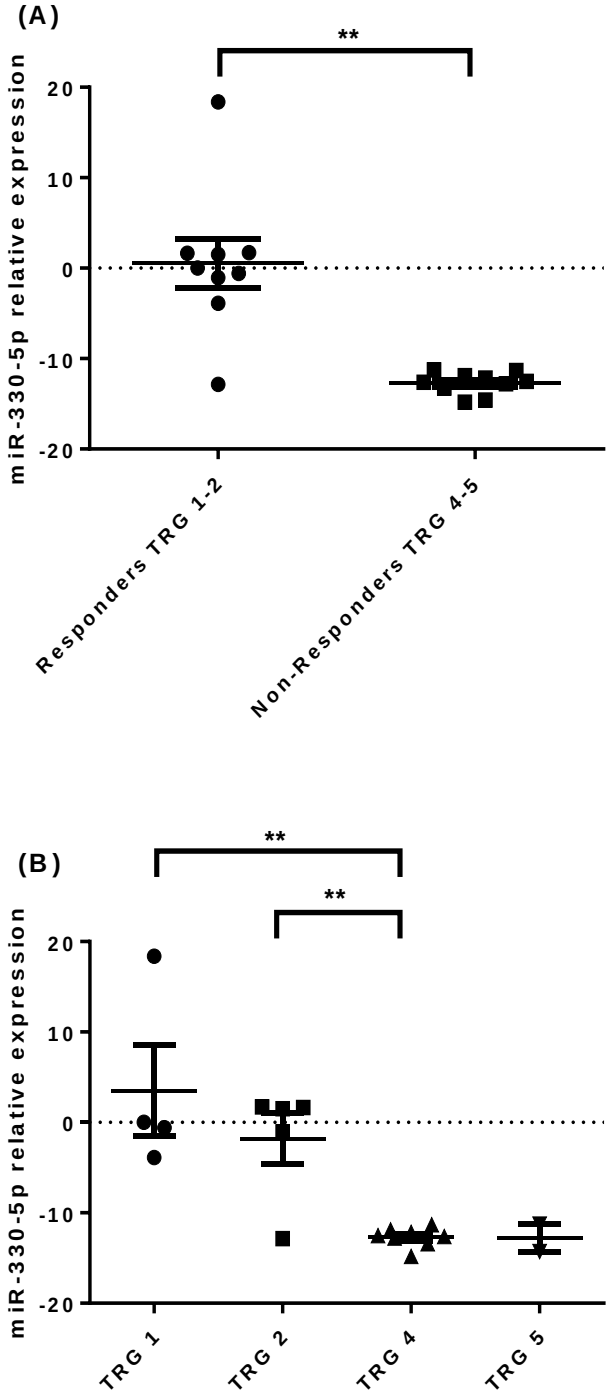

Fig 3.1 MiR-330-5p expression was downregulated in the pre-treatment biopsies from the non-responders. (**A**) MiR-330-5p expression was significantly lower in patients who did not respond to neo-CRT (TRG 4 and 5) when compared with responders (TRG 1 and 2). The two outlier values in the responders data set came from the two patients who were not clinical stage T3. These two outlier values were biopsy specimens from tumours graded T*is* and T2. (**B**) MiR-330-5p expression was significantly lower in patients with TRG 4 (non-responders) compared to patients with TRG 1 and 2 (responders). Analysis was performed using the Mann Whitney U-test; $^{**}p<0.01$. Data are presented as the mean ± SEM.

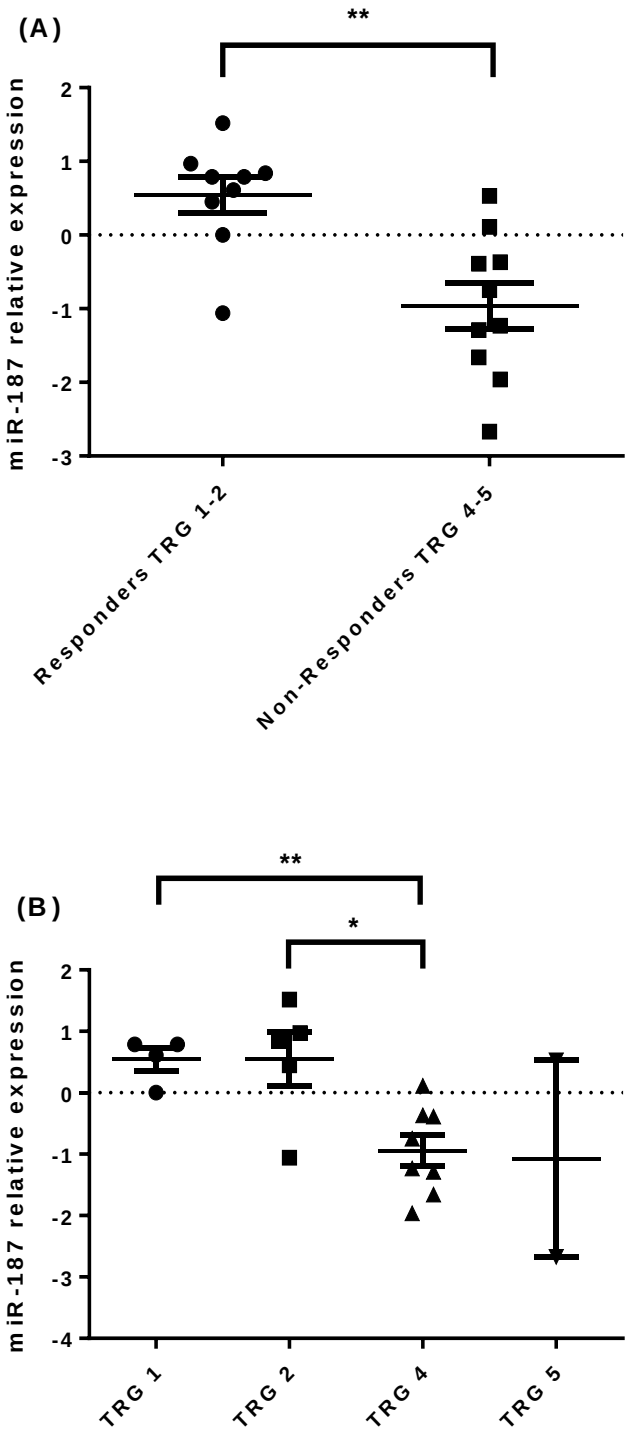

Fig 3.2 MiR-187 expression was downregulated in the pre-treatment biopsies from the non-responders. (**A**) MiR-187 expression was significantly lower in patients who did not respond to neo-CRT (TRG 4 and 5) when compared with responders (TRG 1 and 2). (**B**) MiR-187 expression was significantly lower in patients with TRG 4 (non-responders) compared to patients with TRG 1 and 2 (responders). Analysis was performed using the Mann Whitney U-test; *p<0.05 **p<0.01. Data are presented as the mean ± SEM.

3.5 Discussion

In this chapter the aim was to identify differentially expressed miRNA between OAC responders and non-responders to neo-CRT in a pre-treatment setting. The 67 differentially expressed miRNA identified here are potential biomarkers and therapeutic targets. In a pre-treatment setting miRNA biomarkers could predict the likelihood of a patient responding to neo-CRT. Furthermore, predictive biomarkers could aid treatment stratification in the clinic. The differentially expressed miRNA in pre-treatment biopsies may be 'passenger' biomarkers and their altered expression may be indirectly related to tumour sensitivity and response to CRT. These miRNA could be considered surrogate biomarkers of CRT sensitivity. Conversely, these miRNA could be directly associated with CRT response and sensitivity in patients. The altered expression of these miRNA could profoundly alter the tumour biology associated with patient response and sensitivity to CRT. These miRNA are potential biomarkers and possible therapeutic targets which could be targeted in combination with neo-CRT to enhance tumour sensitivity and patient response to CRT.

The stratification of patients in the clinic, prior to treatment, would have significant benefits for patients. Biomarkers predictive of patient response to neo-CRT could be beneficial to the 70% of patients who receive aggressive treatments from which they gain little or no benefit, whilst compromising their quality of life. In addition, the therapeutic applications of miRNA could have far greater clinical benefits. MiRNA replacement or inhibition could be achieved through therapeutic targeting. Targeting miRNA in conjugation with neo-CRT could enhance tumour sensitivity to CRT furthermore, miRNA therapeutics could have generic tumour suppressor effects independent of modulating sensitivity to CRT. Considering a pCR can increase a patient's 5-year survival rate by 50-60%, therapeutics to enhance the efficacy of CRT could significantly improve prognosis for a large proportion of OAC patients.

The majority of patients in this cohort (89%) were graded clinical stage T3, with the exception of two patients who were graded T*is* and T2 (Table 3.1). These two patients also had lymph node positive disease and received neo-CRT and surgery, both were classified as responders. One biopsy sample was from a patient diagnosed with OSC, this tumour had mixed OAC and OSC histology and was therefore included in the cohort (Table 3.1). The time to surgery for patients after neo-CRT was approximately 5 weeks. In the CROSS trial it was reported that increasing time to surgery from 5 weeks to 12 weeks after neo-CRT, improved the odds of achieving a pCR (van Hagen et al., 2012). This was associated with only a slight increase in the risk of post-operative complications. Based on these findings it is possible that tumours regarded as non-responsive at 5 weeks may have regressed if given additional time to surgery. The tumours most likely to regress in the extended time to surgery would be those classified as TRG 3, which were not included in this study.

Biopsy samples from solid tumours contain multiple cell types including epithelial, mesenchymal, endothethial, pericytes, erythrocytes, neutrophils, monocytes, fibroblasts, lymphocytes, macrophages and plasma cells. In tissue biopsies the contribution of these various cell types to the genetic landscape, including the expression of miRNA, cannot be overlooked. The importance of cell type localisation and miRNA expression has been illustrated by miR-143 and miR-145 studies. In patient biopsy tissues miR-143 and miR-145 were highly expressed in normal colon tissue compared to matched colonic adenocarcinoma that had reduced expression of miR-143 and miR-145 (Michael et al., 2003). Recent findings demonstrated that miR-143 and miR-145 are in fact not expressed in colonic epithelial cells but are highly expressed in mesencymal cells such as fibroblasts and smooth muscle cells (Kent et al., 2014). These studies reaffirm that cells express miRNA not tissue and that multiple cell types contribute to the overall gene expression profile in a tissue sample. Another point to

consider regarding solid tumour biopsy samples is intratumour heterogeneity (Gerlinger et al., 2012). In solid tumour biopsies intratumour heterogeneity has been shown at the RNA expression level and expression signatures associated with treatment resistance and sensitivity have been reported in different regions of a single tumour (Gerlinger et al., 2012). Intratumour heterogeneity and cellular heterogeneity are important factors to consider when interpreting gene expression assays in tissue specimens, an appreciation of the complexity of tumour tissue composition should inform data interpretation (Pichler & Calin, 2015).

In oesophageal cancer, specific miRNA have been identified as potential clinical biomarkers (Sakai et al., 2013; Amin & Lam, 2015). However, few studies focus on miRNA as predictive biomarkers of OAC patient response to neo-CRT (Ko et al., 2012; Lynam-Lennon et al., 2012; Skinner et al., 2014). Several of the most significantly altered miRNA in the data presented here could constitute a miRNA signature predictive of patient response to neo-CRT. This miRNA signature could be validated in a prospective follow-up cohort. This approach has previously been used to validate a miRNA signature predicting pCR in OAC patients receiving neo-CRT (Skinner et al., 2014). Three patient cohorts were used in the study; discovery, model and validation cohorts. In the discovery cohort miRNA array profiling of pre-treatment biopsies identified 44 miRNA that were significantly differentially expressed between patients with pCR and non-pCR. These 44 miRNA were profiled in the model cohort and the 4 most significant miRNA (miR-505-5p, miR-99b-3p, miR-451 and miR-145-3p) predicting pCR were used to generate a miRNA expression profiling (MEP) score. In the validation cohort the MEP score was able to identify patients with a high probability (≥80%) of pCR after neo-CRT (Skinner et al., 2014). A follow up study of similar design could be undertaken using the cohort presented here.

To establish which of these miRNA have the potential to be therapeutic targets in OAC it is necessary to understand the function of the individual miRNA. In the data presented here, miR-31 expression was significantly downregulated in the non-responders (Appendix 4). The downregulated expression of miR-31 was shown to increase the expression of several DNA repair genes and modulated tumour sensitivity to radiation (Lynam-Lennon et al., 2012). The downregulated expression of miR-31 in the non-responders potentially increased DNA repair efficiency and contributed to radioresistance (Lynam-Lennon et al., 2012).

Of the 67 differentially expressed miRNA miR-330-5p was selected because it was the most downregulated miRNA in the non-responder. The expression of miR-187 was also downregulated in the non-responder and was selected because it has previously been implicated in cancer tumorigenesis (Zhao et al., 2013). In this project the aim was to investigate the functions of miR-330-5p and miR-187 as modulators of CRT response and sensitivity in OAC. To identify targets and pathways of miR-330-5p and miR-187 the expression of these miRNA were manipulate and studied using *in vitro* OAC cell models. As the most downregulated miRNA in the non-responders, the initial focus was the function of miR-330-5p as a potential modulator of CRT sensitivity.

Chapter 4 The Role of MiR-330 in OAC Cellular Sensitivity to CRT

Published in part; Bibby BAS, Reynolds JV, Maher SG. MicroRNA-330-5p as a putative modulator of neoadjuvant chemoradiotherapy sensitivity in oesophageal adenocarcinoma. PLoS ONE 2015 doi: 10.1371/journal.pone.013418

4.1 Introduction

In the previous chapter, miRNA expression profiling identified miR-330-5p as the most downregulated miRNA in the pre-treatment tumour biopsies of OAC neo-CRT non-responders. The downregulated expression of miR-330-5p in non-responders is a potential predictive biomarker of tumour sensitivity to neo-CRT. Furthermore, the downregulated expression of miR-330-5p may contribute to tumour resistance to neo-CRT. Therapeutic replacement of miRNA that are known to positively regulate tumour response to therapy could enhance tumour sensitivity to neo-CRT. For the 70% of OAC patients who do not respond to neo-CRT, miRNA replacement therapies which enhance tumour sensitivity to neo-CRT could significant improve patient survival. In this chapter the functional role of miR-330-5p as a modulator of sensitivity to CRT was investigated.

Bioinformatics databases and existing literature do not define which of the miR-330 isoforms, miR-330-3p or miR330-5p, is the functional mature stand and which is the degraded passenger stand. It is possible that both isoforms could independently function as mature miRNA. In this case miR-330-3p and miR-330-5p would have their own specific mRNA targets however, they may also share common mRNA targets. Reported targets of miR-330-3p in various cancer types include *Sp1*, *CDC42* and *E2F1* (Lee et al., 2009; Li et al., 2013; Mao et al., 2013). In prostate cancer miR-330-3p acts as a tumour suppressor by repressing the translation of *E2F1* and *Sp1*. The downregulation of E2F1 protein expression decreases the levels of p-Akt and induces pro-apoptotic pathways, whilst the downregulation of Sp1 protein expression has an anti-metastatic effect (Lee et al., 2009; Mao et al., 2013). In colorectal cancer miR-330-3p represses the translation of *CDC42* and negatively regulates proliferation (Li et al., 2013). Conversely, miR-330-3p acts an oncogenic factor in glioblastoma by enhancing proliferation, invasion and inhibiting apoptosis through activation of ERK and

PI3K/Akt pathways (Qu et al., 2012; Yao et al., 2014). This dichotomy in the biological activities and roles of miRNA in different cell types is well documented. Of particular interest at the start of this project, was the identification of miR-330-3p as a tumour suppressor in prostate cancer. In the prostate study it was reported that miR-330-3p acted as a tumour suppressor by repressing the translation of *E2F1*. The downregulation of E2F1 protein expression subsequently decreased the levels of p-Akt and induced pro-apoptotic pathways (Lee et al., 2009). Furthermore, it has previously been reported that the E2F1/p-Akt pathway promotes cell survival in response to cytotoxic insult induced by both chemotherapeutics and radiation (Winograd-Katz & Levitzki, 2006; Toulany et al., 2007). Interestingly, a bioinformatics search identified a credible binding site for miR-330-5p, as well as miR-330-3p, in the *E2F1* mRNA sequence (Betel et al., 2008).

Using *in vitro* OAC cell models the effect of miR-330-5p expression on cancer cell sensitivity to CRT was investigated. The expression of miR-330-5p was manipulated in OAC cell lines to achieve overexpression or endogenous silencing of the miRNA. In these cell models alterations in the E2F1/p-Akt pathway and cellular sensitivity to cisplatin, 5-FU and radiation were assessed.

4.2 Rationale, aims and objectives

In the pre-treatment tumour biopsies taken from neo-CRT non-responders, miR-330-5p was the most downregulated miRNA. The downregulated expression of miR-330-5p in patient tumours is a potential predictive biomarker of patient response to neo-CRT. Furthermore, miR-330-5p may modulate tumour response and sensitivity to CRT and is a potential therapeutic target. Downregulated miR-330-5p expression is predicted to alter the expression of multiple mRNA targets and subsequently modulate multiple signalling pathways that may confer tumour resistance to CRT. Here, the role of miR-330-5p as a modulator of CRT sensitivity in OAC patients was investigated using an *in vitro* approach.

- Establish OAC cell models of miR-330 overexpression and miR-330-5p silencing.
- Assess alterations in the E2F1/p-Akt pathway with miR-330 overexpression and miR-330-5p silencing.
- Determine the effect of miR-330 overexpression and miR-330-5p silencing on cellular sensitivity to cisplatin, 5-FU and radiation.

4.3 Materials and methods

4.3.1 Transient forward transfection of cell lines

The forward transfection method was used to transfect OE33 cells with the miR-330 or miR-VC vectors (section 2.4.5). In T25 cm^2 flasks ~7×10^5 cells were seeded and allowed to adhere overnight. The following day the media was removed, cells were washed with PBS and 5 mL of Opti-MEM was added to the flasks. Lipofectamine 2000 transfection reagent was diluted; 7.8 µL in 390 µL of Opti-MEM. The plasmid vector was diluted; 4.6 µg in 455 µL of Opti-MEM. The DNA-lipid complexes were prepared by combing the plasmid and transfection reagent; 390 µL of the prepared plasmid solution was added to the 390 µL of lipofectamine solution. The solution was mixed well and incubated at room temperature for 5-10 min. To each flask, 650 µL of the DNA-lipid solution was applied. After 4 h the media was discarded and replaced with complete media.

4.3.2 Stable transfection of cell lines

To establish stable cell lines (OE33 and OE19) expressing the miRZIP-330-5p or miRZIP-VC vectors, the cells were seeded into 10 cm tissue culture dishes and were transfected as previously described (section 4.3.1). The seeding densities and transfection protocol were scaled up according to the surface area of the 10 cm dishes. The media containing the transfection complex was incubated on the cells overnight. The following day the media was discarded and replaced with complete media containing 3 µg/mL of puromycin (Sigma, UK). Cells were cultured under puromycin selection for ~2 weeks before individual colonies were visible. Using a pipette tip containing ~50 µL of media individual colonies were scratched from the surface of the dish, taken up into the pipette tip and transferred into the wells of a 96-well plate. Cells were cultured in 100 µL media with 3µg/mL puromycin until they reached ~80%

confluency. The expression of GFP was confirmed using fluorescent microscopy (section 2.4.6). Clones were scaled up from 96 well plates to 12 well plates, 12 clones which were confirmed to be expressing GFP in the 96 well plates were transferred to 12-well plates. Cells were cultured in media containing puromycin until they reached ~80% confluency. The wells were trypsinsed and 80% of the cells were harvested for western blotting. The remaining cells were again cultured in the 12-well plate to 80% confluency. Based on the expression level of GFP, determined by western blotting, 6 clones were selected. Two clones with high, intermediate and low GFP expression were scaled up into T75 cm^2 flasks, at which stage the puromycin selection was removed. The mixed population was established by harvesting all the clones from the 10 cm dish (as appose to picking individual clones) and reseeding the cells in a larger dish or flask. Puromycin selection was maintained for ~6 weeks. Stable cell lines were checked frequently using fluorescent microscopy and western blotting to confirm continued expression of GFP in long term cell cultures in the absence of puromycin.

4.3.3 qPCR analysis of miRNA and mRNA expression

Cells were harvested and RNA was extracted as previously described (section 2.5.1). To analyse the relative expression of miR-330-3p and miR-330-5p, the miScript II RT Kit was used for cDNA synthesis and the miScript SYBR Green PCR kit was used for the qPCR analysis (as previously described sections 2.5.3 and 2.5.4). The miScript primer assays used for target amplification in the qPCR were miR-330-3p, miR-330-5p and the endogenous control RNU6 (Table 2.1). To analyse the relative expression of *E2F1* mRNA, the QuantiTect RT Kit was used for cDNA synthesis and the QuaniTect SYBR green PCR master mix was used for the qPCR analysis (as previously described in sections 2.5.5 and 2.5.6). The QuantiTect primer assays used for target amplification in the qPCR were E2F1 and the endogenous control B2M (Table 2.1).

4.3.4 Western blotting

Cells were harvested and protein was extracted and quantified as previously described (sections 2.6.1 and 2.6.2). Samples were prepared for SDS-PAGE, a total volume of 25 µL was loaded into the wells of a 12% gel or a precast 4-20% gradient gel (section 2.6.3). SDS-PAGE and western blot were performed as described in sections 2.6.3 and 2.6.4. The PVDF membranes were probed for E2F1 (KH95, Santa Cruz Biotechnology, Texas, USA), turboGFP (Origene, Maryland, USA) and the loading control β-actin (AC-15, Santa Cruz Biotechnology, Texas, USA) (Table 2.2). After incubation with the primary antibody, the blots were washed and then incubated for 1 h at room temperature with the secondary antibody (Table 2.2). After incubation with the secondary antibody, the blots were washed and the chemiluminescent substrate was applied (section 2.6.4). The blots were imaged using a chemiluminescent imaging system or autoradiography (section 2.6.7). Image Lab 3.0 software (BioRad, UK) was used for densitometry analysis of western blots (section 2.6.8).

4.3.5 Phospho-Akt ELISA

Cells were harvested, counted and ~1.8×10^6 cells were seeded into 10 cm t dishes and incubated overnight to allow cells to adhere. The cells were transfected as previously described, scaling up the transfection protocol according to the surface area of the dish (section 4.3.1). The cells were harvested 72 h post transfection and protein was extracted and quantified as previously described (section 2.6.1 and 2.6.2). The ELISA detected phosphorylated Akt1/2/3; the protocol was performed as previously described (section 2.6.9).

4.3.6 Clonogenic assay

Transiently transfected cells were harvested 24 h post-transfection (section 4.3.1). Cells were counted and seeded into 6-well plates. The optimised seeding

densities for the OE33 cell line are reported in Table 4.1. The OE19 cell line was seeded at 500 cells per well for the untreated, PBS, DMSO or mock irradiated controls and 1000 cells per well for the 3 µM cisplatin, 15 µM 5-FU or 2 Gy treatments. The assay was performed as described in section 2.7.1.

The cisplatin and 5-FU clonogenic assays for the OE33 miRZIP-VC and miRZIP-330-5p cell lines produced colonies that could not be accurately counted using the Gel Count. The individual colony boundaries were difficult to define and the Gel Count algorithm could not be optimised to give a reliable and reproducible count. To quantify the clonogenic assays the crystal violet was solubilised and absorbance was measured. To each well 1.5 mL of 1% SDS solution was applied and the plates were incubated overnight at 37°C to solubilise the crystal violet. From each well 200 µL of the solubilised crystal violet was transferred into a 96 well plate and absorbance was measured at 595 nm (Biotech Absorbance Microplate Reader ELx800). The absorbance measurements of the untreated controls was normalised to 1 and the cisplatin and 5-FU absorbance values were calculated relative to the untreated control.

4.3.7 MTS proliferation/viability assay

Transiently transfected cells were harvested 24 h post-transfection (section 4.3.1). Cells were seeded into 96 well plates in 100 µL of media and allowed to adhere overnight. The following day, 50 µL of media was removed and replaced with 50 µL media containing cisplatin or 5-FU. Treatment was diluted 1:2 in the well to give final concentrations of 1µM cisplatin or 12µM 5-FU. The MTS reagent was applied 24, 48 or 72 h post-treatment and the assay protocol was performed as previously described (section 2.7.2)

4.4 Results

4.4.1 Establishing an *in vitro* model of miR-330 overexpression

To study the effect of miR-330 on cellular sensitivity to CRT in OAC cell lines, a model of transient miR-330 overexpression was established. Cells were transfected with a plasmid vector encoding the miR-330 precursor sequence. Control cells were transfected with an identical plasmid vector encoding a non-targeting scrambled sequence (miR-VC). These vectors also encoded GFP and transfection efficiency was assessed using fluorescent microscopy (Fig 4.1). To confirm overexpression of the miRNA, in cells transfected with the miR-330 vector, the relative expression of miR-330 was measure by qPCR. The miR-330 vector encoded the miR-330 precursor sequence and produced both mature miR-330-3p and miR-330-5p. Therefore, overexpression refers to general miR-330 overexpression, as it is not possible to discriminate between the contributions of miR-330-3p and miR-330-5p in this model. In the cells transfected with the miR-330 vector, the expressions of miR-330-3p and miR-330-5p were increased 24, 48 and 72 h post-transfection (Fig 4.2).

It has previously been reported, in prostate cancer, that miR-330 acts as a tumour suppressor by downregulating E2F1 expression and p-Akt levels (Lee et al., 2009). Furthermore, the E2F1/p-Akt pathway promotes cell survival in response to cytotoxic insult and is associated with CRT resistance (Nicholson & Anderson, 2002; Chaussepied & Ginsberg, 2004). Using the transient miR-330 overexpression model alterations in the E2F1/p-Akt pathway was studied.

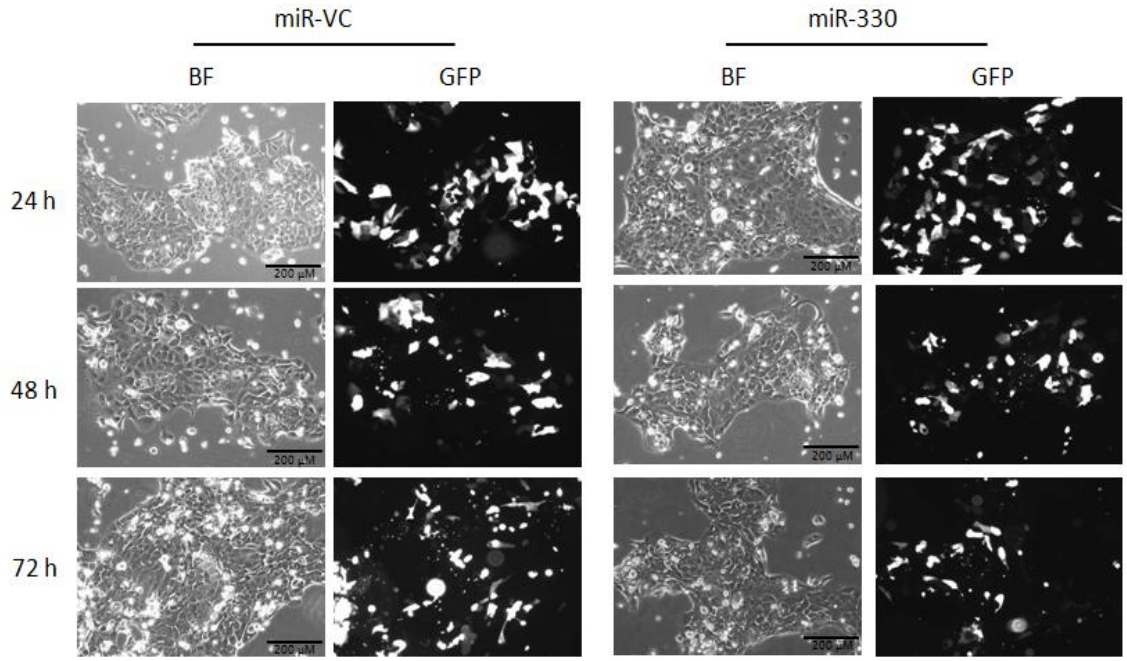

Fig 4.1 Fluorescent microscopy time course of GFP expression in OE33 cells transfected with the miR-VC or miR-330 vectors. The OE33 cells were transiently transfected with the miR-VC or miR-330 vectors and fluorescent microscopy confirmed successful transfection and expression of the plasmids 24, 48 and 72 h post-transfection. There was no GFP expression observed in the control and lipofectamine only treated cells (not shown). BF; bright field. GFP; green fluorescent protein detected via the fluorescein isothiocyanate channel (FITC) ×10 magnification.

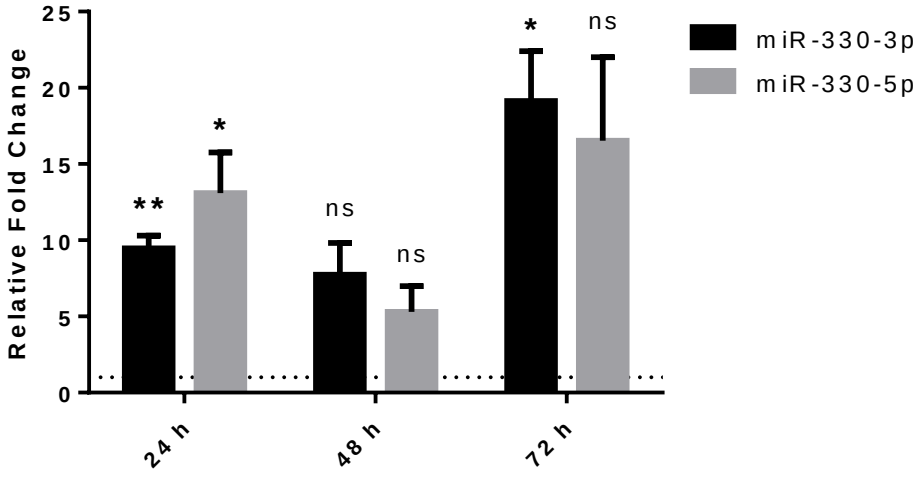

Fig 4.2 Overexpression of miR-330-3p and miR-330-5p in OE33 cells. Cells transfected with the miR-VC or the miR-330 vectors were harvested 24, 48 and 72 h post-transfection for qPCR analysis. The Livak method was used to analyse the data with RNU6 as the endogenous control. The fold change in the expressions of miR-330-3p and miR-330-5p in cells transfected with the miR-330 vector were calculated relative to the expression of miR-330-3p and miR-330-5p in the cells transfect with the miR-VC vector. The miR-VC cells were normalised to 1 (dotted line). Experimental repeats n=3. Data are presented as the mean ± SEM. Statistical analysis was performed using the one-sample t-test; * p<0.05, ** p<0.01, ns not significant.

4.4.2 MiR-330 overexpression downregulated the E2F1 protein and p-Akt levels

It has previously been demonstrated in prostate cancer that miR-330 acts as a tumour suppressor by downregulating E2F1 protein expression and the cellular levels of p-Akt thereby promoting apoptosis of cancer cells (Lee et al., 2009). The E2F1/p-Akt pathway promotes cell survival by inhibiting pro-apoptotic proteins that induce cell death (Nicholson & Anderson, 2002; Chaussepied & Ginsberg, 2004). Furthermore, increased levels of p-Akt are known to be induced in response to the cytotoxic insult of chemotherapeutics and radiation and promotes cell survival and evasion of cell death (Winograd-Katz & Levitzki, 2006; Toulany et al., 2007). Based on these previous studies, it was hypothesised that the downregulated miR-330-5p expression observed in the pre-treatment OAC biopsies from non-responders potentially induced the E2F1/p-Akt cell survival pathway thereby promoting tumour resistance to CRT. In agreement with the previous findings in prostate, the overexpression of miR-330 significantly downregulated E2F1 protein levels and subsequently the levels of p-Akt also decreased (Fig 4.3 and 4.4). Interestingly, *E2F1* mRNA levels did not decrease with the overexpression of miR-330 suggesting that miR-330 repressed *E2F1* mRNA translation without degrading the mRNA (Fig 4.5).

This data indicated that miR-330 regulates, at least partially, the E2F1/pAkt pathway in OAC. Clonogenic survival assays were employed to further investigate the role of miR-330 as a modulator of cellular sensitivity to cisplatin, 5-FU and radiation.

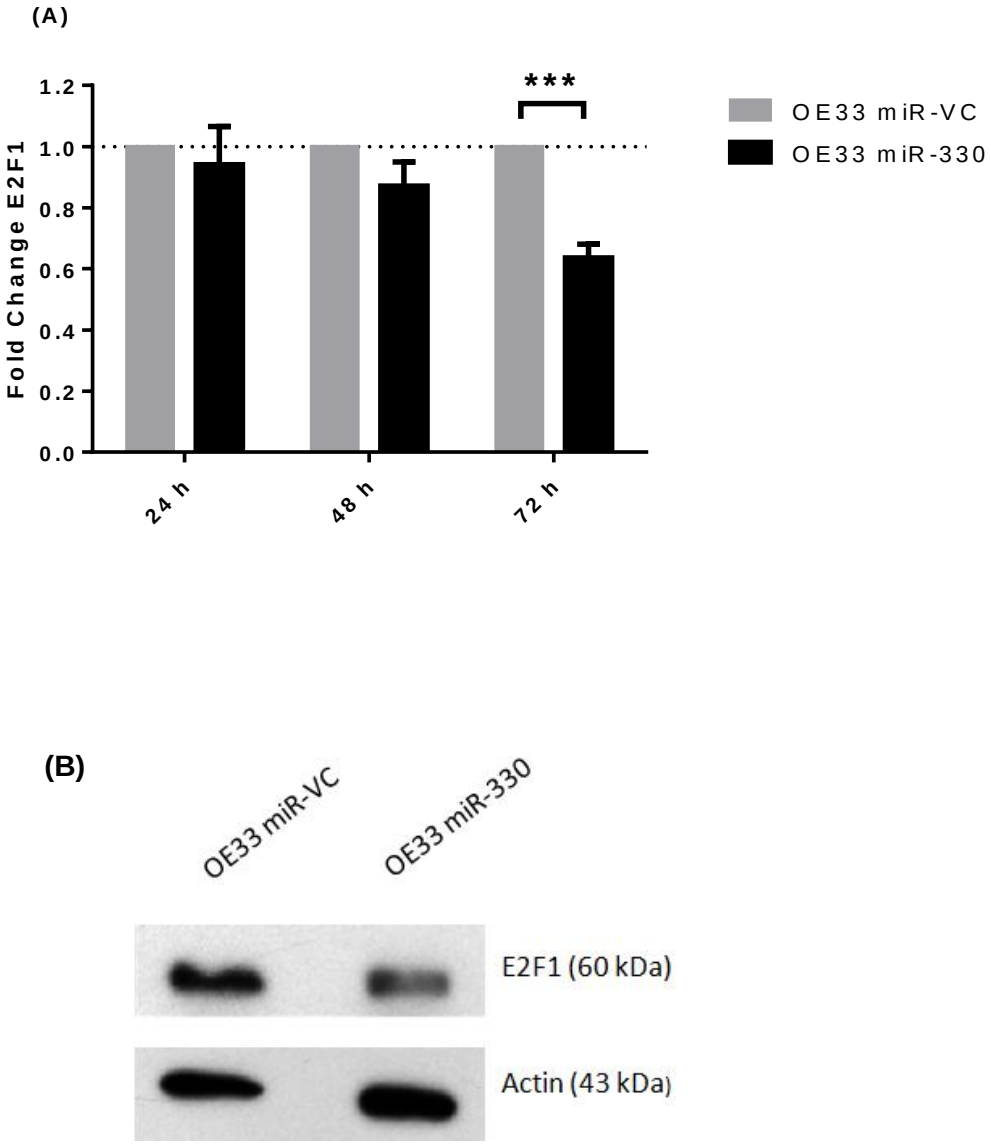

Fig 4.3 MiR-330 overexpression downregulated the E2F1 protein. Transient miR-330 overexpression significantly decreased E2F1 protein expression compared to the miR-VC. (**A**) Densitometry was used to analyse western blot images. Relative to the miR-VC transfected cells there was a ~40% decrease in the E2F1 protein after 72 h of miR-330 overexpression. The dotted line represents the miR-VC E2F1 expression normalised to 1. (**B**) The relative quantity of E2F1 protein was determined via western blot using β-actin as a loading control. Experimental repeats; 24 h n=5, 48 h n=5, 72 h n=6. Data are presented as the mean ± SEM. Analysis was performed using the one-sample t-test; miR-VC 72 h *vs.* miR-330 72 h ***p<0.001.

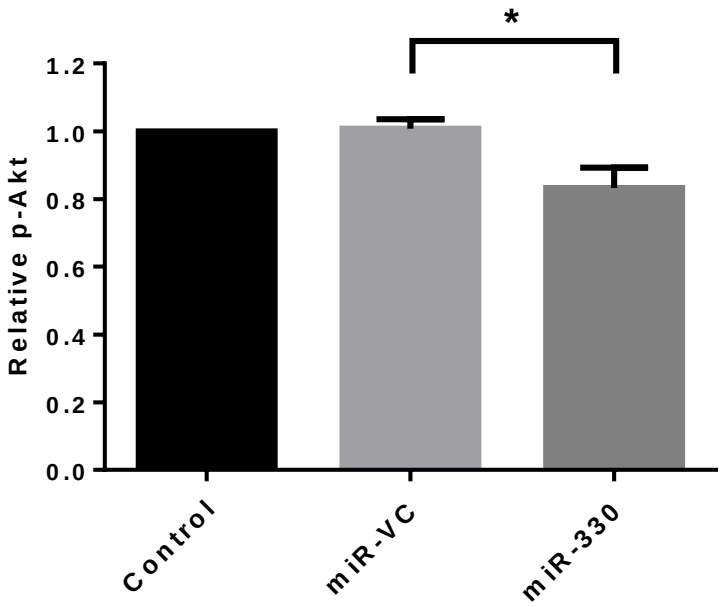

Fig 4.4 MiR-330 overexpression decreased the levels of p-Akt. Transient miR-330 overexpression in the OE33 cell line decreased the levels of p-Akt, 72 h post-transfection, in concordance with a decrease in E2F1 protein expression. There was a 20% decrease in the levels of p-Akt with miR-330 overexpression compared to the miR-VC control. Experimental repeats n=3. Data are presented as the mean ± SEM. Analysis was performed using one-way ANOVA and Tukey post-test; *p<0.05.

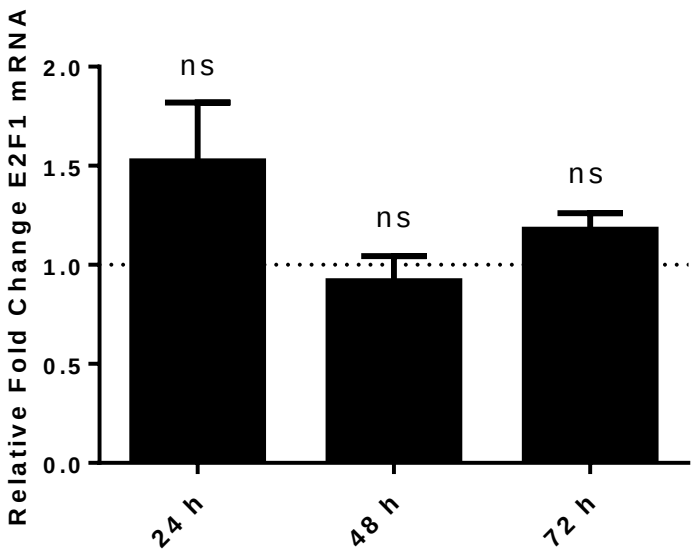

Fig 4.5 MiR-330 overexpression did not alter *E2F1* mRNA expression. Cells were transfected with the miR-VC or the miR-330 overexpression plasmid and harvested 24, 48 and 72 h post-transfection for qPCR analysis. The Livak method was used to analyse the qPCR data with *B2M* as the endogenous control. The fold change in the expression of the E2F1 mRNA in OE33 cells transfected with the miR-330 overexpression plasmid was normalised to the expression of *E2F1* in the miR-VC transfected cells. The dotted line represents the normalised miR-VC equal to 1. There were no significant changes in the *E2F1* mRNA levels with miR-330 overexpression compared to the miR-VC at any time point. Experimental repeats; 24 h *n*=3, 48 h *n*=3, 72 h *n*=4. Data are presented as the mean ± SEM. Statistical analysis was performed by one-way ANOVA; ns not significant.

4.4.3 Clonogenic assay cisplatin and 5-FU dose response curves

The clonogenic assay measures the reproductive integrity of cells following treatment with chemotherapeutic drugs or radiation. Viable cells that survive cytotoxic insult, and maintain the ability to proliferate are able to form colonies. This assay is the 'gold standard' technique for measuring the ability of viable cells to proliferate indefinitely and potentially repopulate a tumour following cytotoxic insult (Franken et al., 2006). Cell seeding densities were optimised so that at least ~100 colonies were counted at the end of the assay (Table 4.1). This is essential for statistical significance in calculating the surviving fraction of cells based on plating efficiency. Dose response curves were used to determine the IC_{50} concentrations of cisplatin and 5-FU for the OE33 cell line (Fig 4.6). The cisplatin IC_{50} dose was approximately 1 µM and the 5-FU IC_{50} dose was approximately 12µM (Fig 4.6). The clonogenic assay was used to assess alterations in cellular sensitivity to cisplatin, 5-FU or radiation in cells with miR-330 overexpression.

4.4.4 MiR-330 overexpression did not alter cellular sensitivity to cisplatin, 5-FU or radiation

To determine if miR-330 overexpression alters cellular sensitivity to cisplatin, 5-FU or radiation the cells were transfected with the miR-330 vector and seeded for the clonogenic assay. The established cisplatin and 5-FU IC_{50} doses were used in the clonogenic assays (Fig 4.6). Radiation was administered at a clinically relevant dose of 2 Gy. The overexpression of miR-330 did not enhance cellular sensitivity to cisplatin, 5-FU or radiation at the selected time points and doses (Fig. 4.7). Although alterations in E2F1 and p-Akt levels were observed with miR-330 overexpression, the negative regulation of this pathway was not sufficient to alter chemosensitivity or radiosensitivity.

Table 4.1 OE33 seeding densities for the clonogenic assay.

Treatment	Cell seeding density	Mean colony no. ± SEM
Untreated	5×10^2	188 ± 3
PBS	5×10^2	189 ± 9
1 µM cisplatin	$1\text{-}1.5 \times 10^3$	238 ± 19
DMSO	7.5×10^2	138 ± 11
15 µM 5-FU	$1.5\text{-}2 \times 10^3$	87 ± 14
Mock irradiated	$5\text{-}7.5 \times 10^2$	179 ± 18
2 Gy	$1\text{-}1.5 \times 10^3$	216 ± 21

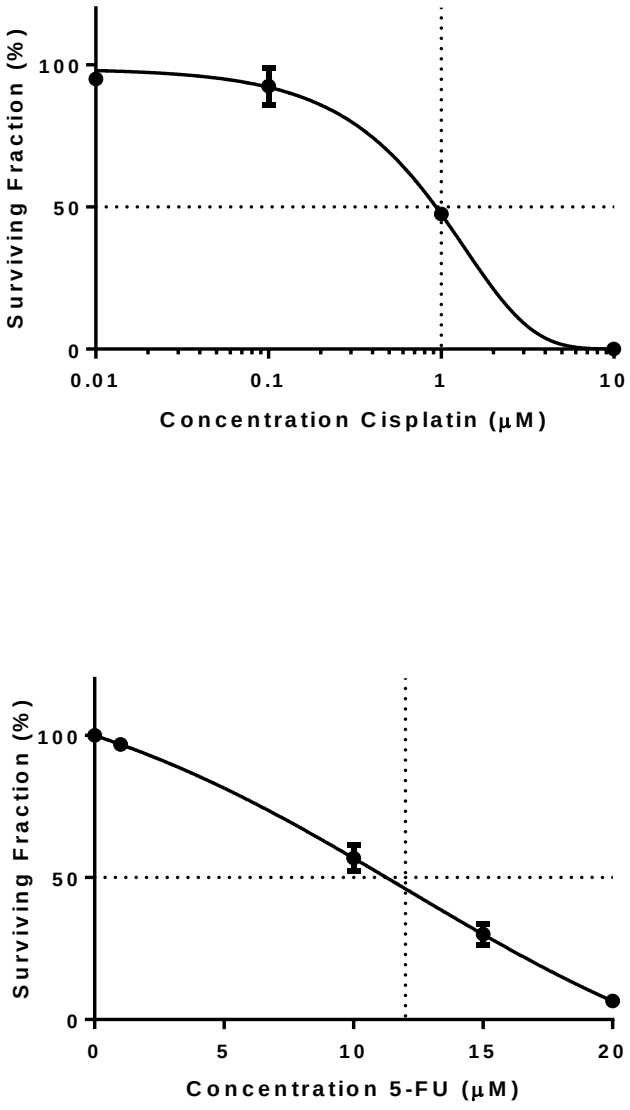

Fig 4.6 Clonogenic assay cisplatin and 5-FU dose response curves for OE33 cells. The dose of cisplatin or 5-FU required to reduce the surviving fraction to 50% were determined from the dose response curves. **(A)** Cells were treated with a 10-fold range of cisplatin concentrations or the corresponding concentration of PBS vehicle control. Cells were treated for 24 h and plates were incubated for ~7 days. The cisplatin IC_{50} concentration was approximately 1 µM (dotted lines). Experimental repeats; 0.01 µM *n*=2, 0.1 µM *n*=2, 1 µM *n*=4, 10 µM *n*=2. **(B)** Cells were treated with a range of 5-FU concentrations or the corresponding concentration of DMSO vehicle control. Cells were treated for 24 h and plates were incubated for ~7 days. The 5-FU IC_{50} concentration was approximately 12 µM (dotted lines). Experimental repeats; 1 µM *n*=7, 10 µM *n*=6, 15 µM *n*=4, 20 µM *n*=4. Data are presented as the mean ± SEM.

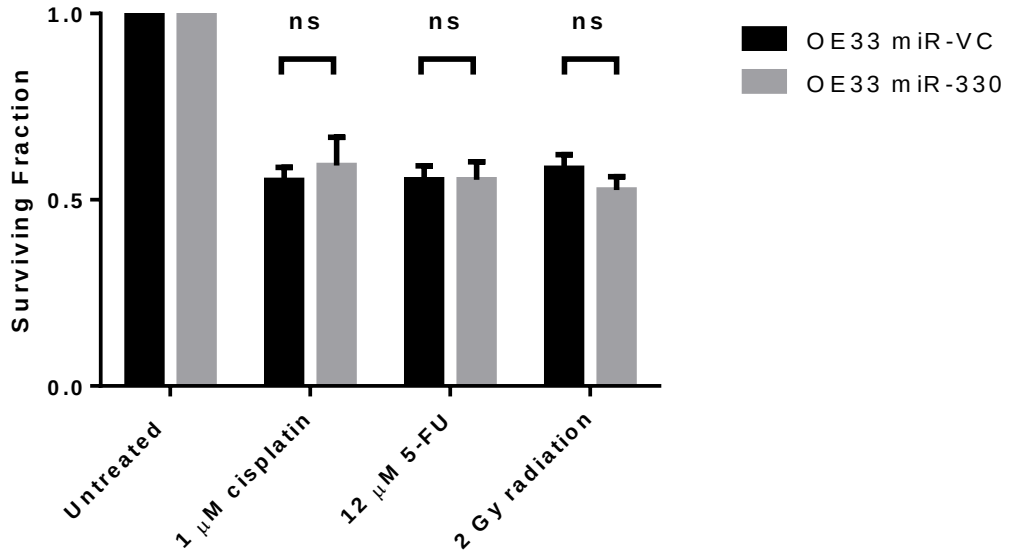

Fig 4.7 MiR-330 overexpression did not alter cellular sensitivity to cisplatin, 5-FU or radiation. OE33 cells were transiently transfected with the miR-VC or miR-330 plasmid, 24 h post-transfection cells were harvested and seeded for the clonogenic assay. The following day cells were treated with radiation or 24 h of chemotherapy. The overexpression of miR-330 in the OE33 cell line did not significantly alter cellular sensitivity to chemotherapy or radiotherapy relative to the miR-VC control. Experimental repeats 1 µM cisplatin *n*=5, 12 µM 5-FU *n*=3, 2 Gy *n*=6**.** Data are presented as mean ± SEM. Statistical analysis was performed using the paired two-tailed *t*-test; ns not significant.

4.4.5 MiR-330 overexpression did not alter cellular viability in response to chemotherapy

Overexpression of miR-330 did not alter the clonogenic potential of OE33 cells treated with cisplatin or 5-FU. To establish if miR-330 overexpression altered cellular viability in response to cisplatin or 5-FU, the MTS assay was employed. The overexpression of miR-330 did not alter cellular viability compared to the non-transfected and miR-VC controls (Fig 4.8). Cisplatin treatment reduced cell viability ~25% and 5-FU reduced cell viability ~50% (Fig 4.9). However, the overexpression of miR-330 did not significantly alter cellular viability in response to cisplatin or 5-FU relative the miR-VC control (Fig 4.9). The overexpression of miR-330 altered E2F1 protein expression and p-Akt levels, however the modulation of this pathway was not sufficient to alter cellular viability or sensitivity to cisplatin, 5-FU or radiation.

4.4.6 Establishing an *in vitro* model of miR-330-5p silencing

In the patient cohort miR-330-5p was the most downregulated miRNA in non-responder to neo-CRT. To establish an *in vitro* model of this observation the expression of endogenous miR-330-5p was silenced in the OE33 and OE19 cell lines.

The miRZIP-330-5p vector produced the miR-330-5p anti-miRNA that bound irreversibly to the endogenously expressed mature miR-330-5p via strict Watson-Crick base paring. The irreversible binding of the anti-sense strand inhibited the function of miR-330-5p. The anti-miRNA produced by the miRZIP-330-5p vector bound specifically to miR-330-5p and did not inhibit miR-330-3p. The miRZIP-330-5p and miRZIP-VC vectors were transfected into cells (section 4.3.2). These vectors encoded the mammalian antibiotic resistance gene for puromycin. The resistance gene enabled only the transfected cells to survive when puromycin treatment was applied.

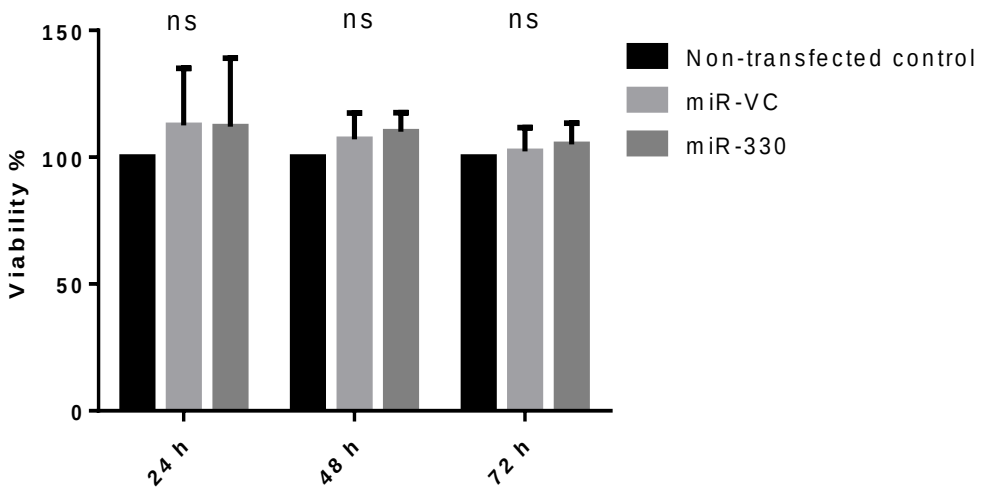

Fig 4.8 MiR-330 overexpression did not alter cellular viability. OE33 cells were transiently transfected and the following day cells were harvested and seeded into the MTS assay. After 24, 48 or 72 h the MTS reagent was added and plates were incubated for 3 h prior to reading Abs 490 nm. The viability of OE33 cells transfected with the miR-VC or miR-330 vector were normalised to the non-transfected control cells. There were no significant changes in viability between any of the groups at any of the time points. Experimental repeats; 24 h *n*=2, 48 h *n*=3, 72 h *n*=3. Data are presented as mean ± SEM. Statistical analysis was performed using the one-way ANOVA; ns not significant.

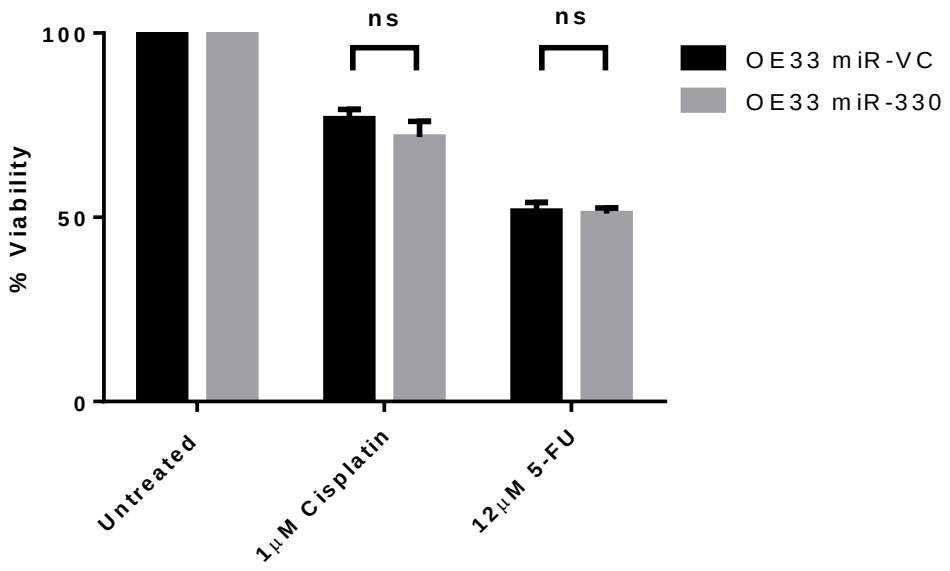

Fig 4.9 MiR-330 overexpression did not alter cellular viability in response to cisplatin or 5-FU treatment. OE33 cells were transiently transfected and the following day cells were harvested and seeded into the MTS assay. The viability of the chemotherapy treated cells was normalised to the vehicle control/untreated cells. MTS reagent added and plates were incubated for 3 h prior to reading Abs 490 nm. There were no significant changes in cellular viability between the miR-330 and miR-VC transfected cells treated for 72 h with 1 μM cisplatin or 12 μM 5-FU. Experimental repeats cisplatin *n*=4, 5-FU *n*=3. Data are presented as mean ± SEM. Statistical analysis was performed using the paired two-tailed *t*-test; ns not significant.

This enabled the selection and propagation of a cell population that had successfully integrated the vector. Furthermore, the vectors encoded the GFP reporter gene and cells with stable expression of the vector were monitored using fluorescent microscopy. The expression of GFP was determined by western blotting to assess the variability of vector expression across multiple clones (Fig 4.10 and 4.11). Amongst the individual clones GFP expression was highly variable. Six clones were selected for expansion and archiving. Of the 6 selected clones there were 2 clones each with high, intermediate or low GFP expression and the selected pairs had similar levels of GFP (Fig 4.10 and 4.11). In addition to the clones with high/intermediate/low expression of the vector, a mixed heterogeneous stable population was also established. The OE33 and OE19 cell line models of miR-330-5p silencing were established to mimic the downregulated miR-330-5p expression observed in neo-CRT non-responders of the patient cohort. These *in vitro* models were used to study the effect of miR-330-5p silencing on cellular sensitivity to CRT and to investigate alterations in the expression of E2F1.

4.4.7 MiR-330-5p silencing did not alter E2F1 expression

Previously miR-330 overexpression was shown to downregulate the expression of the E2F1 protein (Fig 4.3). The *E2F1* mRNA has possible binding sites for both miR-330-3p and miR-330-5p and in the overexpression model it was not possible to discriminate between the contributions of the two miRNA isoforms (Betel et al., 2008). In the silencing model miR-330-5p is specifically silenced, therefore targets and signalling pathways altered in this model are associated with the silencing of only miR-330-5p. Inhibition of endogenous miR-330-5p in the OE33 and OE19 cell lines did not significantly alter the expression of the E2F1 protein (Fig 4.12). Furthermore, the expression of the *E2F1* mRNA was not significantly altered by miR-330-5p silencing (Fig 4.13).

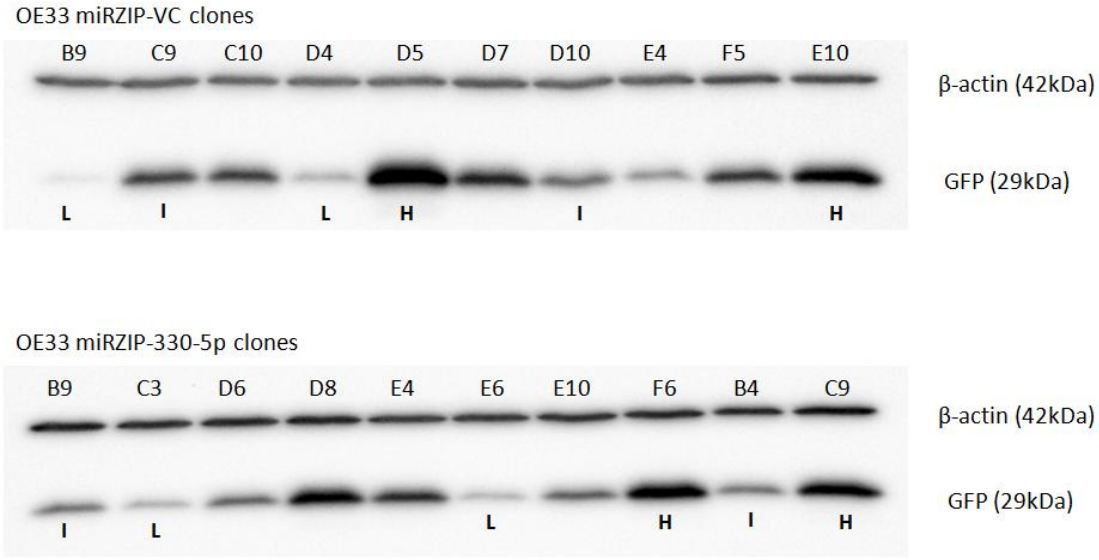

Fig 4.10 GFP expression in OE33 miRZIP-330-5p and miRZIP-VC stable clones. Protein extracts were prepared from each of the 10 clones at the 12 well plate stage (section 4.3.2). Protein samples were quantified and analysed for GFP expression using western blotting. The loading control was β-actin. Variable GFP expression was observed amongst the clones. Six clones were selected; two each of high (H), intermediate (I) and low (L) GFP expression.

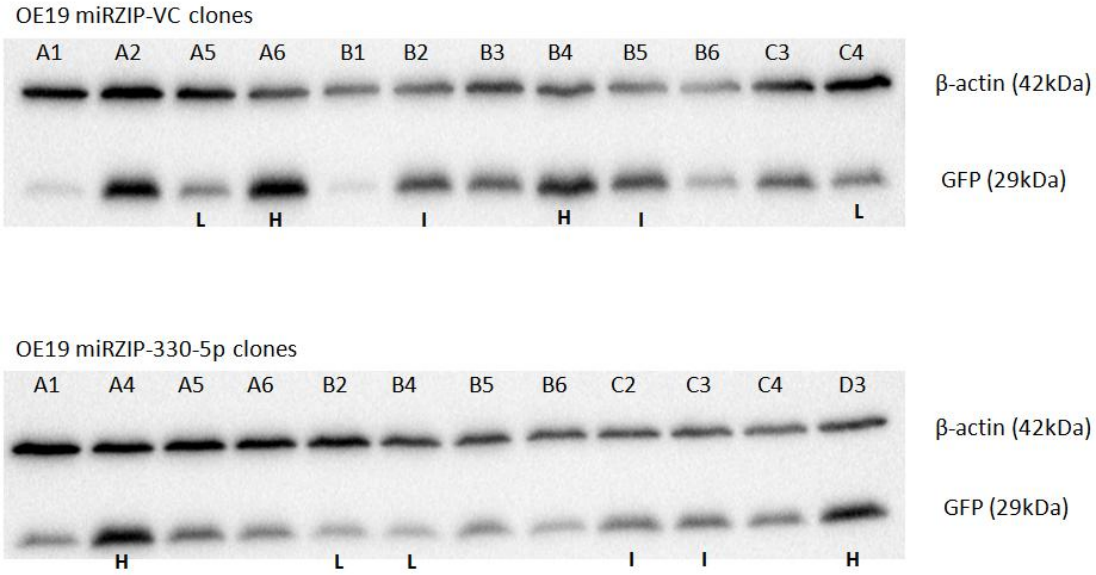

Fig 4.11 GFP expression in OE19 miRZIP-330-5p and miRZIP-VC stable clones. Protein extracts were prepared from each of the 12 clones at the 12 well plate stage (section 4.3.2). Protein samples were quantified and analysed for GFP expression using western blotting. The loading control was β-actin. Variable GFP expression was observed amongst the clones. Six clones were selected; two each of high (H), intermediate (I) and low (L) GFP expression.

(A)

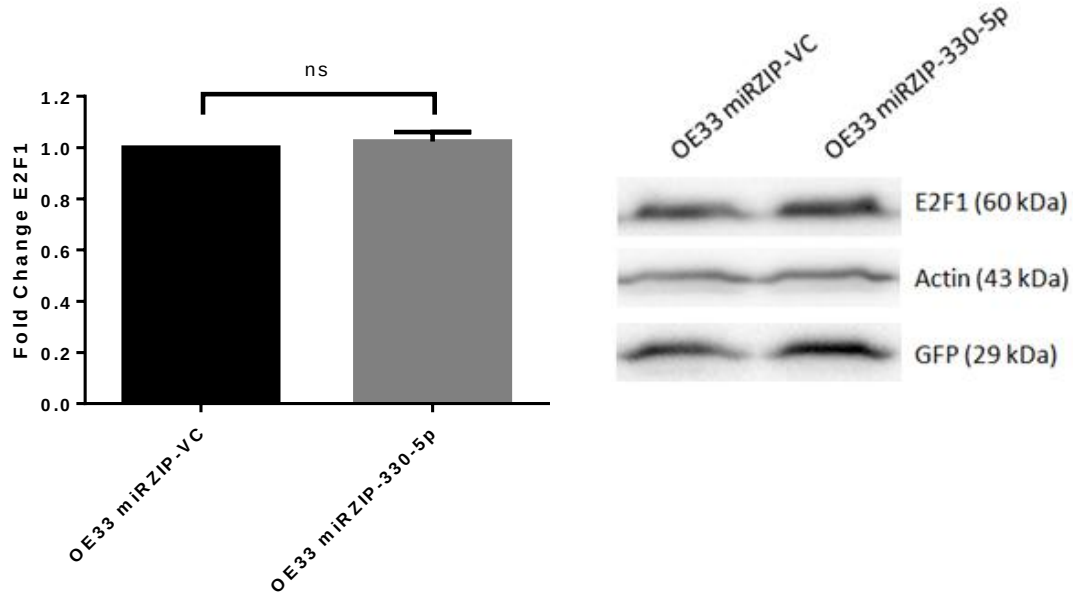

(B)

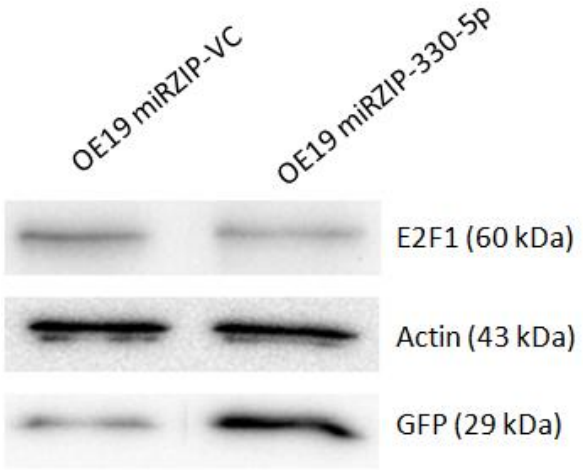

Fig 4.12 Silencing endogenous miR-330-5p did not alter E2F1 protein expression. (**A**) In the OE33 miRZIP-330-5p mixed population stable cell lines, the expression of E2F1 was not significantly altered relative to the miRZIP-VC (*left* densitometry analysis and *right* western blot). (**B**) In the OE19 miRZIP-330-5p mixed population stable cell lines, the expression of E2F1 was not significantly altered relative to the miRZIP-VC. GFP expression confirms the stable transfection of the cell lines and β-actin was used as the loading control. Experimental repeats; OE33 *n*=3 and OE19 *n*=2. Data presented as the mean ± SEM. Statistical analysis was performed using the one-sample *t*-test; ns not significant.

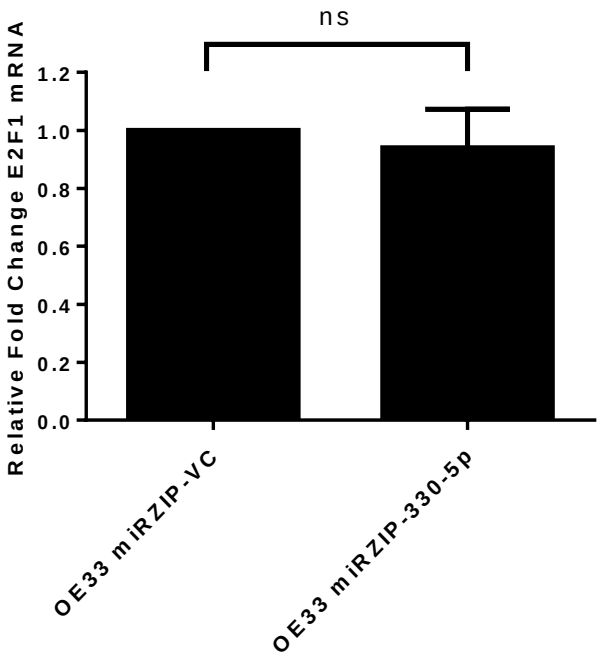

Fig 4.13 Silencing endogenous miR-330-5p did not alter *E2F1* mRNA expression. The fold change in *E2F1* mRNA was measured in stably transfected high GFP clone OE33 miRZIP-330-5p F6 relative to the OE33 miRZIP-VC E10 clone. The Livak method was used to analyse the data with *B2M* as the endogenous control. The expression of *E2F1* in the OE33 miRZIP-VC E10 was normalised to 1. There was no significant difference in the mRNA levels of *E2F1* with miR-330-5p silencing. Experimental repeats n=3. Data are presented as the mean ± SEM. Statistical analysis was performed using the paired *t*-test; ns not significant.

4.4.8 MiR-330-5p silencing enhanced cellular resistance to radiotherapy but not chemotherapy

The silencing of miR-330-5p is a more relevant model of the downregulated expression observed in the non-responder patient biopsies. The clonogenic assay was used to determine if silencing endogenous miR-330-5p altered cellular sensitivity to cisplatin, 5-FU or radiation. In the OE33 and OE19 cell lines, miR-330-5p silencing did not alter cellular sensitivity to cisplatin or 5-FU under the conditions tested (Fig 4.14). In the OE19 cell line miR-330-5p silencing did not enhance radioresistance (Fig 4.14 B) however the OE33 cell line was significantly more radioresistant with miR-330-5p silencing albeit marginally (OE33 miRZIP-VC 0.67 ± 0.05 *vs.* OE33 miRZIP-330-5p 0.74 ± 0.04 p=0.02) (Fig 4.14 A).

4.4.9 MiR-330 silencing did not alter cellular viability in response to chemotherapy

To assess alterations in cellular viability with endogenous miR-330-5p silencing the MTS assay was employed. Silencing miR-330-5p did not alter cellular viability in response to cisplatin or 5-FU treatment, compared to the miRZIP-VC control (Fig 4.15).

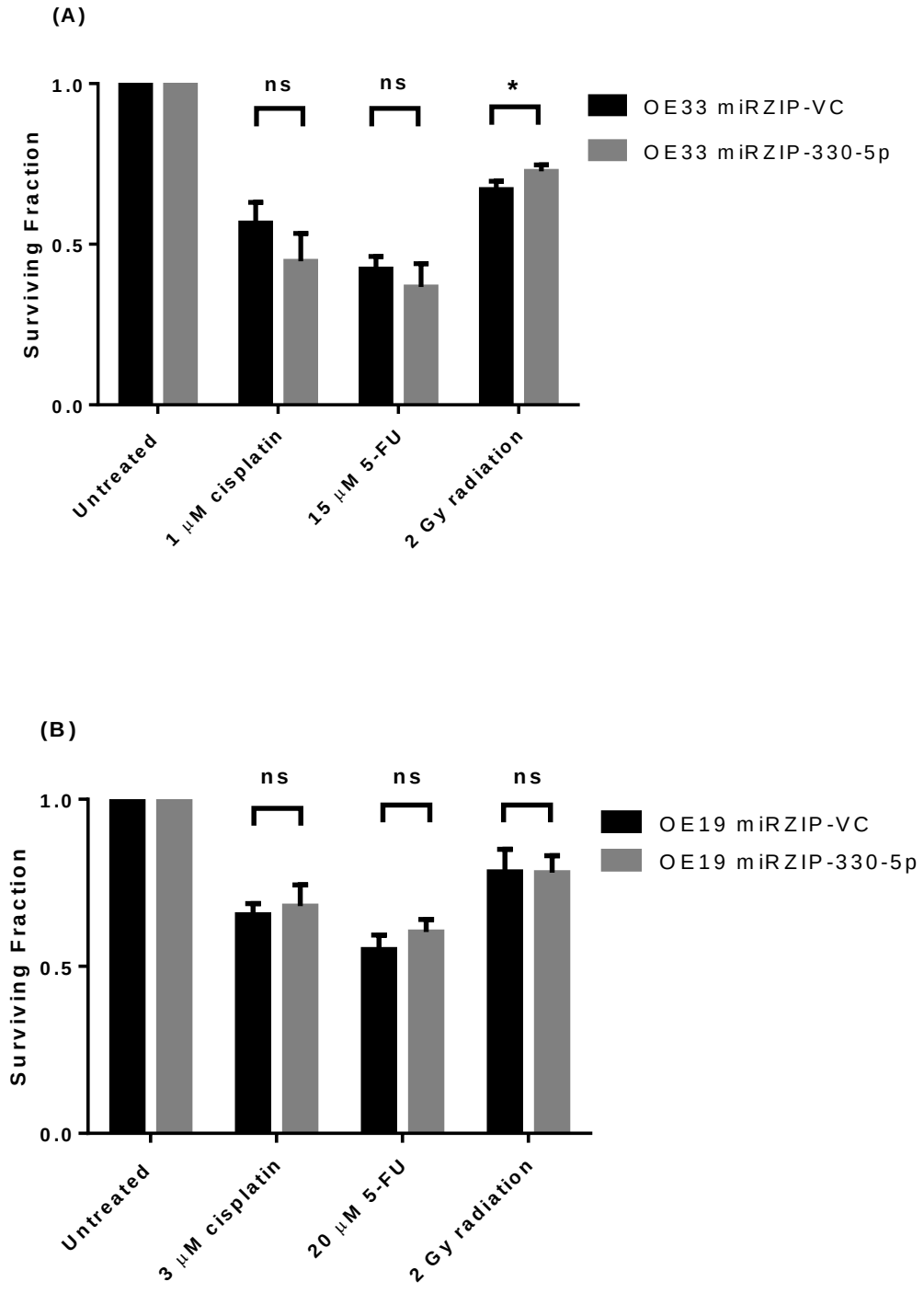

Fig 4.14 Alterations in chemo and radiotherapy sensitivity with miR-330-5p silencing. (**A**) Stable silencing of miR-330-5p in the OE33 cell line did not significantly alter cellular sensitivity to 1 μM cisplatin or 15 μM 5-FU (24 h treatments) compared to the miRZIP-VC control. However, there was a significant increase in resistance to radiotherapy (2 Gy) with miR-330-5p silencing. (**B**) Stable silencing of miR-330-5p in the OE19 cell line did not significantly alter cellular sensitivity to 3 μM cisplatin, 20 μM 5-FU (24 h treatments) or radiation (2 Gy). Experimental repeats n=3 minimum. Data are presented as the mean ± SEM. Analysis was performed using the paired t-test; *p<0.05, ns not significant.

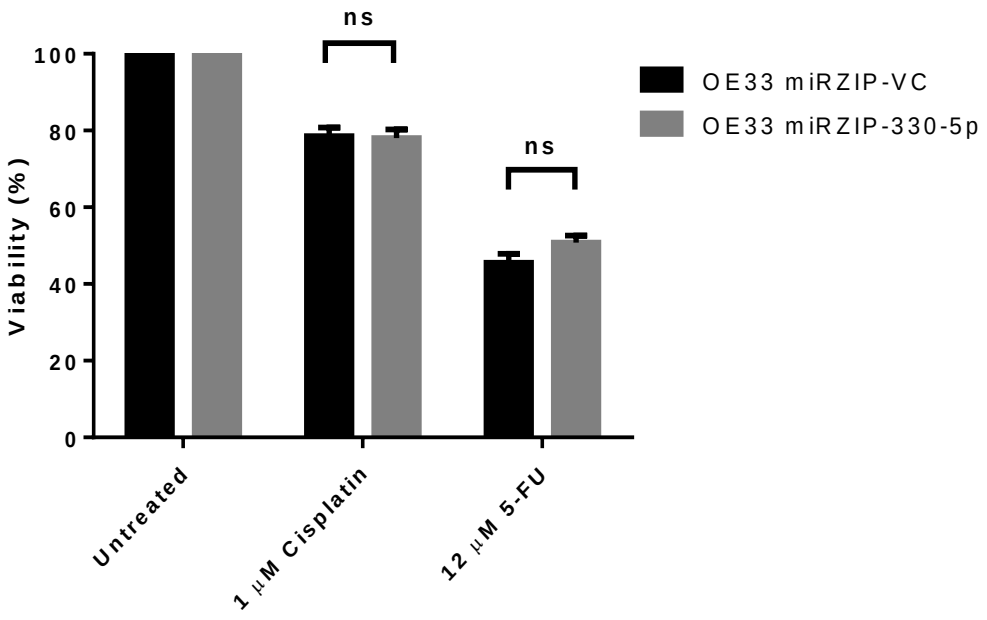

Fig 4.15 MiR-330-5p silencing did not alter cellular viability in response to chemotherapy. Stable silencing of miR-330-5p did not significantly alter cellular viability in response to treatment with 72 h of 1 µM cisplatin or 72 h of 12 µM 5-FU. The OE33 miRZIP-VC E10 and miRZIP-330-5p F6 clones were used in the MTS assay. MTS reagent was added and plates were incubated for 3 h prior to reading Abs 490 nm. Viability was normalised to the vehicle control/untreated cells. Experimental repeats n=4. Data are presented as the mean ± SEM. Statistical analysis was performed using the paired *t*-test; ns not significant.

4.5 Discussion

In the previous chapter, miRNA arrays were used to identify differentially expressed miRNA between neo-CRT responders and non-responders. Of the 67 differentially expressed miRNA miR-330-5p was identified as the most downregulated miRNA in non-responders (Fig 3.1). Hence, it was hypothesised that miR-330-5p may modulate cellular sensitivity to CRT and that the downregulated expression of miR-330-5p in the non-responders contributed to tumour resistance to CRT. In this chapter the role of miR-330-5p as a modulator of CRT sensitivity was investigated using *in vitro* OAC cancer cell models.

Until recently, and prior to the start of this study, few miR-330 related publications were available. Of the available literature, the identification of miR-330-3p as a tumour suppressor in prostate cancer was particularly relevant to this study. MiR-330-3p was reported to act as a tumour suppressor in prostate cancer by repressing the Akt survival pathway (Lee et al., 2009). Using patient biopsies and prostate cancer cell lines, an inverse correlation between miR-330-3p expression and E2F1 protein expression was identified. The E2F1 transcription factor regulates the expression of pro-apoptotic genes and induces or inhibits apoptosis (Johnson & Degregori, 2006). The dual function of E2F1 is context dependent, the initiation or inhibition of apoptosis is influenced by other oncogenic mutations in the cell. In the context of chemoresistant tumours E2F1 functions as an oncogene (Alla et al., 2010; Lee et al., 2010). The overexpression of miR-330-3p in prostate cancer cell lines downregulated E2F1 and p-Akt levels. The E2F1 mediated suppression of Akt phosphorylation activated pro-apoptotic proteins and signalling pathways, thus inducing apoptosis (Chaussepied & Ginsberg, 2004). Furthermore, the E2F1/p-Akt signalling pathway has previously been linked with resistance to CRT (Winograd-Katz & Levitzki, 2006; Toulany et al., 2007). In the context of the patient data it was hypothesised that low miR-330-5p expression in

the non-responders may upregulate the oncogenic activity of the E2F1/p-Akt signalling pathway, thus promoting cell survival in response to CRT.

In the overexpression model both miR-330-3p and miR-330-5p were produced by the miR-330 vector (Fig 4.2). The transient overexpression of miR-330 significantly decreased the expression of the E2F1 protein and the levels of p-Akt (Fig 4.3 and 4.4). This indicates that the E2F1/p-Akt pathway is, at least partially, regulated by miR-330 in OAC. It is not possible to discriminate between the contributions of miR-330-3p and miR-330-5p in the regulation of E2F1 and p-Akt in this model. Although there are predicted binding sites for both miR-330-3p and miR-330-5p in the *E2F1* mRNA, it is not possible to surmise if the regulation of *E2F1* by miR-330 is the result of a direct miRNA:mRNA interaction (Appendix 5). However, it has previously been reported that miR-330-3p binds to a seed site in the 3'UTR of the *E2F1* mRNA (Lee et al., 2009). The decrease in the E2F1 protein did not correlate with a decrease *E2F1* mRNA expression (Fig 4.5). If miR-330-3p or miR-330-5p directly binds to the *E2F1* mRNA then translation is most likely repressed by sequestering the mRNA from the translational machinery of the cell. Alternatively, the alteration in the expression of the E2F1 protein may be indirectly associated with the overexpression of miR-330-3p and/or miR-330-5p. The decrease in p-Akt levels was concomitant with a decrease in E2F1 protein expression, in agreement with the miR-330-3p prostate cancer study (Lee et al., 2009). Interestingly, the overexpression of miR-330-5p has also been reported to decrease p-Akt levels in pancreatic cancer (Trehoux et al., 2015). Here, the simultaneous overexpression of miR-330-3p and miR-330-5p decreased p-Akt levels (Fig 4.4). Based on these previous reports it is conceivable that both miR-330-3p and miR-330-5p regulate different targets upstream of Akt thereby indirectly influencing the phosphorylation status of Akt and its downstream signalling pathways. Silencing miR-330-5p did not alter the expression of the *E2F1* mRNA or E2F1 protein (Fig 4.12). The

inhibition of miR-330-5p is likely to be compensated for by other miRNA which regulate the expression of the E2F1 mRNA such as miR-330-3p, miR-106a, miR-34, miR-223, miR-205 and the miR-15 and miR-17 family clusters all of which are reported to regulate *E2F1* (Knoll et al., 2013).

The clonogenic assay was used determine the effect of miR-330 overexpression and miR-330-5p silencing on cellular sensitivity to CRT. The clonogenic assay measures clonogenicity, the ability of a single cell to proliferate and establish a colony after exposure to treatment, and is the gold standard for measuring response to chemotherapy and radiotherapy *in vitro*. Viable cells which survive treatment but are unable to proliferate are regarded as a positive response to chemotherapy as these cells would be unable to repopulate or increase the size of a tumour (Franken et al., 2006). Although this may be a temporary cellular state, for the patient stalling tumour growth could prolong patient survival. In the clonogenic assay cells were treated for 24 h with the IC_{50} doses of cisplatin or 5-FU. The 2 Gy radiation dose was selected as it is a clinically relevant dose, patients undertaking radiotherapy are treated with fractionated doses of 2-2.67 Gy (Lynam-Lennon et al., 2010).

The overexpression of miR-330 did not alter cellular sensitivity to cisplatin, 5-FU or radiotherapy (Fig 4.7). Despite alterations in the E2F1/p-Akt pathway with miR-330 overexpression, the negative regulation of this pathway was not sufficient to alter CRT sensitivity. Although there were no significant changes in clonogenicity the assay was limited to a single dose and for chemotherapeutics the treatment duration was 24 h. It is feasible that higher/lower doses and longer treatment time points may alter clonogenicity with miR-330 overexpression. Furthermore, the overexpression of miR-330 was a transient expression system and although miR-330 was overexpressed at the time of treatment the expression of the plasmid was gradually depleted during the ~7

day incubation period. It is feasible that the overexpression of miR-330 altered clonogenicity but lost of miR-330 overexpression during the incubation period allowed the cells to recover thus no alteration in clonogenicity was observed at the assay endpoint. In comparison the miR-330-5p silencing model was a stable plasmid expression system which ensured the silencing of the miRNA throughout the duration of the assay. Furthermore, the silencing of miR-330-5p was a more clinically relevant model of the downregulated miR-330-5p expression observed in the pre-treatment biopsies of the non-responders. Whilst there was no alteration in sensitivity to chemotherapeutics at the doses and time points tested, there was a statistically significant increase in radioresistance in the OE33 cell line with miR-330-5p silencing (Fig 4.14). Interestingly, the overexpression of miR-330-5p has been reported to enhance cellular sensitivity to gemcitabine in pancreatic cancer although in the same study the overexpression of miR-330-5p did not alter cellular sensitivity to oxaliplatin or 5-FU (Trehoux et al., 2015). Enhanced radioresistance was not observed in the OE19 cell line at the dose tested and may be linked with the OE19 cell line being inherently more radioresistant than the OE33 cell line, this could be overcome by increasing the radiation dose in the OE19 clonogenic assay (Lynam-Lennon et al., 2012). The increase in radioresistance as a result of miR-330-5p silencing *in vitro* suggests downregulated miR-330-5p expression in patient tumours may alter response and sensitivity to radiotherapy. Furthermore, considering patients receive 40-60 Gy of radiation in fractioned doses, the marginal change observed in the clonogenic assay with a single 2 Gy dose may have more clinical significance in the context of the fractionated treatment regimen administered to patients. Further work is needed to clarify the molecular mechanisms by which miR-330-5p modulates sensitivity to radiotherapy. In addition, repetitive or fractioned doses of radiation as part of the clonogenic assay should be considered for future studies. Although logistically challenging combined cisplatin, 5-

FU and radiation treatment as part of the clonogenic assay would also be a more clinically relevant approach. It is feasible that the combined treatments induce different cellular responses in comparison to a single treatment and this may have agonistic or antagonistic effects on cellular response and sensitivity to CRT.

The proliferation rate of tumour cells alters their sensitivity to chemotherapeutic drugs (Siddik, 2003). The overexpression of miR-330 did not alter cellular proliferation (Fig 4.8). Furthermore, the overexpression of miR-330 or silencing miR-330-5p, in combination with cisplatin or 5-FU treatment did not alter proliferation (Fig 4.9 and 4.15). Together, the clonogenic and proliferation assays indicate that miR-330 does not alter the cellular sensitivity of cancer cells in response to chemotherapy.

Here, the role of miR-330-5p as a modulator of CRT sensitivity was investigated in a simplified OAC cancer cell model. The effects of miR-330-5p on cancer cell sensitivity to CRT cannot be fully explored using an *in vitro* system in the absence of other more complex aspects of the tumour microenvironment. Downregulated miR-330-5p expression was identified in patient biopsies that contained multiple cell types, extracellular matrix, vasculature and regions of altered oxygen tension. These tumour-associated compartments play an integral role in tumour biology and consequently therapeutic sensitivity. Therefore, to further investigate the significance of miR-330-5p downregulation in the pre-treatment biopsy samples of neo-CRT non-responders the targets and pathways of miR-330-5p were investigated and an *in vivo* model of OAC with miR-330-5p silencing was established.

Chapter 5 Identification of MiR-330-5p Targets in OAC

5.1 Introduction

MiRNA expression profiling of OAC pre-treatment biopsies identified miR-330-5p as the most downregulated miRNA in neo-CRT non-responders. The expression of miR-330-5p in treatment naive tumours was hypothesised to modulated tumour response and sensitivity to CRT. In the neo-CRT non-responders, miR-330-5p downregulation was hypothesised to promote tumour resistance to CRT. In the previous chapter, the overexpression and silencing of miR-330-5p *in vitro* did not alter cellular sensitivity to CRT. With the exception of miR-330-5p silencing in the OE33 cell line that marginally enhanced radioresistance. The *in vitro* cell line provided a simplified model that was used to study the affect of miR-330-5p expression on cellular sensitivity to CRT in OAC cell lines. Although miR-330-5p did not directly alter cellular sensitivity to CRT in the *in vitro* models, the expression of miR-330-5p in the cell potentially regulates the expression of proteins with functional roles in the tumour microenvironment.

The tumour microenvironment encompasses cancer cells, stromal cells and immune cells as well as the structural molecules of the extracellular matrix (Bhome et al., 2015). Tumour response and sensitivity to systemic chemotherapeutics and radiation is determined by multiple factors, one of which is the response of the cancer cells to cytotoxic damage. The delivery of systemic treatments such as cisplatin and 5-FU are reliant on the tumour vasculature for efficient delivery of the cytotoxic agents. The vasculature also supplies oxygen that is essential for the generation of ROS following radiation (Overgaard, 2011). Aside from the physiological factors, tumour sensitivity to CRT is also mediated by the response of the immune and stromal cells in addition to the cancer cells. Tumour resistance to CRT could be targeted via the tumour microenvironment. Considering miRNA are produced in all cell types and are known to directly and indirectly modulate the tumour microenvironment, therapeutic intervention

at the miRNA level could alter the biology of the extracellular microenvironment and CRT sensitivity (Chou et al., 2013).

In this chapter the relationship between miR-330-5p expression in the cancer cell and subsequent modulation of the tumour microenvironment was studied. The *in vitro* model of miR-330-5p silencing mimicked the downregulated expression observed in the neo-CRT non-responders. To identify targets and pathways affected by miR-330-5p silencing, gene expression profiling was undertaken in the *in vitro* cell model. Considering the silencing of miR-330-5p did not modulate cellular sensitivity to CRT, the miR-330-5p mediated regulation of extracellular proteins was of particular interest.

5.2 Rationale, aims and objectives

Previously, miR-330-5p was identified as the most downregulated miRNA in the neo-CRT non-responders and was hypothesised to modulate tumour sensitivity to CRT in patients. However, *in vitro* miR-330-5p did not significantly alter cellular sensitivity to CRT. The tumour microenvironment also modulates tumour sensitivity to CRT and the extracellular proteins produced by cancer cells are essential components and regulators of the tumour microenvironment. In this chapter, the initial aim was to identify targets of miR-330-5p with a particular focus on miR-330-5p mediated regulation of the extracellular environment. Considering the complex biology of a solid tumour and the limitations of the *in vitro* model, an *in vivo* model was established to assess tumour sensitivity to CRT with miR-330-5p downregulation.

- Gene expression profiling in the *in vitro* miR-330-5p silencing model
- Validate potential miR-330-5p targets
- Establish an *in vivo* model of miR-330-5p downregulation and assess tumour sensitivity to cisplatin

5.3 Materials and methods

5.3.1 Whole genome digital gene expression analysis

Total RNA was extracted from the OE33 miRZIP-VC E10 and miRZIP-330-5p F6 clones, as previously described in section 2.5.1. Samples of total RNA were prepared for shipping, as previously described section 2.5.7. Digital RNA-seq was outsourced to LC Sciences (Texas, USA). Analysed data sets were provided by LC Sciences. The fold change in gene expression was calculated from the equation; log2 (miRZIP-330-5p FPKM / miRZIP-VC FPMK). Gene expression changes were considered significant when the *p* value was <0.05.

5.3.2 qPCR analysis of mRNA expression in cell lines

Cells were harvested and RNA was extracted as previously described (section 2.5.1). To analyse the relative expressions of *MMP1* and *MMP7*, the QuantiTect RT Kit was used for cDNA synthesis and the QuantiTect SYBR Green PCR master mix was used for qPCR analysis (as previously described in sections 2.5.5 and 2.5.6). The QuantiTect primer assays used for target amplification in the qPCR were MMP1, MMP7 and the endogenous control B2M (Table 2.1).

5.3.3 Western blotting

Condition media was prepared from OE33 miRZIP-VC and miRZIP-330-5p cell lines for western blot analysis of extracellular MMP1 and MMP7 protein expression (as described in section 2.6.6). Conditioned media was also prepared from OE33 cells transiently transfected with the miR-VC or miR-330 plasmid (section 4.3.1). The transfection media was removed after ~5 h and replaced with complete media. The conditioned media was harvested and concentrated using centrifugal filter columns (as describe in section 2.6.6). The concentrated protein samples were quantified using the BCA assay (section 2.6.2). SDS-PAGE and western blotting were performed as

previously described in sections 2.6.3 and 2.6.4. The PVDF membrane was incubated with the primary antibody overnight. Blots were probed for MMP1 (clone # 36665, R and D Systems, Minnesota, USA) and MMP7 (clone # 111433, R and D Systems, Minnesota, USA) (Table 2.2). After incubation with the primary antibody, the blots were washed and incubated for 1 h at room temperature with the secondary antibody (Table 2.2). After incubation with the secondary antibody, the blots were washed and the chemiluminescent substrate was applied (section 2.6.4). The blots were imaged using a chemiluminescent imaging system or autoradiography (section 2.6.7). Image Lab 3.0 software (BioRad, UK) was used for densitometry analysis of western blots (section 2.6.8).

5.3.4 Gelatin zymography

Condition media was prepared from the OE33 miRZIP-VC E10 and miRZIP-330-5p F6 clones for analysis of extracellular MMP1 protein expression using zymography (as described in section 2.6.6). Zymograms were stained with coomassie and then destained to develop the white bands within the blue stained gelatin gel. Zymograms were imaged using an imaging system (Molecular Imager ChemiDoc XRS, BioRad, UK).

5.3.5 Protease and protease inhibitor antibody-based arrays

Condition media was prepared from the OE33 miRZIP-VC E10 and miRZIP-330-5p F6 clones (section 2.6.6) for analysis of extracellular proteases and protease inhibitors using an antibody-based array (Proteome Profiler antibody arrays, R and D Systems, Minnesota, USA). The antibody arrays were performed according to the manufacturer's protocol, as described in section 2.6.5. Densitometry analysis was performed as described in section 2.6.8. Briefly, in the Image lab 3.0 software, the volume tool was used to draw boxes of the same dimensions around each of the spotted

antibody pairs. The pixel density for each pair was recorded and relative fold change was calculated; miRZIP-VC pixel density / miRZIP-330-5p pixel density.

5.3.6 Invasion assay

The Corning BioCoat matrigel invasion chamber assay was used to measure the invasive potential of the OE33 miRZIP-VC and miRZIP-330-5p heterogeneous cell lines. The assay was performed according the manufacturer's instructions as detailed in section 2.7.4. The slides were imaged on the microscope using the DAPI channel at ×10 magnification (section 2.4.6). Several images were taken to capture the entire membrane with minimal overlap. The percentage invasion and the invasion index were calculated as described in section 2.7.4.

5.3.7 qPCR analysis of MMP1 expression in patient biopsies

The relative expression of the *MMP1* mRNA was analysed in RNA extracted from the pre-treatment diagnostic tumour biopsies (section 2.2.3). The cDNA template was produced using random hexamers and the Taqman qPCR analysis was performed using the MMP1 and the B2M probes (as described in sections 2.5.5 and 2.5.6).

5.3.8 *In vivo* tumour implants and ^{18}F-FDG PET-CT imaging

Tumour implants were established from the OE33 miRZIP-VC or miRZIP-330-5p heterogeneous cell lines. The cells were implanted by subcutaneous injection of 4×10^6 cells on the right flank, as described in section 2.8.1. Tumour volume was calculated from caliper measurements taken 2-4 times per week once tumours were palpable. Mice were treated with 2.5 mg/kg cisplatin twice per week (section 2.8.2). Mice were prepared and for imaging as previously described (section 2.8.3).

5.4 Results

5.4.1 Identification of potential miR-330-5p targets

MiR-330-5p was the most downregulated miRNA in the pre-treatment biopsies of neo-CRT non-responders and is considered to be a putative modulator of CRT sensitivity. *In vitro* cell lines were stably transfected with a plasmid vector encoding the miR-330-5p anti-sense sequence, which binds irreversibly to endogenous miR-330-5p, thereby silencing and inhibiting the miRNA. This *in vitro* model of miR-330-5p silencing mimiced the downregulated expression of miR-330-5p in the neo-CRT non-responders. In the previous chapter the silencing of miR-330-5p *in vitro* did not alter cellular sensitivity to cisplatin or 5-FU however radioresistance was marginally enhanced in the OE33 miRZIP-330-5p cell line (Fig 4.14). Although miR-330-5p silencing had little or no effect on cellular sensitivity to CRT, the downregulation of miR-330-5p in cancer cells within a solid tumour potentially modulates the biology of tumour microenvironment and could contribute to patient response to CRT.

To identify gene expression changes associated with miR-330-5p silencing, digital gene expression analyses was performed using the OE33 miRZIP-VC and miRZIP-330-5p cell lines. The downregulated expression of miR-330-5p significantly altered the expression of 37 genes, of these 7 genes (19%) were upregulated and 30 genes (81%) were downregulated (Table 5.1).

Table 5.1 Gene expression analysis in the OE33 miRZIP-330-5p cell line.

Gene	FPKM miRZIP-VC	FPKM miRZIP-330-5p	Log2 Fold Change
PRAME	0.00	146811.00	∞
ADRA2C	0.00	2.63	∞
MMP1	4.78	200.91	5.39
MMP7	145.09	896.33	2.63
DPP4	0.94	5.69	2.60
AQP3	6.70	28.89	2.11
PVRL1	4.60	14.46	1.65
NR4A1	134.88	47.06	-1.52
SLFN5	28.67	9.76	-1.55
DDX60	13.95	4.20	-1.73
COL17A1	18.52	5.33	-1.80
COMMD10	31.26	8.84	-1.82
IFIT3	40.15	11.29	-1.83
S100P	788.57	213.55	-1.88
LCN2	2195.35	588.77	-1.90
SAMD9	33.38	8.93	-1.90
ISG15	638.99	170.69	-1.90
SAMD9L	14.49	3.73	-1.96
FST	88.03	22.60	-1.96
IFI27	442.09	98.28	-2.17
IRF7	162.45	33.04	-2.30
LAMP3	14.89	3.02	-2.30
LOC644100	87.72	15.34	-2.52
WFDC2	303.05	49.36	-2.62
HIST2H2BE	11.08	1.72	-2.69

CMPK2	12.26	1.89	-2.70
RCAN1	16.15	2.48	-2.70
MX1	118.24	17.70	-2.74
IFIT1	79.92	11.00	-2.86
IFITM1	77.69	10.69	-2.86
IFI6	219.34	28.28	-2.96
SLC6A14	3.53	0.43	-3.04
HERC5	5.58	0.64	-3.11
OAS2	46.42	4.32	-3.42
IFI44L	3.77	0.27	-3.78
MX2	22.76	1.62	-3.82
STS	1.52	0.00	∞

FPKM; fragments per kilobase of transcript per million mapped reads.

5.4.2 Validation of MMP1 and MMP7 upregulation in response to miR-330-5p silencing

Digital gene expression sequencing identified a 5.4 fold increase in *MMP1* mRNA expression and a 2.6 fold increase in *MMP7* mRNA expression (Table 5.1). Considering the minimal effect of miR-330-5p silencing on cancer cell sensitivity to CRT and the initial identification of miR-330-5p in the patient biopsies, the possibility that miR-330-5p modulates extracellular proteins in the tumour microenvironment was of particular interest. Furthermore, MMP1 and MMP7 have been previously been identified as markers of poor prognosis in oesophageal cancer (Murray et al., 1998; Yamashita et al., 2001; Tanioka et al., 2003). The increase in *MMP1* and *MMP7* mRNA expression in the miRZIP-330-5p cell line was confirmed by qPCR (Fig 5.1). The increase in *MMP1* mRNA corresponded to an increase in the expression of the MMP1 protein (Fig 5.2). However, the increase in the *MMP7* mRNA did not correspond to an increase in the expression of the MMP7 protein (Fig 5.2).

The MMP1 protein is produced in the cell as a zymogen and is secreted into the extracellular environment as the inactive pro-MMP1. Proteolytic cleavage in the extracellular environment activates the enzymatic activity of MMP1. Gelatin zymography was used to determine if the increase in the MMP1 protein corresponded to an increase in the active MMP1 isoform. Zymography confirmed an increase in both the inactive pro-MMP1 and the active MMP1 protein (Fig 5.3).

There are three predicted binding sites for miR-330-5p in the *MMP1* mRNA (Appendix 6). Conversely there are no predicted binding sites for miR-330-5p in the *MMP7* mRNA (Betel et al., 2008). The silencing of miR-330-5p increased the expression of the MMP1 protein (Fig 5.2). Furthermore, the transient overexpression of miR-330 decreased MMP1 protein expression (Fig 5.4). There are no predicted binding

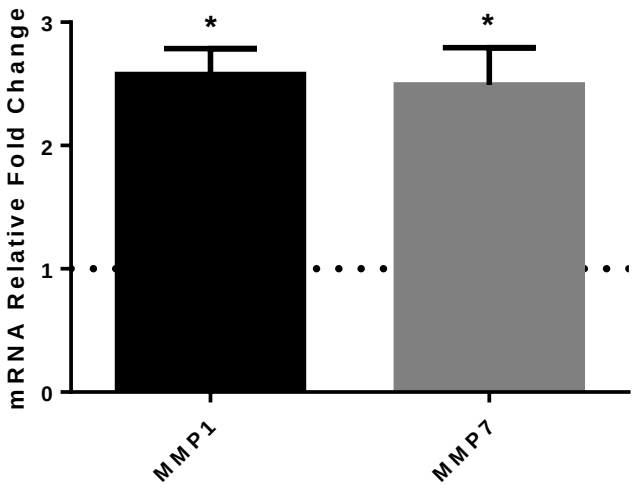

Fig 5.1 Stable silencing of miR-330-5p increased *MMP1* and *MMP7* mRNA expression. The qPCR analysis of *MMP1* and *MMP7* expression confirmed a ~2.5 fold increase in both mRNA, in the OE33 miRZIP-330-5p F6 clone compared to the miRZIP-VC E10 clone. The Livak method was used to analyse the data with *B2M* as the endogenous control. The miRZIP-VC control was normalised to 1 (dotted line), the relative fold change in *MMP1* and *MMP7* in the miRZIP-330-5p cell line was calculated relative to the control. Experimental repeats n=3. Data presented as the mean ± SEM. Statistical analysis was performed using the one-sample *t*-test; * p<0.05

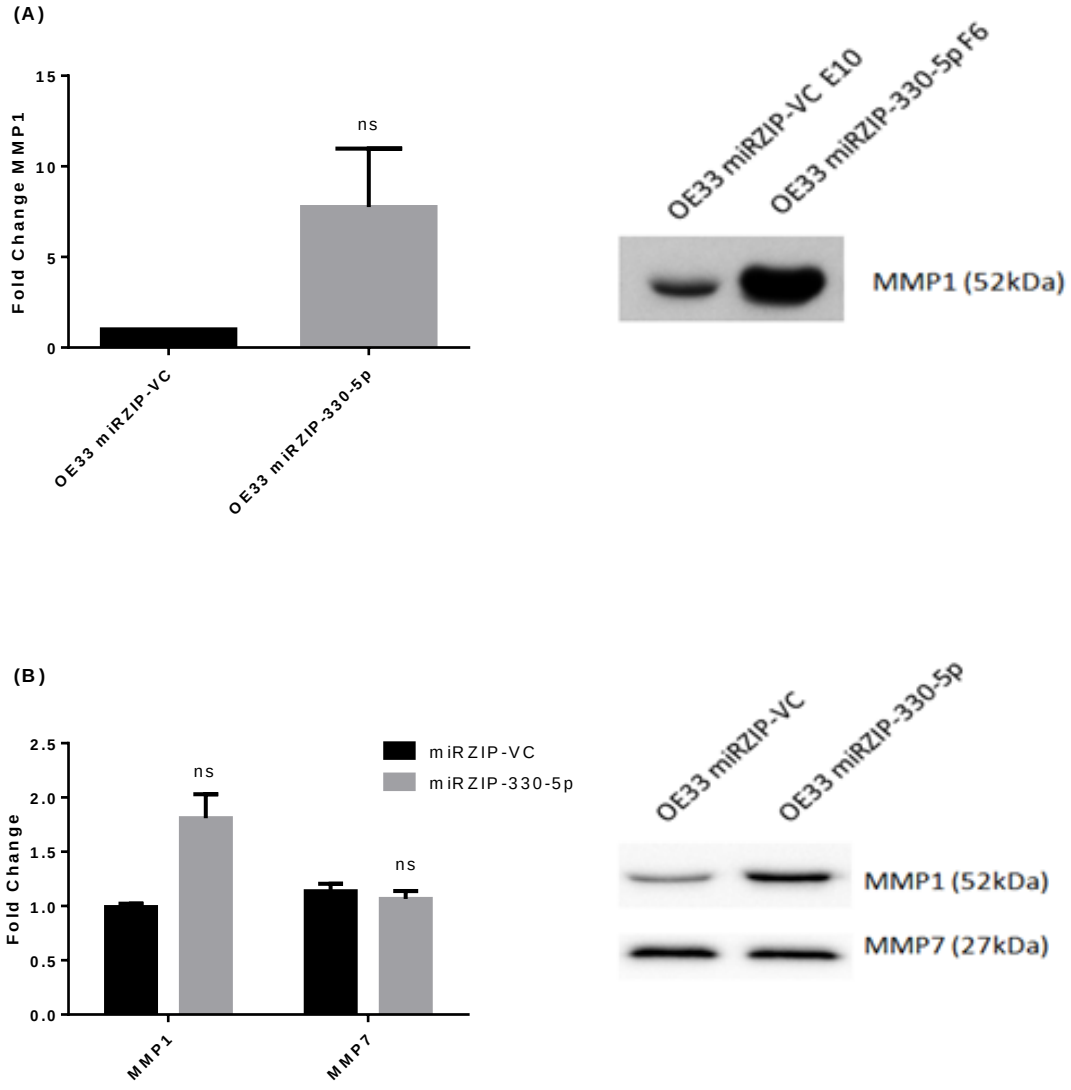

Fig 5.2 Stable silencing of miR-330-5p increased the expression of extracellular MMP1. (**A**) MMP1 protein expression, in the conditioned media, was increased in the OE33 miRZIP-330-5p F6 clone compared to the miRZIP-VC E10 clone. The OE33 miRZIP-VC E10 and miRZIP-330-5p F6 clones were selected as high GFP expressing clones. Experimental repeats *n*=3 (*left* densitometry analysis and *right* western blot). Data presented as the mean ± SEM. Statistical analysis was performed using the one-way one-sample *t*-test; ns not significant (*p*=0.09). (**B**) MMP1 protein expression, in conditioned media, was increased in the OE33 miRZIP-330-5p heterogeneous cell line compared to the miRZIP-VC heterogeneous cell line. The expression of MMP7 protein was not increased by miR-330-5p silencing. Experimental repeats *n*=3 (*left* densitometry analysis and *right* western blot). Statistical analysis was performed using the paired *t*-test; ns not significant (MMP1 *p*=0.07).

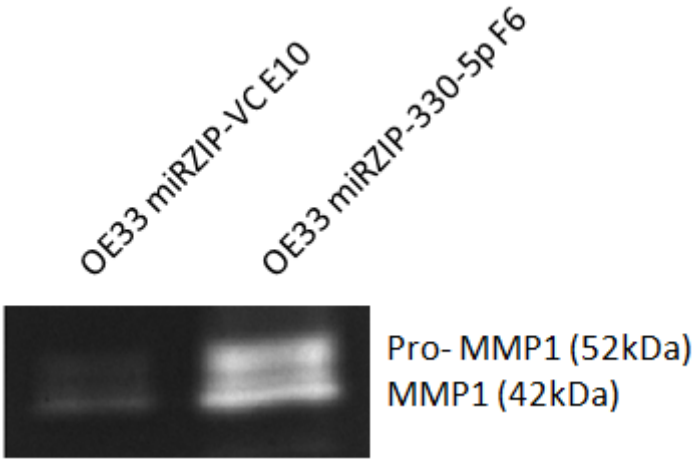

Fig 5.3 Silencing miR-330-5p increased the expression of the inactive and active MMP1 protein isoforms. Gelatine zymography confirmed an increase in MMP1 protein expression. The expression of the inactive pro-MMP1 and active MMP1 were both increased in the 24 h conditioned media from the OE33 miRZIP-330-5p F6 clone compared to the miRZIP-VC E10 clone. Experimental repeats *n*=3.

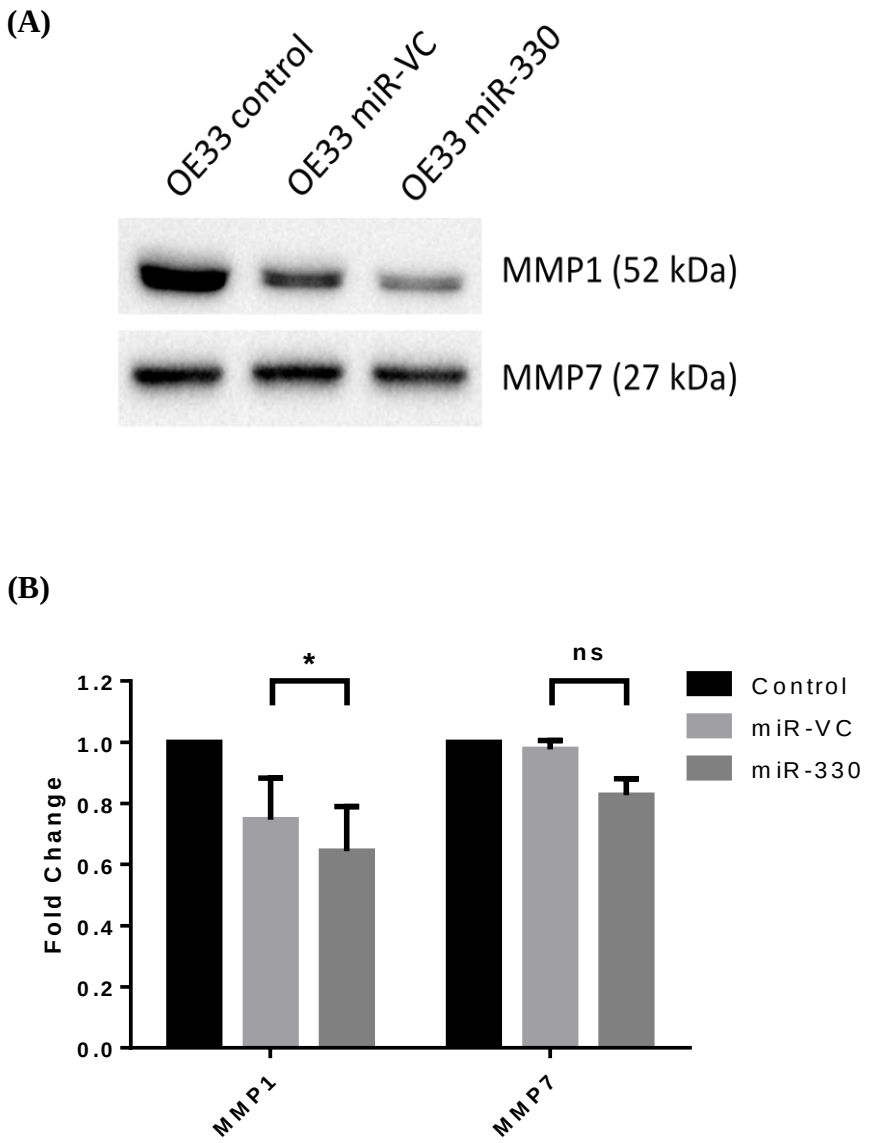

Fig 5.4 Overexpression of miR-330 decreases MMP1 protein expression. (**A**) In the OE33 cell line the transient overexpression of miR-330 significantly decreased the expression of MMP1 protein in the 24 h conditioned media (48h post-transfection) compared to the miR-VC. (**B**) Western blot images were analysed using densitometry to determine the fold change in protein expression. The expression of MMP7 was not significantly altered with miR-330 overexpression. Experimental repeats n=3. Data presented as the mean ± SEM. Statistical analysis performed using paired t-test; * p<0.05, ns not significant.

sites for miR-330-3p in the MMP1 mRNA (Betel et al., 2008). The inverse relationship between miR-330-5p and MMP1 expression and the reported binding site for miR-330-5p in the MMP1 mRNA suggests MMP1 is a direct target of miR-330-5p.

5.4.3 Identification of miR-330-5p targets in the secretome

Antibody-based arrays were used to assess the expression of 35 proteases and 32 protease inhibitors in conditioned media (Appendix 7). The protease antibody-based array confirmed an increase in MMP1 protein expression as a result of miR-330-5p silencing, and no significant change in the expression of MMP7 (Fig 5.5). Furthermore, the expression of cathepsins A, B, S and V were decreased with miR-330-5p silencing (Fig 5.6). The protease inhibitor array indicated high expression of the tissue inhibitors of metalloproteinases, TIMP-1 and TIMP-2, and the expression of HE4 and cystatin B were decreased with miR-330-5p silencing (Fig 5.6).

5.4.4 Silencing miR-330-5p increased MMP1 expression but did not alter invasion

MMP1 is an interstitial collagenase, which degrades collagen type I, II and III in the extracellular environment and is associated with tissue remodelling, metastasis and invasion. Although silencing miR-330-5p increased the expression of MMP1, this did not correspond to an increase in the invasive potential of the OE33 miRZIP-330-5p cell line (Fig 5.7). The high expression of TIMP-1, detected in the antibody-based array, may in part explain why the invasive potential of the cell line was unaltered (Fig 5.6).

Considering the limitations of *in vitro* models to study changes in the extracellular tumour microenvironment, more clinically relevant models were required to investigate the biological significance of miR-330-5p downregulation in neo-CRT non-responders. Firstly, the expression of *MMP1* mRNA was measured in the patient

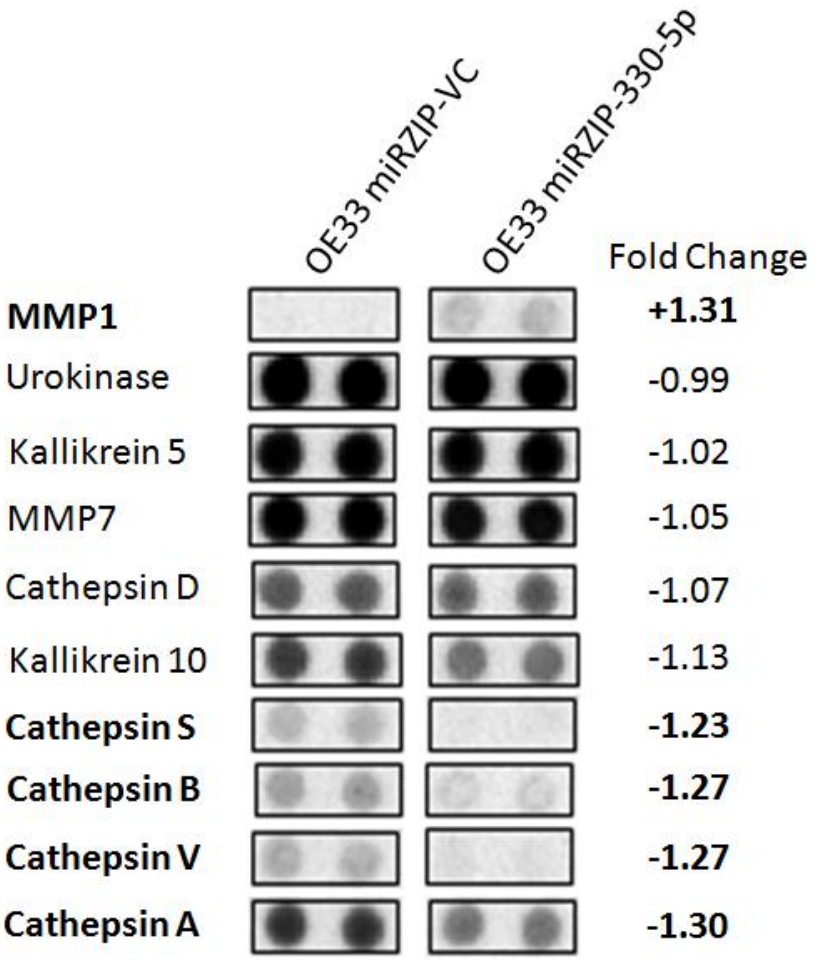

Fig 5.5 Protease antibody-based array profile. Silencing miR-330-5p altered the expression of secreted proteases in 24 h conditioned media. Densitometry analysis was used to calculate the fold change in protein expression in the OE33 miRZIP-330-5p F6 clone relative to the OE33 miRZIP-VC E10 clone. Highlighted in bold are proteins which exceeded ±1.2 fold change. The antibody-based array confirmed an increase in MMP1 expression with miR-330-5p silencing, and confirmed no increase in MMP7 expression. Experimental repeats *n*=1.

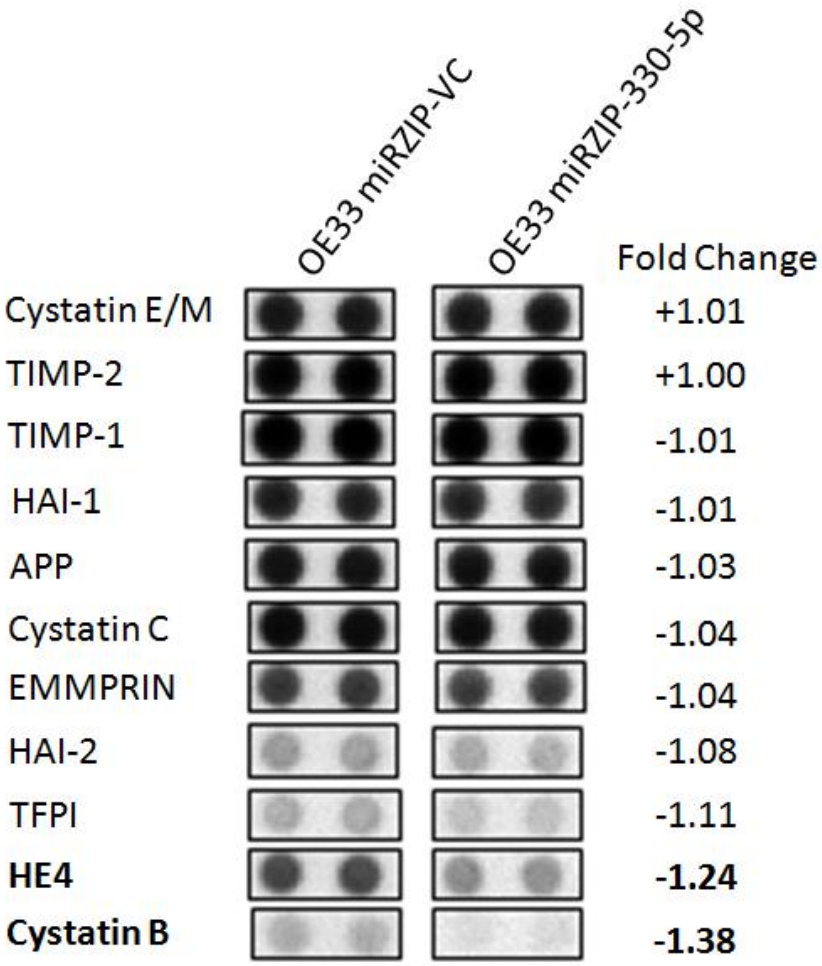

Fig 5.6 Protease inhibitor antibody-based array profile. Silencing miR-330-5p altered the expression of secreted proteases inhibitors in 24 h conditioned media. Densitometry analysis was used to calculate the fold change in protein expression in the OE33 miRZIP-330-5p F6 clone relative to the OE33 miRZIP-VC E10 clone. Highlighted in bold are proteins which exceeded ±1.2 fold change. The antibody-based array confirmed expression of TIMP-1 and TIMP-2 in both the miRZIP-VC and miRZIP-330-5p cell lines. Experimental repeats *n*=1.

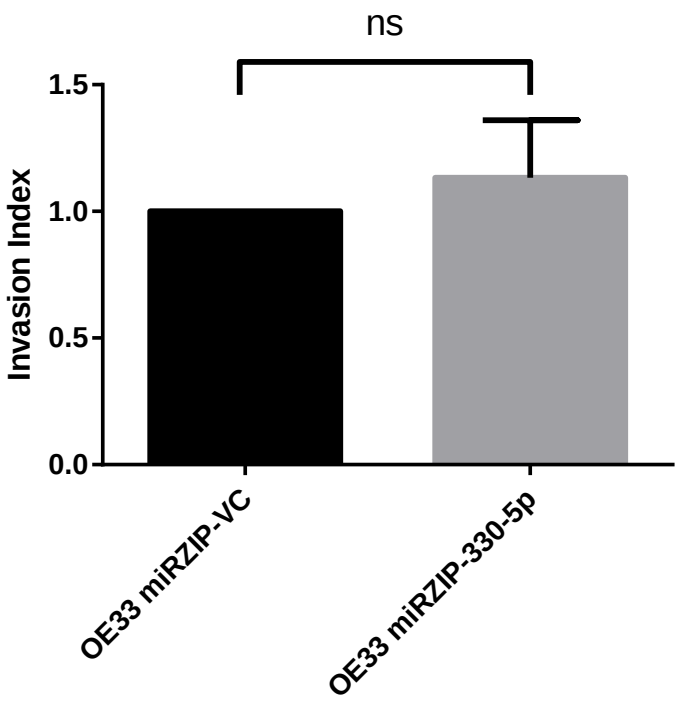

Fig 5.7 Silencing miR-330-5p did not alter invasion. Cells were seeded on top of a layer of matrigel in a Boyden chamber and incubated for 24 h. The invasive potential of the OE33 miRZIP-330-5p heterogeneous cell line was not significantly increased relative to the miRZIP-VC heterogeneous cell line. Experimental repeats *n*=3. Data presented as the mean ± SEM. Statistical analysis performed using the one-sample *t*-test; ns not significant.

biopsy samples. Secondly, *in vivo* tumour models were established from the OE33 miRZIP-VC and miR-330-5p stable cell lines.

5.4.5 MMP1 expression in patient samples

The expression of the *MMP1* mRNA was analysed in the patient biopsy samples from 7 responders and 8 non-responders of the original patient cohort used for the miRNA profiling array (Table 3.1). There was no correlation between *MMP1* mRNA expression and patient response to neo-CRT (Fig 5.8). Furthermore, the relative expressions of *MMP1* and miR-330-5p in the patient biopsies were analysed using the Spearman rank test. There was no statically significant correlation between *MMP1* and miR-330-5p expression in the data set (p=0.075, n=14). There was also no significance between *MMP1* and miR-330-5p in the responders (p=0.713, n=7) or the non-responders (p=0.088, n=7).

5.4.6 *In vivo* miR-330-5p silencing

The growth profiles of the tumours established from the OE33 miRZIP-VC and miRZIP-330-5p cell lines indicated a faster growth rate in tumours with miR-330-5p silencing (Fig 5.9). This may impart be associated with increased MMP1 expression in the OE33 miRZIP-330-5p cell line. In oesophageal cancer MMP1 has been reported to enhance local tumour invasion as appose to invasion and metastasis to secondary sites (Yamashita et al., 2001).

In vitro, silencing miR-330-5p did not alter cellular sensitivity to cisplatin (Fig 4.14). However, the *in vivo* model provided a more clinically relevant system to study the effect of miR-330-5p silencing in a solid tumour treated with cisplatin. This model mimicked the downregulated miR-330-5p expression observed in the pre-treatment biopsy samples of the non-responders. Furthermore, the *in vivo* tumour model incorporated a complex extracellular environment, which may in part be modulated by

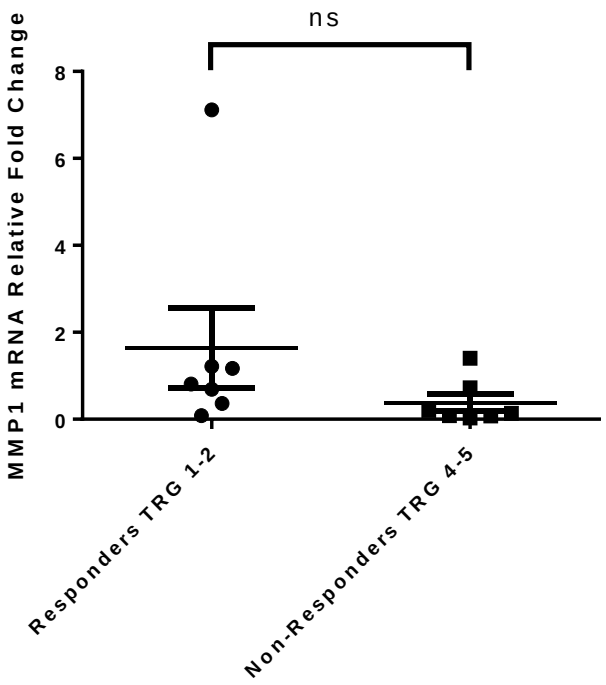

Fig 5.8 *MMP1* mRNA expression did not correlate with neo-CRT response or expression of miR-330-5p in the pre-treatment patient biopsies. *MMP1* expression was analysed in pre-treatment biopsies from 7 responders and 7 non-responders using qPCR. The Livak method was used for data analysis with *B2M* as the endogenous control. The expression of the *MMP1* mRNA did not correlate with patient response to neo-CRT. Statistical analysis was performed using Mann Whitney U-test; ns not significant (p=0.209).

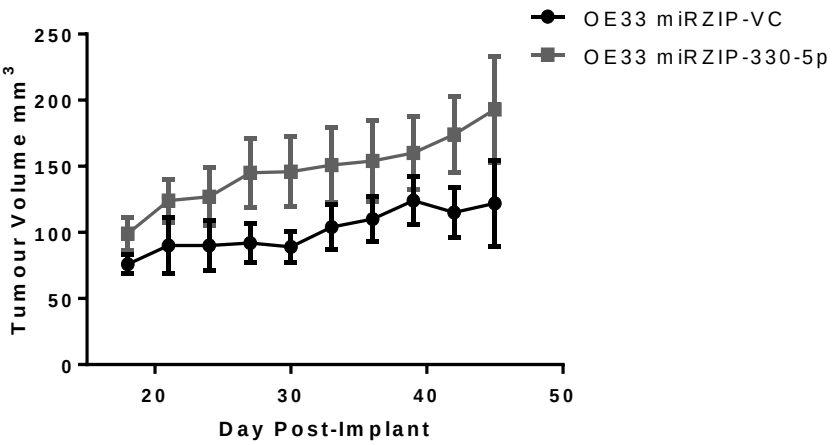

Fig 5.9 Early growth profiles of tumour xenografts established from OE33 miRZIP-VC and miRZIP-330-5p heterogeneous cell lines. Mice were implanted on day 0, tumour measurements are presented from day 18 to day 46. These measurements were taken prior to the administration of cisplatin treatment and before tumour sizes exceeded 200 mm^3. Animals per group miRZIP-VC *n*=6, miRZIP-330-5p *n*=5. Data presented as the mean ± SEM. Statistical analysis was performed using the two-sample *t*-test assuming unequal variance two tail *p*=0.328.

miR-330-5p. Within a solid tumour the vasculature and oxygen tension contribute to response and sensitivity to CRT. The interactions between multiple cell types, the structural matrix and the immune response are also implicated in tumour response to CRT. The *in vivo* model was more clinically relevant and incorporated elements of the more complex biology of a solid tumour.

Mice received 2.5 mg/kg cisplatin twice per week after the tumour volume exceeded ~200 mm^3. The miRZIP-330-5p group (*n*=3) began treatment 47 days post-implant (Fig 5.10). The miRZIP-VC tumours grew more slowly and this group (*n*=3) began treatment on day 105 (Fig 5.10). Of the three mice in the miRZIP-330-5p group, the tumour growth in two mice was unperturbed by cisplatin treatment (Fig 5.10 ■ and▲). The tumour burden of the other mouse did not regress until ~25 days after cisplatin treatment began, at which stage the tumour growth slowly regressed to >200 mm^3 over a 48 day period (Fig 5.10 ●). Of the three mice in the miRZIP-VC group, the tumour growth in two mice regressed immediately in response to cisplatin treatment and continued to regress until the experiment end point on day 150 (Fig 5.10 ■ and▲). The tumour burden of the other mouse did initially plateau in the first 10 days of treatment however tumour growth then increased continually until the experiment end point on day 150 (Fig 5.10 ●). In summary, two out of three miRZIP-330-5p tumours were non-responders and two out of three miRZIP-VC tumours were responders to cisplatin treatment. The data presented here are from a preliminary pilot study which does not provide conclusive findings, but does warrant further *in vivo* investigations into the relevance of the downregulated expression of miR-330-5p in OAC tumours in a pre-treatment setting. Furthermore, the tumours established from the OE33 miRZIP-VC and miRZIP-330-5p cell lines were imaged using ^{18}F-FDG PET-CT and were confirmed to have high metabolic activity (Fig 5.11).

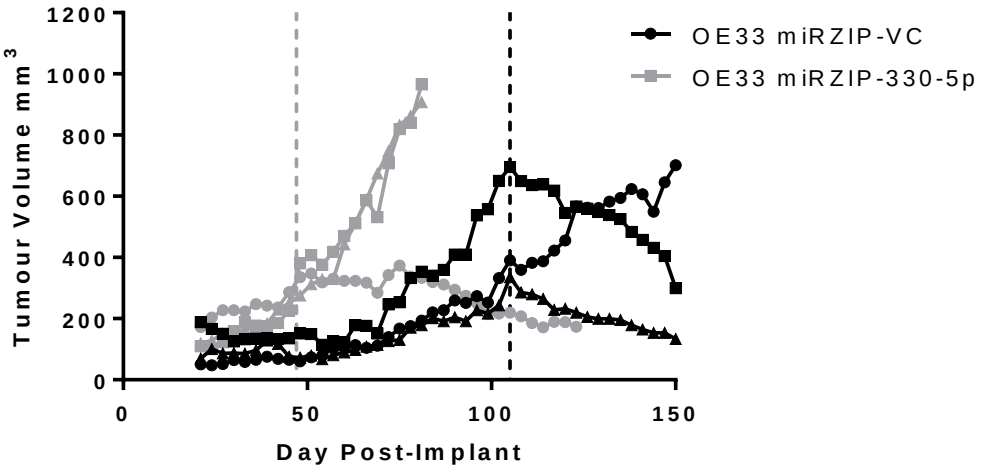

Fig 5.10 OE33 miRZIP-VC and miRZIP-330-5p tumour growth profiles with cisplatin treatment. Cisplatin treatment started when tumours were ~200 mm³, mice received 2.5 mg/kg cisplatin twice per week. The miRZIP-330-5p group (*n*=3) began treatment on day 47 (grey dashed line) and the miRZIP-VC group (*n*=3) began treatment on day 105 (black dashed line). Response to cisplatin was assessed according to tumour volume measurements. In the miRZIP-VC group there were two responders and one non-responder. In the miRZIP-330-5p group there were two non-responders and one responder.

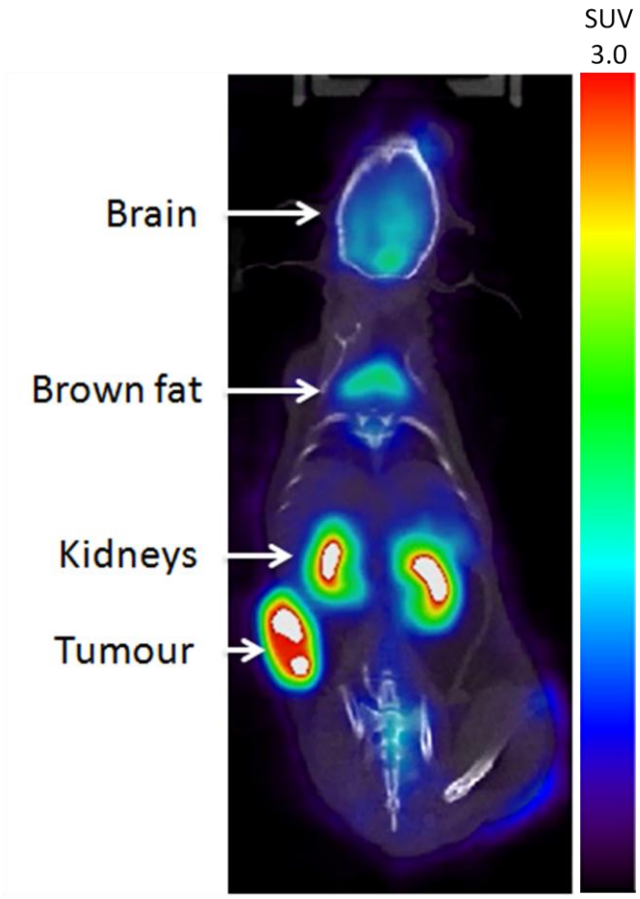

Fig 5.11 ^{18}F-FDG PET-CT image of a CD1 tumour bearing mouse. The uptake of ^{18}F-FDG in the tumour confirms the OE33 cells establish tumours with high metabolic activity. SUV; standardised uptake value.

5.5 Discussion

In the previous chapter miR-330 overexpression and miR-330-5p silencing did not alter cellular sensitivity to cisplatin or 5-FU, but marginally altered radiosensitivity in the miR-330-5p silencing model. Within a solid tumour multiple factors contribute to CRT sensitivity and resistance to treatment is not simply defined by the response of the cancer cells. Tumour sensitivity to chemotherapy and radiation is determined by multiple factors including cancer cells, cancer stem cells, vasculature, hypoxia, immune response and inflammation. These aspects of the tumour microenvironment are directly or indirectly modulated by miRNA that are expressed by all cell types within the tumour microenvironment (Chou et al., 2013). In this chapter the initial aim was to identify targets and pathways of miR-330-5p, using gene expression analysis and antibody-based arrays. Considering miR-330-5p did not significantly alter cellular response to CRT *in vitro*, the identification of miR-330-5p regulated genes and proteins with extracellular functions were of particular interest.

The *in vitro* model of miR-330-5p silencing mimicked the downregulated miR-330-5p expression observed in the biopsies of the neo-CRT non-responders. Gene expression analysis was undertaken for the OE33 miRZIP-VC and miRZIP-330-5p clones which had previously been selected as cell lines with high expression of the vector (Fig 4.10). Gene expression analysis was used to identify potential direct and indirect targets of miR-330-5p. However, direct mRNA targets of miR-330-5p may not be upregulated at the mRNA level as a result of miR-330-5p silencing. The mRNA targets of miR-330-5p that are translationally repressed by mechanism other than degradation or cleavage are unlikely to have altered mRNA expression and these targets will not appear in the gene expression data set. The majority of gene expression changes are likely to be indirectly associated with miR-330-5p silencing. There were 7 genes upregulated in response to miR-330-5p silencing. The most upregulated gene was

PRAME (preferentially expressed antigen of melanoma). PRAME is a tumour antigen which induces cytoxic T-cell immune response (Ikeda et al., 1997). Although the tumour antigen is preferentially expressed in melanoma it has also been identified in a number of other cancers and correlates with prognosis and survival (Epping & Bernards, 2006). In a head and neck squamous cell carcinoma study the expression of *PRAME* was identified in primary lesions and was consistently expressed in metastatic lymph nodes (Figueiredo et al., 2006). PRAME has also been demonstrated to repress retinoic acid receptor (RAR) signalling (Epping et al., 2005). Increased *PRAME* expression was associated with downregulated RAR signalling and enhanced growth and survival (Epping et al., 2005). In melanoma miR-211 expression is frequently downregulated and correlates with increased expression of *PRAME*. The overexpression of miR-211 significantly downregulated *PRAME* expression and the direct interaction between the miRNA and mRNA was confirmed using a luciferase reporter assay (Sakurai et al., 2011). The downregulated expression of miR-330-5p in patient tumours potentially enhances expression of *PRAME* that could repress RAR and promote growth and survival in response to CRT. Although there is no existing literature on the expression of PRAME in OAC, RAR signalling is reportedly reduced in BO dysplasia and OAC (Pavlov et al., 2014). The second most upregulated gene with miR-330-5p silencing was *adrenoreceptor alpha 2C* (*ADRA2C*) that also has a predicted binding site for miR-330-5p (Betel et al., 2008). The alpha-2-adrenergic receptors are a family of g-protein coupled receptors which primarily function in the central nervous system as regulators of neurotransmitter release. Expression of alpha-2-adrenergic receptors has been reported in breast cancer cells and tissue and receptor activation induced proliferation (Vazquez et al., 2006). In colorectal cancer *ADRA2C* gene expression was identified as a predictor of advanced clinical stage (Lee et al., 2013). *Aquaporin 3* (*AQP3*) was also upregulated with miR-330-5p silencing. The aquaporin proteins are a

family of membrane receptors that coordinate the transport of water and glycerol across the cell membrane. In OSC co-expression of *AQP3* and *AQP5* were identified as prognostic markers, high expression of both proteins correlated with poor prognosis in overall and disease free survival (Liu et al., 2013). The expressions of *AQP1*, *AQP3* and *AQP5* were associated with lymph node metastasis in colon cancer patients (Kang et al., 2015). *AQP3* expression is also upregulated in gastric cancer, and is associated with poor prognosis (Chen et al., 2014). The increase in AQP3 expression *in vitro* enhanced cellular proliferation and induced EMT, possibly via the PI3K/Akt/SNAIL pathway (Chen et al., 2014). The expression of *AQP3* in gastric cancer is regulated by miR-874, *in vitro* the ectopic expression of miR-874 inhibited growth, migration and invasion (Jiang et al., 2014). Furthermore, cellular sensitivity to cisplatin is reportedly mediated in part by AQP3 in squamous cell carcinoma and ovarian cell lines (Xuejun et al., 2014).

The upregulated expression of *MMP1* and *MMP7* with miR-330-5p silencing, was of particular interest because MMP1 and MMP7 have previously been reported as prognostic markers in oesophageal cancer (Murray et al., 1998; Yamashita et al., 2001; Tanioka et al., 2003). The first of these studies reported MMP1 as an independent prognostic marker in a cohort of 19 OSC and 27 OAC patients (Murray et al., 1998). In formalin fixed paraffin embedded tissue samples MMP1 protein was detectable in 24%, MMP2 in 78% and MMP9 in 70% of tumours. Survival analysis showed the MMP1 positive group had a median survival of 7 months compared to 16 months in the MMP1 negative group (Murray et al., 1998). In a more recent oesophageal OSC study, qPCR analysis confirmed MMP1 expression in 94% of a 51 patient cohort and almost no expression of MMP1 was detectable in the normal oesophageal specimens (Yamashita et al., 2001). The authors proposed that expression of MMP1 was associated with local tumour invasion in early disease but not invasion and metastasis in advanced disease

(Yamashita et al., 2001). The role of MMP1 in early disease was reported in another study which identified MMP1 as a pre-invasive factor in BO associated OAC (Grimm et al., 2010). The expression of MMP1 was confirmed in 95% of a 41 patient cohort with OAC and BO furthermore, *in vitro* MMP1 expression strongly correlated with proliferation. Although MMP1 expression was not associated with overall survival, high expression of MMP1 was associated with lymph node metastasis (Grimm et al., 2010). The upregulation of MMP1 expression in OAC has been linked to the EST-domain transcription factor PEA3 subfamily (Keld et al., 2010). *In vitro* the ERK-PEA3-MMP1 axis was confirmed to be upregulated and was associated with cellular invasion and proliferation. This study indentified PEA3 regulation of MMP1 in OAC which promotes MMP1 expression and potentially drives metastasis (Keld et al., 2010). Interestingly, PEA3 has previously been shown to regulate both MMP1 and MMP7 (Horiuchi et al., 2003; Xu et al., 2003; Yamamoto et al., 2004). In an OSC study the expression of MMP7 in superficial tumours, which had not invaded into the submucosa, was associated with nodal metastasis (Tanioka et al., 2003). Furthermore, the combined expressions of MMP7 and MMP9 have been identified as potential markers of malignancy and lymphatic metastasis. The identification of MMP1 and MMP7 was also of interests because recent literature report expanding roles for MMPs in cancer development and progression. The MMP family degrade various components of the extracellular matrix and enable cancer cells to invade and metastasis. However, the activities of MMPs are not limited to extracellular matrix remodelling (Kessenbrock et al., 2010). Recently, MMP1 has been implicated as a promoter of angiogenesis (Foley et al., 2014a). In the context of tumour response to CRT the vasculature is a critical factor. The delivery of systemic chemotherapies relies on the tumour vasculature. Furthermore, the vasculature provides the oxygen supply that is essential for the generation of ROS following radiotherapy.

The increase in *MMP1* and *MMP7* identified in the gene expression data was further validated by qPCR and confirmed an increase in mRNA expression with silencing of miR-330-5p (Fig 5.1). The upregulated expression of the *MMP1* mRNA corresponded to an increase in the expression of pro-MMP1 and active MMP1 protein (Fig 5.2 and 5.3). Conversely, the increase in the *MMP7* mRNA did not correspond to an increase in the MMP7 protein (Fig 5.2B). The increase in MMP1 protein expression was far greater in the miRZIP-330-5p clone than the in the heterogeneous miRZIP-330-5p cell line (Fig 5.2). In the clone, high expression of the vector indicated the production of the anti-miRNA that bound irreversibly to endogenous miR-330-5p. Conversely, in the heterogeneous cell line there were multiple clones, some with high and some with low expression of the vector. The silencing of miR-330-5p in heterogeneous cell line was not saturated to the same level as it was in the clonal cell line. This may explain why the expression of MMP1 was increased in the heterogeneous cell line, but not to the same extent as observed in the clonal cell line. There are three possible binding sites for miR-330-5p in the *MMP1* mRNA, suggesting miR-330-5p may directly target and regulate *MMP1* expression (Appendix 6) (Betel et al., 2008). Furthermore, overexpression of miR-330 decreased the expression of MMP1. The transient transfection of the miR-330 vector produced both miR-330-5p and miR-330-3p but there are no predicted binding sites for miR-330-3p in the *MMP1* mRNA (Betel et al., 2008). This suggests miR-330-5p may directly target the *MMP1* mRNA. In future work the direct interaction between miR-330-5p and MMP1 could be investigated using the luciferase reporter assay or a miRNA pull down assay.

Although expression of the MMP1 protein was increased in the miRZIP-330-5p heterogeneous cell line, there was no significant increase in the invasive potential of the cell line compared to the miRZIP-VC (Fig 5.7). The increase in MMP1 protein expression may not have been sufficient to increase the invasive potential of the

heterogeneous cell line but the clonal population, which had a greater increase in MMP1 expression, may be more invasive. In addition, the invasive potential of the cells was assessed using matrigel that contained multiple extracellular matrix components including collagen. The preferred substrates of MMP1 are collagen types I, II and III. There are commercially available collagen invasion assays and in future work the invasive potential of the cells lines should be assessed in a collagen invasion assay. The antibody-based arrays also confirmed expression of the MMP inhibitors TIMP-1 and TIMP-2, this may also explain why there was no increase in the invasive potential (Fig 5.5). The increase in MMP1 with miR-330-5p silencing may not have been sufficient overcome inhibition by the basally expressed TIMPs. The relative expression of *MMP1* did not correlate with patient response to neo-CRT (Fig 5.8). Furthermore, there was no correlation between *MMP1* mRNA expression and miR-330-5p expression in the patient biopsies (p=0.0752, n=14 Spearman rank test). The patient biopsy samples used for this analysis were limited (n=14) and there was insufficient data to analysis *MMP1* expression and nodal status (N0 samples n=11, N1 samples n=3). In the non-responders the correlation between miR-330-5p and *MMP1* was approaching significance. Increasing the sample numbers would be necessary to determine if there is correlation between miR-330-5p and *MMP1* in pre-treatment non-responder tissue biopsies. The current sample size is insufficient and cannot reliably support or disprove the hypothesis that miR-330-5p downregulation enhances *MMP1* expression.

The silencing of miR-330-5p downregulated the expression of extracellular cathepsins (A, B, S and V) and cystatin B (Fig 5.5 and 5.6). The cathepsin family are proteases and the cystatin family are the cathepsin protease inhibitors. Cathepsins, like MMPs, are proteases which remodel the extracellular matrix and are associated with invasion and metastasis (Loser & Pietzsch, 2015). Furthermore, cathepsin B and S are induced by radiation treatment and promote radioresistance (Seo et al., 2009; Malla et

al., 2012). Conversely, cathepsin S has been reported to promote apoptosis and enhance chemosensitivity in hepatocellular carcinoma cells (Wang et al., 2015). Increased cathepsin B activity is associated with tumour progression in various cancer types and is frequently upregulated in OAC due to chromosomal amplification (Hughes et al., 1998; Loser & Pietzsch, 2015). Molecular imaging combines imaging modalities with detectable expression of biological targets in tissues, such as cathepsins (Loser & Pietzsch, 2015). Early detection of OAC improves patients prognosis however, detecting early disease and with conventional white light endoscopy can be challenging as the tissue can appear very similar to the normal mucosa and tissue biopsies can also fail to detect the onset of dysplasia (Parsons, 2010). Near infrared optical imaging combined with fluorescent probes and optical imaging agents have been used to enhance detection of various cancer types. Of particular interest is a study in an orthotopic OAC mouse model that was established to test near infrared cathepsin B activated agents (Habibollahi et al., 2012). The optical imaging agents are immobilised on the endoscope probe and become highly fluorescent when they are activated by the protease activity of cathepsin B within the tissue. The orthotopic tumours were imaged simultaneously with white light and the near infrared custom built cathepsin B probe. The imaging technique was able to detected small neoplastic foci with low background signal from the normal tissue (Habibollahi et al., 2012).

In vivo tumours were established from the OE33 miRZIP-VC and miRZIP-330-5p heterogeneous cell lines. The mixed population of clones was considers to be a more relevant model of tumour heterogeneity, as appose to the single clonal population. Tumours established from the miRZIP-330-5p cell line initially grew faster than the miRZIP-VC tumours. This may in part be due to the increased expression of MMP1 which has previously reported to enhance local tumour invasion as appose to late stage metastasis in OAC patients (Yamashita et al., 2001). The faster growth rate of the

miRZIP-330-5p tumours allowed cisplatin treatment to begin ~50 days before the miRZIP-VC tumours. Of the miRZIP-330-5p tumours two out of three were non-responders and tumour burden increased rapidly despite cisplatin treatment. Of the miRZIP-VC tumours two out of three were responders. These preliminary data are inconclusive with regards to miR-330-5p downregulation modulating tumour sensitivity to cisplatin. Further worked is needed to establish the role of miR-330-5p as a modulator of CRT sensitivity *in vivo*. Considering miR-330-5p silencing enhanced radioresistance *in vitro* it would be of interest to investigate radiosensitivity in this model. It is of importance to note that these tumour xenografts were established in immunocompramised mice which is necessary to prevent immune destruction and rejection of the implanted human cancer cells. The inflammatory response is a critical factor in the development and progression of OAC and in tumour resistance to CRT. The *in vivo* model in this study does not take into account the role of the immune response as a potential modulator of tumour sensitivity to cisplatin.

In addition to the *in vivo* cisplatin study, ^{18}F-FDG PET-CT confirmed high metabolic activity in the tumours established from the stably transfected OE33 cell line (Fig 5.11). Cancer cells generally produce ATP energy via glycolysis, as oppose to oxidative phosphorylation which is a much slower but far more efficient producer of ATP. Hypoxia is a common trait within solid tumours therefore cancer cells utilise glycolysis to produce energy in the absence of oxygen (Hanahan & Weinberg, 2011). However, cancer cells also prefer to use glycolysis to produce energy in the presence of oxygen and this is known as the Warburg effect (Warburg et al., 1927). Why the cancer cell prefers to generate energy using glycolysis in the presence of oxygen is not fully understood. The aerobic oxidative phospshorylation produces far more ATP than the anaerobic glycolysis, albeit at a slower rate. Flurodeoxyglucose ^{18}F is a glucose analogue with the 2' hydroxyl group substituted for the radioactive fluorine isotope

(^{18}F). The ^{18}F-FDG imaging technique is based on the need of cancer cells to rapidly uptake vast amounts of glucose to maintain ATP production from glycolytic metabolism. The uptake of ^{18}F-FDG is a proxy of high glucose uptake and high metabolic activity. In conjunction with PET and CT scanning the uptake of ^{18}F-FDG can be anatomically imaged. Currently, ^{18}F-FDG PET-CT is used in the management of OAC patients in the clinic for staging and assessing the metastatic status of the disease (van Westreenen et al., 2004). There is considerable interest in using ^{18}F-FDG PET-CT as a clinical tool to assess patient response to neo-CRT during treatment (Chen et al., 2011; Bollschweiler et al., 2015). The imaging technique offers a non-invasive approach to measure alterations in tumour metabolism during treatment, which could be a surrogate marker of tumour response to treatment, before regression in tumour growth. The majority of OAC patients who receive neo-CRT show little or no response to treatment. In some cases the patient's disease can progress during treatment and unfavourably delay surgery. Monitoring the efficacy of neo-CRT during treatment could identify those patients who are not responding to CRT. The non-responders would benefit from discontinuation of aggressive treatments in favour of surgery or palliative care. The MUNICON phase II trial was undertaken to assess early response to chemotherapy in OAC, using ^{18}F-FDG PET-CT to measure metabolic response (Lordick et al., 2007). Before the start of chemotherapy and two weeks into the treatment regimen patients undertook an ^{18}F-FDG PET-CT scan. Changes in the tumour metabolism were used to assess early response to chemotherapy. Those patients with a 35% decrease in their tumour glucose standard uptake values (SUV) were considered responders. The responders continued with the chemotherapy regimen and then proceeded to surgery. Those patients who did not have a 35% decrease in their SUV were considered non-responders and discontinued chemotherapy in favour of immediate surgery. The primary endpoint measurement of the trial was median overall survival,

which in metabolic responders was a least twice as a high as the non-responders (Lordick et al., 2007). This trial demonstrated the ^{18}F-FDG PET-CT could be used to monitor early response to neo-CRT and identify responders and non-responders, with the aim of providing individual patients with the most effective therapeutic strategy. In another study a similar approach was taken to assess ^{18}F-FDG PET-CT as a clinic tool for monitoring early response to neo-CRT in OAC patients (van Heijl et al., 2011). Although the SUV significantly decreased in the responders, in agreement with the MUNICON trial, its accuracy in determining non-responders (50% specificity) was not sufficient to justify discontinuation of neo-CRT in these patients (van Heijl et al., 2011). Monitoring patient response to neoadjuvant therapy including radiation using ^{18}F-FDG PET-CT is subject to the confounding factor of a time-dependent 'metabolic flare'. In response to radiation an increase in metabolic activity can be observed as a result of energy dependent repair mechanisms within the tumour cells or radiation-induced oesophagitis, this could be interpreted as a false negative in potential responders (Malik et al., 2010). Studies are ongoing to assess the clinical application of ^{18}F-FDG PET-CT in monitoring OAC patient response to neoadjuvant therapies however, the protocols used across multiple centres are highly variable making it difficult to directly compare individual studies (Krause et al., 2009). ^{18}F-FDG PET-CT has been used to monitor treatment response in other cancer types and has the potential to accelerate drug development by indicating early response to therapeutics and informing drug dosage adjustments (Kelloff et al., 2005). The response of the OE33 miRZIP-VC and miRZIP-330-5p to cisplatin treatment was assesses by tumour volume measurements in this study. The high metabolic activity of the OE33 tumours reported here indicates ^{18}F-FDG PET-CT could be used to measure early response to CRT in the OE33 miRZIP-330-5p model. In future work early response to chemotherapy and radiotherapy could be assess in this miRNA *in vivo* model using ^{18}F-FDG PET-CT. Imaging could

potentially identify early response before regression in tumour growth is measurable and offers the opportunity to detect metastatic disease. Considering the upregulation of MMP1 in the OE33 miRZIP-330-5p cell line, the ability to assess tumour metastasis as well as treatment response would be of significant interest in this model. An alternative approach to studying the role of miRNA as modulators of CRT could be undertaken using *in vivo* tumour models and miRNA therapeutics. For example, in the case of miR-330-5p it would be hypothesised that patients with high expression of the miRNA would be responders to CRT. *In vivo* tumour models could be established using OAC cell lines, and miRNA therapeutics such as miR-330-5p mimics could be administered to enhance miRNA expression in the tumour. The mice could be treated with CRT and early response monitored with ^{18}F-FDG PET-CT to assess altered sensitivity to treatment with enhanced expression of the miRNA. This approach would use imaging to measure early response to CRT and validate the use of miRNA therapeutics to enhance the efficacy of CRT.

In this chapter, gene expression profiling and antibody-based arrays identified potential targets of miR-330-5p. Further work is needed to determine if miR-330-5p mediated regulation of these genes and proteins alters CRT sensitivity *in vivo*. Considering the importance of the tumour microenvironment in CRT response and sensitivity, the miR-330-5p mediated regulation of extracellular proteins is of particular interest. The *in vivo* model established here mimics the downregulated expression of miR-330-5p in OAC non-responder. Future work using this model should firstly investigate alterations in CRT sensitivity in the tumours with silencing of miR-330-5p. Secondly, if miR-330-5p does alter CRT sensitivity *in vivo*, the mechanisms associated with treatment sensitivity should be investigated starting with the targets identified and discussed here.

Chapter 6 The Role of MiR-187 in OAC Cellular Sensitivity to CRT

6.1 Introduction

There were 67 differentially expressed miRNA identified in the OAC neo-CRT responders and non-responders. The expression of miR-187 was significantly downregulated in the non-responders compared to the responders (Fig 3.2). In the literature miR-187 has previously been identified as part of prognostic and diagnostic miRNA signatures in numerous cancer types. In thyroid cancer miR-187 was identified as part of a seven miRNA signature that could potentially be used a preoperative diagnostic tool (Nikiforova et al., 2008). In pancreatic cancer and lung adenocarcinoma, miR-187 was identified as part of prognostic signatures predicting patients overall survival (Schultz et al., 2012; Li et al., 2014b). The eight-miRNA (miR-31, miR-196b, miR-766, miR-519a-1, miR-375, miR-187, miR-331 and miR-101-1) signature identified in a cohort of 372 lung adenocarcinoma patients was an independent prognostic marker of overall survival. Interestingly, three (miR-31, miR-331 and miR-187) of the eight miRNA are also significantly downregulated in the non-responders of the patient cohort presented in this study (Appendix 4). The expression of miR-187 was one of 58 differentially expressed miRNA in prostate cancer specimens, compared to normal prostate tissue specimens (Fuse et al., 2012). The top four downregulated miRNA in the prostate cancer specimens included miR-187 and miR-31, both of which were downregulated in the OAC non-responders of the cohort presented here (Fuse et al., 2012). In another independent prostate cancer study miR-187 was again reported to be downregulated in prostate cancer specimens and was detectable as a non-invasive biomarker in patient urine (Casanova-Salas et al., 2014). The expression of miR-187 was reported as a potential early diagnostic and prognostic tool for prostate cancer patients undergoing radical prostatectomy (Casanova-Salas et al., 2014). In the preoperative and postoperative sera of ovarian clear cell carcinoma patients the expression of miR-187 was one of four upregulated miRNA in preoperative sera (Chao

et al., 2014). The expression of miR-187 was also significantly dysregulated in the blood of gallbladder cancer patients (Li & Pu, 2015). These studies highlight the potential of miR-187 as a cancer biomarker based on miRNA profiling studies in patient tissue specimens and bodily fluids.

Although these studies identify miR-187 as a potential biomarker, miR-187 may also be a therapeutic target. The presence or absence of miR-187 is perhaps a bystander biomarker. Alternatively, miR-187 may be a driver biomarker and a functional contributor to cancer development and progression. Understanding the function of the miRNA and its role in cancer progression will determine if miR-187 is a potential therapeutic target. To date there are few functional miR-187 studies, although the limited experimental evidence indicates miR-187 expression does contribute to disease progression. In ovarian cancer the *Dab2* gene was identified as a direct target of miR-187 and ectopic expression of miR-187 initially enhanced proliferation but also suppressed Dab2 and inhibited migration. Conversely, inhibiting miR-187 increased Dab2 expression and promoted EMT. These findings suggest miR-187 promotes proliferation in the early stages of ovarian cancer tumorigenesis but inhibits invasion in the later stages, hence expression of miR-187 was associated with better patient survival (Chao et al., 2012). The expression of miR-187 was reported as an independent prognostic maker in breast cancer and ectopic expression of miR-187 *in vitro* enhanced cellular invasion and migration (Mulrane et al., 2012). In prostate cancer cell lines the *ALDH1A3* gene was identified as a direct target of miR-187 translational regulation, although the functional implication of altered ALDH1A3 protein expression in the cell lines was not investigated (Casanova-Salas et al., 2015). In clear cell renal cell carcinoma miR-187 downregulation was associated with lower patient survival rates and *in vitro* ectopic expression of miR-187 directly targeted B7-H3 which contributed to suppressed cellular proliferation and migration (Zhao et al., 2013). In the studies

discussed here there are contradictory reports of miR-187 acting as a tumour suppressor and an oncogene in various cancer types, this emphasises the tissue specific functions of miRNA.

Here, miR-187 was downregulated in the pre-treatment biopsies from the neo-CRT non-responders. In a pre-treatment setting miR-187 is a potential biomarker of patient sensitivity to neo-CRT. In this chapter the aim was to investigate miR-187 as a modulator of cellular sensitivity to CRT and to identify targets and pathways regulated by miR-187 which may be associated with sensitivity to CRT.

6.2 Rationale, aims and objectives

In the pre-treatment diagnostic biopsies from OAC neo-CRT non-responders the expression of miR-187 was significantly downregulated, compared to the responders. The downregulated expression of miR-187 prior to neo-CRT potentially enhances tumour resistance to CRT. In this chapter the aim was to investigate the role of miR-187 as a modulator of cellular response and sensitivity to CRT.

- Establish OAC cell models with ectopic miR-187 overexpression.
- Assess cellular sensitivity to radiation in the cell line models using the clonogenic assay.
- Identify mRNA targets regulated by miR-187 using whole genome digital gene expression analysis.

6.3 Materials and methods

6.3.1 Transient reverse transfection of cell lines

The reverse transfection method was used to transfect OE33 P/ OE33 R/ OE33 and SK-GT-4 cells with the pre-miR-187 or miR-VC plasmid vectors (section 4.3.1). The following day cells were harvested or re-seeded for experiments.

6.3.2 Stable transfection of cell lines

To establish stable cell lines expressing the pre-miR-187 (catalogue number; SC400216, Origene, Maryland, USA) or miR-VC (catalogue number; PCMVMIR, Origene, Maryland, USA) plasmid vectors, the cells (OE33 P/ OE33 R/ OE33 and SK-GT-4) were seeded at a density of ~2.5×10^6 cells into 10 cm tissue culture dishes and were transfected as previously described (sections 4.3.1 and 4.3.2). The following day the media was discarded and replaced with complete media containing 500 µg/mL of geneticine (G418) (Thermo Scientific). Cells were cultured under G418 selection for ~2 weeks before individual colonies were visible. The mixed population was established by harvesting all the clones from the dish and reseeding the cells in a larger dish or flask. G418 selection was maintained for ~6 weeks. Stable cell lines were checked frequently using fluorescent microscopy and western blotting to confirm continued expression of GFP in long term cell cultures in the absence of G418.

6.3.3 Clonogenic assay

Transiently transfected cells were harvested 24 h post-transfection. Cells were seeded into 6-well plates with 2 mL of complete media (section 4.3.6). The cell lines were seeded at 500-750 cells per well for the mock irradiated controls and 1000-1500 cells per well for radiation. With the exception of the OE33 cells transiently transfected with miR-187 which were seed at 1500 cells per well for the mock irradiated controls and 3000 cells per well for radiation.

6.3.4 MT cell viability assay

Cells were reverse transfected with the pre-miR-187 or miR-VC plasmid vectors as described in section 6.3.1. The following day cells were counted and seeded into white opaque 96 well plates. The assay was performed as described in section 2.7.3.

6.3.5 Propidium iodide flow cytometry

Cells were reverse transfected with the pre-miR-187 or miR-VC plasmid vector in 6-well plates (section 2.7.5). Of the duplicate wells, one well was harvested and stained with PI and the other well was harvested and was the unstained control. The harvesting and staining protocol is described in section 2.7.5. A minimum of 10,000 events were collected and the data was analysed by histogram plot using CellQuest software (BD Biosciences). The x-axis represents PI fluorescence and the y-axis represents cell number. The M1 gated population represents positive PI staining and % cell death (Appendix 8).

6.3.6 Western blotting

Cells were harvested and protein was extracted and quantified as previously described (sections 2.6.1 and 2.6.2). Samples were prepared for SDS-PAGE, a total volume of 25 µL was loaded into the wells of a 10 or 12% gel (section 2.6.3). SDS-PAGE and western blotting were performed as described in sections 2.6.3 and 2.6.4. The PVDF membrane was incubated with the primary antibody overnight. Blots were probed for cleaved PARP Asp 214 (D64E10 XP, Cell Signaling, Massachusetts, USA), cleaved caspase-3 Asp 175 (5A1E, Cell Signaling, Massachusetts, USA), turboGFP (Origene, Maryland, USA) and the loading control GAPDH (Ambion, Massachusetts, USA) (Table 2.2). After incubation with the primary antibody, the blots were washed and then incubated with the secondary antibody (Table 2.2). After incubation with the secondary antibody, the blots were washed and the chemiluminescent substrate was

applied (section 2.6.4). The blots were imaged using a chemiluminescent imaging system (section 2.6.4). Image Lab 3.0 software (BioRad, UK) was used for densitometry analysis of western blots (section 2.6.8).

6.3.7 Whole genome digital expression analysis

Total RNA was extracted (section 2.5.1) from the OE33 R cells with miR-187 overexpression or the OE33 R control transfected cells. Samples of total RNA were prepared for shipping, as previously described section 2.5.7. Digital RNA-seq was outsourced to LC Sciences (Texas, USA). Analysed data sets were provided by LC Sciences. The fold change in gene expression was calculated from the equation; log2 (miR-187 FPKM / miR-VC FPMK). Gene expression changes were considered significant if the *p* value was <0.05.

6.3.8 qPCR analysis of miRNA *in vitro*

The TaqMan Universal PCR Master Mix and TaqMan miRNA Assays were used to analyse miRNA expression in the cDNA template produced with the TaqMan MicroRNA Reverse Transcription Kit (as previously described sections 2.5.3 and 2.5.4). The TaqMan miRNA Assays used for target amplification in the qPCR were miR-187-3p and the endogenous control RNU48 (Table 2.1).

6.3.9 qPCR analysis of mRNA *in vitro*

To analyse the relative expression of the *PYROXD2*, *APC*, *PTEN*, *JUN*, *TNF*, *CXCL10* and *CDK6* mRNA, the QuantiTect RT Kit was used for cDNA synthesis and the QuaniTect SYBR green PCR master mix was used for the qPCR analysis (as previously described sections 2.5.5 and 2.5.6). QuantiTect primer assays (Qiagen, UK) were used for target amplification in the qPCR (Table 2.1).

To analyse the relative expression of *C3*, *CFB*, *TRANK1*, *APOL2*, *OAS1*, *IL28*, *IFNB1* and *IL22RA1* mRNA, the TaqMan Universal PCR Master Mix and the TaqMan

Gene Expression Assays were used to analyse mRNA expression in the cDNA template produced with the random hexamers (sections 2.5.5 and 2.5.6). TaqMan probes (Applied Biosystems, UK) were used for target amplification in the qPCR (table 2.1).

6.3.10 qPCR analysis of C3 mRNA in patient samples

The relative expression of the *C3* mRNA was analysed in RNA extracted from the pre-treatment diagnostic tumour biopsies. RNA extraction was performed as described in section 2.2.3. The cDNA template was produced with random hexamers (section 2.5.5) and the qPCR analysis was performed as described in section 2.5.6.

6.3.11 Immunohistochemistry

The TMAs of the pre-treatment tumour biopsies (7 responders, 16 non-responders) were used for C3 immunhistochemistry analysis as described in section 2.6.10. Stained sections were scanned using a scanscope XT digital scanner and ImageScope software (Aperio Technologies, UK). The percentage positivity and staining intensity scores were assigned separately for the epithelium and stromal compartments of the TMA cores (section 2.6.10). The three sets of scores were compiled and analysed.

6.4 Results

6.4.1 The radioresistant isogenic model

Prior to the start of this study, an isogenic model of radioresistance was established (Lynam-Lennon et al., 2010). The OE33 cell line was irradiated with fractionated 2 Gy doses, until the cells developed a radioresistant phenotype after a cumulative dose of 50 Gy (OE33 R) (Lynam-Lennon et al., 2010). In addition, a parental OE33 cell line (OE33 P) was mock irritated to maintain a control and passage matched isogenic cell model. The OE33 P and OE33 R are cell lines with the same genetic background but distinct radiosensitivities (Fig 6.1).

The endogenous expression of miR-187 was undetectable in the OE33 P and OE33 R cell lines (Fig 6.2). There was no amplification of miR-187 in the qPCR analysis of the non-transfected cells or the miR-VC transfected cells, suggesting loss of miR-187 expression. However, the cell lines transfected with the pre-miR-187 overexpression vector were confirmed to be expressing mature miR-187 (Fig. 6.2).

6.4.2 MiR-187 overexpression enhances cellular sensitivity to radiation

To investigate the role of miR-187 as a modulator of cellular sensitivity to radiotherapy OAC cell lines were transfected with the pre-miR-187 vector and sensitivity to a clinically relevant dose of radiotherapy was assessed by clonogenic assay (Fig 6.3). The transient overexpression of miR-187, in the OE33 P and OE33 R cell lines, significantly enhanced cellular sensitivity to radiotherapy compared to the miR-VC transfected control (Fig 6.3).

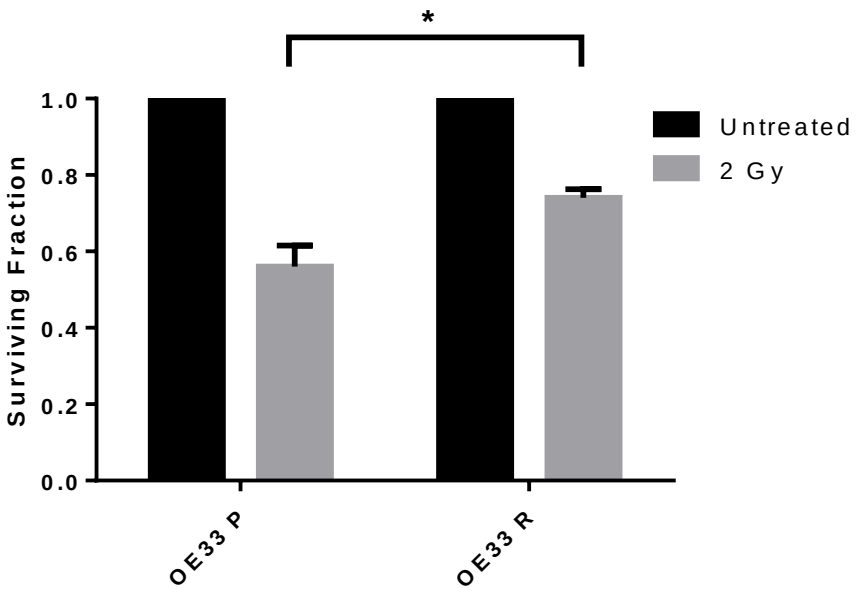

Fig 6.1 The radioresistant isogenic model. The radioresistant phenotype of the isogenic cell model was confirmed using the clonogenic assay. The radioresistance (2 Gy) of the OE33 R cell line is significantly greater than the OE33 P cell line. Experimental repeats n=3. Data presented as the mean ± SEM. Statistical analysis was performed using the paired t-test; * p<0.05

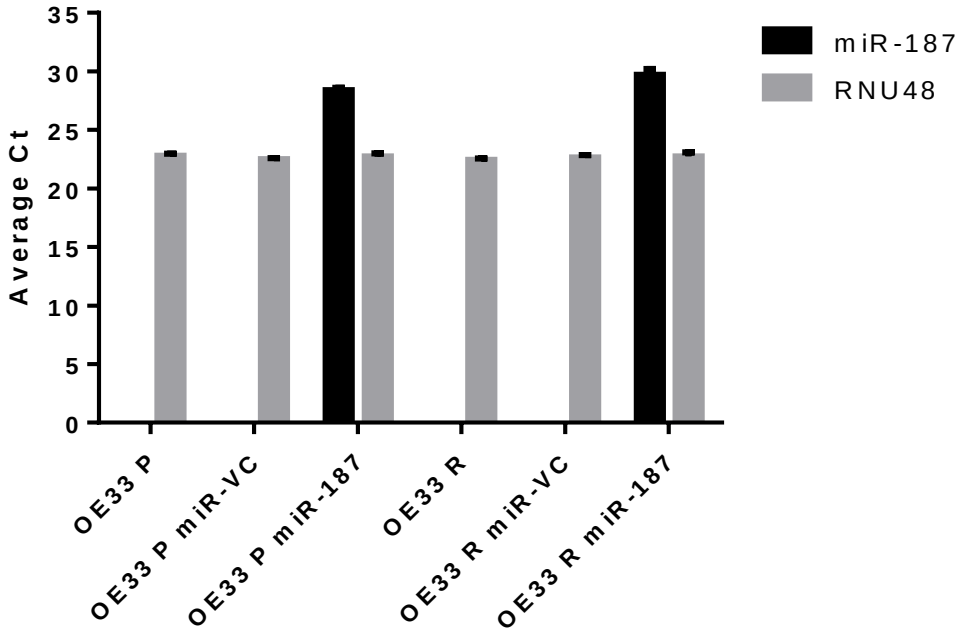

Fig 6.2 Endogenous miR-187 expression was not detectable in the OE33 P and OE33 R cell lines, unless cells were transfected with the pre-miR-187 vector. The expression of mature miR-187 was analysed by qPCR. The Livak method was used for data analysis with RNU48 as the endogenous control. There was no detectable expression of endogenous miR-187 in the OE33 P or OE33 R cell lines. The cell lines were transiently transfected with the miR-VC or pre-miR-187 vectors, the expression of miR-187 was analysed 24 h post-transfection to confirm expression of mature miR-187 in the cells transfected with the pre-miR-187 vector. The average Ct values for miR-187 and the endogenous experimental control RNU48 are presented. There was no endogenous miR-187 expression in the cell lines therefore the data cannot be presented as fold change. Experimental repeats *n*=3. Data presented as the mean ± SEM.

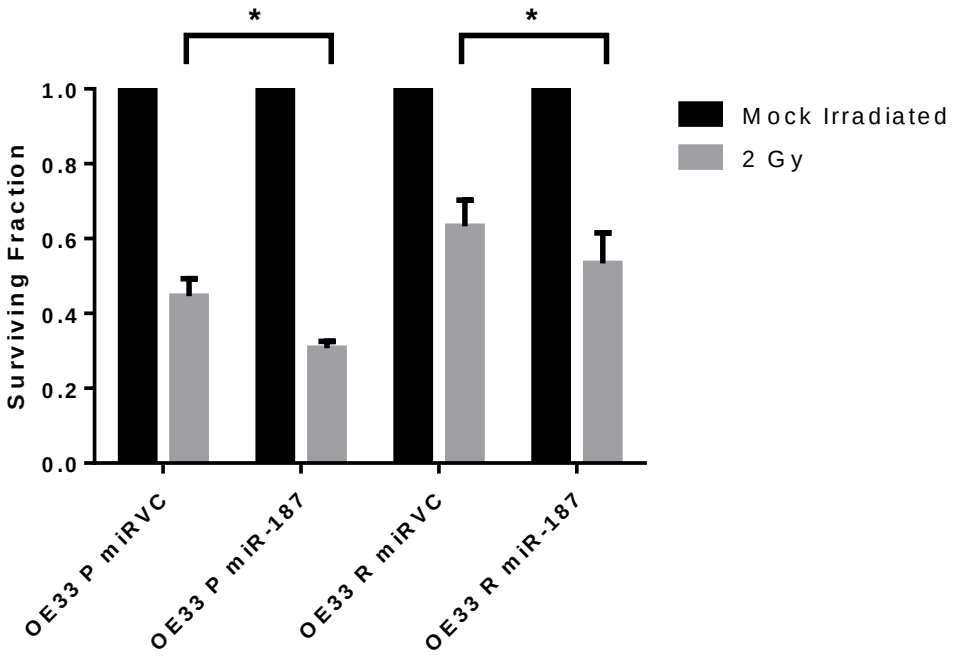

Fig 6.3 Transient miR-187 overexpression enhanced radiosensitivity in the OE33 P and OE33 R cell lines. The OE33 P and OE33 R cell lines were transiently transfected with the pre-miR-187 and miR-VC vectors. The clonogenic assay confirmed miR-187 overexpression significantly enhanced the radiosensitivity (2 Gy) of the OE33 P and OE33 R cell lines. Experimental repeats OE33 P n=3 and OE33 R n=6. Statistical analysis was performed using the paired t-test for the OE33 P data and the Wilcoxon matched pairs test for the OE33 R data; * p<0.05

Conversely, stable overexpression of miR-187 in the OE33 P and OE33 R did not alter the radiosensitivity of the OE33 R cell line and enhanced radioresistance in the OE33 P cell line (Fig 6.4).

The OE33 P and OE33 R cell lines are a model of acquired radioresistance in response to chronic fractioned doses of radiation. To investigate if miR-187 modulates radiosensitivity in OAC cell lines with inherently different radiosensitivities, the OE33 and SK-GT-4 cell lines were transiently transfect with the pre-miR-187 overexpression vector. The SK-GT-4 cell line was inherently more radioresistance compared to the OE33 cell line (OE33 surviving fraction 0.58 ± 0.03 and SK-GT-4 surviving fraction 0.77 ± 0.005). The transient overexpression of miR-187 enhanced the radiosensitivity of the OE33 and SK-GT-4 cell lines, when compared to the miR-VC transfected control (Fig 6.5 and 6.8). The transient overexpression of miR-187 also enhanced cellular sensitivity to cisplatin in the OE33 cell line (Fig 6.7). The stable overexpression of miR-187 in the OE33 cell line enhanced cellular sensitivity to 2 and 4 Gy radiation, when compared to the stable miR-VC cell line (Fig 6.6). However, stable miR-187 overexpression in the SK-GT-4 cell line did not significantly alter cellular sensitivity to 2 or 4 Gy radiation (Fig 6.9).

6.4.3 MiR-187 overexpression alters cellular viability

The transient overexpression of miR-187 in the OAC cell lines enhanced radiosensitivity. To investigate the mechanism by which miR-187 modulates radiosensitivity, viability was measured with 2 Gy radiation or mock irradiation. The overexpression of miR-187 significantly reduced the viability of OE33 cells at 24 and 48 h compared to the miR-VC transfected control (Fig 6.10).

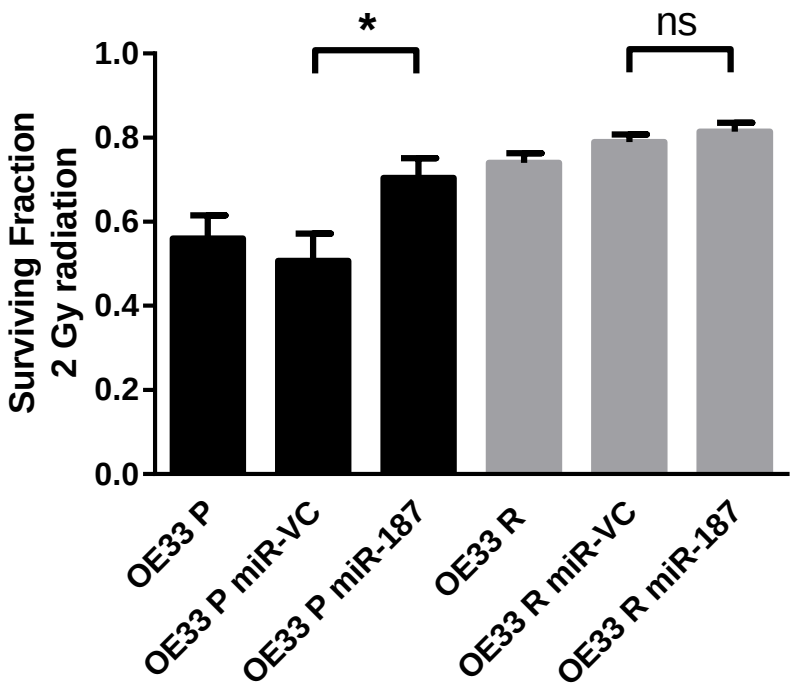

Fig 6.4 Stable miR-187 overexpression enhanced radioresistance in the OE33 P. The OE33 P and OE33 R cell lines were transfected with the miR-VC or pre-miR-187 vector and heterogeneous/mixed clonal stable cell lines were established by mammalian antibiotic selection. The clonogenic assay demonstrated enhanced radioresistance (2 Gy) in the OE33 P miR-187 cell line compared to the OE33 P miR-VC cell line. The stable overexpression of miR-187 did not alter the radiosensitivity of the OE33 R cell line relative to the OE33 R miR-VC cell line. Experimental repeats n=4. Data presented as the mean ± SEM. Statistical analysis was performed using the paired t-test; * p<0.05, ns not significant.

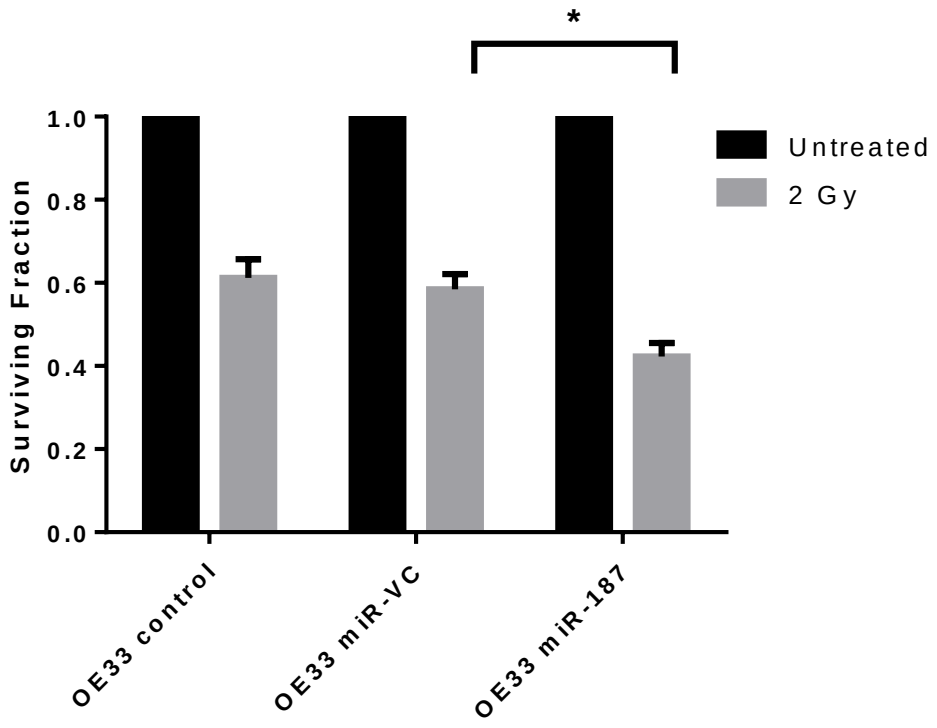

Fig 6.5 Transient miR-187 overexpression enhanced OE33 radiosensitivity. The clonogenic assay demonstrated enhanced cellular sensitivity to 2 Gy radiation with the transient overexpression of miR-187 in the OE33 cell line compared to the OE33 miR-VC transfected control. Experiential repeats n=3. Data presented as the mean ± SEM. Statistical analysis was performed using the unpaired t-test; * p<0.05

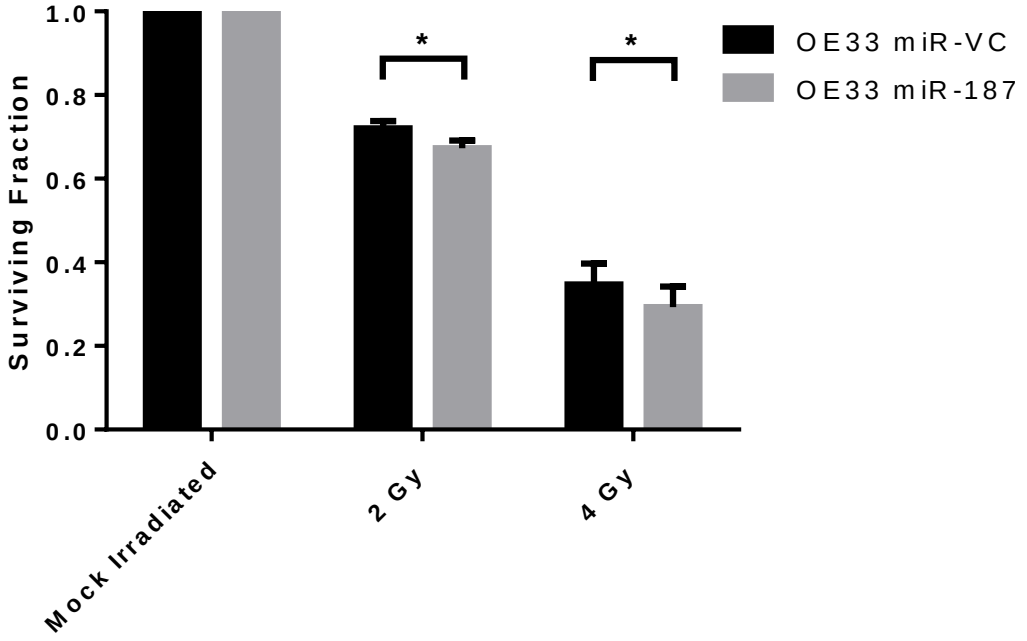

Fig 6.6 Stable miR-187 overexpression enhanced OE33 radiosensitivity. The clonogenic assay demonstrated enhanced cellular sensitivity to 2 and 4 Gy radiation with the stable overexpression of miR-187 in the OE33 cell line compared to the OE33 miR-VC control. Experiential repeats n=4. Data presented as the mean ± SEM. Statistical analysis was performed using the paired *t*-test; * $p<0.05$

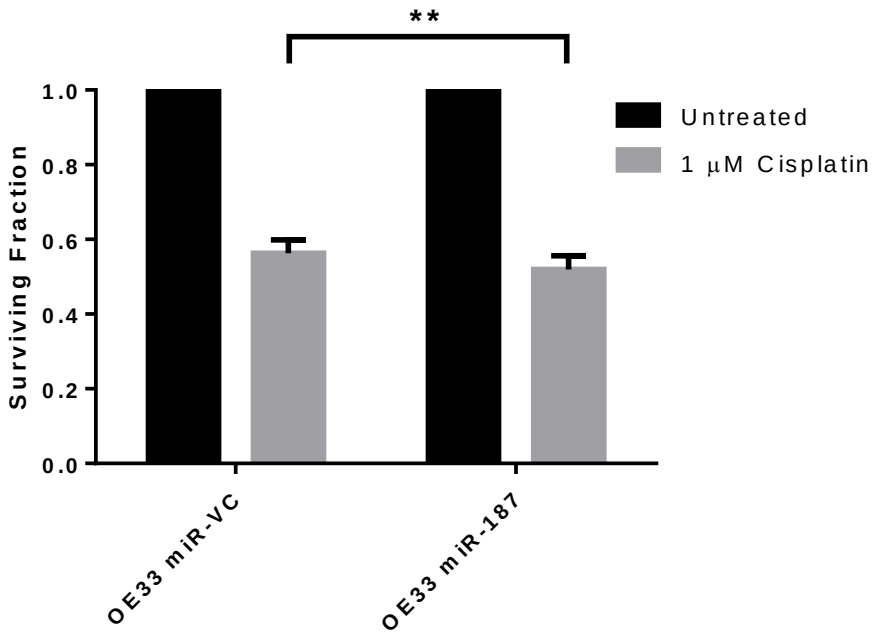

Fig 6.7 Transient miR-187 overexpression enhanced OE33 cellular sensitivity to cisplatin. The clonogenic assay demonstrated enhanced cellular sensitivity to of 1 μM cisplatin (24 h treatment) with the transient overexpression of miR-187 in the OE33 cell line compared to the OE33 miR-VC transfected control. Experiential repeats n=3. Data presented as the mean ± SEM. Statistical analysis was performed using the paired t-test; ** p<0.01

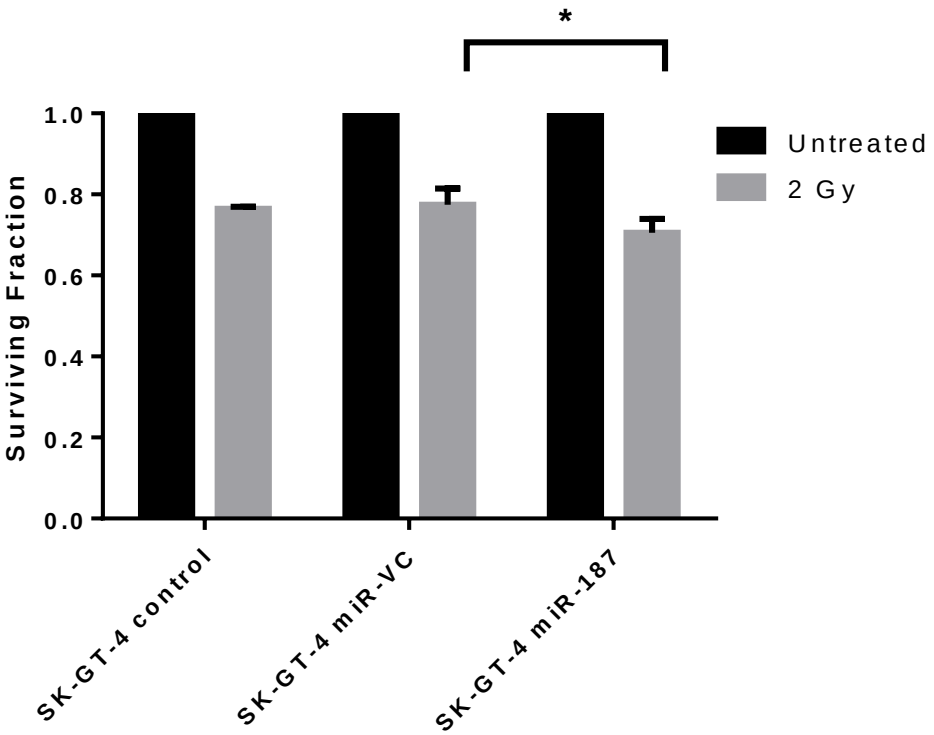

Fig 6.8 Transient miR-187 overexpression enhanced SK-GT-4 radiosensitivity. The clonogenic assay demonstrated enhanced cellular sensitivity to 2 Gy radiation with the transient overexpression of miR-187 in the SK-GT-4 cell line compared to the SK-GT-4 miR-VC transfected control. Experiential repeats n=4. Data presented as the mean ± SEM. Statistical analysis was performed using the paired t-test; * p<0.05

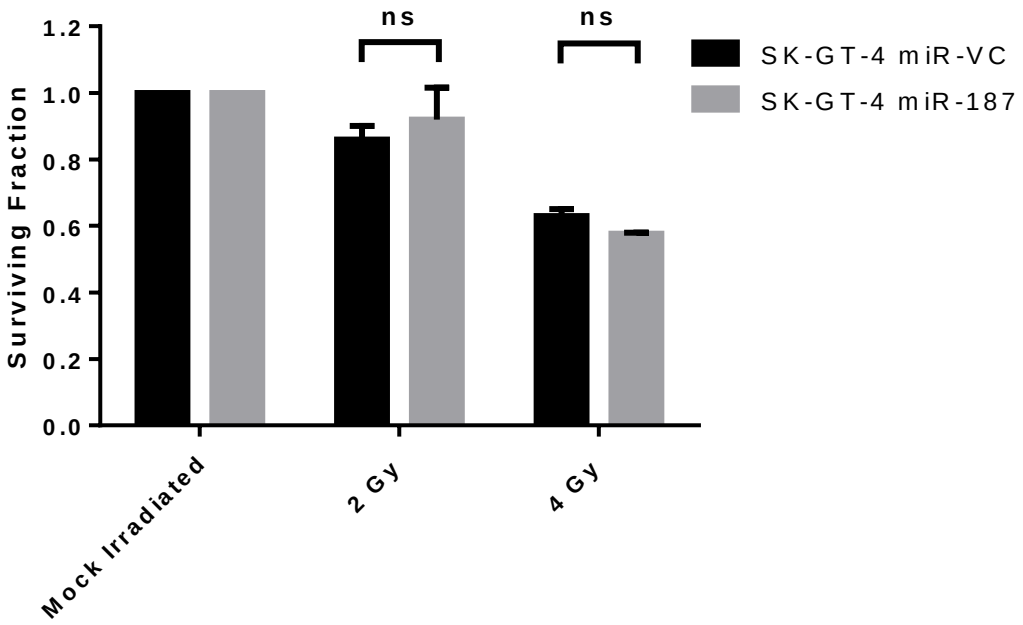

Fig 6.9 Stable miR-187 overexpression did not alter SK-GT-4 radiosensitivity. In the clonogenic assay the stable overexpression of miR-187 in the SK-GT-4 cell line, did not significantly alter cellular sensitivity to 2 or 4 Gy radiation compared to the SK-GT-4 miR-VC control. Experiential repeats *n*=4. Data presented as the mean ± SEM. Statistical analysis was performed using the paired *t*-test; ns not significant.

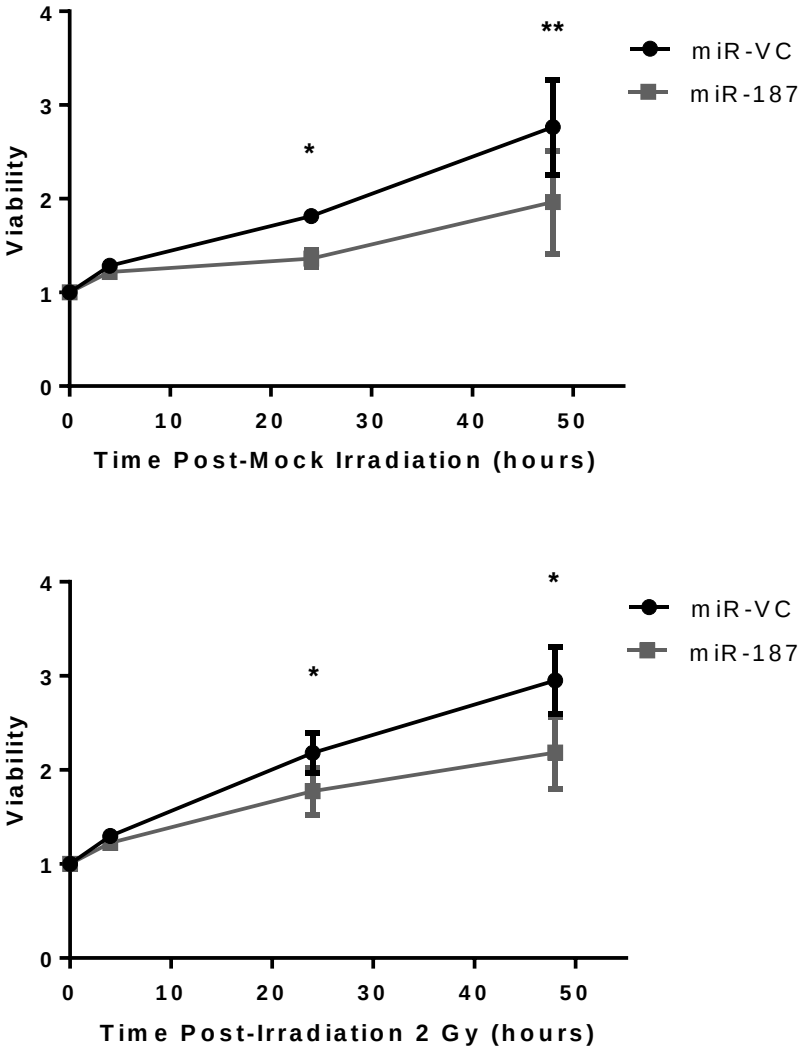

Fig 6.10 The overexpression of miR-187 decreased OE33 cellular viability. Cellular viability was measured in OE33 cells transiently transfected with the miR-VC or pre-miR-187 vectors. Viability was measured using a longitudinal real-time assay. Cellular viability was measured immediately prior (0 h) to 2 Gy radiation or mock-irradiation and after 4, 24 and 48 h. The viability reading at 0 h was normalised to 1 and the relative change in viability was calculated relative to the 0 h reading. (**A**) Mock-irradiated cells transiently transfected with the pre-miR-187 or miR-VC vector. The overexpression of miR-187 significantly reduced cell viability at 24 and 48 h. (**B**) Irradiated cells transiently transfected with the pre-miR-187 or miR-VC vector. The overexpression of miR-187 significantly reduced cell viability at 24 and 48 h. Experimental repeats n=4. Data presented as the mean ± SEM. Statistical analysis was performed using the paired *t*-test to compare miR-VC and miR-187 viability at each time point; * $p<0.05$, ** $p<0.01$

Characterisation of cellular processes associated with cellular response and sensitivity to radiotherapy were to be investigated. Cellular viability and growth was measured using a metabolic assay, the assay allowed for continuous cell viability measurements over 48 h. The viability of cells transiently transfected with the miR-VC or pre-miR-187 vectors irradiated and the irradiated cells, suggesting miR-187 overexpression has a tumour suppressor effect by reducing cell viability. Conversely, the transient overexpression of miR-187 in the SK-GT-4 cell line did not alter cellular viability, in the mock-irradiated or 2 Gy irradiated cells (Fig 6.11).

6.4.4 MiR-187 overexpression induced apoptosis in the OE33 cell line

The decrease in viability in OE33 cells with miR-187 overexpression was determined using a metabolic assay. To assess whether the decrease in cellular viability was the result of an increase in cell death, the cells transfected with the miR-VC or pre-miR-187 vectors were stained with PI for flow cytometry analysis. Viable live cells with an intact cell membrane exclude PI. Cell death, by apoptosis or necrosis, compromises the integrity of the cell membrane thereby permeabilizing the cell to PI, which enters the cell through passive diffusion and intercalates with DNA. The proportion of PI positive cells was measured using flow cytometry. The overexpression of miR-187 in the OE33 cells significantly increased the proportion of dead cells 48 h post-transfection compared to the miR-VC transfected control (Fig 6.12). To determine the mechanism of cell death as either apoptosis or necrosis the expression of the apoptosis specific proteins, cleaved PARP and cleaved caspase-3, were analysed. The overexpression of miR-187 increased the levels of both cleaved PARP and cleaved caspase-3, compared to the miR-VC transfected control, indicating induction of apoptosis 48 h post-transfection (Fig 6.13).

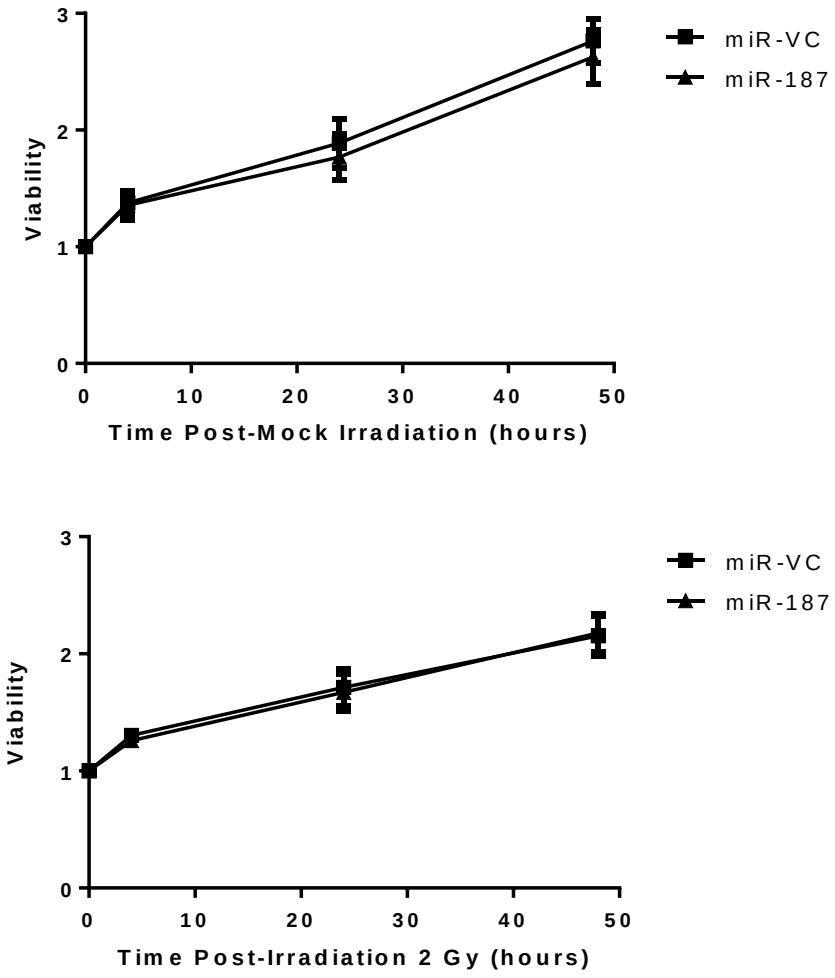

Fig 6.11 The overexpression of miR-187 did not alter SK-GT-4 cellular viability. Cellular viability was measured in SK-GT-4 cells transiently transfected with the pre-miR-187 or miR-VC vectors. Viability was measured using a longitudinal real-time assay. Cellular viability was measured immediately prior (0 h) to 2 Gy radiation or mock-irradiation and after 4, 24 and 48 h. The viability reading at 0 h was normalised to 1 and the relative change in viability was calculated relative to the 0 h reading. (**A**) Mock-irradiated cells transiently transfected with the pre-miR-187 or miR-VC vector. The overexpression of miR-187 did not alter cell viability. (**B**) Irradiated cells transiently transfected with the pre-miR-187 or miR-VC vector. The overexpression of miR-187 did not alter cell viability. Experimental repeats *n*=2. Data presented as the mean ± SEM. Statistical analysis was performed using the paired *t*-test to compare miR-VC and miR-187 viability at each time point.

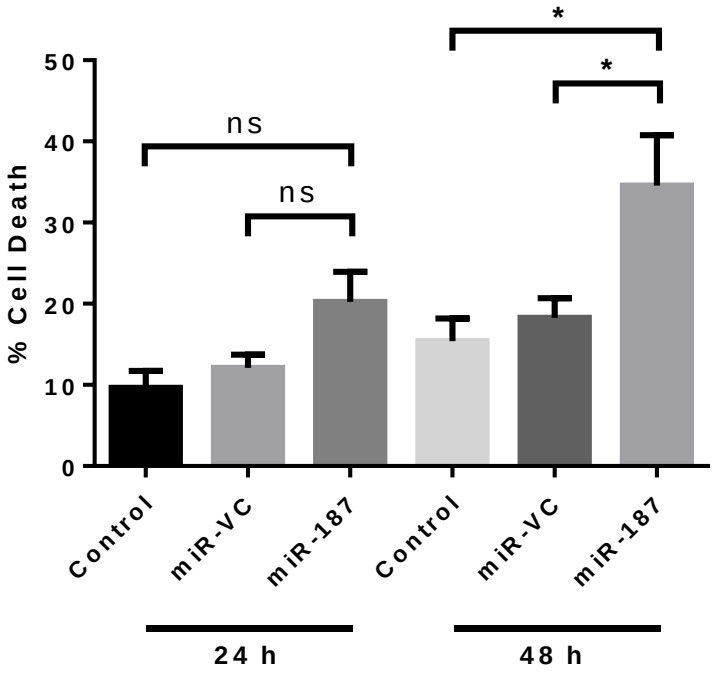

Fig 6.12 The overexpression of miR-187 induced cell death in the OE33 cell line. The transient transfection of the OE33 cell line with the pre-miR-187 vector significantly induced cell death compared to the miR-VC transfected cells, 48 h post-transfection. Cell death was measured by propidium iodide cell staining and flow cytometry. Experimental repeats n=3. Data presented as the mean ± SEM. Statistical analysis was performed using the repeated measures ANOVA with tukey post-test; * p<0.05, ns not significant.

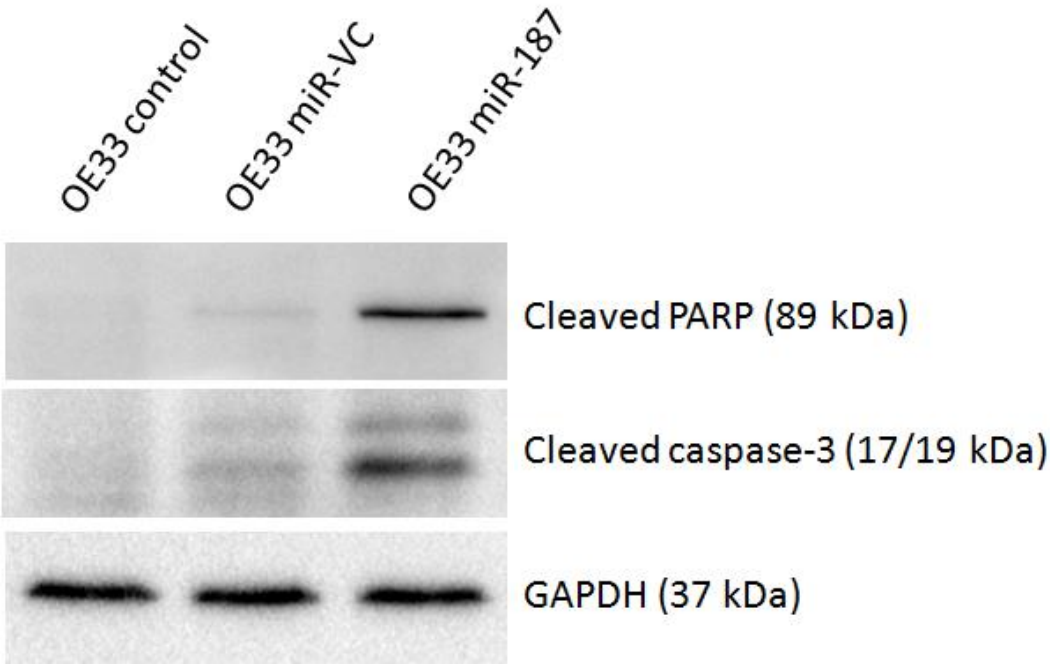

Fig 6.13 The overexpression of miR-187 induced apoptosis in the OE33 cell line. The OE33 cell line was transiently transfected with the pre-miR-187 or miR-VC vector. The overexpression of miR-187 induced PARP cleavage and caspase-3 cleavage, 48 h post-transfection, indicating an induction in apoptosis. GAPDH was probed as a loading control. Experimental repeats *n*=2.

6.4.5 Identification of miR-187 regulated genes

To identify gene expression changes associated with miR-187 overexpression, whole genome digital gene expression analysis was undertaken. The overexpression of miR-187 altered the expression of 303 genes, of these 162 genes (53%) were upregulated and 141 genes (47%) were downregulated (Appendix 9). KEGG (Kyoto encyclopaedia of genes and genomes) analysis identified an enrichment of downregulated genes in RIG-I-like receptor signalling, cytosolic DNA-sensing, cytokine-cytokine receptor interaction, toll-like receptor signalling, Jak-STAT signalling, antigen processing and presentation and chemokine signalling pathways (Table 6.1). The upregulated genes were associated with pathways in cancer and included the tumour suppressors *APC* and *PTEN*, the transcription factor and proto-oncogene *JUN* and the transcriptional regulator *HDAC2* (Table 6.1).

A panel of genes were selected from the data set for further validation based on the fold change in expression or previous identification of the genes in cancer associated pathways. Upregulated genes (*PYROXD2*, *APC*, *PTEN*, *JUN*, *TNF* and *CDK6*) and downregulated genes (*C3*, *CXCL10*, *CFB*, *TRANK1*, *APOL2*, *OAS1*, *IL28A*, *IFNB1*, *IFNL2* and *IL22RA1*) in the transcriptome data set were selected and validated by qPCR. The overexpression of miR-187 significantly increased the mRNA expression of *PTEN* and *TNF* (Fig 6.14 A). Of the 9 downregulated targets, 8 genes were validated and confirmed to be significantly decreased with miR-187 overexpression (Fig 6.14 B).

Table 6.1 KEGG analysis of pathways regulated by miR-187.

KEGG pathway	Fold enrichment	Genes
Pathways in cancer	+3.55	*HDAC2, JUN, KITLG, CDK6, APPL1, PTEN, FH, APC*
Chemokine signalling	-3.09	*CCL22, CXCL11, CCL5, STAT2, CXCL10*
Cytokine-cytokine receptor interaction	-4.41	*CCL22, TNFSF10, IL22RA1, IL29, IFNB1, CXCL11, IL28B, CCL5, IL28A, CXCL10*
Jak-STAT signalling	-4.47	*IL22RA1, IL29, 1FNB1, IL28A, IL28B, STAT2*
Antigen processing and presentation	-5.57	*TAP1, HLA-B, CD74, HLA-F*
Toll-like receptor signalling	-6.87	*IFNB1, IRF7, TLR3, CXCL11, CCL5, CXCL10*
Rig-1-like receptor signalling	-11.39	*DDX58, IFIH1, ISG15, IFNB1, IRF7, DHX58, CXCL10*
Cytosolic DNA-sensing	-12.61	*DDX58, IFNB1, IRF7, CCL5, ZBP1, CXCL10*

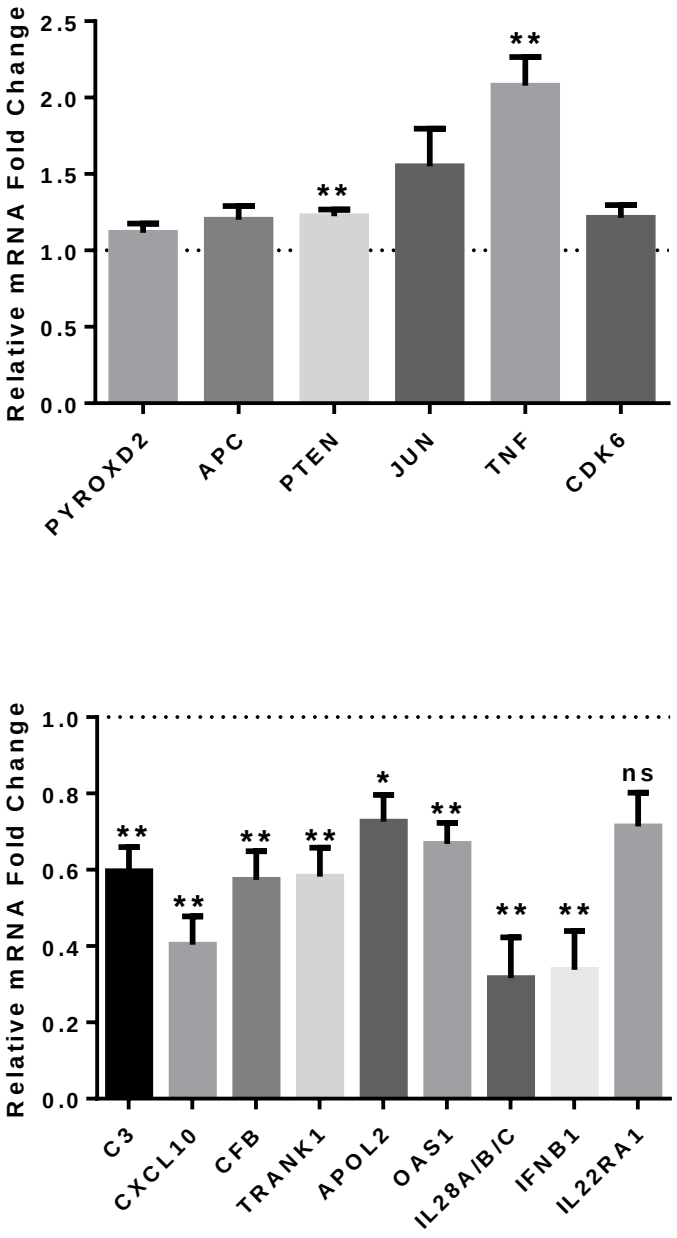

Fig 6.14 Validation of miR-187 regulated targets. Of the differentially expressed genes identified in the digital gene expression analysis, several genes were selected for further validation. The mRNA expression levels of the genes was determined by qPCR analysis in the OE33 R cell line transiently transfected with the miR-VC or pre-miR-187 vectors. (**A**) Of the six upregulated genes selected for validation, *PTEN* and *TNF* were confirmed to be significantly upregulated in the OE33 R cell line with miR-187 overexpression 24 h post-transfection. (**B**) Of the 9 downregulated genes selected for validation, 8 genes were confirmed to be significantly downregulated in the OE33 R cell line with miR-187 overexpression 24 h post-transfection. Experimental repeats n=5. Data presented as the mean ± SEM. Statistical analysis was performed using the one-sample t-test; * p<0.05, ** p<0.01, ns not significant.

6.4.6 *Complement 3* mRNA was upregulated in the non-responder patient biopsies

The overexpression of miR-187 decreased the expression of the *C3* mRNA (Fig 6.14 B). The *C3* gene encodes the C3 protein which is activate by proteolytic cleavage to produce C3a and C3b. The C3 protein is part of the complement system within the innate immune response, the complement system comprises a number of inactive proteins circulating in the blood that are cleaved and activated in response to pathogens. The expression of the C3a in the serum of OAC patients has previously been reported as a potential biomarker of response to CRT in OAC (Maher et al., 2011).

In the patient biopsies the expression of miR-187 was downregulated in the non-responders (Fig 3.2). Concomitant with downregulated expression of miR-187, the expression of the *C3* mRNA was significantly increased in the patient biopsies from the non-responders (Fig 6.15). However, there was no statistically significant correlation between miR-187 and *C3* mRNA expression in the data set (p=0.644 Spearman rank n=9).

In the OAC biopsies, immunohistochemistry confirmed expression of the C3 protein in the tumour epithelium and stromal compartments (Fig 6.16). Although the expression of the C3 mRNA was significantly increased in the non-responders, this did not correspond to an increase in C3 protein expression in the non-responders. There was no significant change in the expression of the C3 protein between the pre-treatment biopsies of the responders and non-responders (Fig 6.16).

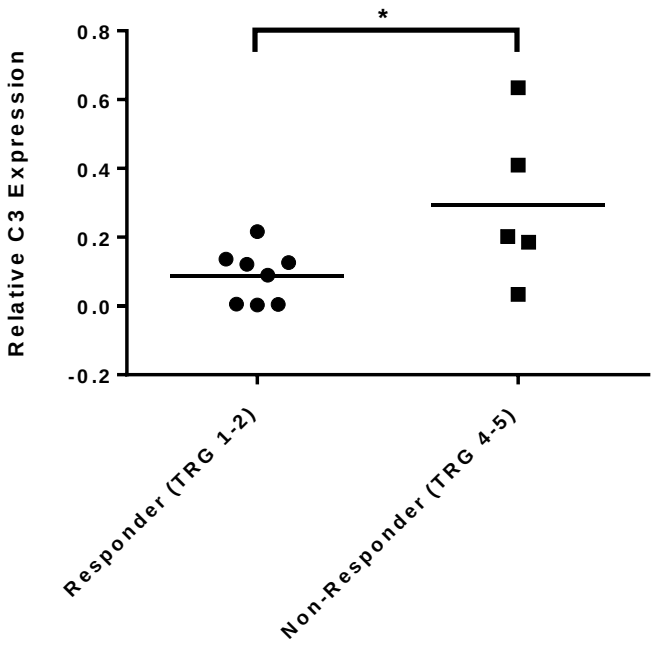

Fig 6.15 *Complement 3* mRNA expression is upregulated in the pre-treatment tumour biopsies of neo-CRT non-responders. The expression of *C3* mRNA was assessed in pre-treatment biopsies from OAC patients (*n*=30 with detectable expression in *n*=13; 8 responders and 5 non-responders). The Livak method was used for data analysis with *B2M* as the endogenous control. The expression of *C3* mRNA was upregulated in the non-responders compared to the responders. Statistical analysis was performed using an unpaired *t*-test; **p*<0.05

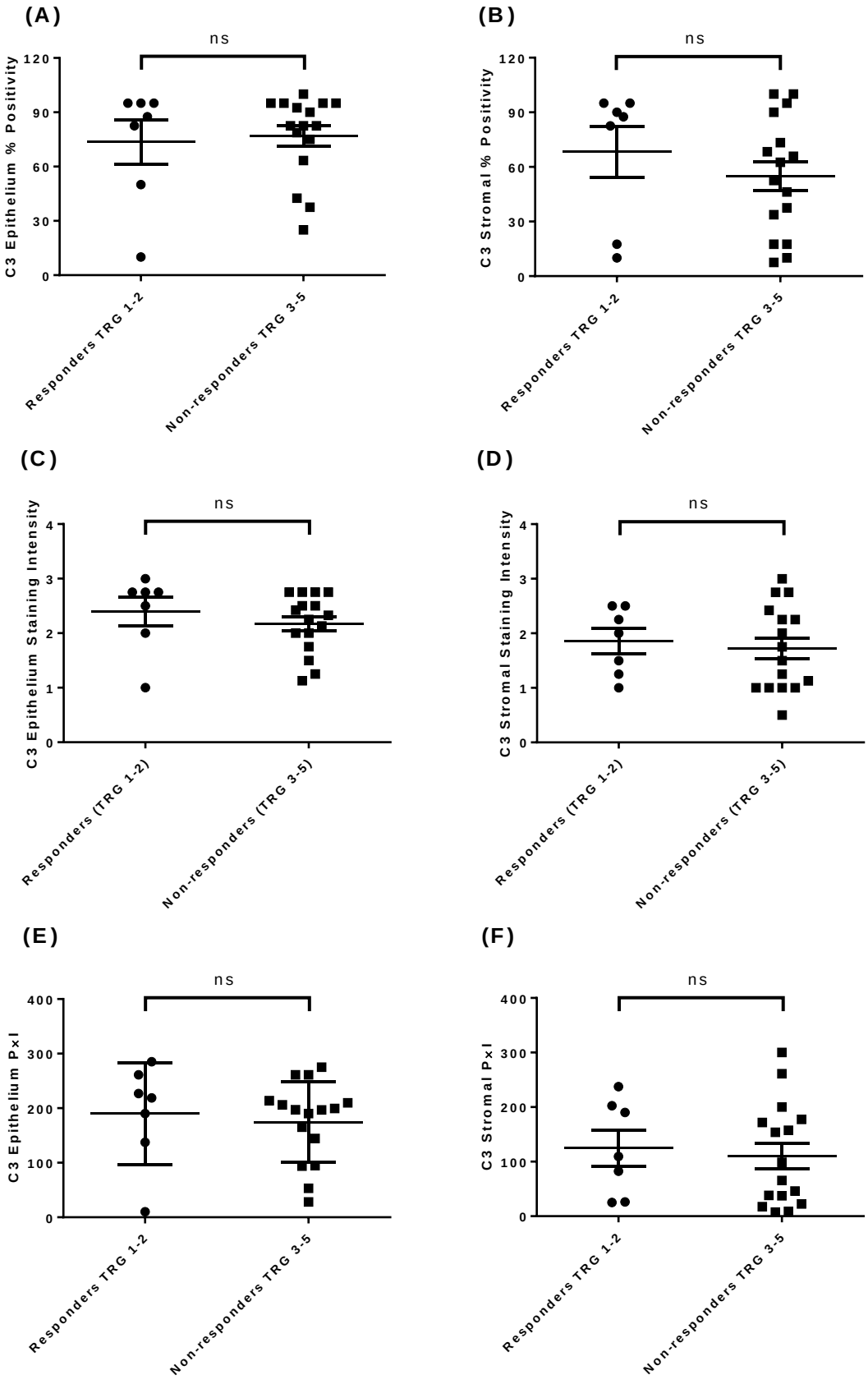
(A)
ns
C3 Epithelium % Positivity
120
90
60
30
0
Responders TRG 1-2
Non-responders TRG 3-5
(B)
ns
C3 Stromal % Positivity
120
90
60
30
0
Responders TRG 1-2
Non-responders TRG 3-5
(C)
ns
C3 Epithelium Staining Intensity
4
3
2
1
0
Responders (TRG 1-2)
Non-responders (TRG 3-5)
(D)
ns
C3 Stromal Staining Intensity
4
3
2
1
0
Responders (TRG 1-2)
Non-responders (TRG 3-5)
(E)
ns
C3 Epithelium P×I
400
300
200
100
0
Responders TRG 1-2
Non-responders TRG 3-5
(F)
ns
C3 Stromal P×I
400
300
200
100
0
Responders TRG 1-2
Non-responders TRG 3-5

Fig 6.16 Complement 3 protein expression does not correlate with patient response to neo-CRT. The expression of the C3 protein was assessed by IHC in the pre-treatment biopsies from OAC patients (*n*=23; 7 responders and 16 non-responders). The expression of C3 was graded separately in the epithelium (**A**, **C** and **E**) and stroma (**B**, **D** and **F**) for each TMA. The C3 staining positivity (**A** and **B**), intensity (**C** and **D**) and positivity × intensity (**E** and **F**) were analysed. There was no statistical significance in the expression of C3 between the responders and non-responder in either the epithelial or stromal tumour tissue. Statistical analysis was performed using the Mann-Whitney test; ns not significant.

6.5 Discussion

In the pre-treatment diagnostic biopsies of the OAC patient cohort, the expression of miR-187 was significantly downregulated in the neo-CRT non-responders (Fig 3.2). MiR-187 was chosen for further investigation as it has previously been reported as a prognostic and diagnostic biomarker as well as a modulator of proliferation, invasion and metastasis in several cancer types. The downregulated expression of miR-187 has previously been reported in taxol resistant ovarian cell lines (Kim et al., 2014). However, miR-187 did not alter sensitivity to tamoxifen or fulvestrant in breast cancer cells (Mulrane et al., 2012). Here, the role of miR-187 as a modulator of chemoradiation cellular sensitivity was investigated, with a particular focus on radiotherapy. Endogenous expression of miR-187 was undetectable in the OAC cell lines (Fig 6.2). This finding is in agreement with existing literature which has previously identified a loss of hyterozygosity on chromosome 18 in OAC (Barrett et al., 1999; Karkera et al., 2000). In the cell models used here the overexpression of miR-187 replaced or restored the expression of the miRNA.

The transient overexpression of miR-187 enhanced radiosensitivity in the OE33 P/ OE33 R/ OE33 and SK-GT-4 cell lines. In the acquired model of radioresistance, reintroducing miR-187 expression into the OE33 P and OE33 R cell lines enhanced cellular sensitivity to radiation in the parent and radioresistant cell lines (Fig 6.3). Furthermore, reintroducing miR-187 into the OE33 and SK-GT-4 cell lines, which have inherently different radiosensitivities, also enhanced cellular sensitivity to radiation (Fig 6.5 and 6.8). However, the stable overexpression of miR-187 only significantly enhanced radiosensitivity in the OE33 cell line (Fig 6.6). Interestingly, the stable overexpression of miR-187 in the OE33 P cell line significantly enhanced radioresistance (Fig 6.4), the opposite of transient miR-187 overexpression in the cell line. The transient and stable overexpression of miR-187 provides two different models

in which to study the function of the miRNA in the cell. The transient model is a system in which the immediate response of the cells to miR-187 expression can be studied, which is particularly significant in the cell lines used here which have no detectable expression of the miRNA. The overexpression of miR-187 introduced the miRNA into miR-187 naive cells, as appose to enhancing the endogenous expression of the miRNA. In comparison establishing a model of stable miR-187 overexpression selects a population of cells which are continually expressing the plasmid vector, and are able to maintain their proliferative integrity. The stable population is established by applying selection pressure to a cell line with inherently clonal instability and genetic diversity (Porter et al., 2014). The surviving cells which constitute the stable cell line model are perhaps the more radioresistant cells within the clonal diversity of the cell line. This may explain why the stable overexpression of miR-187 in the OE33 P generates a cell line with enhanced radioresistance whilst the transient overexpression of miR-187 enhances radiosensitivity. In the OE33 cells the transient or stable overexpression of miR-187 significantly enhanced radiosensitivity (Fig 6.5 and 6.6). In the SK-GT-4 cells the transient overexpression of miR-187 significantly enhanced radiosensitivity (Fig 6.8). However, the stable overexpression of miR-187 did not significantly enhanced radiosensitivity in the SK-GT-4 cells (Fig 6.9).

The stable overexpression model eliminates the initial cellular response to overexpression of the miRNA however, the longevity of the miRNA overexpression is not a concern in the stable model compared to the transient model were the population of cells expressing the plasmid gradually decreases as the cells divide. In the clonogenic assay transiently transfected cells are treated ~48 h after transfection and are expressing the miRNA during treatment, however by the end of the assay it is expected that the cells will no longer be expressing the miRNA. Conversely, in the stable cell miR-187 is constantly expressed during and after treatment. In relation to clinical application, the

transient model more closely represents the concept of miRNA replacement therapy in the clinic. Patients would receive miRNA replacement therapy immediately prior to treatment to ensure the expression of the miRNA was present and active in the tumour during treatment. The miRNA replacement therapy would most likely be administered as a small molecule which would only be transiently expressed in the tumour. However, the stable model provides a more reliable and reproducible system in which to conduct *in vitro* work. The transient transfection of cells inevitably induces some degree of cell death, because the transfection of the plasmid into cells relies on permabilisation and disruption of the cell membrane. The off target effects of transient transfection are not a concern with stable miRNA overexpression. Despite the differences in the two models, the data presented here suggests miR-187 does enhance radiosensitivity and the validation of this finding in the two models and four cell lines provides an extensive validation of miR-187 as a radiosensitising miRNA. In future work the mechanism by which miR-187 modulates cellular sensitivity to radiotherapy will be investigated *in vitro* by assess parameters which contribute to radiation response and sensitivity such as cell cycle disruption, DNA repair and apoptosis. The overexpression of miR-187 also enhanced cellular sensitivity to cisplatin in the OE33 cells (Fig 6.7), and is in agreement with downregulated miR-187 in taxol resistant ovarian cell lines (Kim et al., 2014). Further work is needed to assess miR-187 as a modulator of chemosensitivity.

The overexpression of miR-187 in the OE33 cell line also conferred tumour suppressor effects in addition to enhancing radiosensitivity. The transient overexpression of miR-187 reduced cell viability in the OE33 but not the SK-GT-4 cells (Fig 6.10 and 6.11). The decrease in cell viability in the OE33 cells was observed in the mock and 2 Gy irradiated cells, indicating the decrease in cell viability with miR-187 overexpression is independent of response to radiation at the doses and time points tested. The decrease in viability corresponded to a significant increase in cell death 48 h

post-transfection, relative to the miR-VC transfected control (Fig 6.12). The overexpression of miR-187 induced the cleavage of PARP and caspase-3 indicating cell death was induced by apoptosis and not necrosis (Fig 6.13). In this study miR-187 overexpression enhanced radiosensitivity in the OE33 and SK-GT-4 cells however, apoptosis was only induced in the OE33 cell line and was independent of radiation at the time points tested. In future work it will be necessary to further investigate the combined effects of miR-187 overexpression, apoptosis and radiation to determine if enhanced radiosensitivity is the result of an increase in miR-187 induced apoptosis. Although the overexpression of miR-187 did not decrease cellular viability in the SK-GT-4 cells at the time points and dose tested, the cell line is inherently more resistant to 2 Gy radiation and miR-187 induced apoptosis should be further investigated in the cell line. However, it is also feasible that miR-187 induced apoptosis is specific to the OE33 cells and the induction of apoptosis and enhanced radiosensitivity may be independent cellular pathways. There is evidence of miRNA enhancing radiosensitivity by promoting radiation induced apoptosis, miR-218 is reported to induce apoptosis and enhance radiosensitivity in cervical cancer cells (Yuan et al., 2014). The expression of miR-218 is frequently lost in cervical cancer and correlates with poor prognosis (Yu et al., 2012). *In vitro* the overexpression of miR-218 enhanced radiation-induced apoptosis and suppressed tumour growth. *In vivo* miR-218 overexpression and radiation significantly reduced tumour growth and *ex vivo* analysis confirmed an increase in the expression of cleaved caspase-3. In renal cell carcinoma the overexpression of miR-185 enhanced radiation induced apoptosis via the downregulation of ATR, a master regulator in DNA damage response (Wang et al., 2013). In fact, numerous miRNA have been reported to modulate radiosensitivity in cancer (Zhao et al., 2012). These miRNA modulate radioresponse via the regulation of apoptosis, cell cycle progression, DNA damage response, cell survival pathways, hypoxia and regulation of cancer stem

cells (Zhao et al., 2012; Korpela et al., 2015). The mechanism by which miR-187 enhances OAC radiosensitivity *in vitro* may or may not be associated with apoptosis and this requires further investigation.

Gene expression analysis indentified 303 genes which were significantly differentially expressed as a result of miR-187 overexpression *in vitro* (Appendix 9). These genes may be directly or indirectly modulated by miR-187. However, direct targets of miR-187 which are transitionally repressed without degradation of the mRNA will not be differentially expressed and will not be included in the gene expression data set. Of the 303 genes, six upregulated and nine downregulated genes were selected for further validation (Fig 6.14). These genes were selected from the data set for further validation based on the presence of predicted miR-187 binding sites, the fold change in expression or because they have previously been identified as tumour suppressors or oncogenes. Of the upregulated genes only two, *PTEN* and *TNF*, were significantly upregulated with miR-187 overexpression highlighting the importance of additional validation (Fig 6.14A). *PTEN* is a tumour suppressor and is frequently mutated in cancer. The protein produced by the gene is an upstream negative regulator of the Atk signalling pathway, which is instrumental in cellular response to radiation. The Akt pathway is activated in response to radiation damage and subsequently suppresses pro-apoptotic proteins and activates survival pathways. The *PTEN* gene is regulated by multiple miRNA including miR-21, miR-26, miR-221, miR-222, miR-216a, miR-217 and miR-486 (Zhao et al., 2012). The increase in expression of the *PTEN* tumour suppressor could potentially enhance tumour sensitivity to radiotherapy, and requires further investigation in the models presented here. Restoring or enhancing miR-187 expression in the tumours of the patients could enhance expression of the *PTEN* tumour suppressor, which may improve patient response to CRT via negative regulation of the Akt survival pathway. A similar approach has been suggested in oesophageal squamous

cell carcinoma, the inhibition of oncogenic miR-21 enhanced radiosensitivity possibly through the activation of PTEN protein (Huang et al., 2013).

Complement 3 (*C3)*, C-X-C motif chemokine 10 (*CXCL10*), complement factor B (*CFB*), tetratricopeptide repeat and ankyrin repeat containing 1 (*TRANK1*), apolipoprotein L2 (*APOL2*), 2'-5'-oligoadenylate synthetase 1 (*OAS1*), interferon lambda 2 (*IL28A*) and interferon beta 1 (*IFNβ1*) were validated to be downregulated following overexpression of miR-187, supporting miR-187-mediated negative regulation of these genes (Fig 6.14 B). The expression of *CXCL10* has previously been reported as a prognostic marker of patient response to radiation (Rentoft et al., 2014) (Li et al., 2014a) . In patients with squamous cell carcinoma of the tongue, high expression of *CXCL10* was associated with poor response to radiotherapy (Rentoft et al., 2014). Conversely, high *CXCL10* expression was associated with good response to neoadjuvant CRT in rectal cancer patients, and overexpression of *CXCL10* in HeLa cells enhanced cellular sensitivity to radiation through cell cycle redistribution (Li et al., 2014a) (Yang et al., 2012). APOL2 is a member of the apolipoprotein L family, the function of this lipid binding proteins is unknown (Galindo-Moreno et al., 2014). *APOL1*, *3* and *6* were also downregulated with miR-187 overexpression (Appendix 9). APOL1 and 6 proteins have been identified as regulators of autophagy (Zhaorigetu et al., 2011) (Zhaorigetu et al., 2008). *OAS1* encodes a protein of the 2'-5' oligoadenylate synthetase family, which are involved in the innate immune response, the *OAS2* and *OASL* genes were also downregulated with miR-187 overexpression. The *OAS* genes are induced by interferons and have previously been identified as part of an IFN-related DNA damage resistance signature (Weichselbaum et al., 2008). Radiation resistance has been linked to an overexpression of *IFN* related genes and an interferon-related gene signature has been proposed as a therapy-predictive biomarker to identify patient with

CRT sensitive or resistant breast cancer. In the gene expression data set presented here, a vast number of genes are *IFN* related genes (Weichselbaum et al., 2008).

Inflammation is now considered a hallmark of cancer, impacting all stages of tumorigenesis (Rutkowski et al., 2010; Pio et al., 2013). Chronic inflammation is also implicated in the resistance of tumours to therapy, however, the role of the complement system in resistance to CRT is largely unknown (Multhoff & Radons, 2012). C3 is a central protein of the complement activation cascade, which is an essential component of the innate immune system, and acts as an important bridge between innate and adaptive immunity (Dunkelberger & Song, 2010). In the patient biopsies the expression of the *C3* mRNA was downregulated in the non-responders which correlates with increased miR-187 expression (Fig 6.15). This corroborates with downregulated C3 mRNA expression with miR-187 overexpression *in vitro* (Fig 6.14). However, it is of importance note the small sample size in which *C3* mRNA expression was detectable. There were *n*=13 patient biopsies (*n*=8 responders and *n*=5 non-responders) in which *C3* mRNA expression was detectable and analysed. Sample size should be increased to enhance the statistical power of this analysis as the current sample size is insufficient to support or reject the hypothesis that *C3* mRNA expression is downregulated in non-responders. Furthermore, C3 protein expression was not differentially expressed in the IHC analysis of the patient biopsies (Fig 6.16). This suggests an apparent change in the *C3* mRNA does not correlate to a significant alteration in the expression of the functional protein in tumour tissue. Although sample size is limited and should be expanded, the current data suggests increased expression of *C3* in pre-treatment tumours from non-responders may be a predictive biomarker of tumour response to CRT.

The gene expression analysis presented here identified the altered expression of genes encoding proteins with extracellular functions including *CXCL10*, *CXCL11*, *TNF*,

C3 and *VIM*. These findings support the expanding role of miRNA as modulators of the extracellular environment and the tumour microenvironment (Chou et al., 2013; Suzuki et al., 2015). Within cancer cells and tumour stromal cells, miRNA regulate gene expression including genes encoding proteins with intracellular and extracellular functions, therefore, miRNA modulate intracellular and extracellular processes. In the tumour microenvironment, miRNA have been shown to directly and indirectly modulate angiogenesis, immune response, hypoxia and invasion (Chou et al., 2013; Suzuki et al., 2015). Targeting cancer cells is not the same as targeting tumour tissue, the sensitivity and response of a solid tumour treated with CRT is dictated by the biology of the tumour microenvironment as well as cancer cell sensitivity. For example, a critical factor in tumour response to CRT is tumour vasculature. The vasculature is essential for delivery of systemic chemotherapeutics and the vasculature supplies the tumour with oxygen which enhances tumour sensitivity to radiotherapy. Several miRNA have been reported to directly or indirectly regulate angiogenesis, including miR-9 and miR-126 (Ma et al., 2010; Png et al., 2012) .

Here, miR-187 was shown to alter cellular sensitivity to radiotherapy, the targets and pathways of miR-187 are currently been investigated to understand the mechanism by which miR-187 modulates radiosensitivity in OAC. In future the work, miR-187 should be investigated as a modulator of CRT sensitivity using *in vitro* and *in vivo* models. The replacement or increased expression of miR-187 in patient tumours may offer a therapeutic strategy to enhance sensitivity and efficacy of CRT in OAC patients.

Chapter 7 Generation of an Isogenic Model of Cisplatin Resistance in OAC

7.1 Introduction

Approximately 70% of OAC patients do not respond to neo-CRT which is the standard of care for locally advanced disease. Tumour resistance to CRT is a major obstacle to improving patient survival rates. In this study the aim was to identify and investigate the role of miRNA as modulators of chemoradiation therapy in OAC.

In the previous chapters, cell lines have been used as *in vitro* models to investigate the role of miR-330-5p and miR-187 as modulators of chemoradiation sensitivity in OAC. In chapter 6, the radioresistant isogenic model (OE33 P/OE33 R) was used to identify miR-187 as a radiosensitising miRNA. In this chapter, the aim was to establish a chemoresistant isogenic model in the OE33 cell line. Isogenic cell models are established from a standard cell line which is repeatedly treated alongside an control treated, age and passage matched parent cell line. Treating the cells with low doses enables the cells to adapt and develop an acquired resistance to the therapeutic which induces a stable resistant phenotype. The isogenic model is two cell line of identical genetic background with altered treatment sensitivity. The isogenic model reflects the acquired resistance to therapy observed in cancer patients who initially respond to treatment but subsequently develop therapeutic resistance. Resistant cell line models have been established in multiple cancer types with various therapeutics and provide a valuable insight into the mechanisms and genetic alteration associated with therapeutic resistance (Stordal & Davey, 2007). Furthermore, isogenic models of therapeutic resistance which are established using repetitive treatment cycle and are archived at regular intervals provide a 'time lapse' model of resistance development. In this chapter the aim was to establish and validate an isogenic model of cisplatin resistance. In future studies this model could be used to investigate chemoresistance in OAC and the role of miRNA as modulators of chemosensitivity.

7.2 Rationale, aims and objective

Cell line models of therapeutic resistance are useful tools and systems in which to study acquired molecular mechanism of cancer cell resistance to treatment. Considering OAC patients receive a combination of radiation, cisplatin and 5-FU as part of the neo-CRT regimen, a cell line model of chemoresistance would provide a useful *in vitro* system in which to study the molecular mechanism of acquired resistance. To study chemoresistance in OAC the aim here was to establish an isogenic cell model of cisplatin resistance.

- Establish an OAC isogenic model of cisplatin resistance and confirm cisplatin resistance using the clonogenic assay.
- Assess 5-FU sensitivity in the cisplatin resistant cell line.
- Identify gene expression changes associated with enhanced cisplatin resistance.

7.3 Materials and methods

7.3.1 Induction of cisplatin resistance in the OE33 cell line

The cisplatin resistant variant of the OE33 cell line (OE33 CISR) was derived from the original parent cell line. Cells were treated with 1 µM cisplatin or PBS for 72 h. Treatment was then discarded and replaced with complete media for 72 h, this cyclic treatment regimen was repeated for approximately 6 months. During this time cells were subcultured at 80-90% confluence as previous described (section 2.3.2). Frozen stocks were prepared at regular intervals to archive cell lines with progressive treatment cycles. Prior to freezing cells were cultured for ~14 days in complete media without cisplatin (section 2.3.3).

7.3.2 Clonogenic assay

The clonogenic assay was performed as described in section 2.7.1. Seeding densities were 500 c/w for PBS control and 1000 c/w for 1 µM cisplatin. Cells were incubated for ~8 days prior to fixing and staining with crystal violet. The plating efficiency and surviving fraction were calculated as described in section 2.7.1.

7.3.3 MTS assay

The MTS assays were performed as described in section 2.7.2. Cells were seeded at a density of 1000 c/w and were treated for 72 h with PBS or 1 µM cisplatin. The MTS reagent was added to each well and plates were incubated for a further 3 hours prior to Abs 490 nm measurements.

7.3.4 Whole genome digital gene expression analysis

Total RNA was extracted (section 2.5.1) from the OE33 CISR cells or the OE33 PBS cells. Samples of total RNA were prepared for shipping, as previously described section 2.5.7. Digital RNA-seq was outsourced to LC Sciences (Texas, USA). Analysed

data sets were provided by LC Sciences. The fold change in gene expression was calculated from the equation; log2 (OE33 CISR 29 FPKM / OE33 PBS 29 FPMK). Gene expression changes were considered significant if the *p* value was <0.05.

7.4 Results

7.4.1 Development of a cisplatin resistant isogenic model

To establish an isogenic model of cisplatin resistance the OE33 cell line was cultured with cisplatin or PBS for 72 h followed by 72 h culturing with complete media to allow cells to recover. This cyclic treatment was undertaken for approximately 6 months and alterations in cisplatin sensitivity were assessed during the development of the isogenic model using the clonogenic assay. After 15 cycles of cisplatin treatment there was a slight increase in cisplatin resistance in the OE33 CISR 15 compared to the OE33 PBS 15 cell line (Fig 7.1). The surviving fraction of the OE33 CISR 19 cell line was higher in comparison to the OE33 PBS 19 cell line (Fig 7.1). Similarly, the OE33 CISR 21 and 26 cell lines were more resistant to cisplatin than the age and passage match OE33 PBS cell line, indicating the induction of a stable cisplatin resistant phenotype (Fig 7.1). To confirm cisplatin resistance the clonogenic assay was repeated with OE33 CISR 21 and OE33 PBS 21 cell lines after the cells had been cultured for a minimum of 4 weeks without cisplatin treatment. The OE33 CISR 21 cell line was significantly more resistant to cisplatin treatment in comparison to the OE33 PBS 21 cell line (Fig 7.2).

7.4.2 The cisplatin resistant isogenic model showed enhanced sensitivity to 5-FU

Cellular resistance to cisplatin in the OE33 CISR 21 cell line was also confirmed using the MTS viability assay. The viability of the OE33 CISR 21 cell line was significantly increased compared to the OE33 PBS 21 cell line after 72 h of cisplatin treatment (Fig 7.3 A). In comparison the viability of the OE33 CISR 21 cell line was significantly decreased compared to the OE33 PBS 21 cell line after 72 h of 5-FU treatment (Fig 7.3 B).

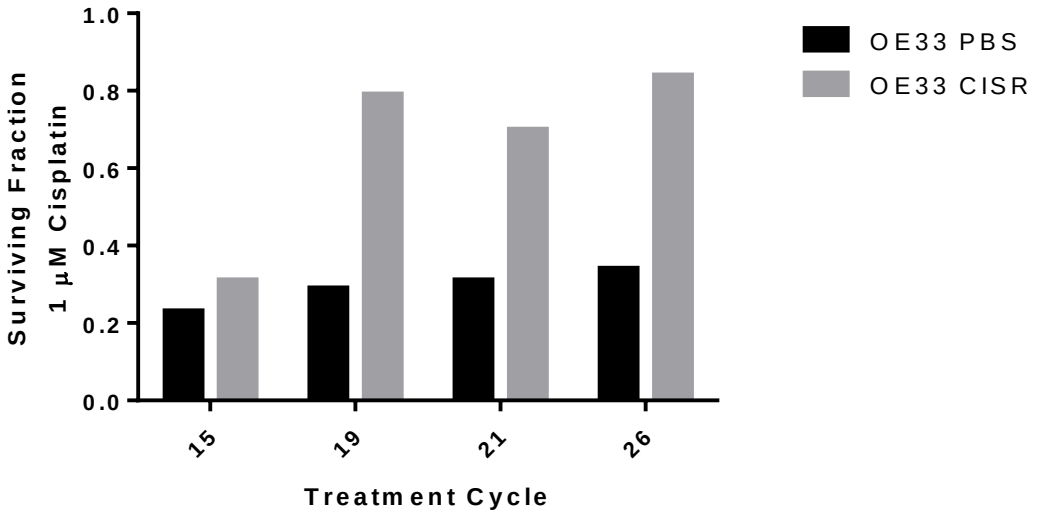

Fig 7.1 Establishing an isogenic model of cisplatin resistance. The development of the cisplatin resistant phenotype was assessed at regular intervals during development of the model using the clonogenic assay. Cells were cultured with 1 µM cisplatin or PBS for 72 h and then cultured without treatment for 72 h in a continuous cycle. The treatment cycle number denotes how many rounds of cisplatin or PBS the cell line was treated with prior to the clonogenic assay. Cells seeded into the clonogenic assay were treated with PBS or 1 µM cisplatin for 24 h. The data indicates enhanced cisplatin resistance developed between cycles 15 and 19. The surviving fraction of the OE33 CISR 19, 21 and 26 increased ~2-fold compared to the OE33 CISR 15 and the OE33 PBS 15, 19, 21 and 26 cell lines. Experimental repeats *n*=1.

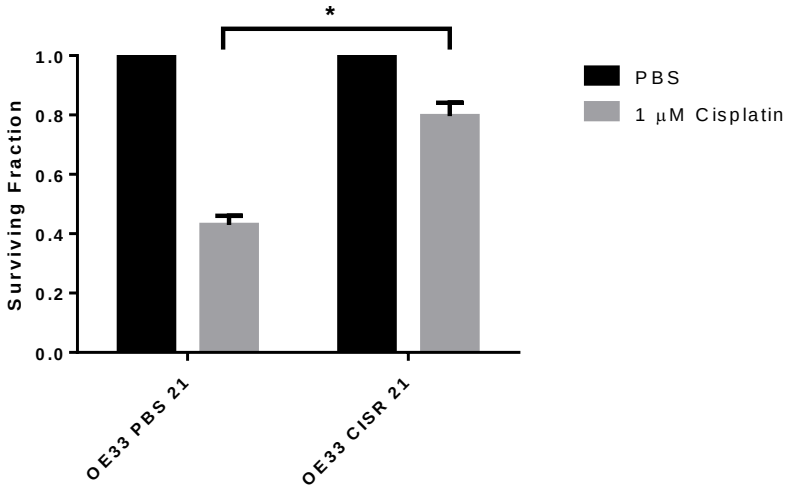

Fig 7.2 The cisplatin resistant isogenic model. The cisplatin resistant phenotype of the isogenic model was confirmed in the OE33 CISR 21 cell line using the clonogenic assay. Cells seeded into the clonogenic assay were treated with PBS or 1 μM cisplatin for 24 h. The surviving fraction of OE33 CISR 21 cells was significantly greater (~35%) than OE33 PBS 21 cells. Experimental repeats *n*=3. Data presented as the mean ± SEM. Statistical analysis was performed using the paired *t*-test; * $p<0.05$

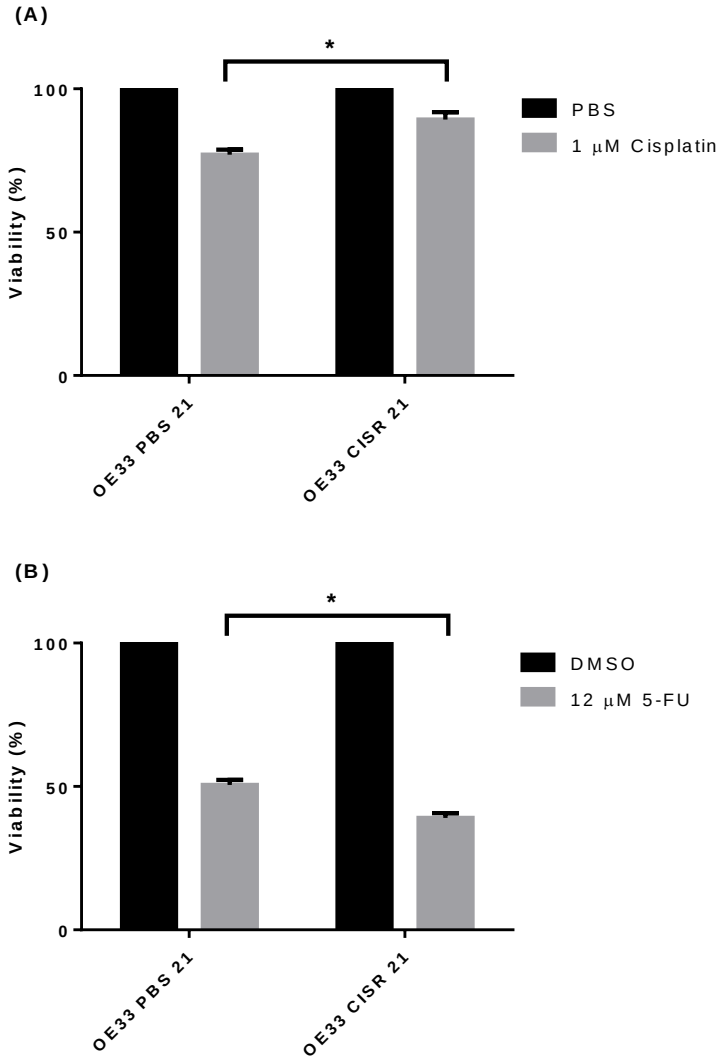

Fig 7.3 The cisplatin resistant isogenic model showed enhanced sensitivity to 5-FU. The viability of the chemotherapy (cisplatin or 5-FU) treated cells was normalised to the vehicle control (PBS or DMSO) treated cells. Cells were treated with either 1 µM cisplatin, 12 µM 5-FU, PBS or DMSO. After 72 h of treatment the MTS reagent was added and plates were incubated for 3 h prior to reading Abs 490 nm. (**A**) The viability of the OE33 CISR 21 was significantly enhanced compared to the OE33 PBS 21 when treated with 1 µM cisplatin. (**B**) The viability of the OE33 CISR 21 was significantly decreased compared to the OE33 PBS 21 when treated with 12 µM 5-FU. Experimental repeats n=3. Data presented as the mean ± SEM. Statistical analysis was performed using the paired t-test; * p<0.05

7.4.3 Gene expression analysis in the cisplatin isogenic model

To identify gene expression changes associated with the cisplatin resistant phenotype, whole genome digital gene expression analysis was undertaken. There were 692 genes significantly differentially expressed between the OE33 CISR 29 and OE33 PBS 29 cell lines. Of these, 278 genes were upregulated and 414 genes were downregulated in the OE33 CISR 29 cell line compared to the OE33 PBS 29 cell line. Applying a threshold of ± 1.5 fold change expression, 90 genes were upregulated and 188 genes were downregulated in the OE33 CISR 29 cell line compared to the OE33 PBS 29 cell line (Appendix 10).

7.5 Discussion

Cisplatin is the original platinum-based chemotherapeutic and has been used in the treatment of cancer for over 30 years (Stordal & Davey, 2007). The platinum-based chemotherapeutics, also known as the alkylating agents, intercalate with DNA forming interstrand and intrastrand adducts. These adducts disrupt DNA replication and translation which subsequently induces cell death. However, cancer cells have molecular mechanism of inherent and acquired cisplatin resistance. The resistance of cancer cell to chemotherapeutics and radiation poses a major challenge in the treatment of cancer. Chemotherapy and radiotherapy are the cornerstones of cancer treatment in the clinic today and will continue to be so for the foreseeable future. Chemo and radiosensitising agent could improve patient response to chemo and radiotherapy and have a significant impact on patient survival. This therapeutic strategy is generally applicably to the treatment of most cancer types, including the 70% of OAC patients who do not respond to neo-CRT and have no alternative treatment options.

Cellular models of therapeutic resistance are useful *in vitro* tools in which to study the cellular mechanisms of resistance. There is no single generic mechanism responsible for therapeutic resistance in a single patient tumour or even a single cancer cell. Previous studies in cisplatin resistant cancer cell lines report multiple mechanisms are responsible for enhanced resistance and the cisplatin resistant phenotype is the result of multiple gene and protein expression changes (Stordal & Davey, 2007). Molecular mechanisms commonly associated with cisplatin resistance include DNA repair, drug influx/efflux, drug detoxification, cell cycle dysregulation and evasion of apoptosis (Shen et al., 2012). In chapter 6, the isogenic model of radioresistance was used to investigate the role of miR-187 as a modulator of cellular sensitivity to radiation. Restoring miR-187 expression enhanced the radiosensitivity of both the OE33 P and OE33 R (Fig 6.3). Furthermore, miR-187 enhanced cisplatin sensitivity in the OE33 cell

line suggesting miR-187 may modulate cellular mechanisms of resistance which are applicable to both cisplatin and radiation sensitivity (Fig 6.7). To investigate the molecular mechanisms of chemoresistance and the role of select miRNA in OAC resistance to chemotherapy an isogenic model of cisplatin resistance was established in the OE33 cell line. Whilst establishing the OE33 CISR cell line the clonogenic assay indicated an alteration in cisplatin sensitivity between cisplatin treatment cycles 15 and 19 (Fig 7.1). The induction of a stable cisplatin resistant phenotype was confirmed in the OE33 CISR 21 vs. OE33 PBS 21 cell lines (Fig 7.2). This is the first study to develop an isogenic model of cisplatin resistance in the OE33 cell line. However, previous studies have established cisplatin and 5-FU resistant OE19 cell lines (Hummel et al., 2011b). Interestingly, miRNA expression profiling in the OE19 cisplatin resistant cell line and the OE19 5-FU resistant cell line identified a large number of miRNA which were significantly differential expressed in comparison to the chemosensitive controls (Hummel et al., 2014). Interestingly, the miRNA expression profile of the cisplatin resistant cell line differed from the miRNA expression profile of the 5-FU resistant cell line (Hummel et al., 2014). The differential miRNA expression profiles may be associated with the different mechanism by which cisplatin and 5-FU induce cytotoxic damage. The enhanced 5-FU sensitivity in the OE33 CISR cell line presented here is also likely attributed to the differential mechanisms of action between the two chemotherapeutics (Fig 7.3). Another study using the same OE19 chemoresistant cell line models demonstrated enhanced cisplatin and 5-FU sensitivity with overexpression of miR-148a in the resistant cell lines (Hummel et al., 2011b). The data from this study supports other studies which suggest miRNA modulate chemoradiation sensitivity in OAC (Hamano et al., 2011; Lynam-Lennon et al., 2012).

During the repetitive cycles of sublethal cisplatin treatment the cells adapted to the cyctoxic insult of cisplatin and developed molecular mechanisms of resistance to

ultimately evade cisplatin induced cell death. This isogenic model reflects the clinical response of patients who initially respond to CRT and later develop resistance to therapy. There are multiple mechanisms by which the cancer cell can develop resistance to cisplatin. Further characterisation of the isogenic model is necessary to reveal the mechanisms of cisplatin resistance. The gene expression data presented here provides indications as to the potential mechanisms associated with enhanced resistance to cisplatin in the OE33 CISR cells compared to the OE33 PBS cells. Cell membrane transporter genes *ATP1A3*, *ABCA12*, *TMEM199* and *TMEM22* were upregulated and *TMEM156* and *TMEM42* were downregulated in the OE33 CISR. The existing literature is limited with regards to these genes however, these genes are members of cell membrane transporter families some of which are associated with transport and cellular accumulation of cisplatin such as ATP7A/B and TMEM205 (Shen et al., 2012). Upregulated Wnt signalling and the EMT pathway are also associated with cisplatin resistance (Singh & Settleman, 2010; Piskareva et al., 2015). The upregulation of the *PRICKLE2* gene may contribute to an increase in Wnt signalling in the OE33 CISR cell line (Katoh, 2007). In addition the upregulation of *MMP1* and downregulation *ICAM* are gene changes associated with the EMT. Evasion of apoptosis is an essential mechanism in therapeutic resistance. The *CDKN1C* gene produces the cyclin-dependent kinase inhibitor p57 which functions as a tumour suppressor in multiple cancer types (Matsuoka et al., 1995). Furthermore, the overexpression of p57 has been shown to enhance cisplatin sensitivity *in vitro* via intrinsic mitochondrial apoptosis (Vlachos et al., 2007). The downregulation of the *CDKN1C* gene in the OE33 CISR cell line may contribute to evasion of apoptosis and cellular resistance to cisplatin.

In future work the isogenic model of cisplatin resistance should be further characterised to identify the molecular mechanisms associated with enhanced cellular resistance to cisplatin. In addition, the resistance mechanisms in the cisplatin and

radiation isogenic models could be compared to identify shared mechanism of resistance which could potentially be targeted to enhance both cisplatin and radiosensitivity simultaneously. In chapter 6, miR-187 overexpression enhanced cisplatin sensitivity in the OE33 cell line and this should also be assessed in the cisplatin isogenic model. The radiosensitivity of the isogenic cisplatin model should also be assessed. As in other related studies discussed here, miRNA expression profiling should be undertaken in the cisplatin isogenic model and the data compared to the miRNA expression profiling in the patient biopsies and the published data on the OE19 cisplatin resistant cell line (Hummel et al., 2014).

Chapter 8 Concluding Discussion

8.1 Discussion

In Europe the prognosis for patients diagnosed with oesophageal cancer is extremely poor, the 1-year survival rate is 40% and the 5-year survival rate is 12% (Anderson et al., 2015). The poorest 5-year survival rate in Europe is in the UK and Ireland, where the most common subtype of oesophageal cancer is OAC (Arnold et al., 2015). The greatest risk factor in the development of OAC is BO. Estimates suggest ~2% of the population have BO, which increases the risk of developing OAC by 30-125 fold (Jankowski et al., 2000a; Solaymani-Dodaran et al., 2004). It is common practise for patients diagnosed with BO to be enrolled in endoscopy surveillance programmes, which monitor changes in the BO segment of the oesophagus to identify early progression and development of OAC. These surveillance programmes are effective in identifying and treating early OAC with curative intent (El-Serag et al., 2015). However, very few BO patients (~0.5%) will progress to OAC and the economic cost of screening BO patients is a contentious issue (Schneider & Corley, 2015). Furthermore, the majority (80-90%) of patients diagnosed with OAC have not previously had a diagnosis of BO (Bhat et al., 2015). Some patients with BO are asymptomatic and 40% of patients diagnosed with OAC have never experienced symptoms of chronic acid reflux or heartburn (Spechler & Souza, 2014). The majority of patients do report symptoms of dysphagia (75%) and are subsequently diagnosed with advanced disease (Khanna & Gress, 2015). Early diagnosis would improve the survival rates for OAC. Patients diagnosed with early disease are treated with curative intent and the 5-year survival rate for these patients is 90% (Visbal et al., 2001). Increasing awareness of the disease, particularly amongst those individual at high risk, could encourage early diagnosis. However, asymptomatic patients may constitute a significant proportion of OAC patients and these patients are very unlikely to receive an early diagnosis. Therefore, it is unavoidable that patients will continue to be diagnosed with OAC at an

advanced stage. With this in mind, the development of more effective treatments for advanced disease will arguably yield the greatest improvements in OAC survival rates.

The majority of OAC patients are diagnosed with advanced disease and approximately half of these patients will receive palliative care (Khanna & Gress, 2015). Patients allocated to palliative care have advanced metastatic disease, or have additional health problems which prevent them receiving neoadjuvant therapy and surgery (Coron et al., 2013). The other half of patients will be treated with curative intent and they will receive neoadjuvant chemotherapy, or neo-CRT, prior to surgical resection. In Ireland the standard of care for OAC patients is neo-CRT and in the UK the standard of care is neoadjuvant chemotherapy (Messager et al., 2015). There is credible and extensive evidence to support neoadjuvant therapy in combination with surgery as the most effective treatment for OAC patients (Sjoquist et al., 2011). There are few studies which have compare neoadjuvant chemotherapy and neo-CRT to determine which is the most effective in combination with surgery (Stahl et al., 2009; Burmeister et al., 2011). However, there is some evidence to suggest that neo-CRT is more effective than neoadjuvant chemotherapy (Sjoquist et al., 2011). Presently, there are a number of on-going definitive trials directly comparing neoadjuvant chemotherapy and neo-CRT (Choi et al., 2015).

Unfortunately the majority of patients will not respond to neo-CRT or neoadjuvant chemotherapy (Allum et al., 2009). The non-responders receive aggressive treatment regimens from which they gain little or no benefit, whilst potentially compromising their quality of life. For some of these patients the disease continues to progress whilst they are receiving neoadjuvant therapy, which reduces the success of surgery and adversely affects the patients prognosis (Kelsen, 2000). The identification of biomarkers which could predict patient response to neoadjuvant therapies, in a pre-

treatment setting, could aid treatment stratification for patients at the point of diagnosis. Those patients who are predicted to be non-responders to neoadjuvant therapy could in some cases benefit from immediate surgery. Alternatively, the predicted non-responders could be allocated palliative care, as appose to aggressive treatments which offer no survival benefits and negatively impact the patient's quality of life. The predictive biomarkers could improve the treatment and care for individual patients, but predictive biomarkers will not confer significant improvements in patient survival. The greatest clinical benefit would be gained from the development of new therapeutics for OAC. Ideally, predictive biomarkers would identify non-responders and those patients would be offered alternative curative therapies. Novel therapeutic agents, which target the functional regulators associated with tumour resistance to chemoradiation therapy, could enhance patient response to conventional neoadjuvant therapies as part of multimodal treatment regimens. Sensitising agents which enhance tumour sensitivity to chemoradiation therapy is an attractive strategy for OAC, as well as the majority of other cancer types.

MiRNA are short non-coding RNA which function to negatively regulate gene expression (Bartel, 2004). Dysregulated miRNA expression plays a causal role in cancer development and progression. Numerous studies have reported miRNA expression profiles and signatures in cancer, highlighting the potential of miRNA as clinical biomarkers (Saumet et al., 2014). MiRNA are also targets for therapeutic intervention. Manipulating the expression of a single miRNA has the potential to alter the expression of multiple genes, proteins and cellular pathways (Lim et al., 2005). Furthermore, miRNA are predictors and modifiers of tumour response to chemotherapeutics and radiation (Hummel et al., 2010). These miRNA are potential biomarkers of patient response to chemotherapy and radiotherapy which, could be utilised in a pre-treatment setting to predict patient response to treatment and inform decisions for patient care.

Furthermore, miRNA which modulate tumour response and sensitivity to CRT are therapeutic targets. Replacing or inhibiting these miRNA with targeted therapies in patients, prior to or during treatment, could enhance tumour sensitivity to the cytotoxic effects of CRT and improve patient response and prognosis.

In this project, the initial aim was to identify miRNA which were differentially expressed between patients who responded to neo-CRT, and patients who did not respond to neo-CRT. In diagnostic pre-treatment biopsies, miRNA expression arrays identified 67 differentially expressed miRNA between responders and non-responders. These miRNA are potential predictive biomarkers of patient response to neo-CRT. Further validation of these miRNA would be necessary to identify a refined miRNA signature which could be applied in the clinic, to stratify patients prior to neoadjuvant therapy. In a recent study, a miRNA signature predictive of pCR after neo-CRT was identified in OAC patients (Skinner et al., 2014). This study used three patient cohorts (discovery, model and validation) to identify and validate a miRNA signature predictive of a pCR in OAC patients with locally advanced disease. In the discovery cohort patient pre-treatment biopsy samples were profiled, using a similar method to the miRNA array profiling presented here in chapter 3. The 44 most significantly altered miRNA were further validated in the model cohort (Skinner et al., 2014). From the model cohort, the four miRNA indentified as reliable predictive biomarkers of a pCR in patients receiving neo-CRT were tested in the validation cohort. The validated miRNA signature identified patients with a high probability (≥80%) of a pCR following neo-CRT. The miRNA expression profiling presented in chapter 3 could be validated in a study of similar design.

The differentially expressed miRNA between responder and non-responders are either surrogate biomarkers of tumour sensitivity to CRT, or active participants which

promote tumour resistance to CRT. The latter are potential therapeutic targets as well as predictive biomarkers. Understanding the molecular biology and functional roles of individual miRNA is necessary for the development of novel miRNA based therapeutics. Replacing or silencing the miRNA which modulate tumour response to cytotoxic agents, prior to or during neoadjuvant therapy, could enhance tumour sensitivity to treatments and improve patient outcomes.

In addition to identify miRNA which were differentially expressed between responders and non-responders, the aim of this project was to determine the functional significance of specific miRNA as modulators of tumour sensitivity to CRT. Of the 67 differentially expressed miRNA the most downregulated miRNA in the non-responders was miR-330-5p. In chapter 4 the aim was to investigate the role of miR-330-5p as a modulator of cellular sensitivity to CRT *in vitro*. It has previously been reported in prostate cancer that miR-330 acts as a tumour suppressor, by downregulating E2F1 and p-Akt to induce apoptosis (Lee et al., 2009). Although the prostate cancer study only reported on miR-330-3p, there are also predicted binding sites for miR-330-5p in the *E2F1* mRNA (Betel et al., 2008). Furthermore, it is not know which strand of the miR-330 duplex, the -3p or -5p, is the functional mature stand and neither strand is denoted as the degraded passenger strand (Griffiths-Jones, 2010). Therefore, it was hypothesised here that both miR-330-3p and miR-330-5p could directly target the *E2F1* mRNA. In this study, miR-330 overexpression downregulated the expression of the E2F1 protein and the levels of p-Akt in an OAC cell line, thus supporting previous findings reported in prostate cancer. It was hypothesised that the downregulation of the E2F1/p-Akt pathway would promote apoptosis and enhanced cellular sensitivity to CRT (Stegeman et al., 2014). To test this hypothesis cells with miR-330 overexpression were treated with cisplatin, 5-FU or radiation and clonogenicity and viability were measured. Despite the alterations in the E2F1/p-Akt pathway, the overexpression of miR-330 did not alter

cellular sensitivity to cisplatin, 5-FU or radiation. To further investigate the role of miR-330-5p as a modulator of CRT sensitivity, a model of miR-330-5p silencing was established. The *in vitro* model of miR-330-5p silencing mimicked the downregulated expression of the miRNA in the non-responder. The silencing of miR-330-5p was hypothesised to enhance cellular resistance to CRT. To test this hypothesis cells with miR-330-5p silencing were treated with cisplatin, 5-FU or radiation and clonogenicity and viability were measured. The silencing of miR-330-5p did not alter cellular sensitivity to cisplatin and 5-FU but marginally enhanced radioresistance.

In addition to the cancer cell population, the tumour microenvironment also mediates tumour resistance to CRT (Castells et al., 2012). The tumour vasculature is essential for the delivery of systemic chemotherapeutics. The vasculature also influences tumour hypoxia and tumour oxygenation is critical for the generation of ROS (Overgaard, 2007). Post-treatment the cytotoxic damage in the tumour tissue induces an immune response with pro- and anti-tumorigenic consequences (Barker et al., 2015). The tumour microenvironment is equally as important as the response of the cancer cells in determining tumour sensitivity to CRT. In addition to modulating intracellular processes and signalling pathways, miRNA also directly and indirectly modulate the extracellular tumour microenvironment (Suzuki et al., 2015). Numerous miRNA have been reported to modulate angiogenesis, hypoxia, the immune response and extracellular matrix remodelling in the tumour microenvironment (Soon & Kiaris, 2013). Within the cancer cells and the tumour associated stromal cells, miRNA regulate the translation of mRNA transcripts which produce proteins with extracellular functions such as MMPs and cytokines (Suzuki et al., 2015). MiRNA mediated regulation of the tumour microenvironment has implications for tumour response and sensitivity to CRT.

Therefore, it was hypothesised that although miR-330-5p did not alter cellular sensitivity to CRT, miR-330-5p could modulate tumour sensitivity to CRT via regulation of the tumour microenvironment. In chapter 5 this hypothesis was supported by digital gene expression analysis and antibody-based arrays which identified the altered expression of several genes and proteins with extracellular functions. The increase in *MMP1* mRNA and protein expression with miR-330-5p silencing was of particular interest because MMP1 has previously been identified as a prognostic marker in OAC and OSC (Murray et al., 1998; Yamashita et al., 2001). The cancer cells and the tumour associated stromal cells can produce MMP1 which has paracrine and autocrine effects in the tumour microenvironment (Tressel et al., 2011). There may be functional differences in the MMP1 produced by cancer cells and fibroblasts which, is mediated by differential post-translational modifications in the different cell types (Saarinen et al., 1999). *MMP1* is frequently upregulated in cancer and is primarily associated with matrix remodelling, invasion and metastasis (Smith et al., 2008). The upregulated expression of MMP1 *in vitro* did not enhance the invasive potential of the cells in a matrigel based invasion assay. The preferred substrate for MMP1 is collagen, and the invasive potential of the cells with miR-330-5p silencing may be enhanced in a collagen specific invasion assay (Tallant et al., 2010). However, the antibody-based array identified high expression of the TIMP-1 protein which is an MMP1 inhibitor (Groblewska et al., 2012). The upregulated expression of MMP1 may not have been sufficient to overcome TIMP-1 inhibition. Silencing miR-330-5p *in vitro* altered the expression of genes and proteins with extracellular functions. To further investigate miR-330-5p as a modulator of tumour sensitivity to CRT within the context of the tumour microenvironment an *in vivo* model was established. The *in vivo* model encompassed the cancer cells and tumour microenvironment and was a more clinically relevant model. The role of miR-330-5p as a mediator of tumour sensitivity to cisplatin

was investigated in the *in vivo* model. The tumour xenografts established from the cells with miR-330-5p silencing grew at a faster rate than the tumour xenografts established from the vector control cells. The significant increase in MMP1 expression with silencing of miR-330-5p *in vitro* potentially enhanced local tumour invasion *in vivo* and may explain the faster growth rate in these tumours (Yamashita et al., 2001). Furthermore, MMP1 has been reported to induce angiogenesis and promote tumour growth (Foley et al., 2014a). The increase in MMP1 production with miR-330-5p silencing *in vitro* may enhance angiogenesis and the development of tumour vasculature *in vivo*. This may also explain the faster growth rate in the miR-330-5p silencing xenografts compared to the vector control xenografts. In response to cisplatin treatment it was hypothesised that the tumours with miR-330-5p silencing would be more resistance to CRT. Two of the three tumours with miR-330-5p silencing were non-responders and one was a responder. Two of the three vector control tumours were responders and one was a non-responder. Experimental repeats are needed to determine if miR-330-5p silencing alters cisplatin sensitivity *in vivo*. In summary, chapters 4 and 5 investigated the role of miR-330-5p as a modulator of CRT sensitivity. The data presented here cannot discount the possibility that miR-330-5p downregulation is only a passenger, or surrogate marker of sensitivity, and not a driver of tumour sensitivity to CRT.

In this project miR-187 was also chosen for further investigation as it has previously been implicated in cancer tumorigenesis (Zhao et al., 2013; Casanova-Salas et al., 2014). In chapter 6, miR-187 was investigated as a modulator of cellular response to CRT. The expression of miR-187 was downregulated in the neo-CRT non-responders and was hypothesised to enhance tumour resistance to neo-CRT. Interestingly, endogenous miR-187 expression was undetectable in the cell line models. The loss of heterozygosity on chromosome 18 has previously been reported in OAC and may be a

common event during OAC development (Barrett et al., 1999). The transient reintroduction of miR-187 enhanced radiosensitivity in the cell line models. Furthermore, the transient reintroduction of miR-187 induced apoptosis in the OE33 cell line, but not in the SK-GT-4 cell line. Studies are ongoing to determine the mechanism by which miR-187 enhances radiosensitivity. The induction of apoptosis in response to radiation is a possible mechanism by which miR-187 enhances radiosensitivity. The downregulated expression of miR-31, in the neo-CRT non-responders of patient cohort presented in chapter 3, has previously been investigated in our group as a modulator of radiosensitivity (Lynam-Lennon et al., 2012). The downregulated expression of miR-31 enhanced radioresistance and was associated with an increase in several DNA repair genes (Lynam-Lennon et al., 2012). Interestingly, a recent study has shown miR-31 enhances radiosensitivity by inducing radiation-dependent intrinsic apoptosis via a novel mechanism (Kumar et al., 2015). Post-irradiation an increase in miR-31 expression subsequently altered Bim mediated translocation of BAX which induced the release of cytochrome c from the mitochondria (Kumar et al., 2015). These studies support a role for miR-31 as a modulator of radiosensitivity via two independent mechanisms, DNA repair and apoptosis (Lynam-Lennon et al., 2012; Kumar et al., 2015). To identify targets and pathways regulated by miR-187 and further elucidate the mechanism by which miR-187 enhances radiosensitivity, digital gene expression analysis was undertaken. Of the validated targets the downregulation of the *C3* mRNA was of particular interest because the C3a protein has previously been identified as a potential serum biomarker of OAC patient response to neo-CRT (Maher et al., 2011). In the serum of the neo-CRT non-responders the expression of the C3a protein was upregulated (Maher et al., 2011). In support of the patient serum study, the expression of the *C3* mRNA was also upregulated in the tumour biopsies of the non-responders. In addition to the immune regulator C3, the

expressions of other immune-related genes were also altered by miR-187 reintroduction *in vitro*. The KEGG analysis identified 5 downregulated pathways associated with the immune response; chemokine signalling, cytokine-cytokine receptor interaction, antigen processing and presentation, Toll-like receptor signalling and RIG-1-like receptor signalling. The tumour immune response induced by radiation can promote both cell death and cell survival (Barker et al., 2015). The findings presented here suggest miR-187 may mediate radiosensitivity via modulation of the immune response in the tumour microenvironment.

In summary, miRNA expression profiling identified 67 miRNA which were differentially expressed between neo-CRT responders and non-responders. These miRNA are potential predictive biomarkers of patient response to neo-CRT which could, with further validation, constitute a miRNA signature for the stratification of patients in a pre-treatment clinical setting. The differentially expressed miRNA are also potential modulators of tumour response and sensitivity to CRT. In this study miR-330-5p and miR-187 were investigated as modulators of tumour sensitivity in response to cisplatin, 5-FU and radiation (Fig 8.1). There is insufficient evidence to support the hypothesis that miR-330-5p modulates tumour sensitivity to CRT, although further investigations *in vivo* are warranted based on the data presented here. The reintroduction of miR-187 *in vitro* enhanced cellular sensitivity to cisplatin and radiation. The mechanisms and pathways downstream of miR-187, which alter chemosensitivity and radiosensitivity, are to be further investigated.

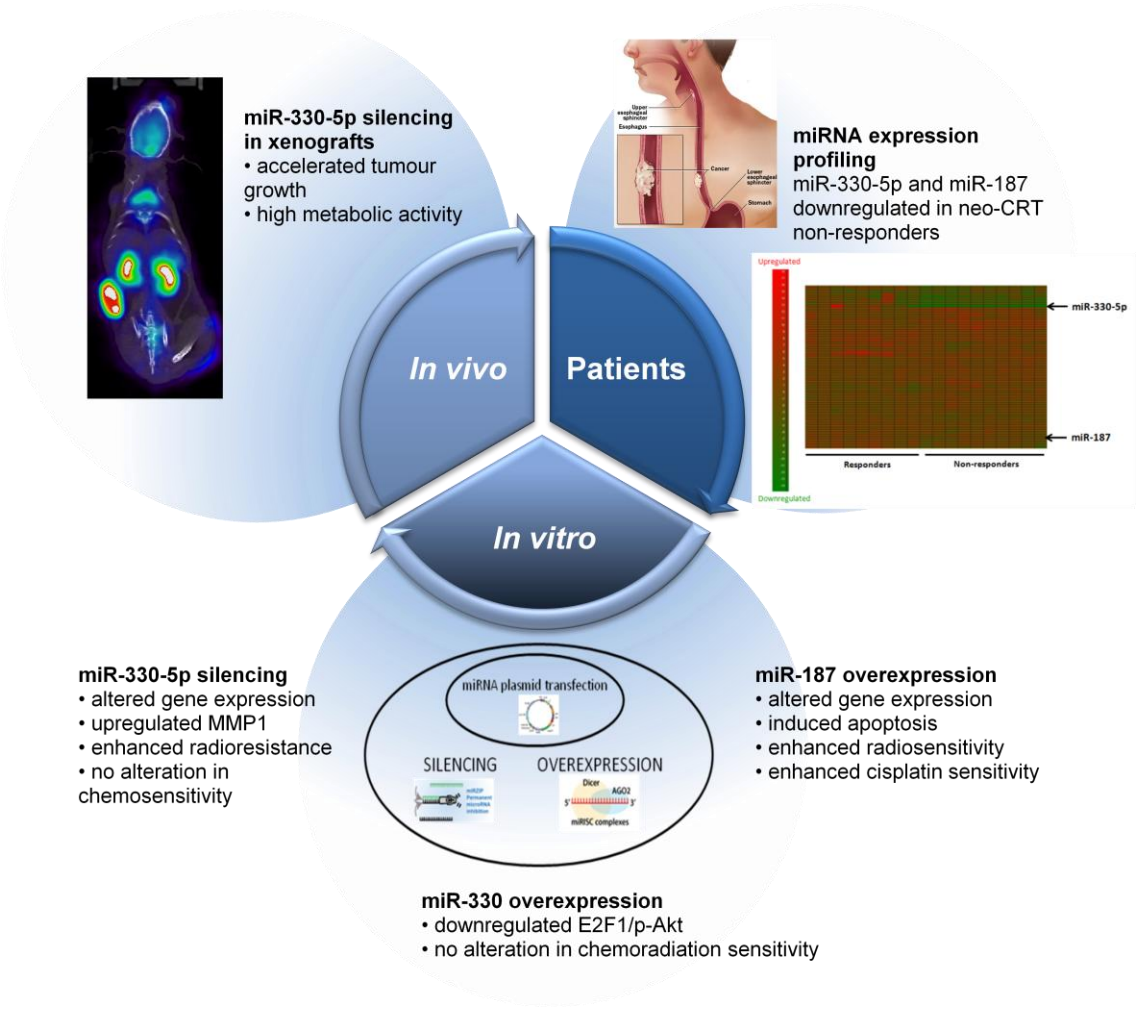

Fig 8.1 Project summary. In this translation research project the aim was firstly, to identify miRNA which were differentially expressed between the diagnostic pre-treatment tumour biopsies of OAC neo-CRT responders and non-responders. The second aim was to investigate selected miRNA, in this study miR-330-5p and miR-187, as modulators of chemoradiation sensitivity using *in vitro* and *in vivo* OAC models. *In vitro*, miRNA expression was manipulated by transfecting OAC cancer cell lines with miRNA overexpression or miRNA silencing vectors. These cell line models were used to assess alterations in cellular sensitivity to chemoradiation therapy with miRNA overexpression or silencing. Furthermore, potential mRNA targets of miR-330-5p and miR-187 were identified using whole genome digital gene expression analysis. *In vivo* tumour xenografts were established from the OE33 miR-330-5p silencing cell model, preliminary data indicated miR-330-5p silencing enhanced tumour growth.

8.2 Future work

The miRNA which were differentially expressed, between the neo-CRT responders and non-responders, are potential clinical biomarkers which could predict patient response to neoadjuvant therapy in a pre-treatment setting. Work is ongoing with an industry partner to develop a miRNA signature for clinical application.

The *in vivo* miR-330-5p tumour model requires further study to determine if miR-330-5p silencing alters tumour sensitivity to cisplatin. The *in vitro* studies indicated miR-330-5p downregulation may enhance radiosensitivity and this should also be investigated the tumour xenograft model. Furthermore, the *in vivo* growth profiles suggested silencing miR-330-5p downregulation may enhance tumour growth and this also warrants further investigation.

In vitro the pathways and targets which are regulated by miR-187 and subsequently enhance radiosensitivity are currently under investigation. The reintroduction of miR-187 may also modulate cellular sensitivity to cisplatin and 5-FU, and this should be tested in other OAC cell lines including the isogenic model of cisplatin resistance. Furthermore, an *in vivo* model should be established to assess reintroduction of miR-187 as a therapeutic radiosensitising agent in OAC tumours.

Bibliography

References

Adams, J. M. & Cory, S. (2007) The Bcl-2 apoptotic switch in cancer development and therapy. *Oncogene*, 26(9), 1324-37.

Aichler, M., Elsner, M., Ludyga, N., Feuchtinger, A., Zangen, V., Maier, S. K., Balluff, B., Schone, C., Hierber, L., Braselmann, H., Meding, S., Rauser, S., Zischka, H., Aubele, M., Schmitt, M., Feith, M., Hauck, S. M., Ueffing, M., Langer, R., Kuster, B., Zitzelsberger, H., Hofler, H. & Walch, A. K. (2013) Clinical response to chemotherapy in oesophageal adenocarcinoma patients is linked to defects in mitochondria. *J Pathol*, 230(4), 410-9.

Albert, J. M., Cao, C., Kim, K. W., Willey, C. D., Geng, L., Xiao, D., Wang, H., Sandler, A., Johnson, D. H., Colevas, A. D., Low, J., Rothenberg, M. L. & Lu, B. (2007) Inhibition of poly(ADP-ribose) polymerase enhances cell death and improves tumor growth delay in irradiated lung cancer models. *Clin Cancer Res*, 13(10), 3033-42.

Alla, V., Engelmann, D., Niemetz, A., Pahnke, J., Schmidt, A., Kunz, M., Emmrich, S., Steder, M., Koczan, D. & Putzer, B. M. (2010) E2F1 in melanoma progression and metastasis. *J Natl Cancer Inst*, 102(2), 127-33.

Allum, W. H., Stenning, S. P., Bancewicz, J., Clark, P. I. & Langley, R. E. (2009) Long-term results of a randomized trial of surgery with or without preoperative chemotherapy in esophageal cancer. *J Clin Oncol*, 27(30), 5062-7.

Ambros, V. & Horvitz, H. R. (1984) Heterochronic mutants of the nematode Caenorhabditis elegans. *Science*, 226(4673), 409-16.

Amin, M. & Lam, A. K. (2015) Current perspectives of mi-RNA in oesophageal adenocarcinoma: Roles in predicting carcinogenesis, progression and values in clinical management. *Exp Mol Pathol*.

Anderson, L. A., Tavilla, A., Brenner, H., Luttmann, S., Navarro, C., Gavin, A. T., Holleczek, B., Johnston, B. T., Cook, M. B., Bannon, F. & Sant, M. (2015) Survival for oesophageal, stomach and small intestine cancers in Europe 1999-2007: results from EUROCARE-5. *Eur J Cancer*.

Apetoh, L., Ghiringhelli, F., Tesniere, A., Obeid, M., Ortiz, C., Criollo, A., Mignot, G., Maiuri, M. C., Ullrich, E., Saulnier, P., Yang, H., Amigorena, S., Ryffel, B., Barrat, F. J., Saftig, P., Levi, F., Lidereau, R., Nogues, C., Mira, J. P., Chompret, A., Joulin, V., Clavel-Chapelon, F., Bourhis, J., Andre, F., Delaloge, S., Tursz, T., Kroemer, G. & Zitvogel, L. (2007) Toll-like receptor 4-dependent contribution of the immune system to anticancer chemotherapy and radiotherapy. *Nat Med*, 13(9), 1050-9.

Arnold, M., Soerjomataram, I., Ferlay, J. & Forman, D. (2015) Global incidence of oesophageal cancer by histological subtype in 2012. *Gut*, 64(3), 381-7.

Bader, A. G. (2012) miR-34 - a microRNA replacement therapy is headed to the clinic. *Front Genet*, 3, 120.

Barker, H. E., Paget, J. T., Khan, A. A. & Harrington, K. J. (2015) The tumour microenvironment after radiotherapy: mechanisms of resistance and recurrence. *Nat Rev Cancer*, 15(7), 409-25.

Barrett, M. T., Sanchez, C. A., Prevo, L. J., Wong, D. J., Galipeau, P. C., Paulson, T. G., Rabinovitch, P. S. & Reid, B. J. (1999) Evolution of neoplastic cell lineages in Barrett oesophagus. *Nat Genet*, 22(1), 106-9.

Bartel, D. P. (2004) MicroRNAs: genomics, biogenesis, mechanism, and function. *Cell*, 116(2), 281-97.

Bassing, C. H. & Alt, F. W. (2004) The cellular response to general and programmed DNA double strand breaks. *DNA Repair (Amst)*, 3(8-9), 781-96.

Begg, A. C., Stewart, F. A. & Vens, C. (2011) Strategies to improve radiotherapy with targeted drugs. *Nat Rev Cancer*, 11(4), 239-53.

Berindan-Neagoe, I., Monroig Pdel, C., Pasculli, B. & Calin, G. A. (2014) MicroRNAome genome: a treasure for cancer diagnosis and therapy. *CA Cancer J Clin*, 64(5), 311-36.

Betel, D., Wilson, M., Gabow, A., Marks, D. S. & Sander, C. (2008) The microRNA.org resource: targets and expression. *Nucleic Acids Res*, 36(Database issue), D149-53.

Bhat, S. K., McManus, D. T., Coleman, H. G., Johnston, B. T., Cardwell, C. R., McMenamin, U., Bannon, F., Hicks, B., Kennedy, G., Gavin, A. T. & Murray, L. J. (2015) Oesophageal

adenocarcinoma and prior diagnosis of Barrett's oesophagus: a population-based study. *Gut*, 64(1), 20-5.

Bhattacharyya, S. N., Habermacher, R., Martine, U., Closs, E. I. & Filipowicz, W. (2006) Relief of microRNA-mediated translational repression in human cells subjected to stress. *Cell*, 125(6), 1111-24.

Bhome, R., Bullock, M. D., Al Saihati, H. A., Goh, R. W., Primrose, J. N., Sayan, A. E. & Mirnezami, A. H. (2015) A top-down view of the tumor microenvironment: structure, cells and signaling. *Front Cell Dev Biol*, 3, 33.

Blasco, M. A. (2005) Telomeres and human disease: ageing, cancer and beyond. *Nat Rev Genet*, 6(8), 611-22.

Blevins, C. H. & Iyer, P. G. (2015) Endoscopic therapy for Barrett's oesophagus. *Best Pract Res Clin Gastroenterol*, 29(1), 167-77.

Bohnsack, M. T., Czaplinski, K. & Gorlich, D. (2004) Exportin 5 is a RanGTP-dependent dsRNA-binding protein that mediates nuclear export of pre-miRNAs. *RNA*, 10(2), 185-91.

Bolderson, E., Richard, D. J., Zhou, B. B. & Khanna, K. K. (2009) Recent advances in cancer therapy targeting proteins involved in DNA double-strand break repair. *Clin Cancer Res*, 15(20), 6314-20.

Bollschweiler, E., Holscher, A. H., Schmidt, M. & Warnecke-Eberz, U. (2015) Neoadjuvant treatment for advanced esophageal cancer: response assessment before surgery and how to predict response to chemoradiation before starting treatment. *Chin J Cancer Res*, 27(3), 221-30.

Bonner, J. A., Harari, P. M., Giralt, J., Cohen, R. B., Jones, C. U., Sur, R. K., Raben, D., Baselga, J., Spencer, S. A., Zhu, J., Youssoufian, H., Rowinsky, E. K. & Ang, K. K. (2010) Radiotherapy plus cetuximab for locoregionally advanced head and neck cancer: 5-year survival data from a phase 3 randomised trial, and relation between cetuximab-induced rash and survival. *Lancet Oncol*, 11(1), 21-8.

Borchert, G. M., Lanier, W. & Davidson, B. L. (2006) RNA polymerase III transcribes human microRNAs. *Nat Struct Mol Biol*, 13(12), 1097-101.

Borst, P., Evers, R., Kool, M. & Wijnholds, J. (2000) A family of drug transporters: the multidrug resistance-associated proteins. *J Natl Cancer Inst*, 92(16), 1295-302.

Botterweck, A. A., Schouten, L. J., Volovics, A., Dorant, E. & van Den Brandt, P. A. (2000) Trends in incidence of adenocarcinoma of the oesophagus and gastric cardia in ten European countries. *Int J Epidemiol*, 29(4), 645-54.

Brengues, M., Teixeira, D. & Parker, R. (2005) Movement of eukaryotic mRNAs between polysomes and cytoplasmic processing bodies. *Science*, 310(5747), 486-9.

Bunting, D. M., Lai, W. W., Berrisford, R. G., Wheatley, T. J., Drake, B. & Sanders, G. (2015) Positron emission tomography-computed tomography in oesophageal cancer staging: a tailored approach. *World J Surg*, 39(4), 1000-7.

Burmeister, B. H., Thomas, J. M., Burmeister, E. A., Walpole, E. T., Harvey, J. A., Thomson, D. B., Barbour, A. P., Gotley, D. C. & Smithers, B. M. (2011) Is concurrent radiation therapy required in patients receiving preoperative chemotherapy for adenocarcinoma of the oesophagus? A randomised phase II trial. *Eur J Cancer*, 47(3), 354-60.

Cahill, D., Connor, B. & Carney, J. P. (2006) Mechanisms of eukaryotic DNA double strand break repair. *Front Biosci*, 11, 1958-76.

Calin, G. A., Dumitru, C. D., Shimizu, M., Bichi, R., Zupo, S., Noch, E., Aldler, H., Rattan, S., Keating, M., Rai, K., Rassenti, L., Kipps, T., Negrini, M., Bullrich, F. & Croce, C. M. (2002) Frequent deletions and down-regulation of micro- RNA genes miR15 and miR16 at 13q14 in chronic lymphocytic leukemia. *Proc Natl Acad Sci U S A*, 99(24), 15524-9.

Calin, G. A., Sevignani, C., Dumitru, C. D., Hyslop, T., Noch, E., Yendamuri, S., Shimizu, M., Rattan, S., Bullrich, F., Negrini, M. & Croce, C. M. (2004) Human microRNA genes are frequently located at fragile sites and genomic regions involved in cancers. *Proc Natl Acad Sci U S A*, 101(9), 2999-3004.

Campbell, N. P. & Villaflor, V. M. (2010) Neoadjuvant treatment of esophageal cancer. *World J Gastroenterol*, 16(30), 3793-803.

Casanova-Salas, I., Masia, E., Arminan, A., Calatrava, A., Mancarella, C., Rubio-Briones, J., Scotlandi, K., Vicent, M. J. & Lopez-Guerrero, J. A. (2015) MiR-187 Targets the Androgen-Regulated Gene ALDH1A3 in Prostate Cancer. *PLoS One*, 10(5), e0125576.

Casanova-Salas, I., Rubio-Briones, J., Calatrava, A., Mancarella, C., Masia, E., Casanova, J., Fernandez-Serra, A., Rubio, L., Ramirez-Backhaus, M., Arminan, A., Dominguez-Escrig, J.,

Martinez, F., Garcia-Casado, Z., Scotlandi, K., Vicent, M. J. & Lopez-Guerrero, J. A. (2014) Identification of miR-187 and miR-182 as biomarkers of early diagnosis and prognosis in patients with prostate cancer treated with radical prostatectomy. *J Urol*, 192(1), 252-9.

Castells, M., Thibault, B., Delord, J. P. & Couderc, B. (2012) Implication of tumor microenvironment in chemoresistance: tumor-associated stromal cells protect tumor cells from cell death. *Int J Mol Sci*, 13(8), 9545-71.

Castro, C., Bosetti, C., Malvezzi, M., Bertuccio, P., Levi, F., Negri, E., La Vecchia, C. & Lunet, N. (2014) Patterns and trends in esophageal cancer mortality and incidence in Europe (1980-2011) and predictions to 2015. *Ann Oncol*, 25(1), 283-90.

Chan, J. A., Krichevsky, A. M. & Kosik, K. S. (2005) MicroRNA-21 is an antiapoptotic factor in human glioblastoma cells. *Cancer Res*, 65(14), 6029-33.

Chan, K. K., Zhang, Q. M. & Dianov, G. L. (2006) Base excision repair fidelity in normal and cancer cells. *Mutagenesis*, 21(3), 173-8.

Chao, A., Lai, C. H., Chen, H. C., Lin, C. Y., Tsai, C. L., Tang, Y. H., Huang, H. J., Lin, C. T., Chen, M. Y., Huang, K. G., Chou, H. H., Chang, T. C., Chen, S. J. & Wang, T. H. (2014) Serum microRNAs in clear cell carcinoma of the ovary. *Taiwan J Obstet Gynecol*, 53(4), 536-41.

Chao, A., Lin, C. Y., Lee, Y. S., Tsai, C. L., Wei, P. C., Hsueh, S., Wu, T. I., Tsai, C. N., Wang, C. J., Chao, A. S., Wang, T. H. & Lai, C. H. (2012) Regulation of ovarian cancer progression by microRNA-187 through targeting Disabled homolog-2. *Oncogene*, 31(6), 764-75.

Chau, Q. & Stewart, D. J. (1999) Cisplatin efflux, binding and intracellular pH in the HTB56 human lung adenocarcinoma cell line and the E-8/0.7 cisplatin-resistant variant. *Cancer Chemother Pharmacol*, 44(3), 193-202.

Chaussepied, M. & Ginsberg, D. (2004) Transcriptional regulation of AKT activation by E2F. *Mol Cell*, 16(5), 831-7.

Chen, J., Wang, T., Zhou, Y. C., Gao, F., Zhang, Z. H., Xu, H., Wang, S. L. & Shen, L. Z. (2014) Aquaporin 3 promotes epithelial-mesenchymal transition in gastric cancer. *J Exp Clin Cancer Res*, 33, 38.

Chen, Q., Zhuang, H. & Liu, Y. (2012) The association between obesity factor and esophageal caner. *J Gastrointest Oncol*, 3(3), 226-31.

Chen, Y. M., Pan, X. F., Tong, L. J., Shi, Y. P. & Chen, T. (2011) Can (1)(8)F-fluorodeoxyglucose positron emission tomography predict responses to neoadjuvant therapy in oesophageal cancer patients? A meta-analysis. *Nucl Med Commun*, 32(11), 1005-10.

Chendrimada, T. P., Finn, K. J., Ji, X., Baillat, D., Gregory, R. I., Liebhaber, S. A., Pasquinelli, A. E. & Shiekhattar, R. (2007) MicroRNA silencing through RISC recruitment of eIF6. *Nature*, 447(7146), 823-8.

Cheng, N., Chytil, A., Shyr, Y., Joly, A. & Moses, H. L. (2008) Transforming growth factor-beta signaling-deficient fibroblasts enhance hepatocyte growth factor signaling in mammary carcinoma cells to promote scattering and invasion. *Mol Cancer Res*, 6(10), 1521-33.

Cho, R. W. & Clarke, M. F. (2008) Recent advances in cancer stem cells. *Curr Opin Genet Dev*, 18(1), 48-53.

Choi, A. H., Kim, J. & Chao, J. (2015) Perioperative chemotherapy for resectable gastric cancer: MAGIC and beyond. *World J Gastroenterol*, 21(24), 7343-8.

Chou, J., Shahi, P. & Werb, Z. (2013) microRNA-mediated regulation of the tumor microenvironment. *Cell Cycle*, 12(20), 3262-71.

Cimmino, A., Calin, G. A., Fabbri, M., Iorio, M. V., Ferracin, M., Shimizu, M., Wojcik, S. E., Aqeilan, R. I., Zupo, S., Dono, M., Rassenti, L., Alder, H., Volinia, S., Liu, C. G., Kipps, T. J., Negrini, M. & Croce, C. M. (2005) miR-15 and miR-16 induce apoptosis by targeting BCL2. *Proc Natl Acad Sci U S A*, 102(39), 13944-9.

Corley, D. A., Levin, T. R., Habel, L. A., Weiss, N. S. & Buffler, P. A. (2002) Surveillance and survival in Barrett's adenocarcinomas: a population-based study. *Gastroenterology*, 122(3), 633-40.

Coron, E. (2013) [In process citation]. *Endoscopy*, 45(7), 684-5.

Coron, E., Robaszkiewicz, M., Chatelain, D., Svrcek, M. & Flejou, J. F. (2013) Advanced precancerous lesions in the lower oesophageal mucosa: high-grade dysplasia and intramucosal carcinoma in Barrett's oesophagus. *Best Pract Res Clin Gastroenterol*, 27(2), 187-204.

Cortez, M. A., Bueso-Ramos, C., Ferdin, J., Lopez-Berestein, G., Sood, A. K. & Calin, G. A. (2011) MicroRNAs in body fluids--the mix of hormones and biomarkers. *Nat Rev Clin Oncol*, 8(8), 467-77.

Cortez, M. A., Valdecanas, D., Zhang, X., Zhan, Y., Bhardwaj, V., Calin, G. A., Komaki, R., Giri, D. K., Quini, C. C., Wolfe, T., Peltier, H. J., Bader, A. G., Heymach, J. V., Meyn, R. E. & Welsh, J. W. (2014) Therapeutic delivery of miR-200c enhances radiosensitivity in lung cancer. *Mol Ther*, 22(8), 1494-503.

Courrech Staal, E. F., Aleman, B. M., Boot, H., van Velthuysen, M. L., van Tinteren, H. & van Sandick, J. W. (2010) Systematic review of the benefits and risks of neoadjuvant chemoradiation for oesophageal cancer. *Br J Surg*, 97(10), 1482-96.

Cronin-Fenton, D. P., Murray, L. J., Whiteman, D. C., Cardwell, C., Webb, P. M., Jordan, S. J., Corley, D. A., Sharp, L. & Lagergren, J. (2010) Reproductive and sex hormonal factors and oesophageal and gastric junction adenocarcinoma: a pooled analysis. *Eur J Cancer*, 46(11), 2067-76.

Cunningham, D., Allum, W. H., Stenning, S. P., Thompson, J. N., Van de Velde, C. J., Nicolson, M., Scarffe, J. H., Lofts, F. J., Falk, S. J., Iveson, T. J., Smith, D. B., Langley, R. E., Verma, M., Weeden, S., Chua, Y. J. & Participants, M. T. (2006) Perioperative chemotherapy versus surgery alone for resectable gastroesophageal cancer. *N Engl J Med*, 355(1), 11-20.

Curto, M., Cole, B. K., Lallemand, D., Liu, C. H. & McClatchey, A. I. (2007) Contact-dependent inhibition of EGFR signaling by Nf2/Merlin. *J Cell Biol*, 177(5), 893-903.

D'Incalci, M., Citti, L., Taverna, P. & Catapano, C. V. (1988) Importance of the DNA repair enzyme O6-alkyl guanine alkyltransferase (AT) in cancer chemotherapy. *Cancer Treat Rev*, 15(4), 279-92.

Dai, T. & Shah, M. A. (2015) Chemoradiation in oesophageal cancer. *Best Pract Res Clin Gastroenterol*, 29(1), 193-209.

DeBerardinis, R. J., Lum, J. J., Hatzivassiliou, G. & Thompson, C. B. (2008) The biology of cancer: metabolic reprogramming fuels cell growth and proliferation. *Cell Metab*, 7(1), 11-20.

Delaney, G., Jacob, S., Featherstone, C. & Barton, M. (2005) The role of radiotherapy in cancer treatment: estimating optimal utilization from a review of evidence-based clinical guidelines. *Cancer*, 104(6), 1129-37.

DeNardo, D. G., Andreu, P. & Coussens, L. M. (2010) Interactions between lymphocytes and myeloid cells regulate pro- versus anti-tumor immunity. *Cancer Metastasis Rev*, 29(2), 309-16.

Derouet, M. F., Liu, G. & Darling, G. E. (2014) MiR-145 expression accelerates esophageal adenocarcinoma progression by enhancing cell invasion and anoikis resistance. *PLoS One*, 9(12), e115589.

Desvignes, T., Batzel, P., Berezikov, E., Eilbeck, K., Eppig, J. T., McAndrews, M. S., Singer, A. & Postlethwait, J. H. (2015) miRNA Nomenclature: A View Incorporating Genetic Origins, Biosynthetic Pathways, and Sequence Variants. *Trends Genet*.

Djuranovic, S., Nahvi, A. & Green, R. (2012) miRNA-mediated gene silencing by translational repression followed by mRNA deadenylation and decay. *Science*, 336(6078), 237-40.

Domper Arnal, M. J., Ferrandez Arenas, A. & Lanas Arbeloa, A. (2015) Esophageal cancer: Risk factors, screening and endoscopic treatment in Western and Eastern countries. *World J Gastroenterol*, 21(26), 7933-43.

Donaldson, K. L., Goolsby, G. L. & Wahl, A. F. (1994) Cytotoxicity of the anticancer agents cisplatin and taxol during cell proliferation and the cell cycle. *Int J Cancer*, 57(6), 847-55.

Dunkelberger, J. R. & Song, W. C. (2010) Complement and its role in innate and adaptive immune responses. *Cell Res*, 20(1), 34-50.

Eastman, A. (1987) The formation, isolation and characterization of DNA adducts produced by anticancer platinum complexes. *Pharmacol Ther*, 34(2), 155-66.

Edgren, G., Adami, H. O., Weiderpass, E. & Nyren, O. (2013) A global assessment of the oesophageal adenocarcinoma epidemic. *Gut*.

El-Serag, H. B. (2007) Time trends of gastroesophageal reflux disease: a systematic review. *Clin Gastroenterol Hepatol*, 5(1), 17-26.

El-Serag, H. B., Naik, A. D., Duan, Z., Shakhatreh, M., Helm, A., Pathak, A., Hinojosa-Lindsey, M., Hou, J., Nguyen, T., Chen, J. & Kramer, J. R. (2015) Surveillance endoscopy is

associated with improved outcomes of oesophageal adenocarcinoma detected in patients with Barrett's oesophagus. *Gut*.

Enzinger, P. C. & Ilson, D. H. (2000) Irinotecan in esophageal cancer. *Oncology (Williston Park)*, 14(12 Suppl 14), 26-30.

Epping, M. T. & Bernards, R. (2006) A causal role for the human tumor antigen preferentially expressed antigen of melanoma in cancer. *Cancer Res*, 66(22), 10639-42.

Epping, M. T., Wang, L., Edel, M. J., Carlee, L., Hernandez, M. & Bernards, R. (2005) The human tumor antigen PRAME is a dominant repressor of retinoic acid receptor signaling. *Cell*, 122(6), 835-47.

Esquela-Kerscher, A. & Slack, F. J. (2006) Oncomirs - microRNAs with a role in cancer. *Nat Rev Cancer*, 6(4), 259-69.

Farazi, T. A., Hoell, J. I., Morozov, P. & Tuschl, T. (2013) MicroRNAs in human cancer. *Adv Exp Med Biol*, 774, 1-20.

Fassan, M., Volinia, S., Palatini, J., Pizzi, M., Baffa, R., De Bernard, M., Battaglia, G., Parente, P., Croce, C. M., Zaninotto, G., Ancona, E. & Rugge, M. (2011) MicroRNA expression profiling in human Barrett's carcinogenesis. *Int J Cancer*, 129(7), 1661-70.

Feber, A., Xi, L., Pennathur, A., Gooding, W. E., Bandla, S., Wu, M., Luketich, J. D., Godfrey, T. E. & Litle, V. R. (2011) MicroRNA prognostic signature for nodal metastases and survival in esophageal adenocarcinoma. *Ann Thorac Surg*, 91(5), 1523-30.

Feng, F. Y., Lopez, C. A., Normolle, D. P., Varambally, S., Li, X., Chun, P. Y., Davis, M. A., Lawrence, T. S. & Nyati, M. K. (2007) Effect of epidermal growth factor receptor inhibitor class in the treatment of head and neck cancer with concurrent radiochemotherapy in vivo. *Clin Cancer Res*, 13(8), 2512-8.

Feng, X., Wang, Z., Fillmore, R. & Xi, Y. (2014) MiR-200, a new star miRNA in human cancer. *Cancer Lett*, 344(2), 166-73.

Ferlay, J., Soerjomataram, I., Dikshit, R., Eser, S., Mathers, C., Rebelo, M., Parkin, D. M., Forman, D. & Bray, F. (2015) Cancer incidence and mortality worldwide: sources, methods and major patterns in GLOBOCAN 2012. *Int J Cancer*, 136(5), E359-86.

Ferrara, N. (2009) Vascular endothelial growth factor. *Arterioscler Thromb Vasc Biol*, 29(6), 789-91.

Figueiredo, D. L., Mamede, R. C., Proto-Siqueira, R., Neder, L., Silva, W. A., Jr. & Zago, M. A. (2006) Expression of cancer testis antigens in head and neck squamous cell carcinomas. *Head Neck*, 28(7), 614-9.

Filipowicz, W., Bhattacharyya, S. N. & Sonenberg, N. (2008) Mechanisms of post-transcriptional regulation by microRNAs: are the answers in sight? *Nat Rev Genet*, 9(2), 102-14.

Fischbach, L. A., Nordenstedt, H., Kramer, J. R., Gandhi, S., Dick-Onuoha, S., Lewis, A. & El-Serag, H. B. (2012) The association between Barrett's esophagus and Helicobacter pylori infection: a meta-analysis. *Helicobacter*, 17(3), 163-75.

Foley, C. J., Fanjul-Fernandez, M., Bohm, A., Nguyen, N., Agarwal, A., Austin, K., Koukos, G., Covic, L., Lopez-Otin, C. & Kuliopulos, A. (2014a) Matrix metalloprotease 1a deficiency suppresses tumor growth and angiogenesis. *Oncogene*, 33(17), 2264-72.

Foley, K. G., Lewis, W. G., Fielding, P., Karran, A., Chan, D., Blake, P. & Roberts, S. A. (2014b) N-staging of oesophageal and junctional carcinoma: is there still a role for EUS in patients staged N0 at PET/CT? *Clin Radiol*, 69(9), 959-64.

Franken, N. A., Rodermond, H. M., Stap, J., Haveman, J. & van Bree, C. (2006) Clonogenic assay of cells in vitro. *Nat Protoc*, 1(5), 2315-9.

Frankowski, H., Gu, Y. H., Heo, J. H., Milner, R. & Del Zoppo, G. J. (2012) Use of gel zymography to examine matrix metalloproteinase (gelatinase) expression in brain tissue or in primary glial cultures. *Methods Mol Biol*, 814, 221-33.

Fridman, R., Benton, G., Aranoutova, I., Kleinman, H. K. & Bonfil, R. D. (2012) Increased initiation and growth of tumor cell lines, cancer stem cells and biopsy material in mice using basement membrane matrix protein (Cultrex or Matrigel) co-injection. *Nat Protoc*, 7(6), 1138-44.

Friedman, R. C., Farh, K. K., Burge, C. B. & Bartel, D. P. (2009) Most mammalian mRNAs are conserved targets of microRNAs. *Genome Res*, 19(1), 92-105.

Fu, Z., Chen, D., Cheng, H. & Wang, F. (2015) Hypoxia-inducible factor-1alpha protects cervical carcinoma cells from apoptosis induced by radiation via modulation of vascular endothelial growth factor and p53 under hypoxia. *Med Sci Monit*, 21, 318-25.

Fuse, M., Kojima, S., Enokida, H., Chiyomaru, T., Yoshino, H., Nohata, N., Kinoshita, T., Sakamoto, S., Naya, Y., Nakagawa, M., Ichikawa, T. & Seki, N. (2012) Tumor suppressive microRNAs (miR-222 and miR-31) regulate molecular pathways based on microRNA expression signature in prostate cancer. *J Hum Genet*, 57(11), 691-9.

Galindo-Moreno, J., Iurlaro, R., El Mjiyad, N., Diez-Perez, J., Gabaldon, T. & Munoz-Pinedo, C. (2014) Apolipoprotein L2 contains a BH3-like domain but it does not behave as a BH3-only protein. *Cell Death Dis*, 5, e1275.

Gebert, L. F., Rebhan, M. A., Crivelli, S. E., Denzler, R., Stoffel, M. & Hall, J. (2014) Miravirsen (SPC3649) can inhibit the biogenesis of miR-122. *Nucleic Acids Res*, 42(1), 609-21.

Geh, J. I., Bond, S. J., Bentzen, S. M. & Glynne-Jones, R. (2006) Systematic overview of preoperative (neoadjuvant) chemoradiotherapy trials in oesophageal cancer: evidence of a radiation and chemotherapy dose response. *Radiother Oncol*, 78(3), 236-44.

Gerlinger, M., Rowan, A. J., Horswell, S., Larkin, J., Endesfelder, D., Gronroos, E., Martinez, P., Matthews, N., Stewart, A., Tarpey, P., Varela, I., Phillimore, B., Begum, S., McDonald, N. Q., Butler, A., Jones, D., Raine, K., Latimer, C., Santos, C. R., Nohadani, M., Eklund, A. C., Spencer-Dene, B., Clark, G., Pickering, L., Stamp, G., Gore, M., Szallasi, Z., Downward, J., Futreal, P. A. & Swanton, C. (2012) Intratumor heterogeneity and branched evolution revealed by multiregion sequencing. *N Engl J Med*, 366(10), 883-92.

Gerson, S. L. (2004) MGMT: its role in cancer aetiology and cancer therapeutics. *Nat Rev Cancer*, 4(4), 296-307.

Gilad, S., Meiri, E., Yogev, Y., Benjamin, S., Lebanony, D., Yerushalmi, N., Benjamin, H., Kushnir, M., Cholakh, H., Melamed, N., Bentwich, Z., Hod, M., Goren, Y. & Chajut, A. (2008) Serum microRNAs are promising novel biomarkers. *PLoS One*, 3(9), e3148.

Gilbert, E. W., Luna, R. A., Harrison, V. L. & Hunter, J. G. (2011) Barrett's esophagus: a review of the literature. *J Gastrointest Surg*, 15(5), 708-18.

Good, J. S. & Harrington, K. J. (2013) The hallmarks of cancer and the radiation oncologist: updating the 5Rs of radiobiology. *Clin Oncol (R Coll Radiol)*, 25(10), 569-77.

Gray, S. (2015) *Epigenetic Cancer Therapy*Elsevier Science.

Greaves, M. & Maley, C. C. (2012) Clonal evolution in cancer. *Nature*, 481(7381), 306-13.

Griffiths-Jones, S. (2010) miRBase: microRNA sequences and annotation. *Curr Protoc Bioinformatics*, Chapter 12, Unit 12 9 1-10.

Grimm, D. (2009) Small silencing RNAs: state-of-the-art. *Adv Drug Deliv Rev*, 61(9), 672-703.

Grimm, M., Lazariotou, M., Kircher, S., Stuermer, L., Reiber, C., Hofelmayr, A., Gattenlohner, S., Otto, C., Germer, C. T. & von Rahden, B. H. (2010) MMP-1 is a (pre-)invasive factor in Barrett-associated esophageal adenocarcinomas and is associated with positive lymph node status. *J Transl Med*, 8, 99.

Grimson, A., Farh, K. K., Johnston, W. K., Garrett-Engele, P., Lim, L. P. & Bartel, D. P. (2007) MicroRNA targeting specificity in mammals: determinants beyond seed pairing. *Mol Cell*, 27(1), 91-105.

Groblewska, M., Siewko, M., Mroczko, B. & Szmitkowski, M. (2012) The role of matrix metalloproteinases (MMPs) and their inhibitors (TIMPs) in the development of esophageal cancer. *Folia Histochem Cytobiol*, 50(1), 12-9.

Guaragnella, N., Giannattasio, S. & Moro, L. (2014) Mitochondrial dysfunction in cancer chemoresistance. *Biochem Pharmacol*, 92(1), 62-72.

Guo, H., Ingolia, N. T., Weissman, J. S. & Bartel, D. P. (2010) Mammalian microRNAs predominantly act to decrease target mRNA levels. *Nature*, 466(7308), 835-40.

Gwynne, S., Falk, S., Gollins, S., Wills, L., Bateman, A., Cummins, S., Grabsch, H., Hawkins, M. A., Maggs, R., Mukherjee, S., Radhakrishna, G., Roy, R., Sharma, R. A., Spezi, E. & Crosby, T. (2013) Oesophageal Chemoradiotherapy in the UK--current practice and future directions. *Clin Oncol (R Coll Radiol)*, 25(6), 368-77.

Habibollahi, P., Figueiredo, J. L., Heidari, P., Dulak, A. M., Imamura, Y., Bass, A. J., Ogino, S., Chan, A. T. & Mahmood, U. (2012) Optical Imaging with a Cathepsin B Activated Probe for the Enhanced Detection of Esophageal Adenocarcinoma by Dual Channel Fluorescent Upper GI Endoscopy. *Theranostics*, 2(2), 227-34.

Haidry, R. J., Butt, M. A., Dunn, J. M., Gupta, A., Lipman, G., Smart, H. L., Bhandari, P., Smith, L., Willert, R., Fullarton, G., Di Pietro, M., Gordon, C., Penman, I., Barr, H., Patel, P., Kapoor, N., Hoare, J., Narayanasamy, R., Ang, Y., Veitch, A., Ragunath, K., Novelli, M. & Lovat, L. B. (2015) Improvement over time in outcomes for patients undergoing endoscopic therapy for Barrett's oesophagus-related neoplasia: 6-year experience from the first 500 patients treated in the UK patient registry. *Gut*, 64(8), 1192-9.

Hamano, R., Miyata, H., Yamasaki, M., Kurokawa, Y., Hara, J., Moon, J. H., Nakajima, K., Takiguchi, S., Fujiwara, Y., Mori, M. & Doki, Y. (2011) Overexpression of miR-200c induces chemoresistance in esophageal cancers mediated through activation of the Akt signaling pathway. *Clin Cancer Res*, 17(9), 3029-38.

Han, J., Lee, Y., Yeom, K. H., Kim, Y. K., Jin, H. & Kim, V. N. (2004) The Drosha-DGCR8 complex in primary microRNA processing. *Genes Dev*, 18(24), 3016-27.

Hanahan, D. & Folkman, J. (1996) Patterns and emerging mechanisms of the angiogenic switch during tumorigenesis. *Cell*, 86(3), 353-64.

Hanahan, D. & Weinberg, R. A. (2000) The hallmarks of cancer. *Cell*, 100(1), 57-70.

Hanahan, D. & Weinberg, R. A. (2011) Hallmarks of cancer: the next generation. *Cell*, 144(5), 646-74.

Hanawalt, P. C. (2002) Subpathways of nucleotide excision repair and their regulation. *Oncogene*, 21(58), 8949-56.

Hardee, M. E., Dewhirst, M. W., Agarwal, N. & Sorg, B. S. (2009) Novel imaging provides new insights into mechanisms of oxygen transport in tumors. *Curr Mol Med*, 9(4), 435-41.

He, L., Thomson, J. M., Hemann, M. T., Hernando-Monge, E., Mu, D., Goodson, S., Powers, S., Cordon-Cardo, C., Lowe, S. W., Hannon, G. J. & Hammond, S. M. (2005) A microRNA polycistron as a potential human oncogene. *Nature*, 435(7043), 828-33.

Helleday, T., Petermann, E., Lundin, C., Hodgson, B. & Sharma, R. A. (2008) DNA repair pathways as targets for cancer therapy. *Nat Rev Cancer*, 8(3), 193-204.

Helwak, A., Kudla, G., Dudnakova, T. & Tollervey, D. (2013) Mapping the human miRNA interactome by CLASH reveals frequent noncanonical binding. *Cell*, 153(3), 654-65.

Hickson, I., Zhao, Y., Richardson, C. J., Green, S. J., Martin, N. M., Orr, A. I., Reaper, P. M., Jackson, S. P., Curtin, N. J. & Smith, G. C. (2004) Identification and characterization of a novel and specific inhibitor of the ataxia-telangiectasia mutated kinase ATM. *Cancer Res*, 64(24), 9152-9.

Horiuchi, S., Yamamoto, H., Min, Y., Adachi, Y., Itoh, F. & Imai, K. (2003) Association of ets-related transcriptional factor E1AF expression with tumour progression and overexpression of MMP-1 and matrilysin in human colorectal cancer. *J Pathol*, 200(5), 568-76.

Horvitz, H. R. & Sulston, J. E. (1980) Isolation and genetic characterization of cell-lineage mutants of the nematode Caenorhabditis elegans. *Genetics*, 96(2), 435-54.

Hu, Y., Correa, A. M., Hoque, A., Guan, B., Ye, F., Huang, J., Swisher, S. G., Wu, T. T., Ajani, J. A. & Xu, X. C. (2011) Prognostic significance of differentially expressed miRNAs in esophageal cancer. *Int J Cancer*, 128(1), 132-43.

Huang, S., Li, X. Q., Chen, X., Che, S. M., Chen, W. & Zhang, X. Z. (2013) Inhibition of microRNA-21 increases radiosensitivity of esophageal cancer cells through phosphatase and tensin homolog deleted on chromosome 10 activation. *Dis Esophagus*, 26(8), 823-31.

Hughes, S. J., Glover, T. W., Zhu, X. X., Kuick, R., Thoraval, D., Orringer, M. B., Beer, D. G. & Hanash, S. (1998) A novel amplicon at 8p22-23 results in overexpression of cathepsin B in esophageal adenocarcinoma. *Proc Natl Acad Sci U S A*, 95(21), 12410-5.

Hummel, R., Hussey, D. J. & Haier, J. (2010) MicroRNAs: predictors and modifiers of chemo- and radiotherapy in different tumour types. *Eur J Cancer*, 46(2), 298-311.

Hummel, R., Hussey, D. J., Michael, M. Z., Haier, J., Bruewer, M., Senninger, N. & Watson, D. I. (2011a) MiRNAs and their association with locoregional staging and survival following surgery for esophageal carcinoma. *Ann Surg Oncol*, 18(1), 253-60.

Hummel, R., Sie, C., Watson, D. I., Wang, T., Ansar, A., Michael, M. Z., Van der Hoek, M., Haier, J. & Hussey, D. J. (2014) MicroRNA signatures in chemotherapy resistant esophageal cancer cell lines. *World J Gastroenterol*, 20(40), 14904-12.

Hummel, R., Watson, D. I., Smith, C., Kist, J., Michael, M. Z., Haier, J. & Hussey, D. J. (2011b) Mir-148a improves response to chemotherapy in sensitive and resistant oesophageal adenocarcinoma and squamous cell carcinoma cells. *J Gastrointest Surg*, 15(3), 429-38.

Hvid-Jensen, F., Pedersen, L., Drewes, A. M., Sorensen, H. T. & Funch-Jensen, P. (2011) Incidence of adenocarcinoma among patients with Barrett's esophagus. *N Engl J Med*, 365(15), 1375-83.

Ikeda, H., Lethe, B., Lehmann, F., van Baren, N., Baurain, J. F., de Smet, C., Chambost, H., Vitale, M., Moretta, A., Boon, T. & Coulie, P. G. (1997) Characterization of an antigen that is recognized on a melanoma showing partial HLA loss by CTL expressing an NK inhibitory receptor. *Immunity*, 6(2), 199-208.

Ikushima, H. & Miyazono, K. (2010) TGFbeta signalling: a complex web in cancer progression. *Nat Rev Cancer*, 10(6), 415-24.

Ishida, S., Lee, J., Thiele, D. J. & Herskowitz, I. (2002) Uptake of the anticancer drug cisplatin mediated by the copper transporter Ctr1 in yeast and mammals. *Proc Natl Acad Sci U S A*, 99(22), 14298-302.

Ishii, H., Iwatsuki, M., Ieta, K., Ohta, D., Haraguchi, N., Mimori, K. & Mori, M. (2008) Cancer stem cells and chemoradiation resistance. *Cancer Sci*, 99(10), 1871-7.

Jankowski, J. A., Harrison, R. F., Perry, I., Balkwill, F. & Tselepis, C. (2000a) Barrett's metaplasia. *Lancet*, 356(9247), 2079-85.

Jankowski, J. A., Perry, I. & Harrison, R. F. (2000b) Gastro-oesophageal cancer: death at the junction. *BMJ*, 321(7259), 463-4.

Jiang, B., Li, Z., Zhang, W., Wang, H., Zhi, X., Feng, J., Chen, Z., Zhu, Y., Yang, L., Xu, H. & Xu, Z. (2014) miR-874 Inhibits cell proliferation, migration and invasion through targeting aquaporin-3 in gastric cancer. *J Gastroenterol*, 49(6), 1011-25.

Johnson, D. G. & Degregori, J. (2006) Putting the Oncogenic and Tumor Suppressive Activities of E2F into Context. *Curr Mol Med*, 6(7), 731-8.

Johnson, R. D. & Jasin, M. (2001) Double-strand-break-induced homologous recombination in mammalian cells. *Biochem Soc Trans*, 29(Pt 2), 196-201.

Johnson, S. M., Grosshans, H., Shingara, J., Byrom, M., Jarvis, R., Cheng, A., Labourier, E., Reinert, K. L., Brown, D. & Slack, F. J. (2005) RAS is regulated by the let-7 microRNA family. *Cell*, 120(5), 635-47.

Jones, R. G. & Thompson, C. B. (2009) Tumor suppressors and cell metabolism: a recipe for cancer growth. *Genes Dev*, 23(5), 537-48.

Junttila, M. R. & Evan, G. I. (2009) p53--a Jack of all trades but master of none. *Nat Rev Cancer*, 9(11), 821-9.

Kaanders, J. H., Bussink, J. & van der Kogel, A. J. (2002) ARCON: a novel biology-based approach in radiotherapy. *Lancet Oncol*, 3(12), 728-37.

Kan, T., Sato, F., Ito, T., Matsumura, N., David, S., Cheng, Y., Agarwal, R., Paun, B. C., Jin, Z., Olaru, A. V., Selaru, F. M., Hamilton, J. P., Yang, J., Abraham, J. M., Mori, Y. & Meltzer, S. J. (2009) The miR-106b-25 polycistron, activated by genomic amplification, functions as an oncogene by suppressing p21 and Bim. *Gastroenterology*, 136(5), 1689-700.

Kang, B. W., Kim, J. G., Lee, S. J., Chae, Y. S., Jeong, J. Y., Yoon, G. S., Park, S. Y., Kim, H. J., Park, J. S., Choi, G. S. & Jeong, J. Y. (2015) Expression of aquaporin-1, aquaporin-3, and aquaporin-5 correlates with nodal metastasis in colon cancer. *Oncology*, 88(6), 369-76.

Karar, J. & Maity, A. (2009) Modulating the tumor microenvironment to increase radiation responsiveness. *Cancer Biol Ther*, 8(21), 1994-2001.

Karkera, J. D., Ayache, S., Ransome, R. J., Jr., Jackson, M. A., Elsayem, A. F., Sridhar, R., Detera-Wadleigh, S. D. & Wadleigh, R. G. (2000) Refinement of regions with allelic loss on chromosome 18p11.2 and 18q12.2 in esophageal squamous cell carcinoma. *Clin Cancer Res*, 6(9), 3565-9.

Katoh, M. (2007) Networking of WNT, FGF, Notch, BMP, and Hedgehog signaling pathways during carcinogenesis. *Stem Cell Rev*, 3(1), 30-8.

Keld, R., Guo, B., Downey, P., Gulmann, C., Ang, Y. S. & Sharrocks, A. D. (2010) The ERK MAP kinase-PEA3/ETV4-MMP-1 axis is operative in oesophageal adenocarcinoma. *Mol Cancer*, 9, 313.

Kelloff, G. J., Hoffman, J. M., Johnson, B., Scher, H. I., Siegel, B. A., Cheng, E. Y., Cheson, B. D., O'Shaughnessy, J., Guyton, K. Z., Mankoff, D. A., Shankar, L., Larson, S. M., Sigman, C. C., Schilsky, R. L. & Sullivan, D. C. (2005) Progress and promise of FDG-PET imaging for cancer patient management and oncologic drug development. *Clin Cancer Res*, 11(8), 2785-808.

Kelsen, D. P. (2000) Multimodality therapy of esophageal cancer: an update. *Cancer J*, 6 Suppl 2, S177-81.

Kent, O. A., McCall, M. N., Cornish, T. C. & Halushka, M. K. (2014) Lessons from miR-143/145: the importance of cell-type localization of miRNAs. *Nucleic Acids Res*, 42(12), 7528-38.

Kessenbrock, K., Plaks, V. & Werb, Z. (2010) Matrix metalloproteinases: regulators of the tumor microenvironment. *Cell*, 141(1), 52-67.

Ketting, R. F., Fischer, S. E., Bernstein, E., Sijen, T., Hannon, G. J. & Plasterk, R. H. (2001) Dicer functions in RNA interference and in synthesis of small RNA involved in developmental timing in C. elegans. *Genes Dev*, 15(20), 2654-9.

Khalifa, M. M., Sharaf, R. R. & Aziz, R. K. (2010) Helicobacter pylori: a poor man's gut pathogen? *Gut Pathog*, 2(1), 2.

Khanna, L. G. & Gress, F. G. (2015) Preoperative evaluation of oesophageal adenocarcinoma. *Best Pract Res Clin Gastroenterol*, 29(1), 179-91.

Kim, R., Emi, M. & Tanabe, K. (2007) Cancer immunoediting from immune surveillance to immune escape. *Immunology*, 121(1), 1-14.

Kim, Y. W., Kim, E. Y., Jeon, D., Liu, J. L., Kim, H. S., Choi, J. W. & Ahn, W. S. (2014) Differential microRNA expression signatures and cell type-specific association with Taxol resistance in ovarian cancer cells. *Drug Des Devel Ther*, 8, 293-314.

Kjellen, E., Joiner, M. C., Collier, J. M., Johns, H. & Rojas, A. (1991) A therapeutic benefit from combining normobaric carbogen or oxygen with nicotinamide in fractionated X-ray treatments. *Radiother Oncol*, 22(2), 81-91.

Klymkowsky, M. W. & Savagner, P. (2009) Epithelial-mesenchymal transition: a cancer researcher's conceptual friend and foe. *Am J Pathol*, 174(5), 1588-93.

Knoll, S., Emmrich, S. & Putzer, B. M. (2013) The E2F1-miRNA cancer progression network. *Adv Exp Med Biol*, 774, 135-47.

Ko, M. A., Zehong, G., Virtanen, C., Guindi, M., Waddell, T. K., Keshavjee, S. & Darling, G. E. (2012) MicroRNA expression profiling of esophageal cancer before and after induction chemoradiotherapy. *Ann Thorac Surg*, 94(4), 1094-102; discussion 1102-3.

Korpela, E., Vesprini, D. & Liu, S. K. (2015) MicroRNA in radiotherapy: miRage or miRador? *Br J Cancer*, 112(5), 777-82.

Kozin, S. V., Kamoun, W. S., Huang, Y., Dawson, M. R., Jain, R. K. & Duda, D. G. (2010) Recruitment of myeloid but not endothelial precursor cells facilitates tumor regrowth after local irradiation. *Cancer Res*, 70(14), 5679-85.

Kozomara, A. & Griffiths-Jones, S. (2014) miRBase: annotating high confidence microRNAs using deep sequencing data. *Nucleic Acids Res*, 42(Database issue), D68-73.

Krause, B. J., Herrmann, K., Wieder, H. & zum Buschenfelde, C. M. (2009) 18F-FDG PET and 18F-FDG PET/CT for assessing response to therapy in esophageal cancer. *J Nucl Med*, 50 Suppl 1, 89S-96S.

Krutzfeldt, J., Rajewsky, N., Braich, R., Rajeev, K. G., Tuschl, T., Manoharan, M. & Stoffel, M. (2005) Silencing of microRNAs in vivo with 'antagomirs'. *Nature*, 438(7068), 685-9.

Kubo, A., Corley, D. A., Jensen, C. D. & Kaur, R. (2010) Dietary factors and the risks of oesophageal adenocarcinoma and Barrett's oesophagus. *Nutr Res Rev*, 23(2), 230-46.

Kumar, A., Ghosh, S. & Chandna, S. (2015) Evidence for microRNA-31 dependent Bim-Bax interaction preceding mitochondrial Bax translocation during radiation-induced apoptosis. *Sci Rep*, 5, 15923.

Lagergren, J. (2011) Influence of obesity on the risk of esophageal disorders. *Nat Rev Gastroenterol Hepatol*, 8(6), 340-7.

Lagos-Quintana, M., Rauhut, R., Lendeckel, W. & Tuschl, T. (2001) Identification of novel genes coding for small expressed RNAs. *Science*, 294(5543), 853-8.

Lane, D. P. (1992) Cancer. p53, guardian of the genome. *Nature*, 358(6381), 15-6.

Lau, N. C., Lim, L. P., Weinstein, E. G. & Bartel, D. P. (2001) An abundant class of tiny RNAs with probable regulatory roles in Caenorhabditis elegans. *Science*, 294(5543), 858-62.

Lee, H., Flaherty, P. & Ji, H. P. (2013) Systematic genomic identification of colorectal cancer genes delineating advanced from early clinical stage and metastasis. *BMC Med Genomics*, 6, 54.

Lee, J. S., Leem, S. H., Lee, S. Y., Kim, S. C., Park, E. S., Kim, S. B., Kim, S. K., Kim, Y. J., Kim, W. J. & Chu, I. S. (2010) Expression signature of E2F1 and its associated genes predict superficial to invasive progression of bladder tumors. *J Clin Oncol*, 28(16), 2660-7.

Lee, K. H., Chen, Y. L., Yeh, S. D., Hsiao, M., Lin, J. T., Goan, Y. G. & Lu, P. J. (2009) MicroRNA-330 acts as tumor suppressor and induces apoptosis of prostate cancer cells through E2F1-mediated suppression of Akt phosphorylation. *Oncogene*, 28(38), 3360-70.

Lee, R. C. & Ambros, V. (2001) An extensive class of small RNAs in Caenorhabditis elegans. *Science*, 294(5543), 862-4.

Lee, R. C., Feinbaum, R. L. & Ambros, V. (1993) The C. elegans heterochronic gene lin-4 encodes small RNAs with antisense complementarity to lin-14. *Cell*, 75(5), 843-54.

Lee, Y., Jeon, K., Lee, J. T., Kim, S. & Kim, V. N. (2002) MicroRNA maturation: stepwise processing and subcellular localization. *EMBO J*, 21(17), 4663-70.

Lee, Y., Kim, M., Han, J., Yeom, K. H., Lee, S., Baek, S. H. & Kim, V. N. (2004) MicroRNA genes are transcribed by RNA polymerase II. *EMBO J*, 23(20), 4051-60.

Lerman, O. Z., Greives, M. R., Singh, S. P., Thanik, V. D., Chang, C. C., Seiser, N., Brown, D. J., Knobel, D., Schneider, R. J., Formenti, S. C., Saadeh, P. B. & Levine, J. P. (2010) Low-dose radiation augments vasculogenesis signaling through HIF-1-dependent and -independent SDF-1 induction. *Blood*, 116(18), 3669-76.

Leung, A. K. (2015) The Whereabouts of microRNA Actions: Cytoplasm and Beyond. *Trends Cell Biol*, 25(10), 601-10.

Lewis, B. P., Shih, I. H., Jones-Rhoades, M. W., Bartel, D. P. & Burge, C. B. (2003) Prediction of mammalian microRNA targets. *Cell*, 115(7), 787-98.

Li, C., Wang, Z., Liu, F., Zhu, J., Yang, L., Cai, G., Zhang, Z., Huang, W., Cai, S. & Xu, Y. (2014a) CXCL10 mRNA expression predicts response to neoadjuvant chemoradiotherapy in rectal cancer patients. *Tumour Biol*, 35(10), 9683-91.

Li, G. & Pu, Y. (2015) MicroRNA signatures in total peripheral blood of gallbladder cancer patients. *Tumour Biol*.

Li, M., Li, J., Ding, X., He, M. & Cheng, S. Y. (2010) microRNA and cancer. *AAPS J*, 12(3), 309-17.

Li, X., Shi, Y., Yin, Z., Xue, X. & Zhou, B. (2014b) An eight-miRNA signature as a potential biomarker for predicting survival in lung adenocarcinoma. *J Transl Med*, 12, 159.

Li, Y., Zhu, X., Xu, W., Wang, D. & Yan, J. (2013) miR-330 regulates the proliferation of colorectal cancer cells by targeting Cdc42. *Biochem Biophys Res Commun*, 431(3), 560-5.

Liao, L. M., Vaughan, T. L., Corley, D. A., Cook, M. B., Casson, A. G., Kamangar, F., Abnet, C. C., Risch, H. A., Giffen, C., Freedman, N. D., Chow, W. H., Sadeghi, S., Pandeya, N., Whiteman, D. C., Murray, L. J., Bernstein, L., Gammon, M. D. & Wu, A. H. (2012) Nonsteroidal anti-inflammatory drug use reduces risk of adenocarcinomas of the esophagus and esophagogastric junction in a pooled analysis. *Gastroenterology*, 142(3), 442-452 e5; quiz e22-3.

Lim, L. P., Lau, N. C., Garrett-Engele, P., Grimson, A., Schelter, J. M., Castle, J., Bartel, D. P., Linsley, P. S. & Johnson, J. M. (2005) Microarray analysis shows that some microRNAs downregulate large numbers of target mRNAs. *Nature*, 433(7027), 769-73.

Liu, L., Hofstetter, W. L., Rashid, A., Swisher, S. G., Correa, A. M., Ajani, J. A., Hamilton, S. R. & Wu, T. T. (2005) Significance of the depth of tumor invasion and lymph node metastasis in superficially invasive (T1) esophageal adenocarcinoma. *Am J Surg Pathol*, 29(8), 1079-85.

Liu, S., Zhang, S., Jiang, H., Yang, Y. & Jiang, Y. (2013) Co-expression of AQP3 and AQP5 in esophageal squamous cell carcinoma correlates with aggressive tumor progression and poor prognosis. *Med Oncol*, 30(3), 636.

Livak, K. J. & Schmittgen, T. D. (2001) Analysis of relative gene expression data using real-time quantitative PCR and the 2(-Delta Delta C(T)) Method. *Methods*, 25(4), 402-8.

Longley, D. B., Harkin, D. P. & Johnston, P. G. (2003) 5-fluorouracil: mechanisms of action and clinical strategies. *Nat Rev Cancer*, 3(5), 330-8.

Longley, D. B. & Johnston, P. G. (2005) Molecular mechanisms of drug resistance. *J Pathol*, 205(2), 275-92.

Lordick, F., Ott, K., Krause, B. J., Weber, W. A., Becker, K., Stein, H. J., Lorenzen, S., Schuster, T., Wieder, H., Herrmann, K., Bredenkamp, R., Hofler, H., Fink, U., Peschel, C., Schwaiger, M. & Siewert, J. R. (2007) PET to assess early metabolic response and to guide treatment of adenocarcinoma of the oesophagogastric junction: the MUNICON phase II trial. *Lancet Oncol*, 8(9), 797-805.

Loser, R. & Pietzsch, J. (2015) Cysteine cathepsins: their role in tumor progression and recent trends in the development of imaging probes. *Front Chem*, 3, 37.

Lu, J., Getz, G., Miska, E. A., Alvarez-Saavedra, E., Lamb, J., Peck, D., Sweet-Cordero, A., Ebert, B. L., Mak, R. H., Ferrando, A. A., Downing, J. R., Jacks, T., Horvitz, H. R. & Golub, T. R. (2005) MicroRNA expression profiles classify human cancers. *Nature*, 435(7043), 834-8.

Luthra, R., Singh, R. R., Luthra, M. G., Li, Y. X., Hannah, C., Romans, A. M., Barkoh, B. A., Chen, S. S., Ensor, J., Maru, D. M., Broaddus, R. R., Rashid, A. & Albarracin, C. T. (2008) MicroRNA-196a targets annexin A1: a microRNA-mediated mechanism of annexin A1 downregulation in cancers. *Oncogene*, 27(52), 6667-78.

Lynam-Lennon, N., Maher, S. G., Maguire, A., Phelan, J., Muldoon, C., Reynolds, J. V. & O'Sullivan, J. (2014) Altered mitochondrial function and energy metabolism is associated with a radioresistant phenotype in oesophageal adenocarcinoma. *PLoS One*, 9(6), e100738.

Lynam-Lennon, N., Reynolds, J. V., Marignol, L., Sheils, O. M., Pidgeon, G. P. & Maher, S. G. (2012) MicroRNA-31 modulates tumour sensitivity to radiation in oesophageal adenocarcinoma. *J Mol Med (Berl)*, 90(12), 1449-58.

Lynam-Lennon, N., Reynolds, J. V., Pidgeon, G. P., Lysaght, J., Marignol, L. & Maher, S. G. (2010) Alterations in DNA repair efficiency are involved in the radioresistance of esophageal adenocarcinoma. *Radiat Res*, 174(6), 703-11.

Lytle, J. R., Yario, T. A. & Steitz, J. A. (2007) Target mRNAs are repressed as efficiently by microRNA-binding sites in the 5' UTR as in the 3' UTR. *Proc Natl Acad Sci U S A*, 104(23), 9667-72.

Ma, L., Young, J., Prabhala, H., Pan, E., Mestdagh, P., Muth, D., Teruya-Feldstein, J., Reinhardt, F., Onder, T. T., Valastyan, S., Westermann, F., Speleman, F., Vandesompele, J. & Weinberg, R. A. (2010) miR-9, a MYC/MYCN-activated microRNA, regulates E-cadherin and cancer metastasis. *Nat Cell Biol*, 12(3), 247-56.

Maher, S. G., Gillham, C. M., Duggan, S. P., Smyth, P. C., Miller, N., Muldoon, C., O'Byrne, K. J., Sheils, O. M., Hollywood, D. & Reynolds, J. V. (2009) Gene expression analysis of diagnostic biopsies predicts pathological response to neoadjuvant chemoradiotherapy of esophageal cancer. *Ann Surg*, 250(5), 729-37.

Maher, S. G., McDowell, D. T., Collins, B. C., Muldoon, C., Gallagher, W. M. & Reynolds, J. V. (2011) Serum proteomic profiling reveals that pretreatment complement protein levels are predictive of esophageal cancer patient response to neoadjuvant chemoradiation. *Ann Surg*, 254(5), 809-16; discussion 816-7.

Malhotra, V. & Perry, M. C. (2003) Classical chemotherapy: mechanisms, toxicities and the therapeutic window. *Cancer Biol Ther*, 2(4 Suppl 1), S2-4.

Malik, V., Lucey, J. A., Duffy, G. J., Wilson, L., McNamara, L., Keogan, M., Gillham, C. & Reynolds, J. V. (2010) Early repeated 18F-FDG PET scans during neoadjuvant chemoradiation fail to predict histopathologic response or survival benefit in adenocarcinoma of the esophagus. *J Nucl Med*, 51(12), 1863-9.

Malla, R. R., Gopinath, S., Alapati, K., Gorantla, B., Gondi, C. S. & Rao, J. S. (2012) uPAR and cathepsin B inhibition enhanced radiation-induced apoptosis in gliomainitiating cells. *Neuro Oncol*, 14(6), 745-60.

Mandard, A. M., Dalibard, F., Mandard, J. C., Marnay, J., Henry-Amar, M., Petiot, J. F., Roussel, A., Jacob, J. H., Segol, P., Samama, G. & et al. (1994) Pathologic assessment of tumor regression after preoperative chemoradiotherapy of esophageal carcinoma. Clinicopathologic correlations. *Cancer*, 73(11), 2680-6.

Mao, Y., Chen, H., Lin, Y., Xu, X., Hu, Z., Zhu, Y., Wu, J., Zheng, X. & Xie, L. (2013) microRNA-330 inhibits cell motility by downregulating Sp1 in prostate cancer cells. *Oncol Rep*, 30(1), 327-33.

Masclee, G. M., Coloma, P. M., de Wilde, M., Kuipers, E. J. & Sturkenboom, M. C. (2014) The incidence of Barrett's oesophagus and oesophageal adenocarcinoma in the United Kingdom and The Netherlands is levelling off. *Aliment Pharmacol Ther*, 39(11), 1321-30.

Masclee, G. M., Coloma, P. M., Spaander, M. C., Kuipers, E. J. & Sturkenboom, M. C. (2015) NSAIDs, statins, low-dose aspirin and PPIs, and the risk of oesophageal adenocarcinoma among patients with Barrett's oesophagus: a population-based case-control study. *BMJ Open*, 5(1), e006640.

Matsuoka, S., Edwards, M. C., Bai, C., Parker, S., Zhang, P., Baldini, A., Harper, J. W. & Elledge, S. J. (1995) p57KIP2, a structurally distinct member of the p21CIP1 Cdk inhibitor family, is a candidate tumor suppressor gene. *Genes Dev*, 9(6), 650-62.

McGowan, P. M., Kirstein, J. M. & Chambers, A. F. (2009) Micrometastatic disease and metastatic outgrowth: clinical issues and experimental approaches. *Future Oncol*, 5(7), 1083-98.

Medina, P. P., Nolde, M. & Slack, F. J. (2010) OncomiR addiction in an in vivo model of microRNA-21-induced pre-B-cell lymphoma. *Nature*, 467(7311), 86-90.

Mendell, J. T. & Olson, E. N. (2012) MicroRNAs in stress signaling and human disease. *Cell*, 148(6), 1172-87.

Messager, M., de Steur, W. O., van Sandick, J. W., Reynolds, J., Pera, M., Mariette, C., Hardwick, R. H., Bastiaannet, E., Boelens, P. G., van deVelde, C. J. & Allum, W. H. (2015) Variations among 5 European countries for curative treatment of resectable oesophageal and gastric cancer: A survey from the EURECCA Upper GI Group (EUropean REgistration of Cancer CAre). *Eur J Surg Oncol*.

Michael, M. Z., SM, O. C., van Holst Pellekaan, N. G., Young, G. P. & James, R. J. (2003) Reduced accumulation of specific microRNAs in colorectal neoplasia. *Mol Cancer Res*, 1(12), 882-91.

Morita, Y., Iwamoto, I., Mizuma, N., Kuwahata, T., Matsuo, T., Yoshinaga, M. & Douchi, T. (2006) Precedence of the shift of body-fat distribution over the change in body composition after menopause. *J Obstet Gynaecol Res*, 32(5), 513-6.

Mukherjee, S., Hurt, C. N., Gwynne, S., Bateman, A., Gollins, S., Radhakrishna, G., Hawkins, M., Canham, J., Lewis, W., Grabsch, H. I., Sharma, R. A., Wade, W., Maggs, R., Tranter, B., Roberts, A., Sebag-Montefiore, D., Maughan, T., Griffiths, G. & Crosby, T. (2015) NEOSCOPE: a randomised Phase II study of induction chemotherapy followed by either oxaliplatin/capecitabine or paclitaxel/carboplatin based chemoradiation as pre-operative regimen for resectable oesophageal adenocarcinoma. *BMC Cancer*, 15, 48.

Mulrane, L., Madden, S. F., Brennan, D. J., Gremel, G., McGee, S. F., McNally, S., Martin, F., Crown, J. P., Jirstrom, K., Higgins, D. G., Gallagher, W. M. & O'Connor, D. P. (2012) miR-187

is an independent prognostic factor in breast cancer and confers increased invasive potential in vitro. *Clin Cancer Res*, 18(24), 6702-13.

Multhoff, G. & Radons, J. (2012) Radiation, inflammation, and immune responses in cancer. *Front Oncol*, 2, 58.

Murray, G. I., Duncan, M. E., O'Neil, P., McKay, J. A., Melvin, W. T. & Fothergill, J. E. (1998) Matrix metalloproteinase-1 is associated with poor prognosis in oesophageal cancer. *J Pathol*, 185(3), 256-61.

Nagy, J. A., Chang, S. H., Shih, S. C., Dvorak, A. M. & Dvorak, H. F. (2010) Heterogeneity of the tumor vasculature. *Semin Thromb Hemost*, 36(3), 321-31.

Neviani, P. & Fabbri, M. (2015) Exosomic microRNAs in the Tumor Microenvironment. *Front Med (Lausanne)*, 2, 47.

Newnham, A., Quinn, M. J., Babb, P., Kang, J. Y. & Majeed, A. (2003) Trends in oesophageal and gastric cancer incidence, mortality and survival in England and Wales 1971-1998/1999. *Aliment Pharmacol Ther*, 17(5), 655-64.

Nguyen, G. H., Schetter, A. J., Chou, D. B., Bowman, E. D., Zhao, R., Hawkes, J. E., Mathe, E. A., Kumamoto, K., Zhao, Y., Budhu, A., Hagiwara, N., Wang, X. W., Miyashita, M., Casson, A. G. & Harris, C. C. (2010) Inflammatory and microRNA gene expression as prognostic classifier of Barrett's-associated esophageal adenocarcinoma. *Clin Cancer Res*, 16(23), 5824-34.

Nicholson, K. M. & Anderson, N. G. (2002) The protein kinase B/Akt signalling pathway in human malignancy. *Cell Signal*, 14(5), 381-95.

Nikiforova, M. N., Tseng, G. C., Steward, D., Diorio, D. & Nikiforov, Y. E. (2008) MicroRNA expression profiling of thyroid tumors: biological significance and diagnostic utility. *J Clin Endocrinol Metab*, 93(5), 1600-8.

Nitiss, J. L. (2009) Targeting DNA topoisomerase II in cancer chemotherapy. *Nat Rev Cancer*, 9(5), 338-50.

Ogunwobi, O. O. & Beales, I. L. (2008) Leptin stimulates the proliferation of human oesophageal adenocarcinoma cells via HB-EGF and Tgfalpha mediated transactivation of the epidermal growth factor receptor. *Br J Biomed Sci*, 65(3), 121-7.

Old, O., Moayyedi, P., Love, S., Roberts, C., Hapeshi, J., Foy, C., Stokes, C., Briggs, A., Jankowski, J. & Barr, H. (2015) Barrett's Oesophagus Surveillance versus endoscopy at need Study (BOSS): protocol and analysis plan for a multicentre randomized controlled trial. *J Med Screen*, 22(3), 158-64.

Orlando, R. C. (2006) Current understanding of the mechanisms of gastro-oesophageal reflux disease. *Drugs*, 66 Suppl 1, 1-5; discussion 29-33.

Overgaard, J. (2007) Hypoxic radiosensitization: adored and ignored. *J Clin Oncol*, 25(26), 4066-74.

Overgaard, J. (2011) Hypoxic modification of radiotherapy in squamous cell carcinoma of the head and neck--a systematic review and meta-analysis. *Radiother Oncol*, 100(1), 22-32.

Parker, R. & Song, H. (2004) The enzymes and control of eukaryotic mRNA turnover. *Nat Struct Mol Biol*, 11(2), 121-7.

Parker, W. B. (2009) Enzymology of purine and pyrimidine antimetabolites used in the treatment of cancer. *Chem Rev*, 109(7), 2880-93.

Parsons, S. (2010) Are we missing Gastro-Oesophageal Cancer at Endoscopy? *Ann R Coll Surg Engl*.

Pasquinelli, A. E., Reinhart, B. J., Slack, F., Martindale, M. Q., Kuroda, M. I., Maller, B., Hayward, D. C., Ball, E. E., Degnan, B., Muller, P., Spring, J., Srinivasan, A., Fishman, M., Finnerty, J., Corbo, J., Levine, M., Leahy, P., Davidson, E. & Ruvkun, G. (2000) Conservation of the sequence and temporal expression of let-7 heterochronic regulatory RNA. *Nature*, 408(6808), 86-9.

Pavlov, K., Meijer, C., van den Berg, A., Peters, F. T., Kruyt, F. A. & Kleibeuker, J. H. (2014) Embryological signaling pathways in Barrett's metaplasia development and malignant transformation; mechanisms and therapeutic opportunities. *Crit Rev Oncol Hematol*, 92(1), 25-37.

Pawlik, T. M. & Keyomarsi, K. (2004) Role of cell cycle in mediating sensitivity to radiotherapy. *Int J Radiat Oncol Biol Phys*, 59(4), 928-42.

Peter, M. E. (2010) Targeting of mRNAs by multiple miRNAs: the next step. *Oncogene*, 29(15), 2161-4.

Peters, L. & Meister, G. (2007) Argonaute proteins: mediators of RNA silencing. *Mol Cell*, 26(5), 611-23.

Petersen, C. P., Bordeleau, M. E., Pelletier, J. & Sharp, P. A. (2006) Short RNAs repress translation after initiation in mammalian cells. *Mol Cell*, 21(4), 533-42.

Picardo, S. L., Maher, S. G., O'Sullivan, J. N. & Reynolds, J. V. (2012) Barrett's to oesophageal cancer sequence: a model of inflammatory-driven upper gastrointestinal cancer. *Dig Surg*, 29(3), 251-60.

Pichler, M. & Calin, G. A. (2015) MicroRNAs in cancer: from developmental genes in worms to their clinical application in patients. *Br J Cancer*.

Pietras, K. & Ostman, A. (2010) Hallmarks of cancer: interactions with the tumor stroma. *Exp Cell Res*, 316(8), 1324-31.

Pio, R., Ajona, D. & Lambris, J. D. (2013) Complement inhibition in cancer therapy. *Semin Immunol*, 25(1), 54-64.

Piskareva, O., Harvey, H., Nolan, J., Conlon, R., Alcock, L., Buckley, P., Dowling, P., O'Sullivan, F., Bray, I. & Stallings, R. L. (2015) The development of cisplatin resistance in neuroblastoma is accompanied by epithelial to mesenchymal transition in vitro. *Cancer Lett*, 364(2), 142-55.

Png, K. J., Halberg, N., Yoshida, M. & Tavazoie, S. F. (2012) A microRNA regulon that mediates endothelial recruitment and metastasis by cancer cells. *Nature*, 481(7380), 190-4.

Pohl, H., Sirovich, B. & Welch, H. G. (2010) Esophageal adenocarcinoma incidence: are we reaching the peak? *Cancer Epidemiol Biomarkers Prev*, 19(6), 1468-70.

Pohl, H. & Welch, H. G. (2005) The role of overdiagnosis and reclassification in the marked increase of esophageal adenocarcinoma incidence. *J Natl Cancer Inst*, 97(2), 142-6.

Pohl, H., Wrobel, K., Bojarski, C., Voderholzer, W., Sonnenberg, A., Rosch, T. & Baumgart, D. C. (2013) Risk factors in the development of esophageal adenocarcinoma. *Am J Gastroenterol*, 108(2), 200-7.

Porter, S. N., Baker, L. C., Mittelman, D. & Porteus, M. H. (2014) Lentiviral and targeted cellular barcoding reveals ongoing clonal dynamics of cell lines in vitro and in vivo. *Genome Biol*, 15(5), R75.

Qian, B. Z. & Pollard, J. W. (2010) Macrophage diversity enhances tumor progression and metastasis. *Cell*, 141(1), 39-51.

Qu, S., Yao, Y., Shang, C., Xue, Y., Ma, J., Li, Z. & Liu, Y. (2012) MicroRNA-330 is an oncogenic factor in glioblastoma cells by regulating SH3GL2 gene. *PLoS One*, 7(9), e46010.

Rajendra, S. (2015) Barrett's oesophagus: can meaningful screening and surveillance guidelines be formulated based on new data and rejigging the old paradigm? *Best Pract Res Clin Gastroenterol*, 29(1), 65-75.

Rakoczy, J., Fernandez-Valverde, S. L., Glazov, E. A., Wainwright, E. N., Sato, T., Takada, S., Combes, A. N., Korbie, D. J., Miller, D., Grimmond, S. M., Little, M. H., Asahara, H., Mattick, J. S., Taft, R. J. & Wilhelm, D. (2013) MicroRNAs-140-5p/140-3p modulate Leydig cell numbers in the developing mouse testis. *Biol Reprod*, 88(6), 143.

Rasanen, K. & Vaheri, A. (2010) Activation of fibroblasts in cancer stroma. *Exp Cell Res*, 316(17), 2713-22.

Reinhart, B. J., Slack, F. J., Basson, M., Pasquinelli, A. E., Bettinger, J. C., Rougvie, A. E., Horvitz, H. R. & Ruvkun, G. (2000) The 21-nucleotide let-7 RNA regulates developmental timing in Caenorhabditis elegans. *Nature*, 403(6772), 901-6.

Rentoft, M., Coates, P. J., Loljung, L., Wilms, T., Laurell, G. & Nylander, K. (2014) Expression of CXCL10 is associated with response to radiotherapy and overall survival in squamous cell carcinoma of the tongue. *Tumour Biol*, 35(5), 4191-8.

Rice, T. W., Blackstone, E. H. & Rusch, V. W. (2010) 7th edition of the AJCC Cancer Staging Manual: esophagus and esophagogastric junction. *Ann Surg Oncol*, 17(7), 1721-4.

Rischin, D., Peters, L. J., O'Sullivan, B., Giralt, J., Fisher, R., Yuen, K., Trotti, A., Bernier, J., Bourhis, J., Ringash, J., Henke, M. & Kenny, L. (2010) Tirapazamine, cisplatin, and radiation versus cisplatin and radiation for advanced squamous cell carcinoma of the head and neck (TROG 02.02, HeadSTART): a phase III trial of the Trans-Tasman Radiation Oncology Group. *J Clin Oncol*, 28(18), 2989-95.

Roberts, T. C. (2014) The MicroRNA Biology of the Mammalian Nucleus. *Mol Ther Nucleic Acids*, 3, e188.

Ruan, K., Fang, X. & Ouyang, G. (2009) MicroRNAs: novel regulators in the hallmarks of human cancer. *Cancer Lett*, 285(2), 116-26.

Rubenstein, J. H. & Thrift, A. P. (2015) Risk factors and populations at risk: selection of patients for screening for Barrett's oesophagus. *Best Pract Res Clin Gastroenterol*, 29(1), 41-50.

Rutkowski, M. J., Sughrue, M. E., Kane, A. J., Ahn, B. J., Fang, S. & Parsa, A. T. (2010) The complement cascade as a mediator of tissue growth and regeneration. *Inflamm Res*, 59(11), 897-905.

Saarinen, J., Welgus, H. G., Flizar, C. A., Kalkkinen, N. & Helin, J. (1999) N-glycan structures of matrix metalloproteinase-1 derived from human fibroblasts and from HT-1080 fibrosarcoma cells. *Eur J Biochem*, 259(3), 829-40.

Saito, T. & Saetrom, P. (2010) MicroRNAs--targeting and target prediction. *N Biotechnol*, 27(3), 243-9.

Sakai, N. S., Samia-Aly, E., Barbera, M. & Fitzgerald, R. C. (2013) A review of the current understanding and clinical utility of miRNAs in esophageal cancer. *Semin Cancer Biol*, 23(6 Pt B), 512-21.

Sakurai, E., Maesawa, C., Shibazaki, M., Yasuhira, S., Oikawa, H., Sato, M., Tsunoda, K., Ishikawa, Y., Watanabe, A., Takahashi, K., Akasaka, T. & Masuda, T. (2011) Downregulation of microRNA-211 is involved in expression of preferentially expressed antigen of melanoma in melanoma cells. *Int J Oncol*, 39(3), 665-72.

Saumet, A., Mathelier, A. & Lecellier, C. H. (2014) The potential of microRNAs in personalized medicine against cancers. *Biomed Res Int*, 2014, 642916.

Schaue, D. & McBride, W. H. (2010) Links between innate immunity and normal tissue radiobiology. *Radiat Res*, 173(4), 406-17.

Schneider, J. L. & Corley, D. A. (2015) A review of the epidemiology of Barrett's oesophagus and oesophageal adenocarcinoma. *Best Pract Res Clin Gastroenterol*, 29(1), 29-39.

Schultz, N. A., Andersen, K. K., Roslind, A., Willenbrock, H., Wojdemann, M. & Johansen, J. S. (2012) Prognostic microRNAs in cancer tissue from patients operated for pancreatic cancer--five microRNAs in a prognostic index. *World J Surg*, 36(11), 2699-707.

Schwarz, D. S., Hutvagner, G., Du, T., Xu, Z., Aronin, N. & Zamore, P. D. (2003) Asymmetry in the assembly of the RNAi enzyme complex. *Cell*, 115(2), 199-208.

Scott, S. P. & Pandita, T. K. (2006) The cellular control of DNA double-strand breaks. *J Cell Biochem*, 99(6), 1463-75.

Semenza, G. L. (2008) Tumor metabolism: cancer cells give and take lactate. *J Clin Invest*, 118(12), 3835-7.

Semenza, G. L. (2010) Defining the role of hypoxia-inducible factor 1 in cancer biology and therapeutics. *Oncogene*, 29(5), 625-34.

Seo, H. R., Bae, S. & Lee, Y. S. (2009) Radiation-induced cathepsin S is involved in radioresistance. *Int J Cancer*, 124(8), 1794-801.

Shabbits, J. A., Hu, Y. & Mayer, L. D. (2003) Tumor chemosensitization strategies based on apoptosis manipulations. *Mol Cancer Ther*, 2(8), 805-13.

Shah, M. A. & Schwartz, G. K. (2001) Cell cycle-mediated drug resistance: an emerging concept in cancer therapy. *Clin Cancer Res*, 7(8), 2168-81.

Shen, D. W., Pouliot, L. M., Hall, M. D. & Gottesman, M. M. (2012) Cisplatin resistance: a cellular self-defense mechanism resulting from multiple epigenetic and genetic changes. *Pharmacol Rev*, 64(3), 706-21.

Siddik, Z. H. (2003) Cisplatin: mode of cytotoxic action and molecular basis of resistance. *Oncogene*, 22(47), 7265-79.

Singh, A. & Settleman, J. (2010) EMT, cancer stem cells and drug resistance: an emerging axis of evil in the war on cancer. *Oncogene*, 29(34), 4741-51.

Sjoquist, K. M., Burmeister, B. H., Smithers, B. M., Zalcberg, J. R., Simes, R. J., Barbour, A. & Gebski, V. (2011) Survival after neoadjuvant chemotherapy or chemoradiotherapy for resectable oesophageal carcinoma: an updated meta-analysis. *Lancet Oncol*, 12(7), 681-92.

Skinner, H. D., Lee, J. H., Bhutani, M. S., Weston, B., Hofstetter, W., Komaki, R., Shiozaki, H., Wadhwa, R., Sudo, K., Elimova, E., Song, S., Ye, Y., Huang, M., Ajani, J. & Wu, X. (2014) A validated miRNA profile predicts response to therapy in esophageal adenocarcinoma. *Cancer*, 120(23), 3635-41.

Smith, V., Wirth, G. J., Fiebig, H. H. & Burger, A. M. (2008) Tissue microarrays of human tumor xenografts: characterization of proteins involved in migration and angiogenesis for applications in the development of targeted anticancer agents. *Cancer Genomics Proteomics*, 5(5), 263-73.

Solaymani-Dodaran, M., Logan, R. F., West, J., Card, T. & Coupland, C. (2004) Risk of oesophageal cancer in Barrett's oesophagus and gastro-oesophageal reflux. *Gut*, 53(8), 1070-4.

Soon, P. & Kiaris, H. (2013) MicroRNAs in the tumour microenvironment: big role for small players. *Endocr Relat Cancer*, 20(5), R257-67.

Sottoriva, A., Kang, H., Ma, Z., Graham, T. A., Salomon, M. P., Zhao, J., Marjoram, P., Siegmund, K., Press, M. F., Shibata, D. & Curtis, C. (2015) A Big Bang model of human colorectal tumor growth. *Nat Genet*, 47(3), 209-16.

Spechler, S. J. & Souza, R. F. (2014) Barrett's esophagus. *N Engl J Med*, 371(9), 836-45.

Stahl, M., Walz, M. K., Stuschke, M., Lehmann, N., Meyer, H. J., Riera-Knorrenschild, J., Langer, P., Engenhart-Cabillic, R., Bitzer, M., Konigsrainer, A., Budach, W. & Wilke, H. (2009) Phase III comparison of preoperative chemotherapy compared with chemoradiotherapy in patients with locally advanced adenocarcinoma of the esophagogastric junction. *J Clin Oncol*, 27(6), 851-6.

Stark, A., Brennecke, J., Bushati, N., Russell, R. B. & Cohen, S. M. (2005) Animal MicroRNAs confer robustness to gene expression and have a significant impact on 3'UTR evolution. *Cell*, 123(6), 1133-46.

Steevens, J., Botterweck, A. A., Dirx, M. J., van den Brandt, P. A. & Schouten, L. J. (2010) Trends in incidence of oesophageal and stomach cancer subtypes in Europe. *Eur J Gastroenterol Hepatol*, 22(6), 669-78.

Stegeman, H., Span, P. N., Kaanders, J. H. & Bussink, J. (2014) Improving chemoradiation efficacy by PI3-K/AKT inhibition. *Cancer Treat Rev*, 40(10), 1182-91.

Stewart, D. J. (2007) Mechanisms of resistance to cisplatin and carboplatin. *Crit Rev Oncol Hematol*, 63(1), 12-31.

Stordal, B. & Davey, M. (2007) Understanding cisplatin resistance using cellular models. *IUBMB Life*, 59(11), 696-9.

Strumberg, D., Pilon, A. A., Smith, M., Hickey, R., Malkas, L. & Pommier, Y. (2000) Conversion of topoisomerase I cleavage complexes on the leading strand of ribosomal DNA into 5'-phosphorylated DNA double-strand breaks by replication runoff. *Mol Cell Biol*, 20(11), 3977-87.

Suzuki, H. I., Katsura, A., Matsuyama, H. & Miyazono, K. (2015) MicroRNA regulons in tumor microenvironment. *Oncogene*, 34(24), 3085-94.

Takeuchi, O. & Akira, S. (2010) Pattern recognition receptors and inflammation. *Cell*, 140(6), 805-20.

Tallant, C., Marrero, A. & Gomis-Ruth, F. X. (2010) Matrix metalloproteinases: fold and function of their catalytic domains. *Biochim Biophys Acta*, 1803(1), 20-8.

Tanioka, Y., Yoshida, T., Yagawa, T., Saiki, Y., Takeo, S., Harada, T., Okazawa, T., Yanai, H. & Okita, K. (2003) Matrix metalloproteinase-7 and matrix metalloproteinase-9 are associated with unfavourable prognosis in superficial oesophageal cancer. *Br J Cancer*, 89(11), 2116-21.

Tay, Y., Zhang, J., Thomson, A. M., Lim, B. & Rigoutsos, I. (2008) MicroRNAs to Nanog, Oct4 and Sox2 coding regions modulate embryonic stem cell differentiation. *Nature*, 455(7216), 1124-8.

Theisen, J., Peters, J. H. & Stein, H. J. (2003) Experimental evidence for mutagenic potential of duodenogastric juice on Barrett's esophagus. *World J Surg*, 27(9), 1018-20.

Thrift, A. P., Kramer, J. R., Richardson, P. A. & El-Serag, H. B. (2014) No significant effects of smoking or alcohol consumption on risk of Barrett's esophagus. *Dig Dis Sci*, 59(1), 108-16.

Toulany, M., Baumann, M. & Rodemann, H. P. (2007) Stimulated PI3K-AKT signaling mediated through ligand or radiation-induced EGFR depends indirectly, but not directly, on constitutive K-Ras activity. *Mol Cancer Res*, 5(8), 863-72.

Toulany, M., Kasten-Pisula, U., Brammer, I., Wang, S., Chen, J., Dittmann, K., Baumann, M., Dikomey, E. & Rodemann, H. P. (2006) Blockage of epidermal growth factor receptor-phosphatidylinositol 3-kinase-AKT signaling increases radiosensitivity of K-RAS mutated human tumor cells in vitro by affecting DNA repair. *Clin Cancer Res*, 12(13), 4119-26.

Tredan, O., Galmarini, C. M., Patel, K. & Tannock, I. F. (2007) Drug resistance and the solid tumor microenvironment. *J Natl Cancer Inst*, 99(19), 1441-54.

Trehoux, S., Lahdaoui, F., Delpu, Y., Renaud, F., Leteurtre, E., Torrisani, J., Jonckheere, N. & Van Seuningen, I. (2015) Micro-RNAs miR-29a and miR-330-5p function as tumor suppressors by targeting the MUC1 mucin in pancreatic cancer cells. *Biochim Biophys Acta*, 1853(10 Pt A), 2392-2403.

Tressel, S. L., Kaneider, N. C., Kasuda, S., Foley, C., Koukos, G., Austin, K., Agarwal, A., Covic, L., Opal, S. M. & Kuliopulos, A. (2011) A matrix metalloprotease-PAR1 system regulates vascular integrity, systemic inflammation and death in sepsis. *EMBO Mol Med*, 3(7), 370-84.

Tuddenham, L., Wheeler, G., Ntounia-Fousara, S., Waters, J., Hajihosseini, M. K., Clark, I. & Dalmay, T. (2006) The cartilage specific microRNA-140 targets histone deacetylase 4 in mouse cells. *FEBS Lett*, 580(17), 4214-7.

van Hagen, P., Hulshof, M. C., van Lanschot, J. J., Steyerberg, E. W., van Berge Henegouwen, M. I., Wijnhoven, B. P., Richel, D. J., Nieuwenhuijzen, G. A., Hospers, G. A., Bonenkamp, J. J., Cuesta, M. A., Blaisse, R. J., Busch, O. R., ten Kate, F. J., Creemers, G. J., Punt, C. J., Plukker, J. T., Verheul, H. M., Spillenaar Bilgen, E. J., van Dekken, H., van der Sangen, M. J., Rozema, T., Biermann, K., Beukema, J. C., Piet, A. H., van Rij, C. M., Reinders, J. G., Tilanus, H. W. & van der Gaast, A. (2012) Preoperative chemoradiotherapy for esophageal or junctional cancer. *N Engl J Med*, 366(22), 2074-84.

van Heijl, M., Omloo, J. M., van Berge Henegouwen, M. I., Hoekstra, O. S., Boellaard, R., Bossuyt, P. M., Busch, O. R., Tilanus, H. W., Hulshof, M. C., van der Gaast, A., Nieuwenhuijzen, G. A., Bonenkamp, H. J., Plukker, J. T., Cuesta, M. A., Ten Kate, F. J., Pruim, J., van Dekken, H., Bergman, J. J., Sloof, G. W. & van Lanschot, J. J. (2011) Fluorodeoxyglucose positron emission tomography for evaluating early response during neoadjuvant chemoradiotherapy in patients with potentially curable esophageal cancer. *Ann Surg*, 253(1), 56-63.

van Heijl, M., van Lanschot, J. J., Koppert, L. B., van Berge Henegouwen, M. I., Muller, K., Steyerberg, E. W., van Dekken, H., Wijnhoven, B. P., Tilanus, H. W., Richel, D. J., Busch, O. R., Bartelsman, J. F., Koning, C. C., Offerhaus, G. J. & van der Gaast, A. (2008) Neoadjuvant

chemoradiation followed by surgery versus surgery alone for patients with adenocarcinoma or squamous cell carcinoma of the esophagus (CROSS). *BMC Surg*, 8, 21.

van Kouwenhove, M., Kedde, M. & Agami, R. (2011) MicroRNA regulation by RNA-binding proteins and its implications for cancer. *Nat Rev Cancer*, 11(9), 644-56.

van Westreenen, H. L., Westerterp, M., Bossuyt, P. M., Pruim, J., Sloof, G. W., van Lanschot, J. J., Groen, H. & Plukker, J. T. (2004) Systematic review of the staging performance of 18F-fluorodeoxyglucose positron emission tomography in esophageal cancer. *J Clin Oncol*, 22(18), 3805-12.

Vasudevan, S., Tong, Y. & Steitz, J. A. (2007) Switching from repression to activation: microRNAs can up-regulate translation. *Science*, 318(5858), 1931-4.

Vazquez, S. M., Mladovan, A. G., Perez, C., Bruzzone, A., Baldi, A. & Luthy, I. A. (2006) Human breast cell lines exhibit functional alpha2-adrenoceptors. *Cancer Chemother Pharmacol*, 58(1), 50-61.

Veuger, S. J., Curtin, N. J., Richardson, C. J., Smith, G. C. & Durkacz, B. W. (2003) Radiosensitization and DNA repair inhibition by the combined use of novel inhibitors of DNA-dependent protein kinase and poly(ADP-ribose) polymerase-1. *Cancer Res*, 63(18), 6008-15.

Visbal, A. L., Allen, M. S., Miller, D. L., Deschamps, C., Trastek, V. F. & Pairolero, P. C. (2001) Ivor Lewis esophagogastrectomy for esophageal cancer. *Ann Thorac Surg*, 71(6), 1803-8.

Vlachos, P., Nyman, U., Hajji, N. & Joseph, B. (2007) The cell cycle inhibitor p57(Kip2) promotes cell death via the mitochondrial apoptotic pathway. *Cell Death Differ*, 14(8), 1497-507.

Wahl, D. R. & Lawrence, T. S. (2015) Integrating chemoradiation and molecularly targeted therapy. *Adv Drug Deliv Rev*.

Walsh, T. N., Noonan, N., Hollywood, D., Kelly, A., Keeling, N. & Hennessy, T. P. (1996) A comparison of multimodal therapy and surgery for esophageal adenocarcinoma. *N Engl J Med*, 335(7), 462-7.

Wang, J., He, J., Su, F., Ding, N., Hu, W., Yao, B., Wang, W. & Zhou, G. (2013) Repression of ATR pathway by miR-185 enhances radiation-induced apoptosis and proliferation inhibition. *Cell Death Dis*, 4, e699.

Wang, X., Xiong, L., Yu, G., Li, D., Peng, T., Luo, D. & Xu, J. (2015) Cathepsin S silencing induces apoptosis of human hepatocellular carcinoma cells. *Am J Transl Res*, 7(1), 100-10.

Warburg, O., Wind, F. & Negelein, E. (1927) THE METABOLISM OF TUMORS IN THE BODY. *J Gen Physiol*, 8(6), 519-30.

Weichselbaum, R. R., Ishwaran, H., Yoon, T., Nuyten, D. S., Baker, S. W., Khodarev, N., Su, A. W., Shaikh, A. Y., Roach, P., Kreike, B., Roizman, B., Bergh, J., Pawitan, Y., van de Vijver, M. J. & Minn, A. J. (2008) An interferon-related gene signature for DNA damage resistance is a predictive marker for chemotherapy and radiation for breast cancer. *Proc Natl Acad Sci U S A*, 105(47), 18490-5.

Wightman, B., Burglin, T. R., Gatto, J., Arasu, P. & Ruvkun, G. (1991) Negative regulatory sequences in the lin-14 3'-untranslated region are necessary to generate a temporal switch during Caenorhabditis elegans development. *Genes Dev*, 5(10), 1813-24.

Wilczynska, A. & Bushell, M. (2015) The complexity of miRNA-mediated repression. *Cell Death Differ*, 22(1), 22-33.

Winograd-Katz, S. E. & Levitzki, A. (2006) Cisplatin induces PKB/Akt activation and p38(MAPK) phosphorylation of the EGF receptor. *Oncogene*, 25(56), 7381-90.

Witsch, E., Sela, M. & Yarden, Y. (2010) Roles for growth factors in cancer progression. *Physiology (Bethesda)*, 25(2), 85-101.

Wohlhueter, R. M., McIvor, R. S. & Plagemann, P. G. (1980) Facilitated transport of uracil and 5-fluorouracil, and permeation of orotic acid into cultured mammalian cells. *J Cell Physiol*, 104(3), 309-19.

Wouters, B. G. & Brown, J. M. (1997) Cells at intermediate oxygen levels can be more important than the "hypoxic fraction" in determining tumor response to fractionated radiotherapy. *Radiat Res*, 147(5), 541-50.

Wu, P. C., Wang, Q., Grobman, L., Chu, E. & Wu, D. Y. (2012) Accelerated cellular senescence in solid tumor therapy. *Exp Oncol*, 34(3), 298-305.

Xu, H., Tanimoto, A., Murata, Y., Kimura, S., Wang, K. Y. & Sasaguri, Y. (2003) Difference in responsiveness of human esophageal squamous cell carcinoma lines to epidermal growth factor for MMP-7 expression. *Int J Oncol*, 23(2), 469-76.

Xuejun, C., Weimin, C., Xiaoyan, D., Wei, Z., Qiong, Z. & Jianhua, Y. (2014) Effects of aquaporins on chemosensitivity to cisplatin in ovarian cancer cells. *Arch Gynecol Obstet*, 290(3), 525-32.

Yamamoto, H., Horiuchi, S., Adachi, Y., Taniguchi, H., Nosho, K., Min, Y. & Imai, K. (2004) Expression of ets-related transcriptional factor E1AF is associated with tumor progression and over-expression of matrilysin in human gastric cancer. *Carcinogenesis*, 25(3), 325-32.

Yamashita, K., Mori, M., Kataoka, A., Inoue, H. & Sugimachi, K. (2001) The clinical significance of MMP-1 expression in oesophageal carcinoma. *Br J Cancer*, 84(2), 276-82.

Yang, H., Gu, J., Wang, K. K., Zhang, W., Xing, J., Chen, Z., Ajani, J. A. & Wu, X. (2009) MicroRNA expression signatures in Barrett's esophagus and esophageal adenocarcinoma. *Clin Cancer Res*, 15(18), 5744-52.

Yang, L. L., Wang, B. Q., Chen, L. L., Luo, H. Q. & Wu, J. B. (2012) CXCL10 enhances radiotherapy effects in HeLa cells through cell cycle redistribution. *Oncol Lett*, 3(2), 383-386.

Yao, Y., Xue, Y., Ma, J., Shang, C., Wang, P., Liu, L., Liu, W., Li, Z., Qu, S., Li, Z. & Liu, Y. (2014) MiR-330-mediated regulation of SH3GL2 expression enhances malignant behaviors of glioblastoma stem cells by activating ERK and PI3K/AKT signaling pathways. *PLoS One*, 9(4), e95060.

Ye, C., Zhang, X., Wan, J., Chang, L., Hu, W., Bing, Z., Zhang, S., Li, J., He, J., Wang, J. & Zhou, G. (2013) Radiation-induced cellular senescence results from a slippage of long-term G2 arrested cells into G1 phase. *Cell Cycle*, 12(9), 1424-32.

Yu, J., Wang, Y., Dong, R., Huang, X., Ding, S. & Qiu, H. (2012) Circulating microRNA-218 was reduced in cervical cancer and correlated with tumor invasion. *J Cancer Res Clin Oncol*, 138(4), 671-4.

Yuan, W., Xiaoyun, H., Haifeng, Q., Jing, L., Weixu, H., Ruofan, D., Jinjin, Y. & Zongji, S. (2014) MicroRNA-218 enhances the radiosensitivity of human cervical cancer via promoting radiation induced apoptosis. *Int J Med Sci*, 11(7), 691-6.

Zaffaroni, N., Silvestrini, R., Orlandi, L., Bearzatto, A., Gornati, D. & Villa, R. (1998) Induction of apoptosis by taxol and cisplatin and effect on cell cycle-related proteins in cisplatin-sensitive and -resistant human ovarian cells. *Br J Cancer*, 77(9), 1378-85.

Zhao, J., Lei, T., Xu, C., Li, H., Ma, W., Yang, Y., Fan, S. & Liu, Y. (2013) MicroRNA-187, down-regulated in clear cell renal cell carcinoma and associated with lower survival, inhibits cell growth and migration though targeting B7-H3. *Biochem Biophys Res Commun*, 438(2), 439-44.

Zhao, L., Bode, A. M., Cao, Y. & Dong, Z. (2012) Regulatory mechanisms and clinical perspectives of miRNA in tumor radiosensitivity. *Carcinogenesis*, 33(11), 2220-7.

Zhaorigetu, S., Wan, G., Kaini, R., Jiang, Z. & Hu, C. A. (2008) ApoL1, a BH3-only lipid-binding protein, induces autophagic cell death. *Autophagy*, 4(8), 1079-82.

Zhaorigetu, S., Yang, Z., Toma, I., McCaffrey, T. A. & Hu, C. A. (2011) Apolipoprotein L6, induced in atherosclerotic lesions, promotes apoptosis and blocks Beclin 1-dependent autophagy in atherosclerotic cells. *J Biol Chem*, 286(31), 27389-98.

Zhou, S., Schuetz, J. D., Bunting, K. D., Colapietro, A. M., Sampath, J., Morris, J. J., Lagutina, I., Grosveld, G. C., Osawa, M., Nakauchi, H. & Sorrentino, B. P. (2001) The ABC transporter Bcrp1/ABCG2 is expressed in a wide variety of stem cells and is a molecular determinant of the side-population phenotype. *Nat Med*, 7(9), 1028-34.

Appendix 1

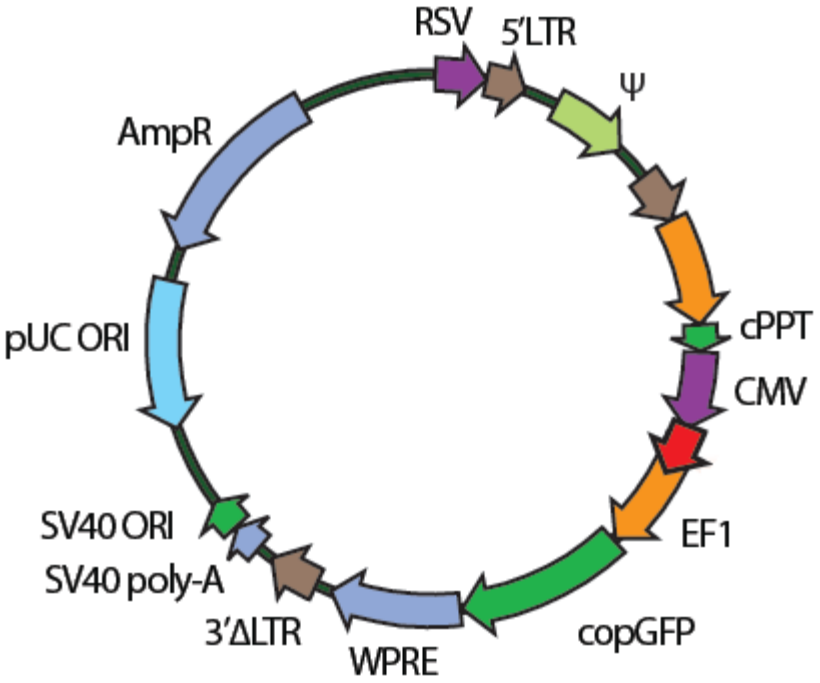

Fig A1a The pre-miR-330, pre-miR-187 and miR-VC plasmid vector map (System Biosciences catalogue numbers; PMIRH330PA-1, PMIRH187PA-1 and CD511B-1). The red arrow indicates the region encoding the pre-miR-330 sequence, the pre-miR-187 sequence or the non-targeting scrambled sequence. The plasmid encodes the reporter protein GFP (copGFP) which was used to assess transfection efficiency in the mammalian cell lines. The plasmid also encodes the ampicillin resistance gene (Amp^R) for bacterial plasmid propagation. These plasmids were used for transient overexpression of miRNA in OAC cell lines.

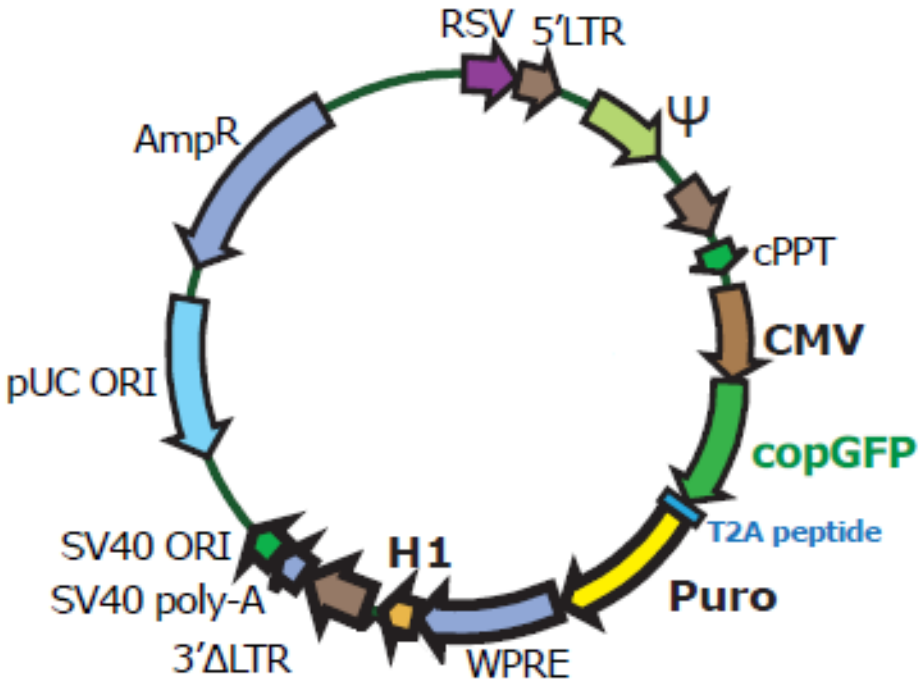

Fig A1b The miRZIP-330-5p and miRZIP-VC plasmid vector map (System Biosciences catalogue numbers; MZIP-330-5p-PA-1 and MZIP000-PA-1). The region encoding the precursor anti-miR-330-5p sequence or the scrambled non-targeting sequence is located between the H1 and 3'ΔLTR sites. The plasmid encodes the reporter protein GFP (copGFP), which was used to assess transfection efficiency and stable plasmid expression in the mammalian cell lines. The plasmid encodes the ampicillin resistance gene (Amp^R) for bacterial plasmid propagation. These plasmids also encode the puromycin resistance gene (Puro) and were used to established stable OAC cell line models.

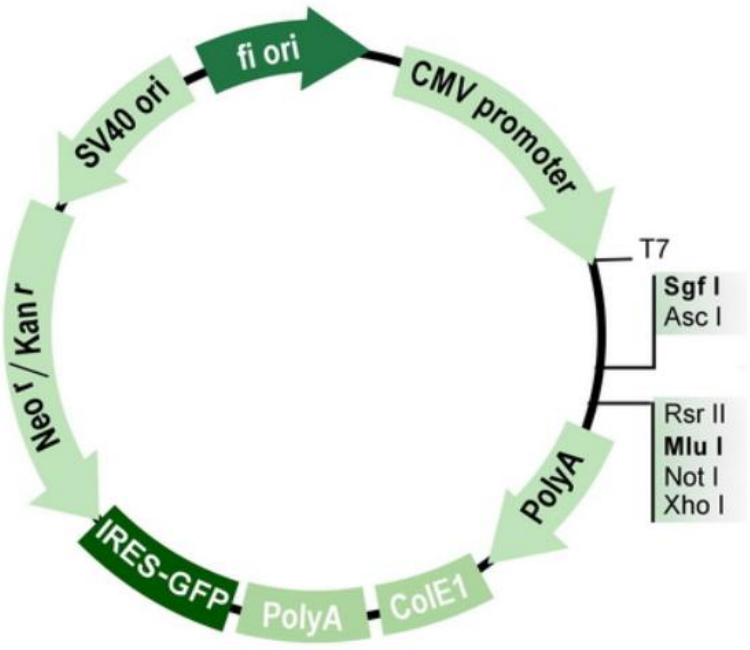

Fig A1c The pre-miR-187 and miR-VC plasmid vector map (Origene catalogue numbers; PCMVMIR187 and PCMVMIR). The region encoding the precursor miR-187 sequence is between the Sgf I and Mlu I sites. The plasmid encodes the reporter protein GFP (IRES-GFP) and the kanamycin resistance gene (Kan^R) for bacterial plasmid propagation. These plasmids also encode the neomycin resistance gene (Neo^R) and were used to established stable OAC cell line models.

Appendix 2

Table A2.1 Recipe for hand cast gels: resolving gel (makes 2 gels)

	10%	**12%**
H_2O	6.1 mL	5.2 mL
1.5M Tris pH 8.8	3.75 mL	3.75 mL
Acrylamide	4.95 mL	5.8 mL
10% SDS	150 µL	150 µL
10% APS	75 µL	75 µL
TEMED	18 µL	18 µL

Table A2.2 Recipe for hand cast gels: stacking gel (for two gels)

	5%
H_2O	6.1 mL
0.5M Tris pH 6.8	2.5 mL
Acrylamide	1.3 mL
10% SDS	100 µL
10% APS	100 µL
TEMED	20 µL

Appendix 3

Table A3 CHARM algorithm settings

Panel	Function	Setting
F1 Pre-processed	Smoothing	5
F2 Edge detection	Edge detection sensitivity	91.6/100
F3 Centre detection	Detection mode	Dark on light
	Centre detection sensitivity	50/100
	Soft colony diameter range	Lower 60 µm
		Upper 3000 µm
	Min centre to centre separation	60 µm
	Auto-select	Yes
	Smoothing	3 (range 0-3)
F4 Shape controls	Circularity factor	74/100
	Edge distance threshold	0.85 (range 0.7 to 1)
	No. spokes	32
	Shape filtering	Fast Gaussian
		Filter size 5
	Shape processing	Best fit circle
F5 Filtering controls	Colony diameter filter	Min 60 µM Max 3000
	Colony intensity (OD)	Min 0.1 Max 2.0
	Good edge factor	0.9/1
	Borders from centroids	Yes
F6 Overlap controls	Merge overlapping objects	Yes
	Overlap threshold	60%
	Overlap calculation	Area
	Retain the	Most intense
	Calculate new cluster boundaries	Yes

Appendix 4

Table A4 Relative expressions (Log_{10}) of the significantly differentially expressed miRNA in the OAC patient cohort

microRNA	Responders (*n*=9)	Non-responders (*n*=10)
hsa-let-7a-2*	2.74	1.56
hsa-let-7d	0.22	1.11
hsa-let-7f-1*	-0.94	-0.21
hsa-let-7g	-0.57	0.09
hsa-miR-103-2*	-0.36	-5.33
hsa-miR-1184	0.46	0.07
hsa-miR-1236	2.13	-0.06
hsa-miR-1237	-0.51	-1.21
hsa-miR-1248	1.00	2.36
hsa-miR-125a-3p	-0.57	0.09
hsa-miR-125a-5p	0.28	0.23
hsa-miR-1296	-0.80	1.01
hsa-miR-140-3p	0.12	-1.12
hsa-miR-142-3p	0.34	2.22
hsa-miR-145*	0.56	-1.32
hsa-miR-147	1.94	0.85
hsa-miR-147b	1.53	0.48
hsa-miR-151-5p	0.07	0.57
hsa-miR-155*	-0.31	-2.97
hsa-miR-16-2*	0.22	1.11
hsa-miR-17	1.00	2.36
hsa-miR-181a-2*	-1.17	-6.10
hsa-miR-187	**0.54**	**-0.97**
hsa-miR-1979	-0.55	0.18
hsa-miR-21	0.46	0.07
hsa-miR-212	3.56	0.15
hsa-miR-220c	-0.55	0.66
hsa-miR-26a	-0.11	0.95
hsa-miR-296-3p	0.26	-2.61
hsa-miR-30c	-0.11	0.79
hsa-miR-30c-1*	-0.11	0.95
hsa-miR-31	1.94	0.85
hsa-miR-320a	-0.51	-1.21
hsa-miR-320b	1.40	0.12
hsa-miR-330-5p	**0.54**	**-12.74**
hsa-miR-331-3p	-0.94	-0.21
hsa-miR-339-3p	-1.43	-4.62
hsa-miR-340*	-0.71	0.13
hsa-miR-370	0.54	-0.43

hsa-miR-373*	0.54	-0.50
hsa-miR-431*	0.38	-1.08
hsa-miR-432*	0.78	3.62
hsa-miR-448	-0.27	0.72
hsa-miR-452*	-4.02	-2.53
hsa-miR-488*	0.02	1.01
hsa-miR-495	-0.71	0.13
hsa-miR-502-5p	-0.22	1.56
hsa-miR-513a-3p	-0.11	0.79
hsa-miR-518d-5p	1.49	0.98
hsa-miR-519c-3p	0.27	1.71
hsa-miR-532-5p	0.39	2.15
hsa-miR-555	2.93	1.86
hsa-miR-556-3p	-0.40	-3.60
hsa-miR-556-5p	-2.07	-0.64
hsa-miR-558	0.21	-0.64
hsa-miR-592	-2.02	-5.80
hsa-miR-630	0.34	2.22
hsa-miR-634	-0.40	0.61
hsa-miR-640	-1.49	0.49
hsa-miR-647	-0.22	1.56
hsa-miR-661	-0.55	0.18
hsa-miR-720	0.21	-0.64
hsa-miR-769-3p	0.25	2.80
hsa-miR-769-5p	1.34	-0.11
hsa-miR-886-5p	1.40	0.12
hsa-miR-99b*	5.27	2.52

Appendix 5

Fig A5 The miR-330-3p and miR-330-5p predicted binding sites in the *E2F1* mRNA transcript (Betel et al., 2008). There are two predicted miR-330-3p binding sites and one predicted miR-330-5p binding site. The vertical lines represent Watson-Crick base pairing, the horizontal lines represent bulges between the miRNA and mRNA and the G:U represents wobble base paring.

Appendix 6

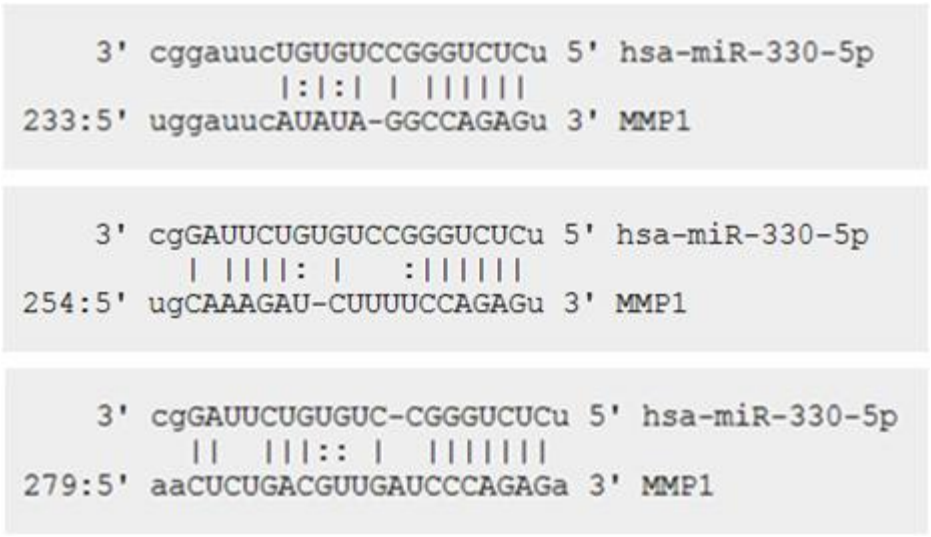

Fig A6 The miR-330-5p predicted binding sites in the *MMP1* mRNA transcript (Betel et al., 2008). There are three predicted miR-330-5p binding sites. The vertical lines represent Watson-Crick base pairing, the horizontal lines represent bulges between the miRNA and mRNA and the G:U represents wobble base paring.

Appendix 7

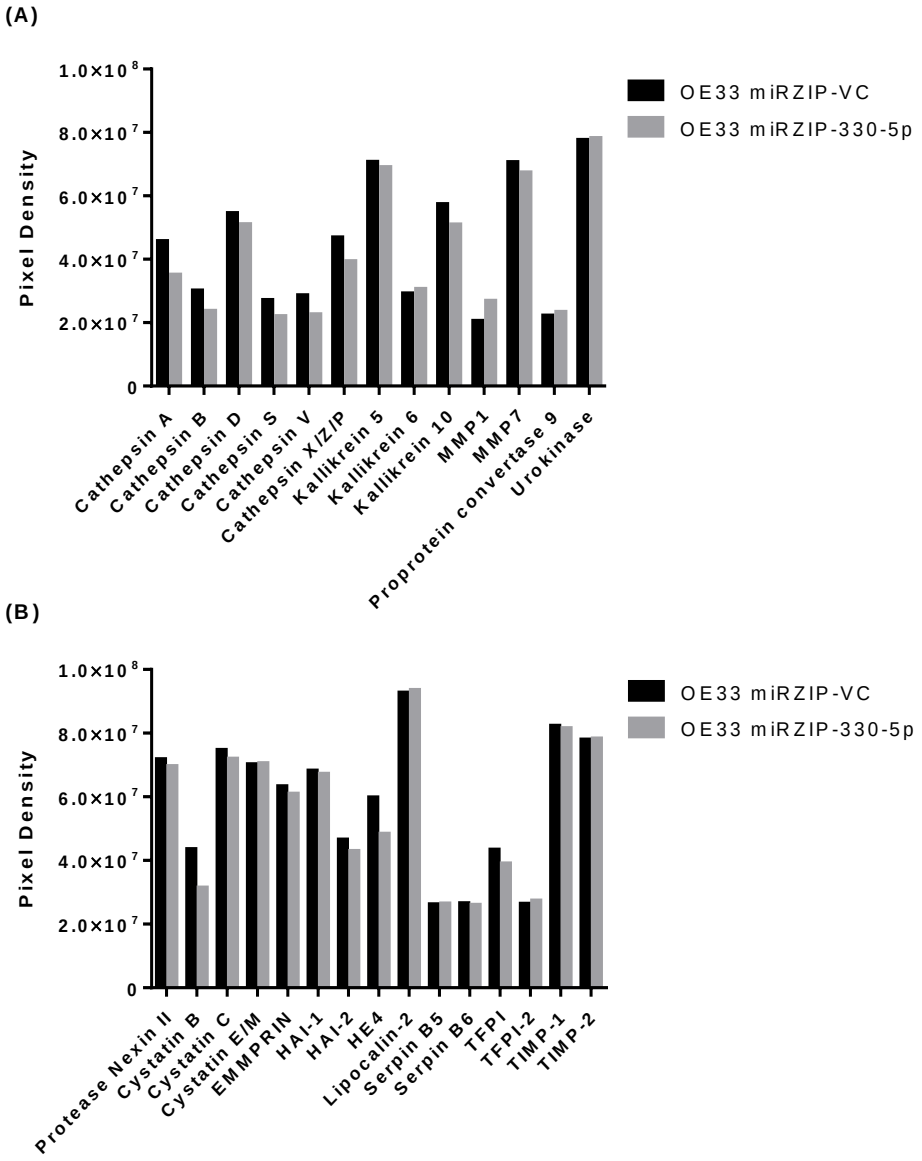

Fig A7 Densitometry analysis, presented as pixel density, for the antibody-based proteome profiler arrays. The relative expression of 32 proteases and 35 protease inhibitors were assessed in conditioned medium from the OE33 miRZIP-VC and the OE33 miRZIP-330-5p cell lines. **(A)** Of the 32 proteases analysed, 13 proteins were expressed. **(B)** Of the 35 protease inhibitors analysed, 15 proteins were expressed.

Appendix 8

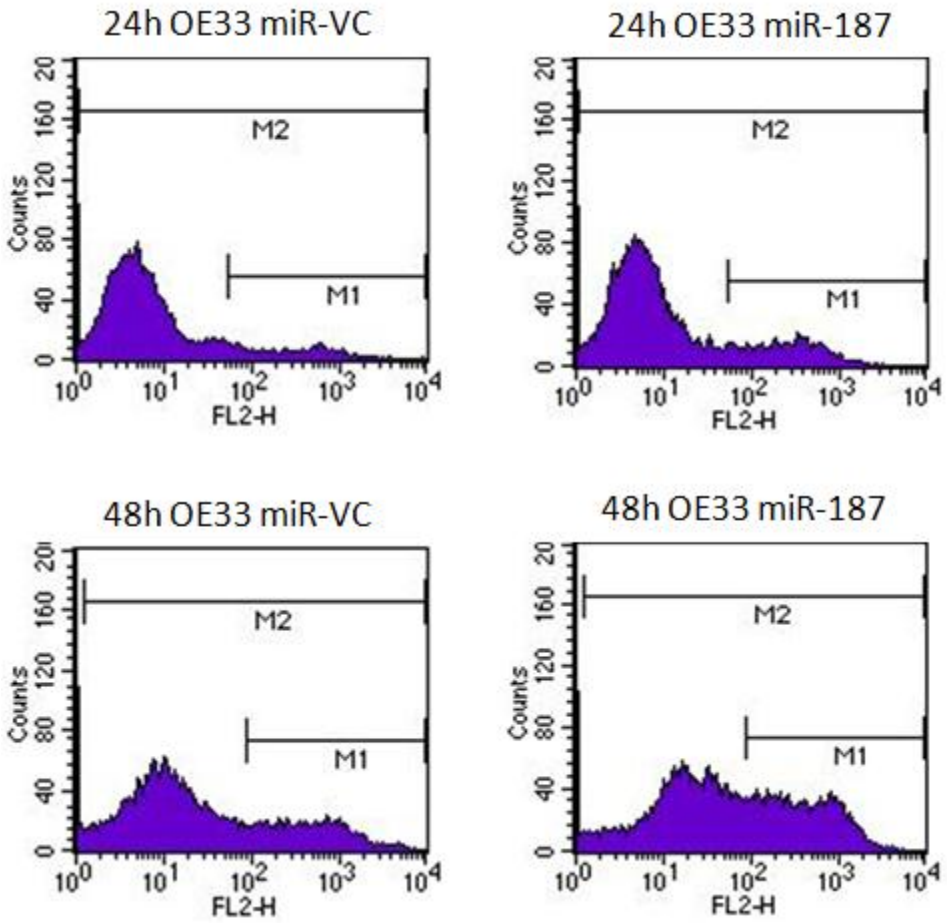

Fig A8 Flow cytometry histogram plots for PI cell staining. The number of cells counted are plotted on the y-axis. PI fluorescence is detected in the FL2 channel and fluorescence intensity is plotted on the x-axis. Marker 2 (M2) designates the total number of events and marker 1 (M1) indicates the number of positive events. In this analysis the positive events are the cells with PI staining and the histograms show the shift in the fraction of PI positive cells. These histograms are example data from one experimental repeat *n*=1.

Appendix 9

Table A9 Gene expression analysis in the OE33 R miR-VC and OE33 R miR-187

Gene	FPMK miR-VC	FPMK miR-187
Non-annotated	0.00	33,194.70
Non-annotated	0.00	7.51
Non-annotated	0.00	2,719,370.00
Non-annotated	0.00	1.20
Non-annotated	0.00	18,485.90
Non-annotated	0.00	23,569.90
HIST1H4D	0.00	1.87
MIR34B	0.00	150.23
MIRLET7E	0.00	114.62
Non-annotated	0.00	1.89
MIR130B	0.00	125.23
MIR183	0.00	37.99
Non-annotated	0.00	5.56
Non-annotated	0.00	106.59
MIR187	**71.73**	**19,891.10**
Non-annotated	37,426.10	1,612,040.00
RNF170	2.51	35.48
APC	1.48	12.49
VIM	0.51	2.41
C10orf118	4.33	17.29
LOC642587	4.85	18.40
HIST1H4H	3.54	11.23
CA5B	0.46	1.38
ZBED3	2.38	6.50
TNF	1.54	3.68
DNAJC12	1.44	3.16
FILIP1L	5.39	11.30
SNORD60	1,329.19	2,715.33
ZNF182	1.08	2.13
GEM	8.72	16.62
NSUN3	2.24	4.16
GAS2L3	1.37	2.54
CLDN5	9.70	17.85
ICK	1.03	1.89
Non-annotated	15.08	26.67
LYRM5	4.69	8.24
SLC9A2	0.81	1.42
Non-annotated	392.11	683.51
ANKRD18A	1.69	2.81
MYLIP	6.30	10.31

PIGX	4.09	6.65
ZNF431	2.26	3.57
PBX3	2.32	3.66
C5orf24	3.19	5.00
ATPBD4	2.93	4.56
RSRC2	31.68	49.25
FAM173B	3.57	5.54
FAM81A	1.60	2.48
STAU2	1.82	2.80
ZNF430	3.48	5.37
CAPN7	3.55	5.43
R3HDM1	8.77	13.38
LOC339290	1.73	2.64
HRSP12	10.95	16.69
VWDE	1.27	1.94
KLHL15	1.17	1.78
TOP2B	8.40	12.75
LYRM7	1.86	2.81
MIB1	2.50	3.78
SH3BGRL2	3.31	5.00
NHLRC2	3.40	5.12
COMMD8	8.50	12.79
ZNF143	6.23	9.36
CDC42BPA	1.92	2.87
LRP6	1.14	1.71
PEX13	4.60	6.88
JUN	61.03	91.12
RNGTT	2.90	4.32
FAM171B	1.71	2.54
STAG3L4	4.44	6.60
PBK	13.63	20.17
CDK8	9.48	13.98
TMEM38B	5.83	8.59
SMC4	35.59	52.39
FAM126A	2.54	3.74
RAB11FIP2	1.79	2.62
SNAPC1	3.72	5.45
NAA30	4.81	7.06
IDI1	27.34	40.10
HINT3	10.40	15.21
IMPACT	3.17	4.62
CUL3	10.91	15.91
SOX4	23.72	34.59
PDZD8	16.55	24.07

SACS	1.93	2.81
GULP1	32.23	46.83
TMEM168	3.71	5.37
PFDN4	23.76	34.40
KITLG	6.74	9.75
KIAA1430	3.91	5.66
PPIL4	8.14	11.76
GPAM	2.06	2.97
ADK	34.76	49.99
KIAA0907	10.99	15.79
RCN2	28.03	40.19
THAP1	7.16	10.22
PSD3	1.93	2.75
CUL5	6.33	9.03
TWSG1	4.68	6.67
ZNF644	7.40	10.52
CENPE	5.83	8.30
ABCE1	30.23	42.94
UTP15	7.82	11.10
SPAST	3.70	5.25
DPY19L4	2.80	3.97
RNF130	18.89	26.79
GNPTAB	3.30	4.66
SAMD12	2.51	3.55
MON2	1.94	2.74
ZNF292	4.02	5.65
KIF14	3.44	4.84
TMTC3	3.17	4.46
LUC7L3	59.53	83.71
PHIP	3.21	4.52
JMJD1C	7.22	10.14
PCNP	30.81	43.27
PTPLB	10.26	14.39
PRKDC	14.82	20.76
TCF12	6.04	8.44
TSEN15	12.72	17.74
GNAI1	13.31	18.55
PRPF4B	9.25	12.89
SSX2IP	3.14	4.37
MYNN	3.61	5.03
SLC4A7	2.41	3.35
GTF2A1	4.55	6.32
TECR	94.10	130.46
UBR3	2.91	4.04

KIDINS220	5.08	7.03
PRPF38B	14.29	19.75
PTEN	4.70	6.48
OPA1	12.27	16.92
NUDT4	20.06	27.63
CDK6	13.82	19.02
RFC3	31.68	43.59
TMEM33	9.76	13.43
APPL1	4.43	6.09
FOPNL	19.49	26.77
ATF3	106.51	146.18
UBE2D1	14.33	19.64
SMC2	8.04	11.02
PREPL	5.14	7.03
AKAP9	9.52	13.03
DDX46	11.74	16.01
EID1	32.44	44.23
SLC12A2	5.25	7.14
DCTN4	12.38	16.85
ZNF706	16.70	22.71
NIPBL	6.10	8.30
THUMPD1	10.76	14.62
FH	66.40	90.13
BICD2	15.73	21.34
MAP3K2	4.38	5.92
KIF5B	28.64	38.72
RBM27	7.85	10.61
SRSF1	36.19	48.83
CENPF	7.59	10.24
ARHGAP5	8.66	11.64
BCLAF1	18.24	24.52
PCM1	8.30	11.14
HDAC2	16.85	22.63
ARPP19	19.13	25.65
APOL6	20.79	15.48
UNC93B1	104.27	77.21
MXD1	11.79	8.70
SP110	72.40	53.15
IFI16	73.84	53.76
MOV10	70.83	51.54
CDKN1A	67.61	49.12
BST2	331.99	240.67
IRF7	583.49	422.58
B3GNT3	22.21	16.00

IRF1	63.81	45.74
HIP1R	30.53	21.87
PLAUR	214.19	153.42
C3	11.28	8.05
PRIC285	145.23	102.85
C19orf66	54.39	38.21
SEMA7A	34.69	24.36
PPM1K	4.89	3.43
HLA-H	40.39	28.26
CMPK2	18.99	13.23
LY6E	259.50	180.62
IFIH1	90.99	63.03
TINF2	15.54	10.76
IFI44L	11.61	8.02
MX2	144.97	99.56
MOBKL2C	6.40	4.39
SECTM1	58.35	40.00
TMEM27	16.72	11.45
APOL1	151.91	103.86
NLRC5	14.27	9.75
PARP10	102.75	69.68
CD274	8.70	5.89
PLEKHA4	22.95	15.51
DDX58	51.03	34.44
RARRES3	302.42	203.64
KRT16	13.75	9.26
UBE2L6	263.53	176.45
STAT2	47.35	31.64
RAPGEF3	5.15	3.42
MT2A	2,148.53	1,423.24
PSMB9	61.40	40.59
IFITM3	1,117.03	733.92
LAMP3	35.28	23.17
CD68	23.11	15.17
HLA-B	891.68	584.92
TLR3	3.78	2.47
RNF19B	24.03	15.45
Non-annotated	43.51	27.97
TRANK1	5.02	3.21
APOL2	101.98	65.27
BTN3A1	4.97	3.16
LMO2	35.88	22.74
Non-annotated	6.74	4.27
SLFN12	4.57	2.88

ISG15	3,842.28	2,426.24
NT5C3	136.34	85.44
PRR15	22.43	14.02
SP100	163.96	102.11
EPSTI1	43.15	26.58
IFIT2	254.00	155.35
CEACAM1	7.49	4.58
IFIT1	752.85	458.37
ETV7	44.38	27.02
IFI6	1,168.40	710.37
CCL5	41.73	25.30
IFI27	504.97	304.57
TAP1	183.81	110.65
HLA-F	162.54	97.30
IL22RA1	5.37	3.21
GSDMB	71.93	42.66
HERC5	8.88	5.25
OAS1	319.96	188.88
LGALS9	78.64	46.38
USP18	107.23	62.64
PXK	3.12	1.81
RTP4	12.38	7.17
PLXNA2	1.96	1.13
Non-annotated	7.14	4.11
CD74	7.00	4.01
MMP13	7.99	4.54
IFIT3	203.75	114.78
APOL3	3.63	2.03
SAMD9L	47.86	26.58
OASL	369.93	204.92
IFITM1	302.78	167.71
MX1	83.31	45.71
GBP4	2.35	1.26
GBP1	13.46	7.21
OAS2	152.63	81.47
KRT17	100.46	53.47
IFI35	138.41	72.82
NCF2	7.42	3.89
SAA1	14.82	7.66
IDO1	13.66	7.04
CFB	19.83	10.20
XAF1	16.81	8.60
TNFSF10	21.43	10.76
BTN3A3	2.98	1.48

ZNF526	17.39	8.38
ISG20	180.28	86.55
HRASLS2	17.91	8.58
DHX58	5.44	2.59
Non-annotated	2.49	1.18
CCL22	1.51	0.71
RHEBL1	4.01	1.83
PRICKLE4	4.52	2.06
UBA7	4.80	2.13
GBP5	1.67	0.71
BCL2L14	2.17	0.91
GMPR	6.45	2.65
RSAD2	65.43	26.56
TRIM22	27.00	10.92
Non-annotated	3.44	1.33
HECTD2	16.63	6.37
NUPR1	5.20	1.91
ZBP1	10.09	3.56
IL29	29.40	10.09
Non-annotated	58.96	19.39
BATF2	25.57	8.38
RAB11FIP4	18.08	5.91
CXCL11	5.92	1.93
Non-annotated	6.88	2.10
CXCL10	14.99	4.39
RRAD	38.20	10.51
KRT14	4.73	1.27
IL28B	16.25	4.16
Non-annotated	35,256.90	8,685.15
C7orf43	122.98	29.26
IL28A	25.53	5.96
IFNB1	6.94	1.24
Non-annotated	35,226.00	4,943.46
PYROXD2	10.25	0.97
Non-annotated	56,946,600.00	0.00
Non-annotated	1.96	0.00
Non-annotated	8,256.79	0.00
Non-annotated	10,740.30	0.00
Non-annotated	22.99	0.00
KRT19P2,MIR492	23.85	0.00
Non-annotated	1,018.30	0.00
Non-annotated	3.90	0.00
Non-annotated	8.63	0.00

FPKM; fragments per kilobase of transcript per million mapped reads

Appendix 10

Table A10 Gene expression analysis in the OE33 PBS 29 and OE33 CISR 29

Gene	FPMK PBS	FPMK CISR
Non-annotated	0.00	155.09
Non-annotated	0.00	3.30
Non-annotated	0.00	4.97
Non-annotated	0.00	7.63
Non-annotated	0.00	5.15
Non-annotated	0.00	2.38
Non-annotated	0.00	1.12
Non-annotated	0.00	4.47
ADAMTS19	0.00	2.13
Non-annotated	0.00	46.36
Non-annotated	0.00	15.70
Non-annotated	0.00	16.28
PTGS2	0.11	2.49
RNF170	2.24	48.99
VCAN	0.44	8.71
COL17A1	4.70	68.72
ACTL8	14.38	197.92
FAM3B	0.64	7.84
ACP5	0.91	10.59
KIAA1199	0.21	2.18
Non-annotated	0.60	5.96
INHBA	0.11	1.09
MB	0.99	9.30
Non-annotated	0.30	2.72
DPP4	0.33	2.77
IGFBP1	0.57	4.68
ATP1A3	1.70	13.47
PRICKLE2	0.21	1.62
SPOCD1	0.68	5.05
LOC100130581	1.31	9.53
C6orf223	2.48	17.17
ANXA10	10.10	66.55
SCIN	0.30	1.90
C7orf43	27.05	171.37
LOC149773	0.89	5.54
UGT2B7	0.22	1.31
TRIM29	1.35	8.02
WISP3	0.66	3.88
MMP1	1.44	8.18
NR5A2	0.27	1.51

SKG2	2.80	15.01
UST	0.25	1.25
FST	10.51	52.09
FRMD3	1.32	6.53
ITGA5	2.08	10.24
SOX21	1.59	7.76
TSPAN33	0.43	2.07
TRIB2	0.35	1.59
IFI27	19.36	88.09
TAGLN3	4.47	18.88
TLEA	0.34	1.39
LOC 339894	0.72	2.97
APOL2	18.55	76.23
BMP2	0.41	1.68
GOLGA7B	1.92	7.55
NAV1	0.55	2.06
OSBP2	1.11	4.15
KITLG	2.70	10.07
TNS4	0.65	2.39
HR	1.42	5.28
PPP1R14C	1.12	4.06
TBC1D17	70.63	253.83
O3FAR1	0.37	1.34
ABCA12	0.24	0.86
HCAR1	0.38	1.34
SERPINE2	0.72	2.55
C2orf89	1.23	4.34
TMEM199	16.23	56.86
TMEM22	1.37	4.80
APOL1	59.39	201.22
RAB36	0.62	2.09
TNIK	0.72	2.41
SLC17A9	4.83	16.04
Non-annotated	1.68	5.53
Non-annotated	2.92	9.63
SBK1	0.59	1.93
SYBU	1.63	5.20
C9orf116	3.58	11.26
LOC257396	0.71	2.21
GIPC2	1.20	3.72
SCAMP5	1.13	3.44
SYNJ2	3.66	10.97
BAHCC1	1.09	3.22
MEF2C	0.30	0.88

IGFBP3	149.15	427.36
C3orf14	6.24	17.75
FREM2	0.46	1.31
UCA1	86.27	244.48
AKAP12	65.67	186.09
PRKAR2A	2.22	6.27
ACE	1.82	5.13
SLC15A1	2.29	0.81
CMTM3	15.72	5.54
DDAH2	53.78	18.89
ZNF816	4.71	1.65
PCDHA1	1.47	0.51
NR4A1	16.27	5.67
ELF5	7.50	2.59
SH3PXD2B	2.46	0.84
FGFR3	12.61	4.31
KLKL5	9.22	3.15
PLAG1	1.08	0.37
TNNC1	14.57	4.95
DUSP6	67.47	22.83
DOCK9	6.31	2.13
CD82	12.00	4.04
ZNF250	0.85	0.29
FYN	2.61	0.87
LCN2	579.97	191.85
ETNK2	9.11	3.00
SOCS2	9.26	3.05
PRSS8	302.94	99.61
TMPRSS2	3.72	1.21
WNT10A	20.83	6.79
SERPINA1	1.22	0.39
PDE9A	13.91	4.51
Non-annotated	544.97	176.01
Non-annotated	28.42	9.11
Non-annotated	9.59	3.07
NDRG2	5.93	1.89
CHRNB1	10.49	3.34
BEAN1	4.34	1.38
OVOL2	5.57	1.77
SNCG	21.66	6.86
NCKAP5L	3.15	0.99
CTGF	6.81	2.15
Non-annotated	4.20	1.32
SLC2A12	1.01	0.32

EPS8L3	9.48	2.96
UPK3B	18.52	5.71
GABARAPL1	7.95	2.44
NEBL	1.05	0.32
GAD1	15.39	4.68
FAM164A	2.09	0.63
PPM1K	2.75	0.83
KRT16	12.66	3.68
GLS2	10.19	3.17
LGALS9	14.92	4.31
Non-annotated	11.69	3.37
FAM46B	3.65	1.05
IL18	69.23	19.78
Non-annotated	7.11	1.97
CDA	37.24	10.28
TTYH1	16.35	4.48
CST6	625.07	169.52
UPK1B	1.98	0.53
PLEKHB1	3.13	0.84
KRT17	8.57	2.28
STXBP1	3.36	0.88
PIAS4	90.60	23.81
CDC42EP5	164.61	43.19
NOS3	10.56	2.77
NAV3	1.04	0.27
GCNT3	1.995	0.50
CERCAM	22.10	5.61
SCEL	34.18	8.58
DUSP16	1.73	0.43
PDZK1IP1	8.68	2.16
Non-annotated	22.67	5.63
SKAP1	15.99	3.94
XK	1.06	0.26
FIBCD1	14.40	3.49
ICAM1	25.26	6.08
CYP2S1	26.02	6.22
GLRX	22.28	5.30
SLAIN1	1.27	0.30
GCHFR	51.38	12.19
PHACTR3	7.32	1.74
LOC642587	18.69	4.42
GABRP	1.08	0.26
TRIM17	7.95	1.85
NDE1	56.89	13.19

IRF7	37.51	8.06
MX1	20.40	4.37
DHRS2	10.33	2.18
CDK14	4.94	1.02
ATG9B	8.10	1.66
CFD	29.21	5.99
CA11	4.48	1.02
CSRP2	10.33	2.08
EDA	1.09	0.22
EMP3	8.90	1.77
IRF9	18.77	3.68
EDN1	11.58	2.26
IL17RD	1.63	0.32
CD22	8.12	1.56
MATN2	1.97	0.38
NCCRP1	2.28	0.43
CCDC92	5.17	0.97
PSCA	74.47	13.88
Non-annotated	29.23	5.44
KCNQ1	9.28	1.72
ITGB8	6.36	1.18
TMEM156	5.04	0.93
TLE3	1.83	0.31
PCDHB3	1.46	0.24
PSG4	1.25	0.20
TMEM42	66.07	10.28
MUC1	13.73	2.13
CDKN1C	12.65	1.96
COL13A1	1.99	0.31
EPPK1	2.97	0.46
DHX58	2.49	0.38
NAV2	1.60	0.24
PPP1R1C	4.81	0.73
CHST11	3.60	0.51
EBF4	4.32	0.59
UPK2	12.48	1.68
SLCO1B3	8.29	1.08
STIM1	62.55	7.93
XAF1	0.76	0.09
GPR35	9.73	1.16
UBD	5.97	0.65
PADI3	3.37	0.36
L1CAM	1.19	0.13
EEF1A2	55.71	5.66

LGALS1	105.00	10.45
IL8	7.68	0.73
SOX2	4.10	0.39
IFI6	62.65	5.73
CCDC160	3.99	0.36
SCARA3	2.23	0.19
HERC5	0.82	0.07
NOXO1	38.38	3.02
IGFBP2	30.76	2.41
CLIC3	20.63	1.61
TGM2	529.64	40.69
FCGRT	11.75	0.88
QPRT	12.08	0.81
IFIT1	16.03	1.03
KISS1R	21.98	1.41
FMNL1	3.74	0.24
C3	15.77	0.99
CFB	4.24	0.26
ACHE	2.76	0.17
MX2	3.01	0.18
HOPX	1.88	0.11
SHROOM2	1.40	0.08
SULF2	4.08	0.22
NXN	4.75	0.25
LOC730755	2.00	1.31
PLAC8	4.29	0.21
UGT1A1	9.09	0.45
MIR675	1169.86	55.33
SUSD2	12.13	0.52
SLC2A3	7.67	0.20
CAPN6	8.38	0.19
ANKRD1	75.31	1.64
BST2	52.26	0.93
OAS2	3.89	0.07
TESC	64.77	1.12
KISS1	346.70	4.11
S100A9	4.10	0.00
HES5	1.13	0.00
Non-annotated	11.21	0.00
IGF2	0.74	0.00
USH1C	1.49	0.00
Non-annotated	6.19	0.00
Non-annotated	85090.00	0.00
RNASE1	1.47	0.00

MT1G	5.21	0.00
VAV1	2.08	0.00
LOC100507003	0.83	0.00
C19orf77	1.52	0.00
MYCN	0.91	0.00
ARHGEF9	0.81	0.00
Non-annotated	2.98	0.00
CHST13	1.17	0.00
Non-annotated	20160.80	0.00
Non-annotated	14.63	0.00
Non-annotated	1.61	0.00

FPKM; fragments per kilobase of transcript per million mapped reads